

Rosslare ORE Hub

EIAR Technical Appendices

Technical Appendix 8:

Coastal Processes

TABLE OF CONTENTS

Chapter	Page
Glossary	vi
8 Introduction	1
8.1 Wave Propagation	2
8.1.1 Methodology	2
8.1.2 Offshore Wave Conditions	15
8.1.3 Nearshore Wave Conditions	21
8.2 Hydrodynamic Assessment	33
8.2.1 Methodology	33
8.2.2 Model Calibration	34
8.3 Dredging Dispersal Assessment	41
8.3.1 Dredging Operations	43
8.3.2 Modelling Software	45
8.3.3 Methodology	47
8.3.4 Model Results	51
8.4 Sediment Transport Modelling	69
8.4.1 Methodology	69
8.4.2 Results	76
8.5 Conclusions and Recommendations	84
8.5.1 Wave Propagation	84
8.5.2 Dredging Dispersal Assessment	84
8.5.3 Sediment Transport Modelling	85
References	86
Appendix A – Offshore Metocean Conditions: Joint Probability Tables	88
Appendix B – Offshore Metocean Conditions: Extreme Analysis Results	90
Appendix C – Nearshore Metocean Conditions: Density Diagram and Non-Exceedance Curves	92
C.1 Point A – NE Rosslare Port	92
C.2 Point B – N Rosslare Port	93
Appendix D – Nearshore Metocean Conditions: Extreme Conditions Diagrams	94
D.1 Point A – NE Rosslare Port	94
D.2 Point B – N Rosslare Port	95
Appendix E – Metocean Survey Report	96
Appendix F – Walkover Survey Report	97
F.1 Introduction	97
F.1.1 Applicable Standards and References	99
F.2 Methodology	99
F.3 Results	101
F.3.1 Overview	101
F.3.2 Eastern Area Location 1 Summary – Small Boat Harbour	104
F.3.3 Eastern Area Location 2 – Further Along Coast from Boat Harbour	111
F.3.4 Eastern Area Location 3	113

F.3.5	Eastern Area Location 1- Beach	115
F.3.6	Eastern Area Location 2 – Rosslare Europort Environs	120
F.3.7	Western Area Location 3 – Harbour Wall & Lighthouse	126

LIST OF TABLES

Table 8-1: Key Wave Model Parameters	8
Table 8-2: Main Sensitivity Cases Performed in the Calibration Process	12
Table 8-3: Offshore data points - Maximum and Average Hs and Tp (1979-2022)	19
Table 8-4: Extreme wave heights in offshore location (in metres)	19
Table 8-5 Nearshore Point Coordinates	24
Table 8-6: Extreme significant wave heights in metres for Point A – NE Rosslare ORE Port	32
Table 8-7: Extreme peak wave period in seconds for Point A – NE Rosslare ORE Port	32
Table 8-8: Extreme Wave Heights in metres in Point B – N Rosslare ORE Port	32
Table 8-9: Extreme peak wave period in seconds for Point B – N Rosslare ORE Port	32
Table 8-10 Key Flow Model Parameters	34
Table 8-11: Total estimated dredged fractions for considering all the dredging area	43
Table 8-12: Sediment material considered for Stage 1	44
Table 8-13: Sediment Material considered for Stage 2	44
Table 8-14: Sediment Material considered for Stage 3	45
Table 8-15: Duration of dredge cycle components	48
Table 8-16: Determination settling velocity coefficients b and n determined based on drag coefficient K	50
Table 8-17 Model input sediment properties for dredging and disposal operations	50
Table 8-18: Spilling rates for both Dredging and disposal activities at each stage.	51
Table 8-19 Point locations for the extracted numerical results.	51
Table 8-20: Maximum total Suspended Sediment Concentration SSC for the extracted numerical results (Perimeter Bunds Stage)	55
Table 8-21: Maximum total Suspended Sediment Concentration SSC for the extracted numerical results (Stage 2)	58
Table 8-22: Maximum total Suspended Sediment Concentration SSC for the extracted numerical results (Stage 3)	61
Table 8-23: Total bed thickness change for the extracted numerical results (Perimeter Bunds Stage)	63
Table 8-24: Total bed thickness change for the extracted numerical results (Stage 2)	66
Table 8-25: Total bed thickness change for the extracted numerical results (Stage 3)	68
Table 8-26: Key Model Parameters for Sediment transport modelling	72
Table 8-27: Bed level Change throughout the modelled period of January 2022 for both Current and Proposed Development Layout	83

LIST OF FIGURES

Figure 8-1: Bathymetry used within the Model Boundaries	4
Figure 8-2: Wind Data Points Location	5
Figure 8-3: Wind Rose for ERA 5 Point (52.25, -6.25)	5
Figure 8-4: Scatter Plot Wind Speed vs Wind Direction for ERA 5 Point (52.25, -6.25)	6
Figure 8-5: Wave Data Points Location	7
Figure 8-6: Model mesh including Proposed Development	7
Figure 8-7: MIKE 21SW Boundary Conditions	9
Figure 8-8: Measurement Buoys Location (Techworks Marine, 2024)	10
Figure 8-9: Hs Time Series for WB001 (Techworks Marine, 2024)	12
Figure 8-10: Comparison of Measured Hs (WB001) and Simulated Hs (Source: MIKE21 Time Series Comparator)	13
Figure 8-11: Modelled Hs vs Observed Hs (WB001) Plot	13
Figure 8-12: Wave Rose in WB001 location (modelled vs observed)	14

Figure 8-13: Scatter Plot H_s vs T_p in WB001 location (modelled vs observed)	14
Figure 8-14: Offshore wave data points used as input data to obtain wave conditions in the Proposed Development by using MIKE21 SW model	15
Figure 8-15: Wave Roses - Offshore Data Points (1979-2022)	16
Figure 8-16: Peak period (T_p) rose diagrams - Offshore Data Points (1979-2022)	17
Figure 8-17: Scatter plot H_s vs T_p with probability density - offshore data points (1979-2022)	18
Figure 8-18: Joint probability table H_s vs T_p - Offshore data points (1979-2022)	19
Figure 8-19: Location of the nearshore points of interest (Extracted from Google Earth)	25
Figure 8-20: Point A – NE Rosslare Port – significant wave height (H_s) and peak period (T_p) rose diagrams (2002-2022)	26
Figure 8-21: Significant wave height and mean wave direction during a south-westerly wave event to illustrate the nature of wave diffraction in Rosslare Port regional area	27
Figure 8-22: Point A – NE Rosslare Port – Scatter Plots (H_s vs Dir, left) (H_s vs T_p , right) (2002-2022)	27
Figure 8-23: Point A – NE Rosslare Port – Joint probability table (H_s vs Dir) (2002-2022)	28
Figure 8-24: Point A – NE Rosslare Port – Joint probability table (H_s vs T_p) (2002-2022)	28
Figure 8-25: Point B – N Rosslare Port - Wave Rose and Peak Period Rose (2002-2022)	29
Figure 8-26: Point B – N Rosslare Port – Scatter Plots (H_s vs Dir, left) (H_s vs T_p , right) (2002-2022)	29
Figure 8-27: Point B – N Rosslare Port – Joint probability table (H_s vs Dir) (2002-2022)	30
Figure 8-28: Point B – N Rosslare Port – Joint probability table (H_s vs T_p) (2002-2022)	31
Figure 8-29: Measurement Buoys Location	35
Figure 8-30: Comparison of Measured Depth-Average Current Speed (WB001) and Simulated Depth-Average Current Speed (Source: MIKE21 Time Series Comparator)	36
Figure 8-31: Comparison of Measured Depth-Average Current Direction (WB001) and Simulated Depth-Average Current Direction (Source: MIKE21 Time Series Comparator)	37
Figure 8-32: Comparison of Measured Depth-Average Current Speed (WB002) and Simulated Depth-Average Current Speed (Source: MIKE21 Time Series Comparator)	38
Figure 8-33: Comparison of Measured Depth-Average Current Direction (WB002) and Simulated Depth-Average Current Direction (Source: MIKE21 Time Series Comparator)	39
Figure 8-34: Comparison of Measured Water Level (ODM) and Simulated Surface Elevation (Source: MIKE21 Time Series Comparator)	40
Figure 8-35: Preliminary Indicative Construction Sequence considering dredging and reclamation area	42
Figure 8-36: Marine Borehole locations within the dredging area	43
Figure 8-37: Model Mesh	48
Figure 8-38: Dredging and disposal locations considered for the sediment dispersal	49
Figure 8-39: Location of the extracted results points.	52
Figure 8-40: Maximum total Suspended Sediment Concentration (SSC) from the 3-month disposal simulation (Perimeter Bunds Stage)	53
Figure 8-41: Close-up view of the port area showing the results of the maximum total Suspended Sediment Concentration (SSC) from the 3-month disposal simulation (Perimeter Bunds Stage)	54
Figure 8-42: Average total Suspended Sediment Concentration (SSC) from the 3-month disposal simulation (Perimeter Bunds Stage)	54
Figure 8-43: Maximum total Suspended Sediment Concentration (SSC) from the 2-month dredging and disposal simulation (Stage 2)	56
Figure 8-44: Close-up view of the port area showing the results of the maximum total Suspended Sediment Concentration (SSC) from the 2-month dredging and disposal simulation (Stage 2)	56
Figure 8-45: Average total Suspended Sediment Concentration (SSC) from the 2-month dredging and disposal simulation (Stage 2)	57
Figure 8-46: Maximum total Suspended Sediment Concentration (SSC) from the 8-month dredging and disposal simulation (Stage 3)	59

Figure 8-47: Close-up view of the port area showing the results of the maximum total Suspended Sediment Concentration (SSC) from the 8-month dredging and disposal simulation (Stage 3)	59
Figure 8-48: Average total Suspended Sediment Concentration (SSC) from the 8-month dredging and disposal simulation (Stage 3)	60
Figure 8-49: Maximum Bed thickness change from the 3-month disposal simulation (Perimeter Bunds Stage)	62
Figure 8-50: Close-up view of the port area showing the results of the maximum bed thickness change from the 3-month disposal simulation (Perimeter Bunds Stage)	62
Figure 8-51: Average bed thickness change from the 3-month disposal simulation (Perimeter Bunds Stage)	63
Figure 8-52: Maximum Bed thickness change from the 2-month dredging and disposal simulation (Stage 2)	64
Figure 8-53: Close-up view of the port area showing the results of the maximum bed thickness change from the 2-month dredging and disposal simulation (Stage 2)	65
Figure 8-54: Average bed thickness change from the 2-month dredging and disposal simulation (Stage 2)	65
Figure 8-55: Maximum Bed thickness change from the 8-month dredging and disposal simulation (Stage 3)	67
Figure 8-56: Close-up view of the port area showing the results of the maximum bed thickness change from the 8-month dredging and disposal simulation (Stage 3)	67
Figure 8-57: Average bed thickness change from the 8-month dredging and disposal simulation (Stage 3)	68
Figure 8-58: Model Boundaries	71
Figure 8-59: Coastal seabed substrate of the Rosslare Europort adjacent area, EMODnet (2020)	73
Figure 8-60: Coastal seabed substrate of the Rosslare Europort adjacent area, INFOMAR (2020, 2023)	75
Figure 8-61: Statistical Mean of Bed Level Change for current layout (top) and Proposed Development layout (bottom)	77
Figure 8-62: Statistical Maximum of Bed Level Change for current layout (top) and Proposed Development layout	78
Figure 8-63: Statistical Mean of Total Load for current port layout (top) and Proposed Development layout (bottom)	79
Figure 8-64: Statistical Maximum of Total Load for current port layout (top) and Proposed Development layout (bottom)	80
Figure 8-65: Statistical Mean of Suspended Sediment Concentration (SSC) for current port layout (top) and Proposed Development layout (bottom)	81
Figure 8-66: Statistical Maximum of Suspended Sediment Concentration (SSC) for current port layout (top) and Proposed Development layout (bottom)	82
Figure A-1: Joint probability table H_s vs wave direction - offshore data points (1979-2022)	88
Figure A-2: Joint probability table H_s vs T_p - offshore data points (1979-2022)	88
Figure A-3: Joint probability table T_p vs wave direction - offshore data points (1979-2022)	89
Figure B-1: Return Period Analysis for each point	90
Figure B-2: Density Diagrams and Residual Quantile Plots for each point	91
Figure C-1: Density Diagram Point A	92
Figure C-2: Non-exceedance probability Point A	92
Figure C-3: Density Diagram Point B	93
Figure C-4: Non-Exceedance Probability Point B	93
Figure D-1: Return Period analysis, Density plot and Residual quantile and probability for point A	94
Figure D-2: Return Period analysis, Density plot and Residual quantile and probability for point B	95

GLOSSARY

AIS	Automatic Identification System
CD	Chart Datum
ECMWF	European Centre for Medium-Range Weather Forecasts
EMODnet	European Marine Observation and Data Network
Hs	Significant Wave Height
ICWWS	Irish Coastal Wave and Water Level Modelling Study
INFOMAR	Integrated Mapping for the Sustainable Development of Ireland's Marine Resource
IPCC	Intergovernmental Panel on Climate Change
LAT	Lowest Astronomical Tide
ORE	Offshore Renewable Energy
Tp	Peak Period

8 COASTAL PROCESSES

8.1 INTRODUCTION

This technical appendix has been prepared to accompany Volume 2: Chapter 8: Coastal Processes of the Rosslare Europort ORE Hub (hereafter the 'Proposed Development') Environmental Impact Assessment Report (EIAR).

This technical appendix details the numerical modelling undertaken to inform the assessment of impacts from the Proposed Development on Coastal Processes receptors (this report and appendices A-D) and includes reports detailing the project-specific metocean (Appendix E) and walkover survey (Appendix F) data gathering completed.

Numerical modelling undertaken for the Proposed Development described in this report include:

- Wave Propagation Modelling (Section 8.1)
- Hydrodynamic Modelling (Section 8.2)
- Dredging Dispersal Modelling (Section 8.3)
- Sediment Transport Modelling (Section 8.4)

This report was prepared by Diogo Neves (PhD) and Laura Ecenarro Díaz-Tejeiro.

Diogo is a graduate in Geophysics – Meteorology and Oceanography with a master's degree in physical Oceanography and a PhD in Civil Engineering. He worked for 10 years in the Ports and Harbours division at the National Laboratory of Civil Engineering in Lisbon (LNEC) (PT) regarding wave propagation and wave-structure interaction studies. He fulfilled the position of geophysical data processor and data scientist at Bibby Hydromap Ltd. (UK) for 2 years. He was also the Head of the Sea Technologies unit for the Institute of Science and innovation in Mechanical and Industrial Engineering (INEGI) at Oporto (PT) for 2 years. He was involved in several types of projects involving Coastal/Offshore studies (Wave propagation, Sediment/constituent transport, Coastal Protection) and the Development of new marine technology studies (Marine devices, Wave energy, Floating platforms, Moorings, Computational Fluid Dynamics (CFD)). He has more than 60 publications in scientific journals and conferences. His skills range between coastal/offshore engineering, Hydrodynamics, CFD, and data analysis.

Laura is a Senior Engineer with more than 7 years of experience in international projects mainly related to ports, coastal infrastructure and marine terminals. She has wide experience working in multidisciplinary projects within the Oil and Gas (O&G) industry, being part of the team responsible for the design of marine facilities and the definition of port operations. Her recent participation in renewable energy projects includes working in the design of NH₃/H₂/CO₂ import and export berths as well as collaborating in Offshore Wind Projects. Her academic background provides an accurate knowledge of coastal dynamics, wave climate, numerical modelling (wave generation, propagation and nearshore interaction) and overall coastal management.

The report has been checked by Mohammed Alaa Almoghayer (PhD), senior offshore project manager, and reviewed by Shauna Creane (BSc. (Hons) Geoscience, PhD in Civil and Environmental Engineering), senior marine geoscientist and Joey O'Connor (BSc. (Hons) Marine Science, MSc. Engineering in the Coastal Environment).

Independent peer review of this Technical Appendix has been undertaken by Partrac Ltd. Partrac provide the owners and developers of complex engineering environmental projects in challenging marine environments with high-quality, science-led metocean and geo-surveys. The Partrac team comprises PhD grade specialists, with expertise in advanced metocean analysis, coastal processes, coastal modelling, geomorphology and flow-sediment-structure interactions and deliver desktop projects and studies for major blue-chip clients which include metocean design criteria, seabed morphodynamic assessments, scour and seabed mobility studies, physical marine environment chapters for EIA and site characterisation studies.

8.2 WAVE PROPAGATION

This section presents the analysis performed to evaluate the wave propagation phenomena in the Proposed Development. This section is structured as follows:

- Presentation of the methodology used in the wave propagation study
- Analysis of the offshore metocean conditions in the Irish Sea, used as an input in the wave propagation analysis presented in this document
- Analysis of nearshore metocean conditions obtained from the wave propagation analysis performed with MIKE21 SW (Spectral Wave model)

8.2.1 METHODOLOGY

8.2.1.1 GENERAL

This section summarises the methodology and key assumptions used in the numerical model for transforming offshore wave conditions to the vicinity of Rosslare Europort. For further information about MIKE21 SW model, refer to the software manual available in DHI website (DHI Group, 2023).

8.2.1.2 NUMERICAL MODEL

The wave propagation analysis is performed with the model MIKE 21 SW (Spectral Wave), which is a new generation spectral wind-wave model based on unstructured meshes. The model simulates the growth, decay and transformation of wind-generated waves and swell waves in offshore and coastal areas (DHI Group, 2023a). MIKE 21 SW includes the following physical phenomena:

- Wave growth by action of wind
- Non-linear wave-wave interaction
- Dissipation due to white-capping, bottom friction and depth-induced wave breaking
- Refraction and shoaling due to depth variations
- Wave-current interaction

- Effect of time-varying water depth

MIKE 21 SW is employed to evaluate wave conditions in both historical analysis (hindcast) and predictive modelling (forecast) modes, particularly focusing on offshore and coastal regions. Its primary use lies in the engineering design of offshore platforms, coastal infrastructure, and port facilities, where precise evaluation of wave-induced loads is critical to guarantee the safety and cost-effectiveness of these structures.

8.2.1.3 INPUT DATA

BATHYMETRY

Offshore regional bathymetry data for the Irish Sea was derived from the European Marine Observation and Data Network (EMODnet, 2023) data, which has a resolution of $1/16^\circ \times 1/16^\circ$ arc minutes (circa. 115 m grid). In the Irish sector of the Irish Sea, this dataset was combined with higher resolution bathymetry data, ranging from 2 to 10 m, collected by the Integrated Mapping for the Sustainable Development of Ireland's Marine Resource (INFOMAR) programme. The data was obtained through the INFOMAR Interactive Web Data Delivery System (IWDDS) (INFOMAR, 2023). INFOMAR data is levelled to the lowest astronomical tide (LAT), according to a Vertical Offshore Reference Frame (VORF) datum. For model input, the EMODnet data was kept referenced to Mean Sea Level (MSL) whereas INFOMAR data was converted from LAT to Malin ordnance datum (OD).

The Proposed Development was defined based on site-specific survey data available at this stage (GDG, 2024). These geotechnical and geophysical surveys were undertaken in 2022 and 2023 (Table 3-2). The bathymetry data has a resolution of 5 m grid and has been converted to Malin ordnance datum (OD) for modelling purposes. Additionally, to represent the future port development, a preliminary approximation of the proposed dredging areas has been included.

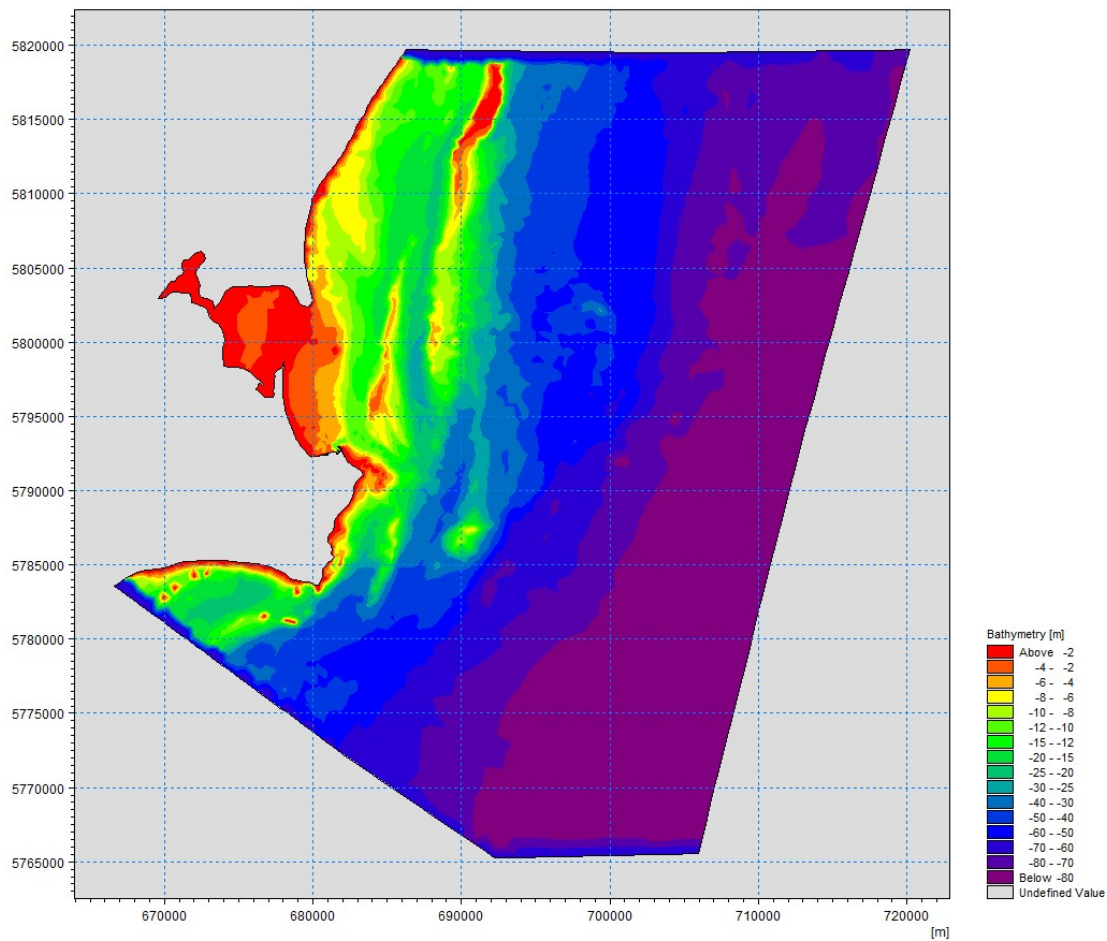


Figure 8-1: Bathymetry used within the Model Boundaries

TIDAL LEVELS

The tidal level is defined as a parameter that varies in time and space to represent the water level variability within the model domain. A grid file of tidal level values has been defined for the model domain via MIKE 21 Tide Prediction Tool in conjunction with the Global Tide Model included in the MIKE 21 package.

The Global Tide Model, developed by DTU Space (DTU10), is available on a $0.125^\circ \times 0.125^\circ$ resolution grid for the major 10 constituents in the tidal spectra. The model utilised the latest 17 years' multi-mission measurements from TOPEX/Poseidon (phase A and phase B), Jason-1 (phase A and phase B) and Jason-2 satellite altimetry for sea level residuals analysis. Based on these measurements, harmonic coefficients have been calculated. The provided constituents consider the semidiurnal M2, S2, K2, N2, the diurnal S1, K1, O1, P1, Q1, and the shallow water constituent M4 (DHI Group, 2023b).

WIND

Wind data was obtained from ERA5 dataset (CDS, 2023), the fifth-generation European Centre for Medium-Range Weather Forecasts (ECMWF) reanalysis for the global climate and weather over the previous eight decades. This dataset offers hourly estimates for diverse atmospheric, oceanographic, and land-surface parameters. The wind forcing component was integrated into the model as a grid

file to capture varied wind conditions across the model mesh. Wind characteristics were defined by their respective components (u and v) combined with atmospheric pressure. Figure 8-2 presents the wind data point locations selected from ERA5 dataset.



Figure 8-2: Wind Data Points Location

As shown in Figure 8-3 and Figure 8-4, wind conditions near the Proposed Development are driven by winds coming from the WSW-SSW with predominant wind speeds between 5 and 12 m/s. The maximum wind speed registered in the point of interest is 25 m/s whereas the average wind speed is approximately 7.2 m/s.

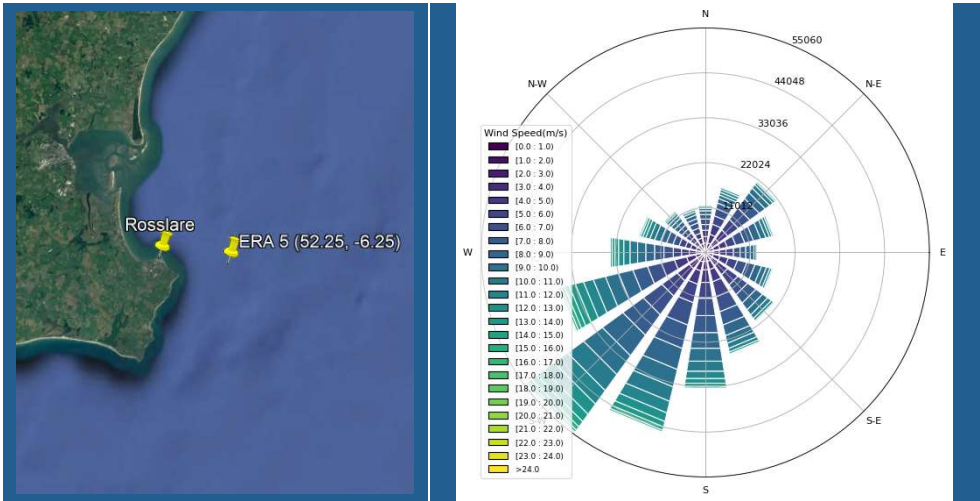


Figure 8-3: Wind Rose for ERA 5 Point (52.25, -6.25)

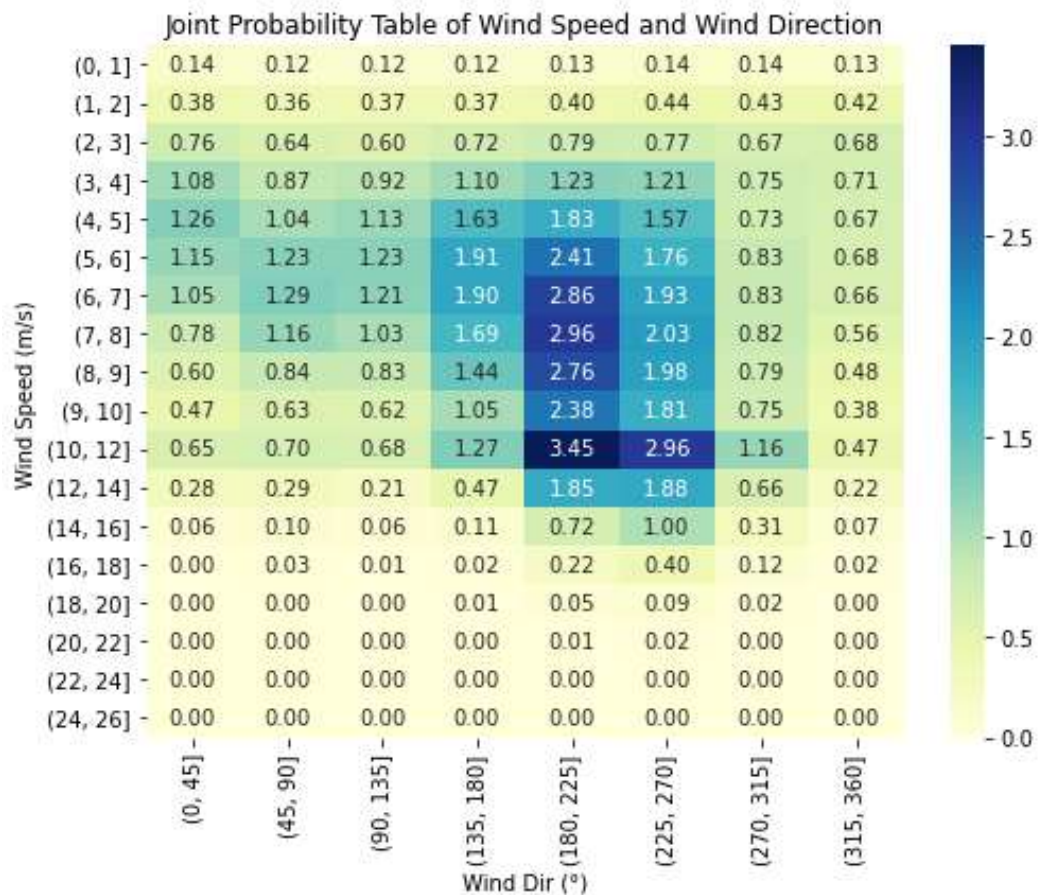


Figure 8-4: Scatter Plot Wind Speed vs Wind Direction for ERA 5 Point (52.25, -6.25)

WAVES

Wave boundary conditions were defined based on the information provided in ERA5 dataset. Four data points were utilised to define conditions in the different model boundaries (Figure 8-5). Hourly data were provided for the following wave parameters: Significant wave height H_s , peak wave period T_p , mean wave direction and the directional spreading index n for both wind and swell seas. Further information about the definition of the boundary conditions is provided in section 8.1.1.4 Boundary Conditions.

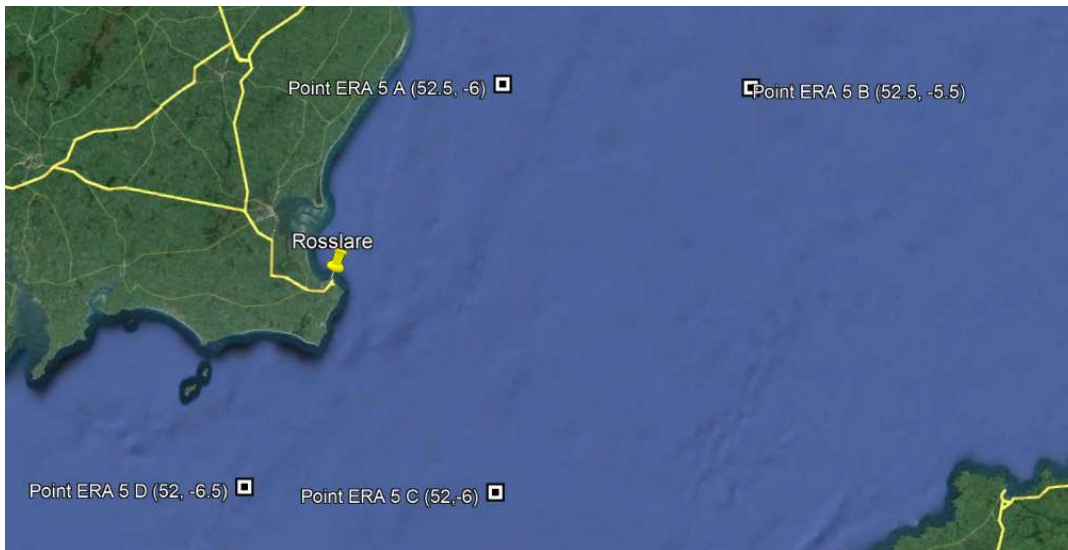


Figure 8-5: Wave Data Points Location

8.2.1.4 MODEL SET UP

MESH

A triangular mesh was utilised in the numerical models, covering an approximate area of 2,400 km². The mesh resolutions vary according to the desired precision level for the simulations: a mesh resolution of 2 km is set in offshore regions where water depth exceeds 75mMSL, while in shallower areas near to the Rosslare Europort, mesh resolution increases to approximately 20 m.

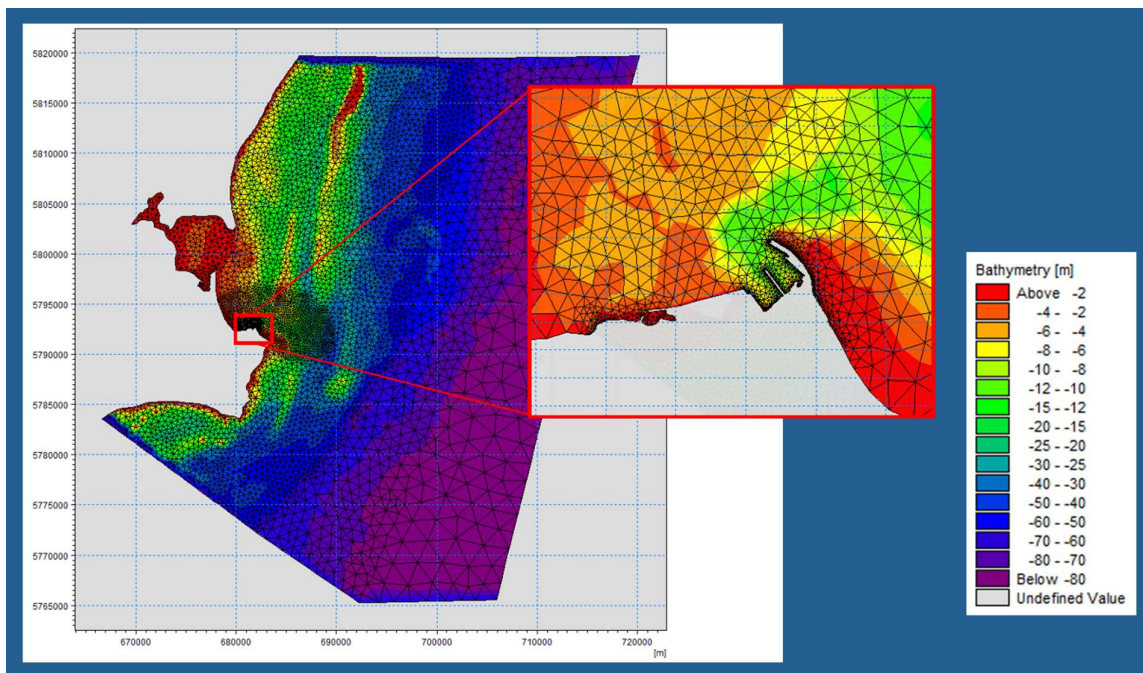


Figure 8-6: Model mesh including Proposed Development

KEY PARAMETERS

The key model parameters are outlined in the table below. These parameters were determined following the model calibration using wave data obtained in the metocean survey performed within this project. Detailed information about the calibration process is provided in section 8.1.1.4 Model Calibration.

Table 8-1: Key Wave Model Parameters

Model Parameter	Description
Time Step	3,600 s ⁽¹⁾
Simulation Period	2002 – 2022
Spectral Formulation	Directionally decoupled parametric formulation ⁽²⁾ . 18 directions considered.
Time Formulation	Quasi-stationary formulation ⁽³⁾ Geographical space discretization: Low order, fast logarithm
Wave Breaking ⁽⁴⁾	Gamma = 1 Alpha=1 Wave Steepness = 5
Bottom Friction ⁽⁴⁾	No bottom friction

Notes:

- 1) Aligned with input data time-step and considered sufficient to represent wave propagation phenomena from offshore to nearshore
- 2) For the assessment of wave conditions in nearshore and coastal areas which most often involves transformation of known offshore wave statistics (derived from e.g. measurement, regional/global models, remote sensing data, etc.) the directionally decoupled parametric formulation is typically used (DHI Group, 2023a)
- 3) Selected as wind forcing using the directionally decoupled parametric formulation is only possible for the quasi-stationary time formulation (DHI Group, 2023a)
- 4) These values have been fixed after the model calibration as presented in section 8.1.1.4 Model Calibration.

BOUNDARY CONDITIONS

Various boundary conditions were set considering ERA5 data available near the respective mesh limit, as illustrated in Figure 8-7. Wave conditions along the different defined mesh boundaries remained spatially constant but varied temporally. These conditions are characterized by the significant wave height (H_s), peak wave period (T_p), directional spreading and wave directions for both swell and wind-wave seas.

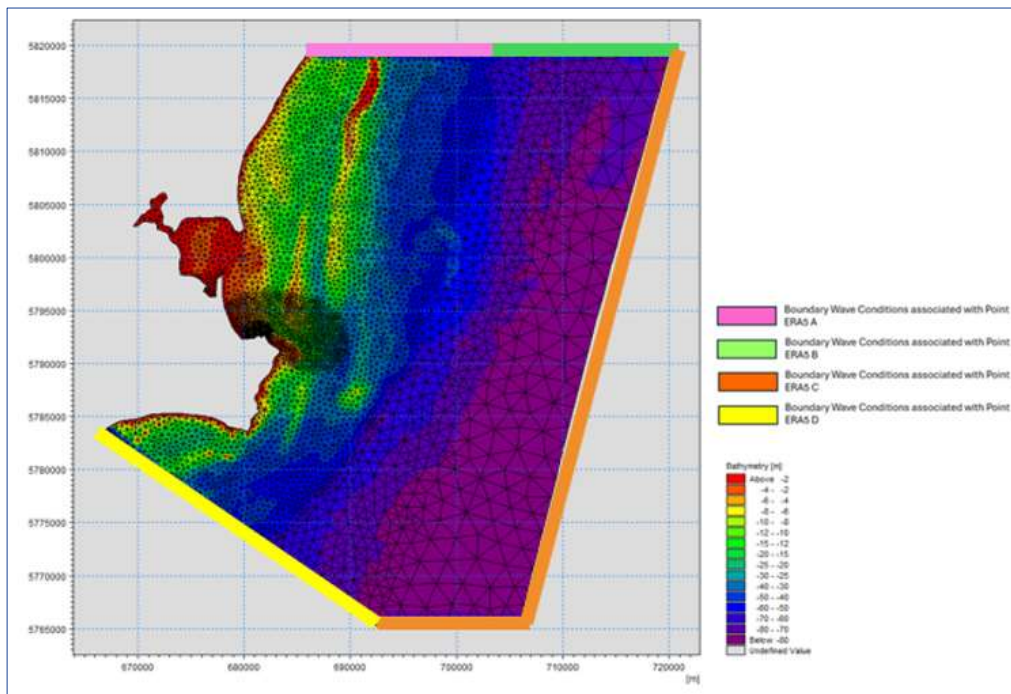


Figure 8-7: MIKE 21SW Boundary Conditions

MODEL CALIBRATION

A metocean survey has been undertaken as part of the Proposed Development to obtain current and wave data to calibrate the hydrodynamic and wave studies performed in this project stage. Two measurement devices were installed at the North and North-East of Rosslare port as indicated in Figure 8-8.

The calibration of the spectral wave model has been based on the wave data obtained from the northern buoy WB001 (indicated in green in Figure 8-8). This dataset was selected as it provides reliable measurements for the study area, while wave conditions recorded at buoy WB002 (indicated in red) were not used due to potential interference from wave reflections against the existing port structures. It should be noted that publicly available wave data for this nearshore region is limited and primarily derived from numerical modelling. The metocean measurements used in this study were specifically designed to validate the numerical modelling within the EIAR, ensuring their suitability for this purpose.

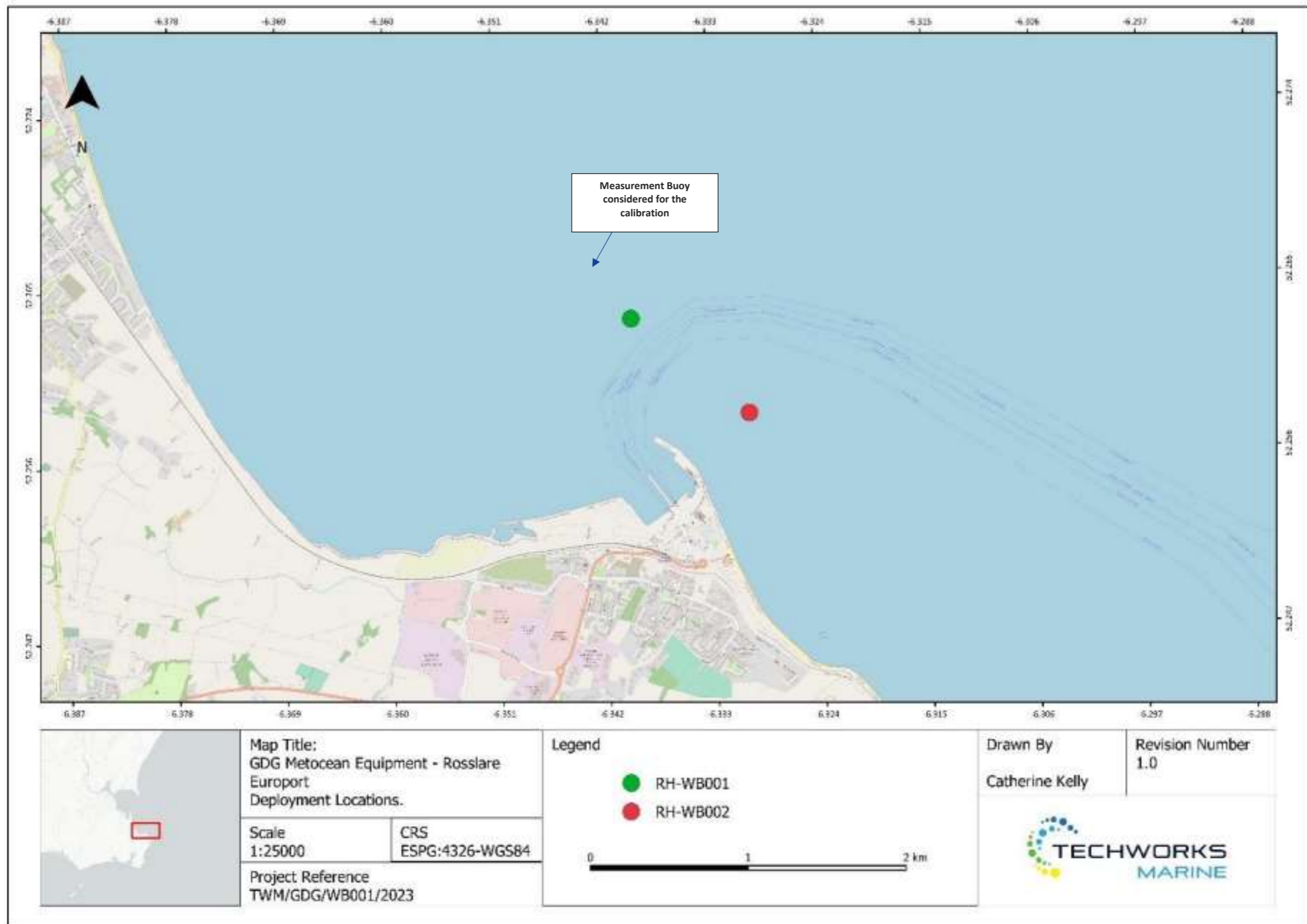


Figure 8-8: Measurement Buoys Location (Techworks Marine, 2024)

As shown in Figure 8-9, there is a data gap in WB001 due to maintenance activities in the measurement device as well as navigation operations within the access channel. Due to this, the survey campaign was extended by an additional week beyond the previously defined completion date (i.e. to March 14th). For further information refer to the metocean survey report provided in Appendix E.

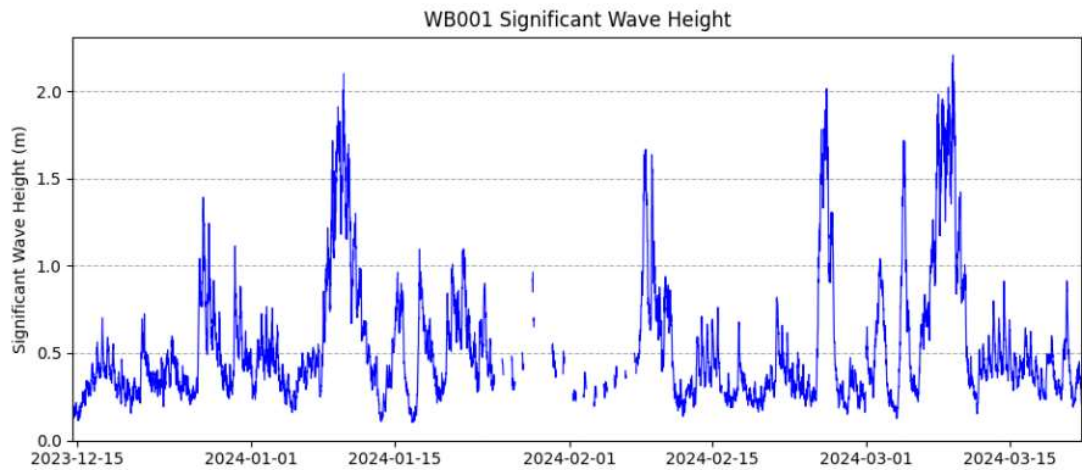


Figure 8-9: Hs Time Series for WB001 (Techworks Marine, 2024)

Table 8-2 presents the key sensitivity cases performed for the model calibration. The number of wave directions applied was set to 18, as this was concluded to suffice the level of directional detail required in the spectral wave model.

Table 8-2: Main Sensitivity Cases Performed in the Calibration Process

Parameter	Base Case (Presented in rev00 report)	Sensitivity Case 1	Sensitivity Case 2	Sensitivity Case 3	Sensitivity Case 4
Time step (s)	3600	3600	3600	3600	3600
Gamma data	0.9	0.9	1	1	1
Alpha	1	1	1	1	1
Wave_steepness	5	5	5	5	5
Number of directions	16	16	18	24	32
Bottom friction	fw=0.005	fw=0.003	N/A	N/A	N/A
Mean Error	0.078	0.062	0.039	0.053	0.070
Mean Absolute Error	0.152	0.149	0.151	0.155	0.166
Root Mean Square Error	0.201	0.197	0.206	0.210	0.225
Std. dev of Residuals	0.185	0.187	0.202	0.203	0.213
Coefficient of Determination	0.861	0.859	0.844	0.843	0.831
Coefficient of Efficiency	0.836	0.843	0.828	0.821	0.795

Parameter	Base Case (Presented in rev00 report)	Sensitivity Case 1	Sensitivity Case 2	Sensitivity Case 3	Sensitivity Case 4
Index of Agreement	0.953	0.956	0.956	0.955	0.949
Max Hs value model	1.760	1.791	1.925	1.928	1.958
Max Hs value survey	2.207	2.207	2.207	2.207	2.207

Figure 8-10 and Figure 8-11 illustrate the comparison between the significant wave height (H_s) time series derived from both the wave buoy WB001 and the MIKE21 SW model, spanning the period from December 2023 to March 2024. The comparison reveals that the wave model values generally align with the trends observed in the buoy data, showing good agreement with both the average and peak values.

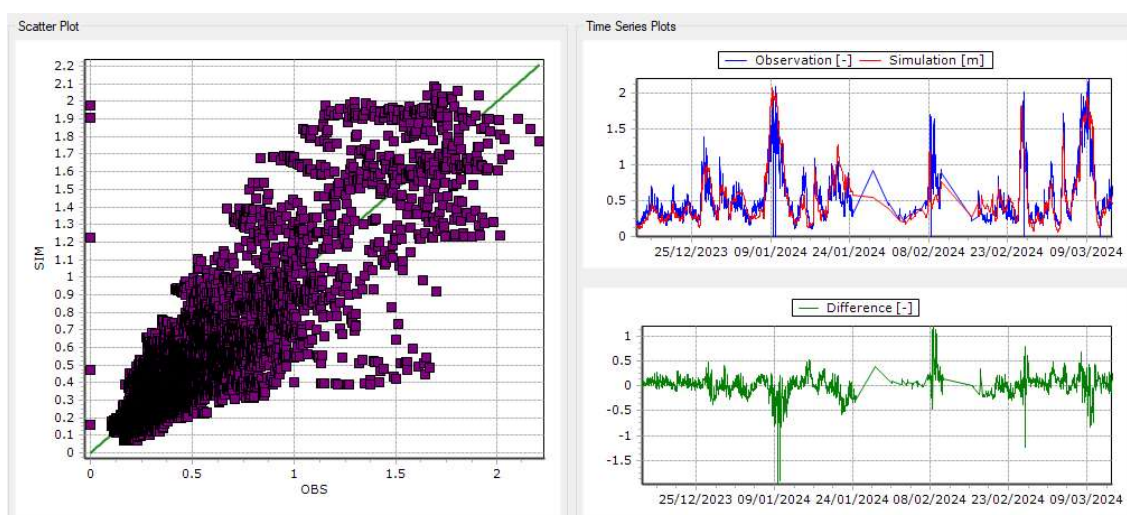


Figure 8-10: Comparison of Measured H_s (WB001) and Simulated H_s (Source: MIKE21 Time Series Comparator)

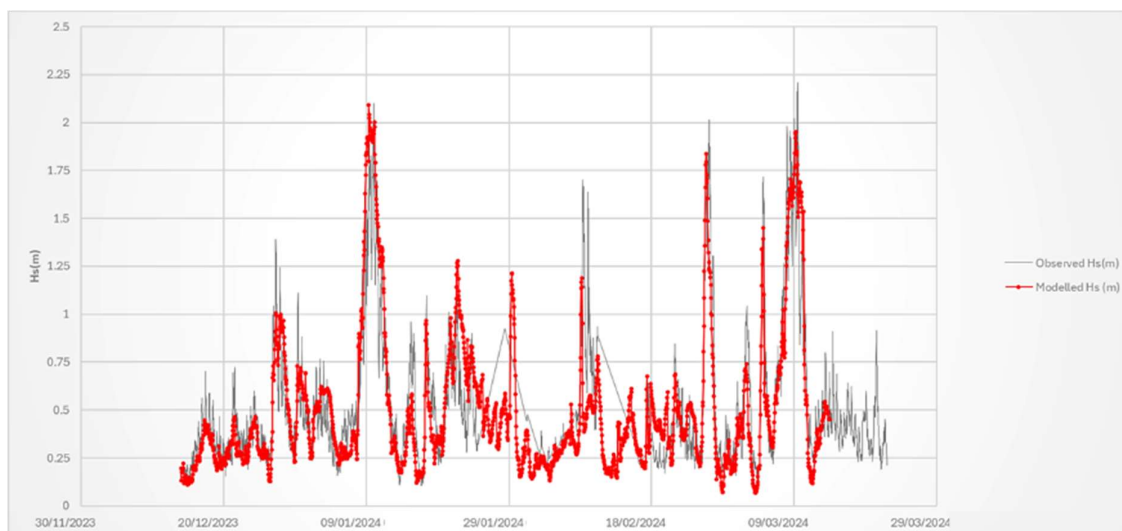


Figure 8-11: Modelled H_s vs Observed H_s (WB001) Plot

The spectral model shows the agreement in terms of wave directionality as shown in Figure 8-12. However, it tends to overestimate the peak periods in some cases, as shown in Figure 8-13.

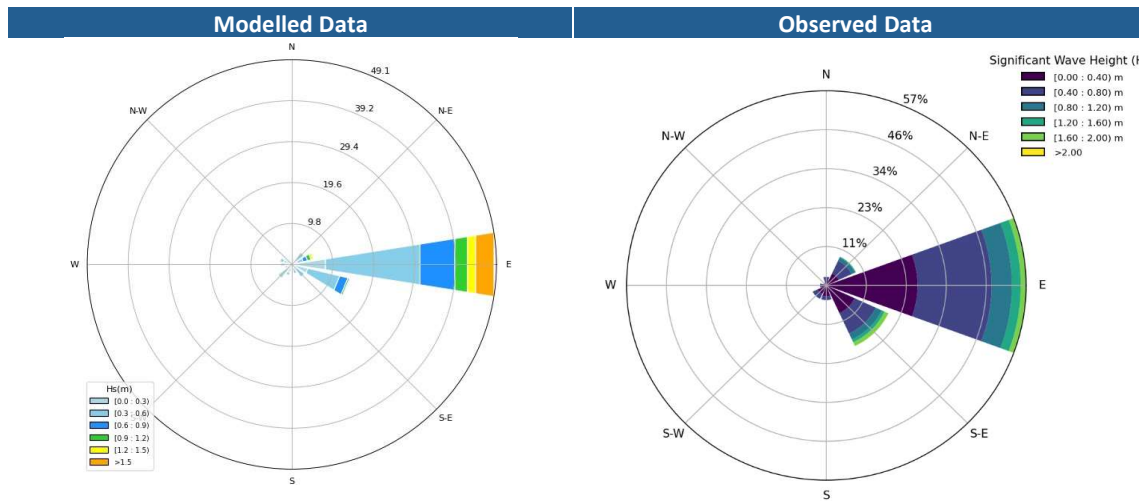


Figure 8-12: Wave Rose in WB001 location (modelled vs observed)

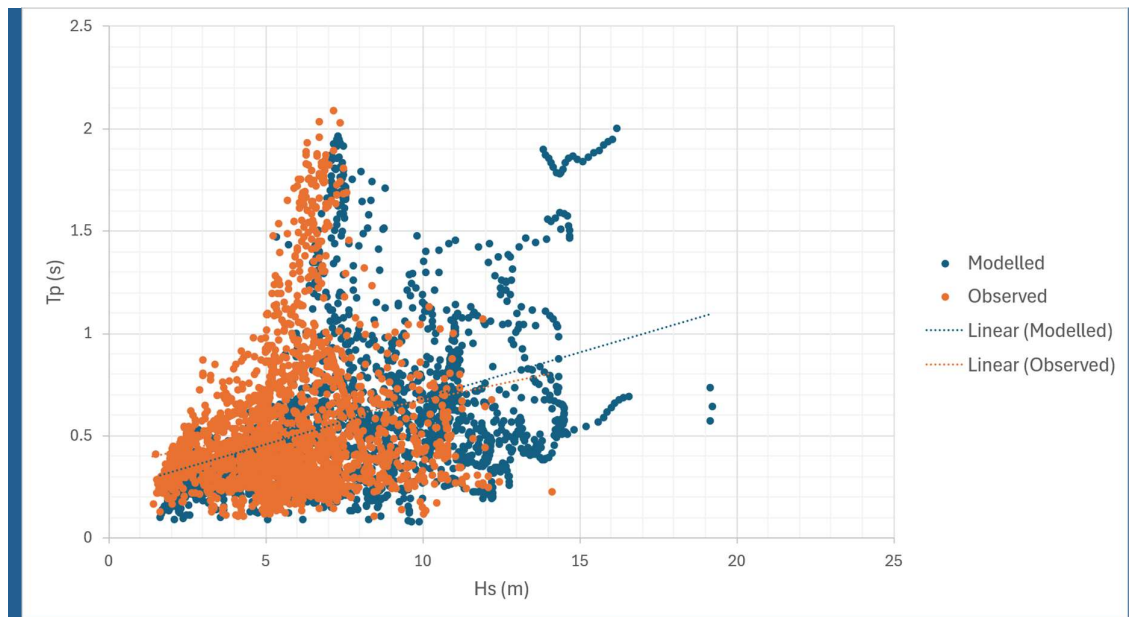


Figure 8-13: Scatter Plot Hs vs Tp in WB001 location (modelled vs observed)

Based on the analysis, it was concluded that although there are some discrepancies between the measured data and the simulation results, the applied model effectively generates wave conditions that accurately represent near-shore real wave conditions.

8.2.1.5 RUN MATRIX

To establish a comprehensive dataset of wave conditions, 21 years of hourly wave data, spanning from 2002 to 2022, were propagated from offshore to the area near the Proposed Development.

8.2.2 OFFSHORE WAVE CONDITIONS

8.2.2.1 GENERAL

This section presents a summary of the offshore metocean conditions obtained from ERA5 dataset (CDS, 2023) and used to define the boundary conditions to obtain wave conditions in the Proposed Development by using MIKE21 SW model.

8.2.2.2 WAVES

Offshore wave climate obtained from ERA5 dataset (CDS, 2023) is used as input data to obtain wave conditions in the Proposed Development by using MIKE21 SW model. Four different data points are used to define offshore wave climate in the Proposed Development as shown in Figure 8-14. Note that the period of time considered in the definition of offshore wave conditions is from 1979 to 2022.



Figure 8-14: Offshore wave data points used as input data to obtain wave conditions in the Proposed Development by using MIKE21 SW model

AVERAGE REGIME

Waves in the South area of the Irish Sea are predominantly driven by waves coming from the WSW and S sector with a low incidence of northern sea states as shown in Figure 8-15.

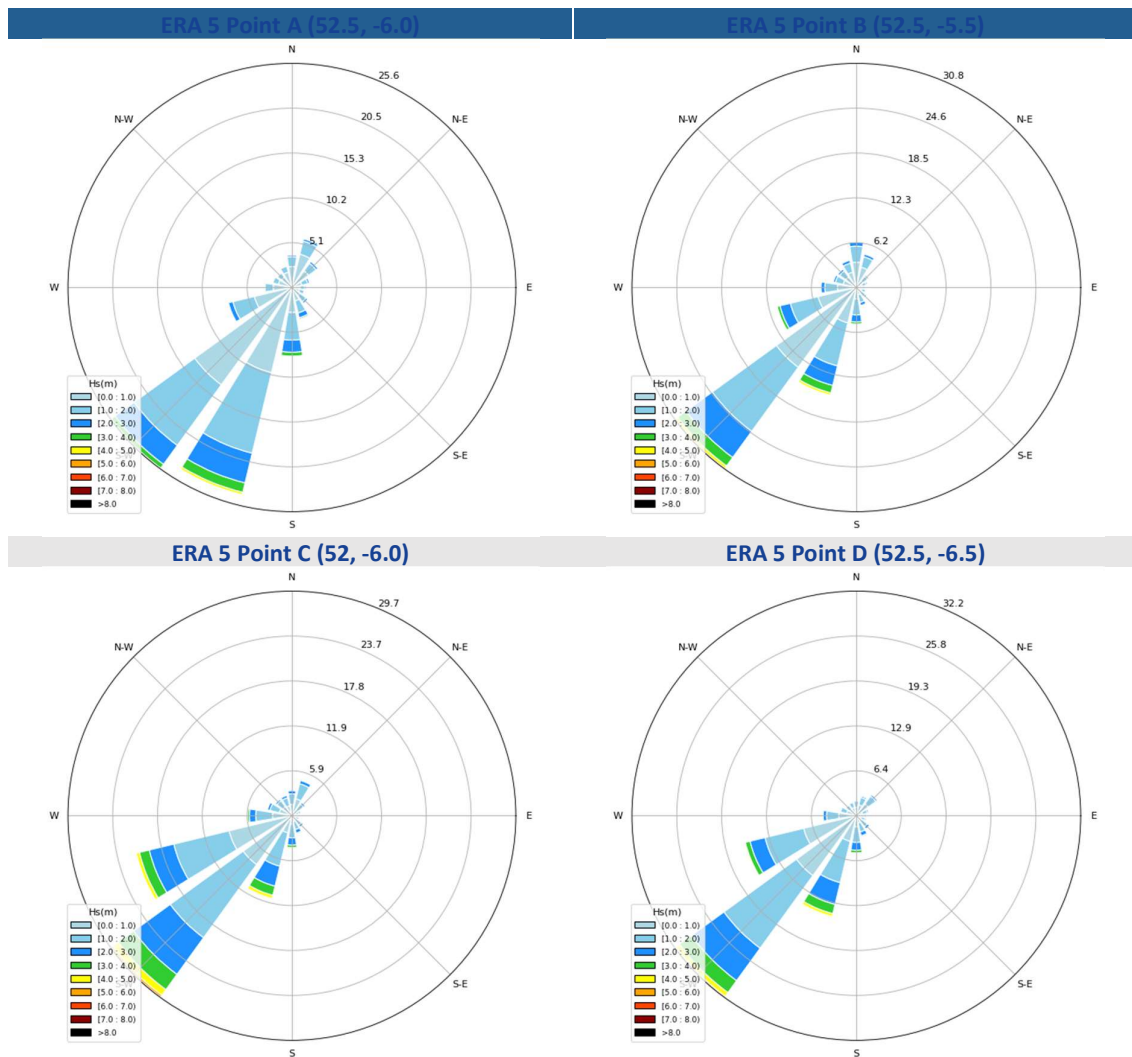


Figure 8-15: Wave Roses - Offshore Data Points (1979-2022)

As shown in Figure 8-16 SSE waves are associated with various wind-seas and swells ($T_p > 10$ s) whereas waves coming from the north are associated with lower wave periods, indicating they are predominantly caused by wind. The wave from northern directions has a higher incidence in the points located at higher latitudes (A & B).

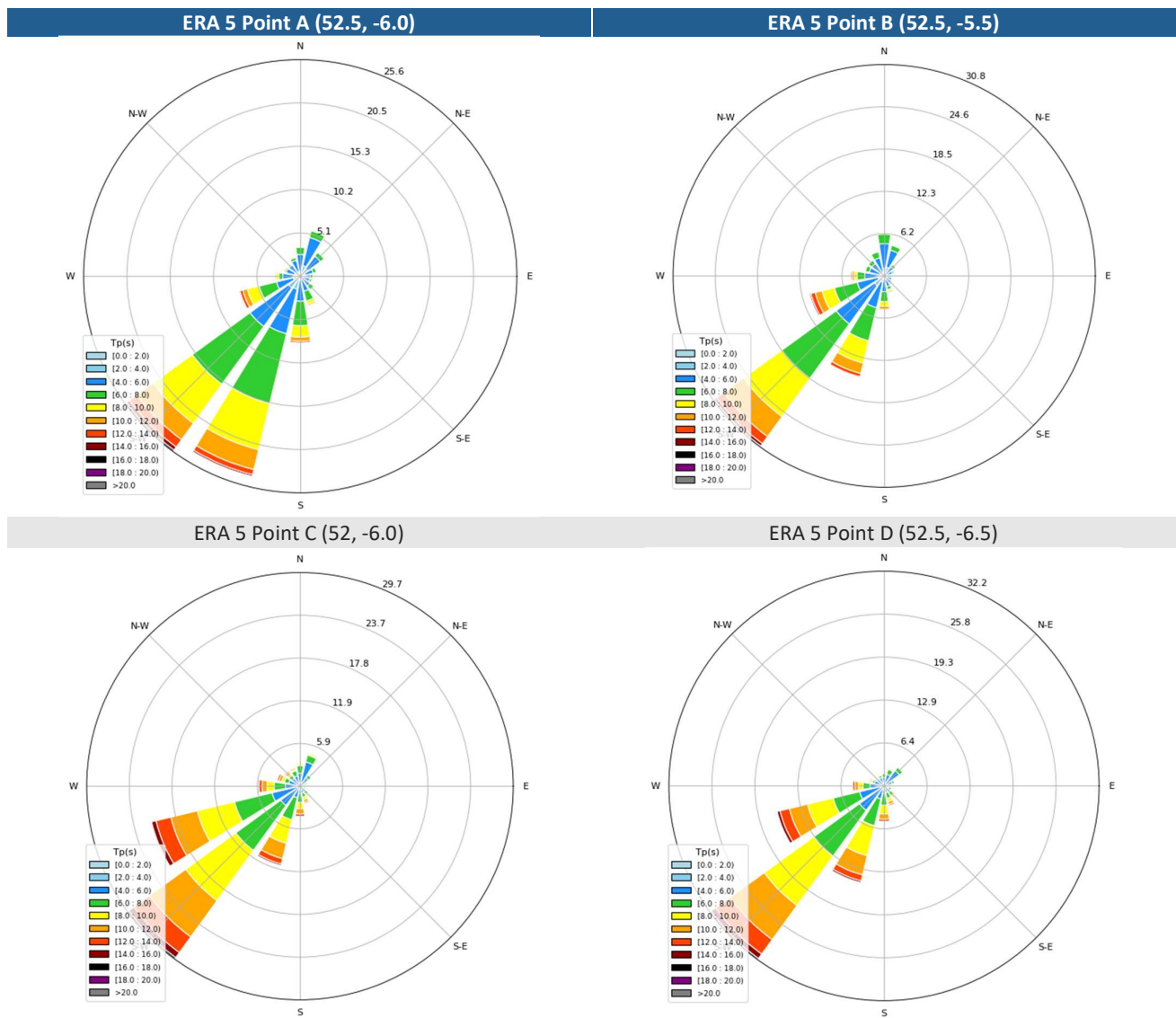


Figure 8-16: Peak period (T_p) rose diagrams - Offshore Data Points (1979-2022)

There is a noticeable reduction in the maximum significant wave height (H_s) values with the wave propagation towards the interior of the Irish Sea: in the limit between the Celtic Sea and the Irish Sea (points C & D) H_s reaches values close to 10 m whereas the maximum H_s in points A & B is close to 8 m as presented in Figure 8-17 and

ERA 5 Point A (52.5, -6.0)																		ERA 5 Point B (52.5, -5.5)																	
Joint Probability Table of Hs and Tp																		Joint Probability Table of Hs and Tp																	
Hs (m)	(0, 1]	20.30	11.35	6.24	3.19	2.70	1.30	0.54	0.11	0.00	0.00	0.00	45.73	(0, 1]	16.62	7.70	6.53	3.79	2.46	1.04	0.40	0.06	0.00	38.60											
	(1, 2]	16.47	12.64	6.62	2.57	0.40	0.07	0.01	0.00	0.00	0.00	0.00	38.79	(1, 2]	21.57	9.98	4.79	3.14	0.73	0.16	0.04	0.00	0.00	40.42											
	(2, 3]	0.42	6.67	3.01	1.33	0.27	0.03	0.01	0.00	0.00	0.00	0.00	11.75	(2, 3]	1.14	10.22	1.96	1.21	0.43	0.08	0.03	0.00	0.00	15.06											
	(3, 4]	0.00	0.94	1.50	0.45	0.07	0.01	0.00	0.00	0.00	0.00	0.00	2.97	(3, 4]	0.00	1.92	2.01	0.40	0.13	0.01	0.01	0.00	0.00	4.48											
	(4, 5]	0.00	0.01	0.45	0.16	0.03	0.00	0.00	0.00	0.00	0.00	0.00	0.65	(4, 5]	0.00	0.06	0.86	0.18	0.03	0.01	0.00	0.00	0.00	1.15											
	(5, 6]	0.00	0.00	0.04	0.05	0.01	0.00	0.00	0.00	0.00	0.00	0.00	0.10	(5, 6]	0.00	0.00	0.12	0.10	0.02	0.00	0.00	0.00	0.00	0.23											
	(6, 7]	0.00	0.00	0.00	0.01	0.00	0.00	0.00	0.00	0.00	0.00	0.00	0.01	(6, 7]	0.00	0.00	0.00	0.03	0.00	0.00	0.00	0.00	0.00	0.04											
	(7, 8]	0.00	0.00	0.00	0.00	0.00	0.00	0.00	0.00	0.00	0.00	0.00	0.00	(7, 8]	0.00	0.00	0.00	0.00	0.00	0.00	0.00	0.00	0.00	0.01											
	(8, 9]	0.00	0.00	0.00	0.00	0.00	0.00	0.00	0.00	0.00	0.00	0.00	0.00	(8, 9]	0.00	0.00	0.00	0.00	0.00	0.00	0.00	0.00	0.00	0.00											
	Total	37.19	31.62	17.86	7.75	3.48	1.42	0.57	0.11	0.00	0.00	0.00	100.00	Total	39.33	29.88	16.27	8.87	3.80	1.30	0.48	0.07	0.00	100.00											
		(4, 6]	(6, 8]	(8, 10]	(10, 12]	(12, 14]	(14, 16]	(16, 18]	(18, 20]	(20, 22]			(4, 6]	(6, 8]	(8, 10]	(10, 12]	(12, 14]	(14, 16]	(16, 18]	(18, 20]	(20, 22]														

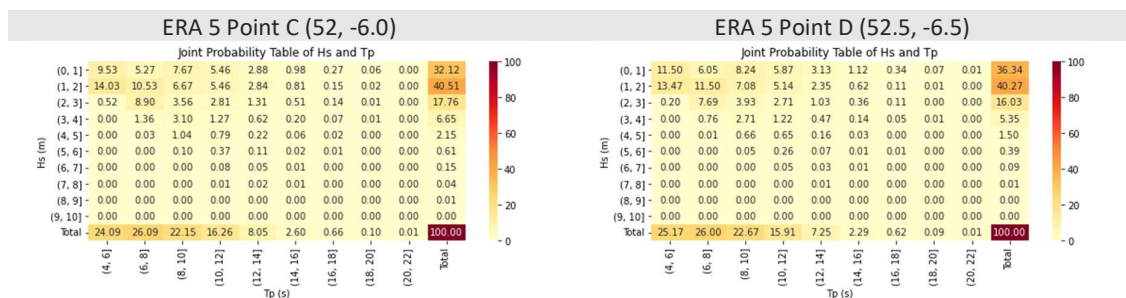


Figure 8-18. A similar phenomenon occurs with the peak wave period (T_p), with a higher percentage of high values in the data points at the entrance of the Irish Sea (C&D) compared to those at the north boundary of the area of interest (A&B). Further joint probability plots are provided in Appendix A.

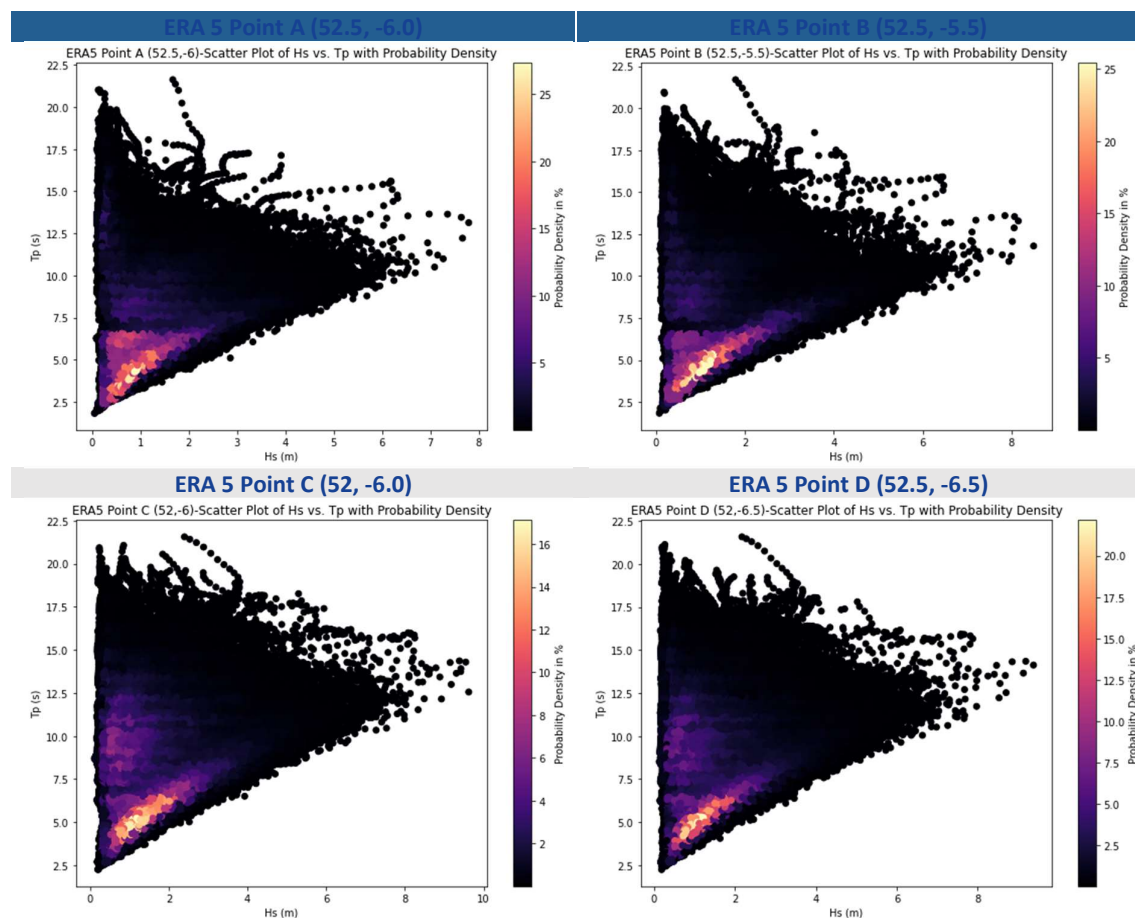


Figure 8-17: Scatter plot H_s vs T_p with probability density - offshore data points (1979-2022)

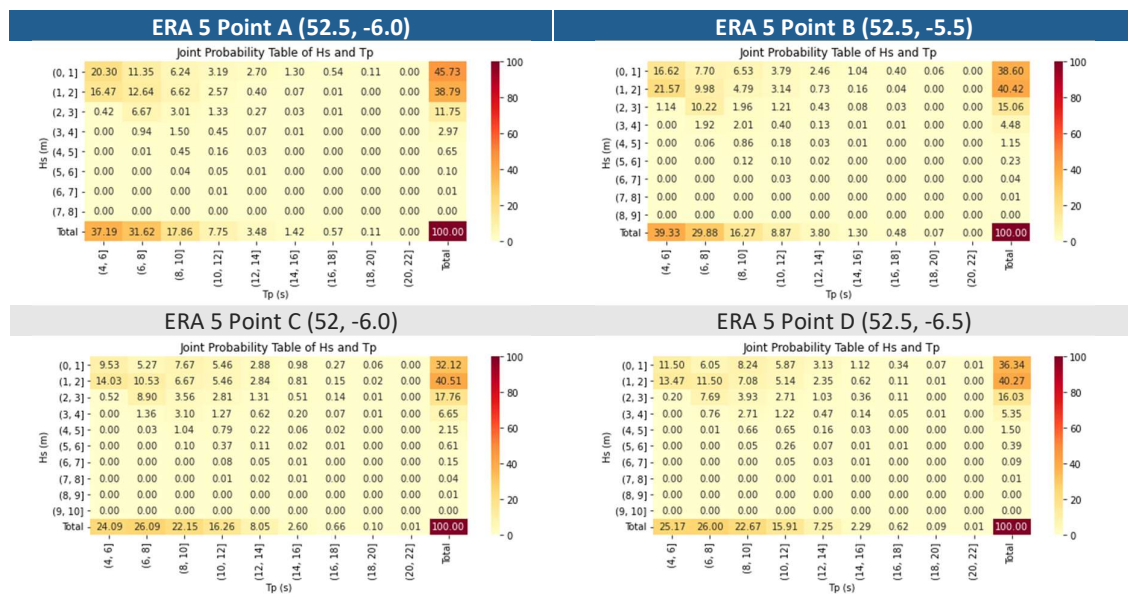


Figure 8-18: Joint probability table H_s vs T_p - Offshore data points (1979-2022)

The maximum and average significant wave heights (H_s) and peak wave period (T_p) values obtained in the selected offshore data points are presented in Table 8-3. As mentioned before, the south boundaries are associated with higher wave heights and wave periods.

Table 8-3: Offshore data points - Maximum and Average H_s and T_p (1979-2022)

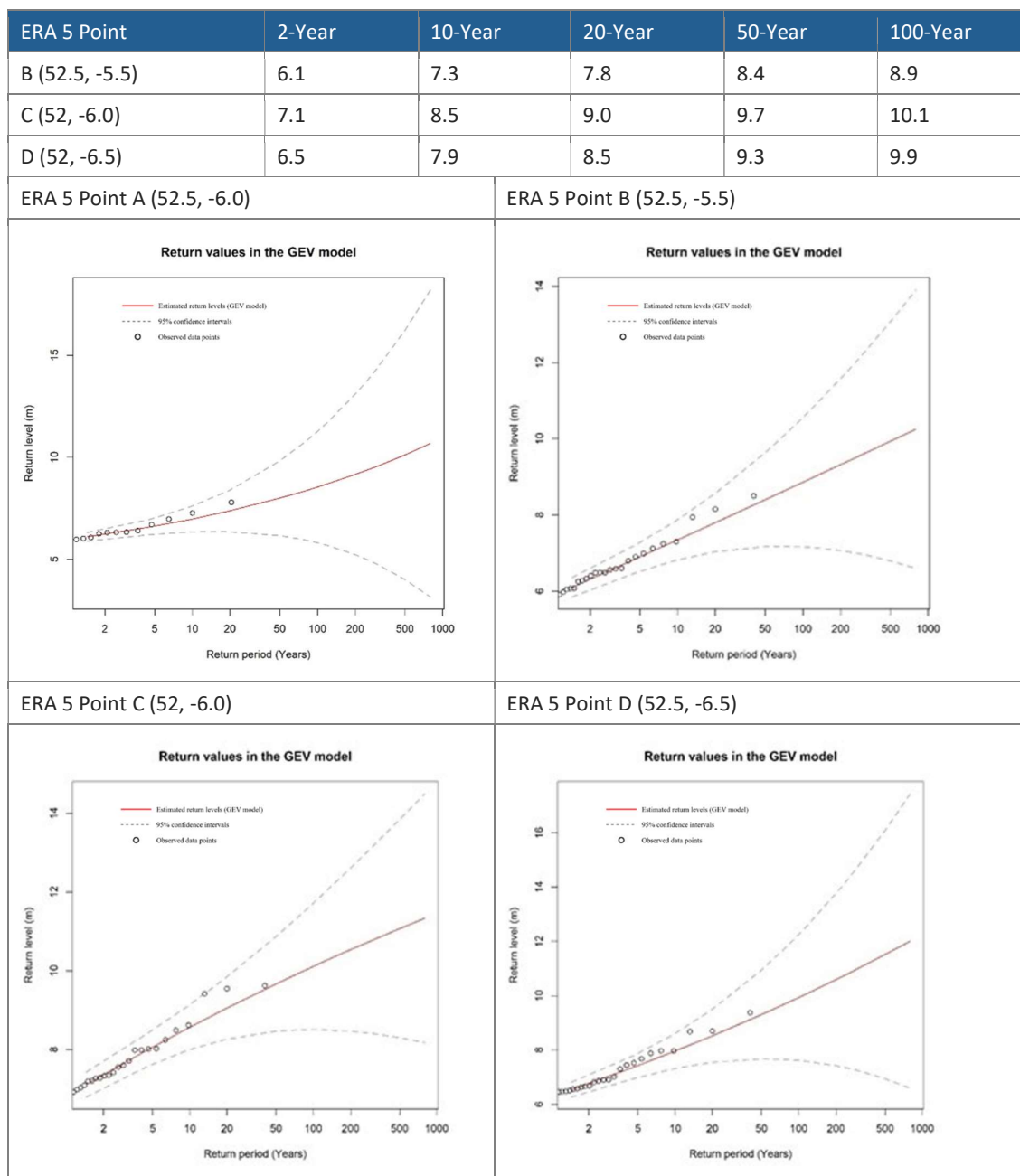
ERA 5 Data Point	H_s (m)		T_p (s)	
	Max	Mean	Max	Mean
A (52.5, -6)	7.8	1.2	21.6	6.8
B (52.5, -5.5)	8.5	1.3	21.7	6.8
C (52, -6)	9.6	1.6	21.6	8.2
D (52.5, -6.5)	9.4	1.5	21.6	8.1

EXTREME ANALYSIS

The Generalized Extreme Value (GEV) method combined with the block maxima data selection is utilised in the estimate of extreme wave events. The number of extreme events considered in the analysis (block maxima) is defined based on the distribution best fit and our expert judgement in the return levels. The data fitting analysis between the GEV distribution and the data is done based on study of the quantile-quantile (QQ) plot and density diagram provided in Appendix B for each offshore point. The extreme offshore wave conditions associated with a return period (RP) up to 100-years are presented in Table 8-4.

Table 8-4: Extreme wave heights in offshore location (in metres)

ERA 5 Point	2-Year	10-Year	20-Year	50-Year	100-Year
A (52.5, -6.0)	6.1	6.9	7.4	8.0	8.5



8.2.3 NEARSHORE WAVE CONDITIONS

8.2.3.1 GENERAL

This section summarizes the wave conditions near the port derived from the MIKE21 SW wave propagation analysis. Two points of interest, shown in

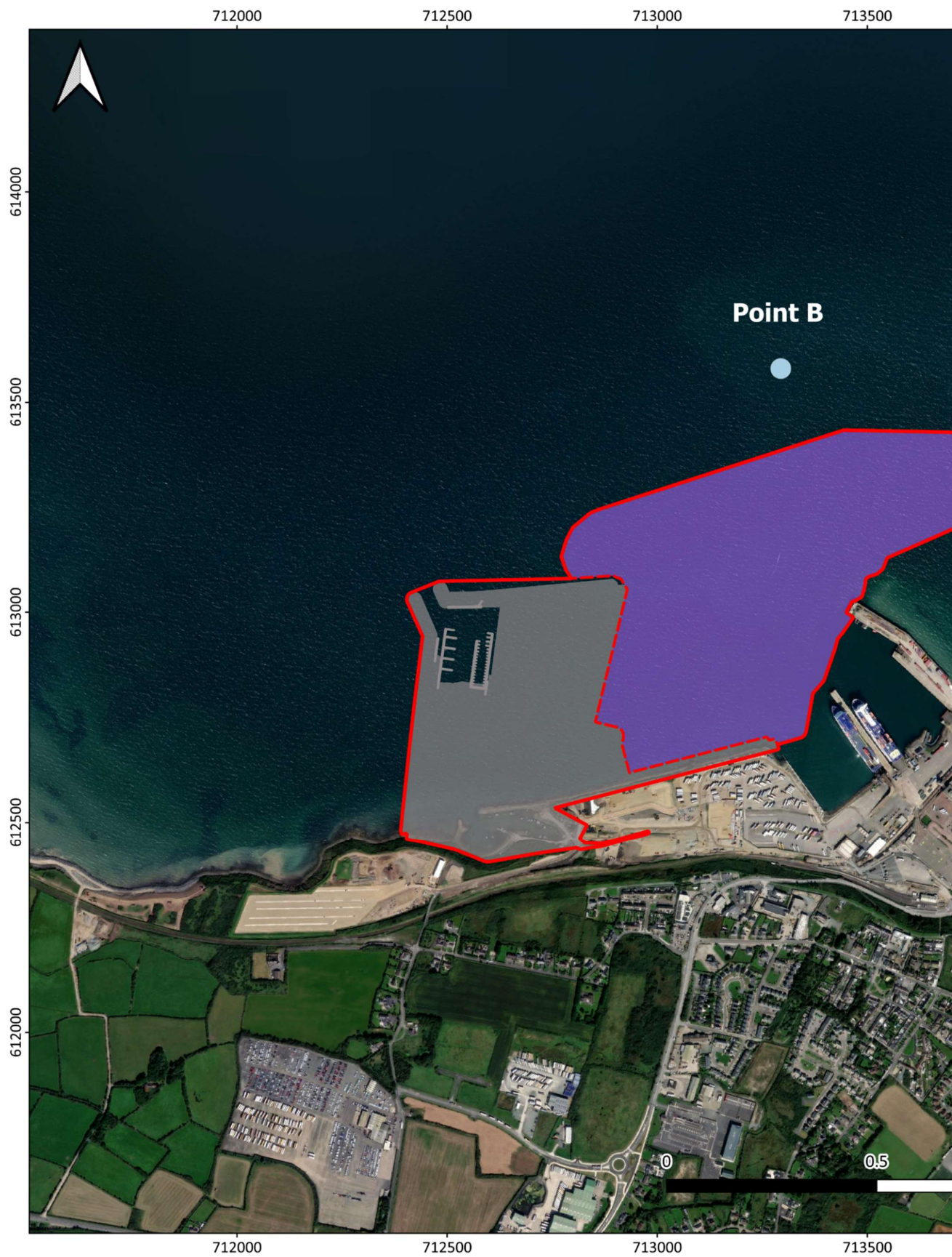


Figure 8-19 and Table 8-5, were selected to characterize wave conditions at the Proposed Development.

Table 8-5 Nearshore Point Coordinates

Point	Water Depth (m ODMalin)	LAT/LONG	UTM (Zone 29)
A	≈10	52.264°, -6.326°	682500.00 m E, 5793800.00 m N
B	≈6	52.262°, -6.340°	681500.00 m E, 5793500.00 m N

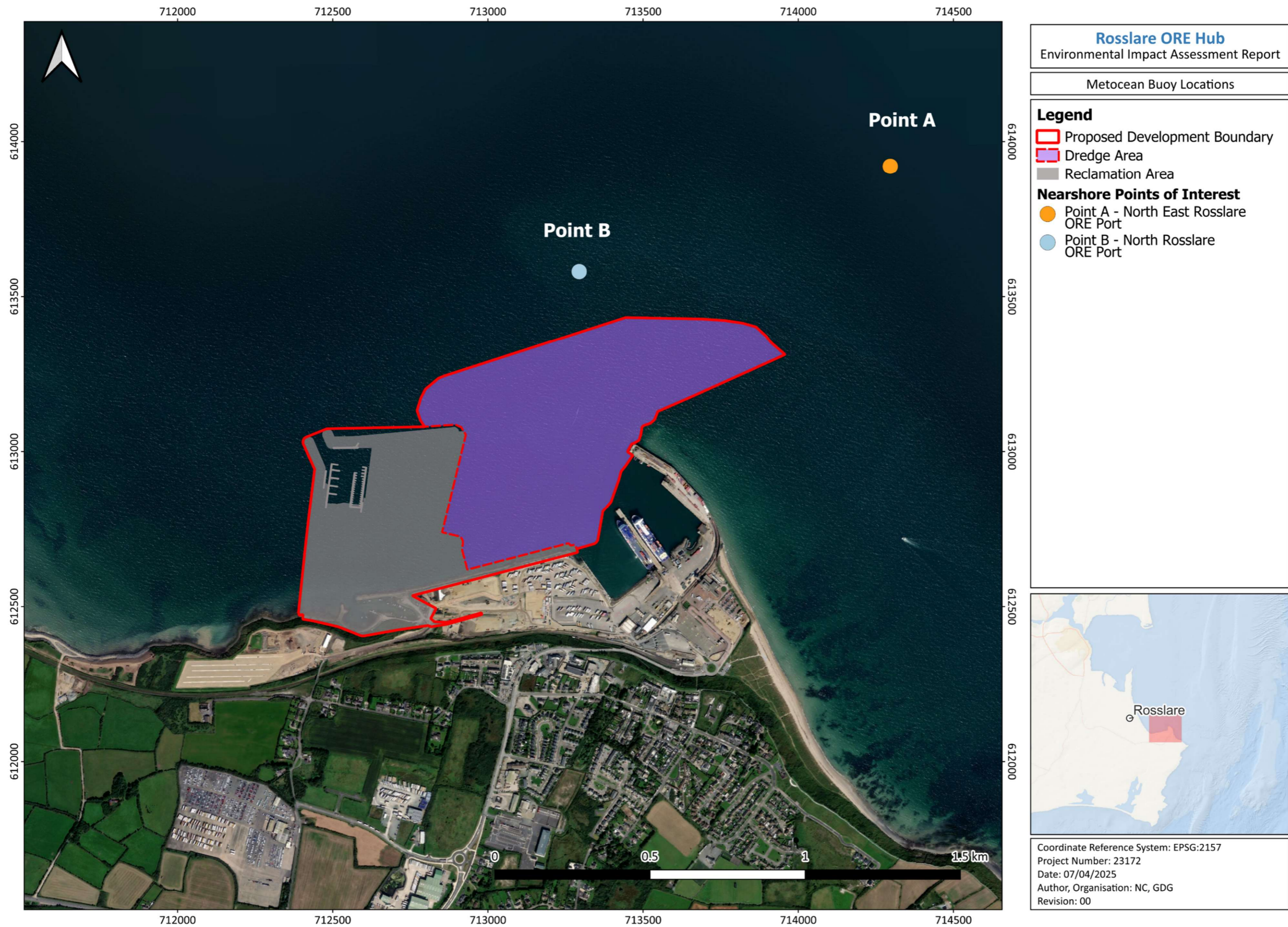


Figure 8-19: Location of the nearshore points of interest (Extracted from Google Earth)

8.2.3.2 WAVES

This section provides a statistical analysis of the 21 years of wave data estimated with MIKE21 SW model at a location near Rosslare Port.

AVERAGE REGIME AT POINT A – NORTHEAST OF THE PROPOSED DEVELOPMENT

The analysis conducted for Point A, located northeast of the port, is detailed in this section. As shown in Figure 8-20, both the significant wave height rose and the peak period rose illustrate that waves at Point A primarily come from the sector covering from East (E) to East-Southeast (ESE), while occurrences of waves from the northeast (NE) and southwest (SW) are comparatively less frequent.

Westerly waves are associated with more energetic sea conditions, characterized by a more significant presence of long wave periods (up to 20 s) and high significant wave heights (above 2 m). These conditions result from offshore swells diffracting as they propagate within the Irish Sea and enter shallower waters as illustrated by an extracted model timestep in Figure 8-21.

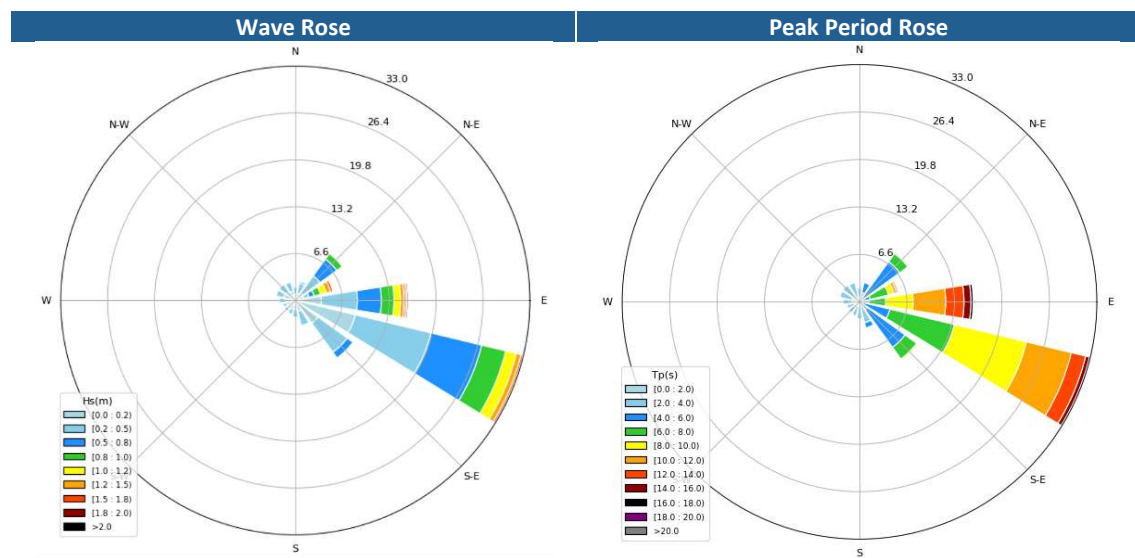


Figure 8-20: Point A – NE Rosslare Port – significant wave height (H_s) and peak period (T_p) rose diagrams (2002-2022)

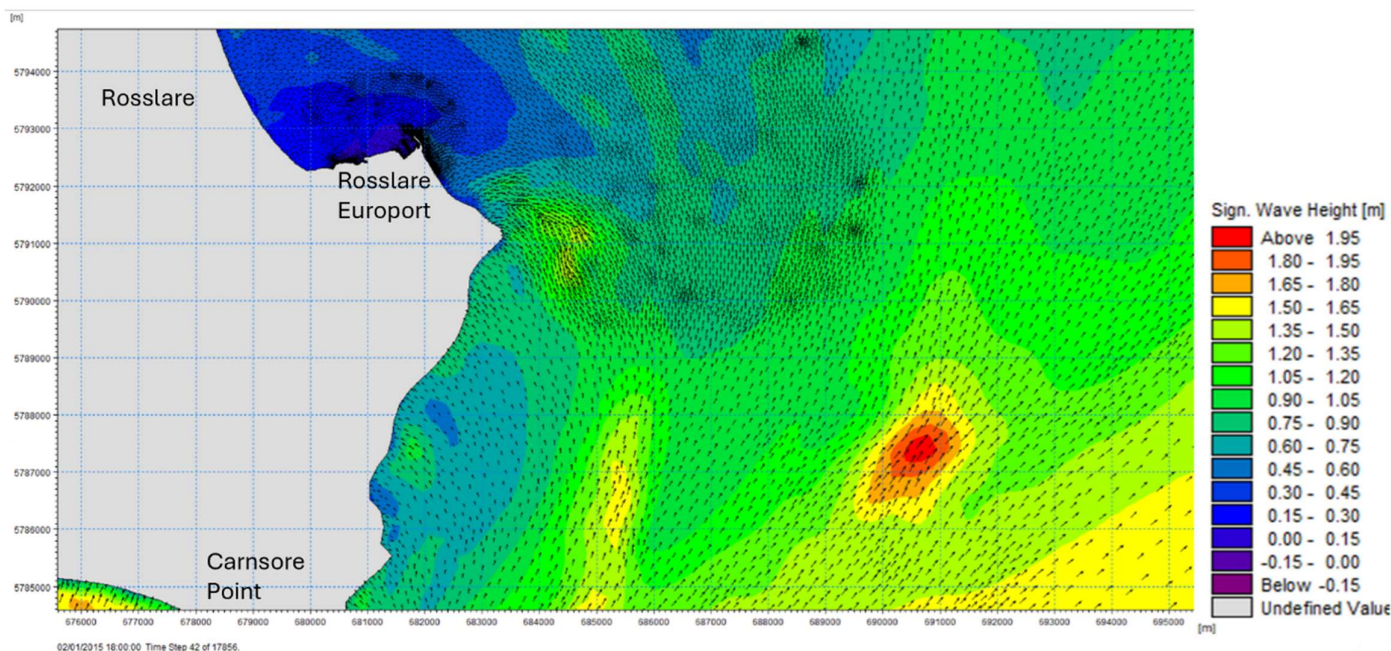


Figure 8-21: Significant wave height and mean wave direction during a south-westerly wave event to illustrate the nature of wave diffraction in Rosslare Port regional area

Regarding the combination of wave height and peak period, prevailing conditions are characterized by wave heights below 1m coupled with peak periods of up to 12s as illustrated in Figure 8-22, Figure 8-23 and Figure 8-24. When analysed individually, wave heights below 1 m and peak periods of up to 10 s are associated with an approximate occurrence probability of 90%.

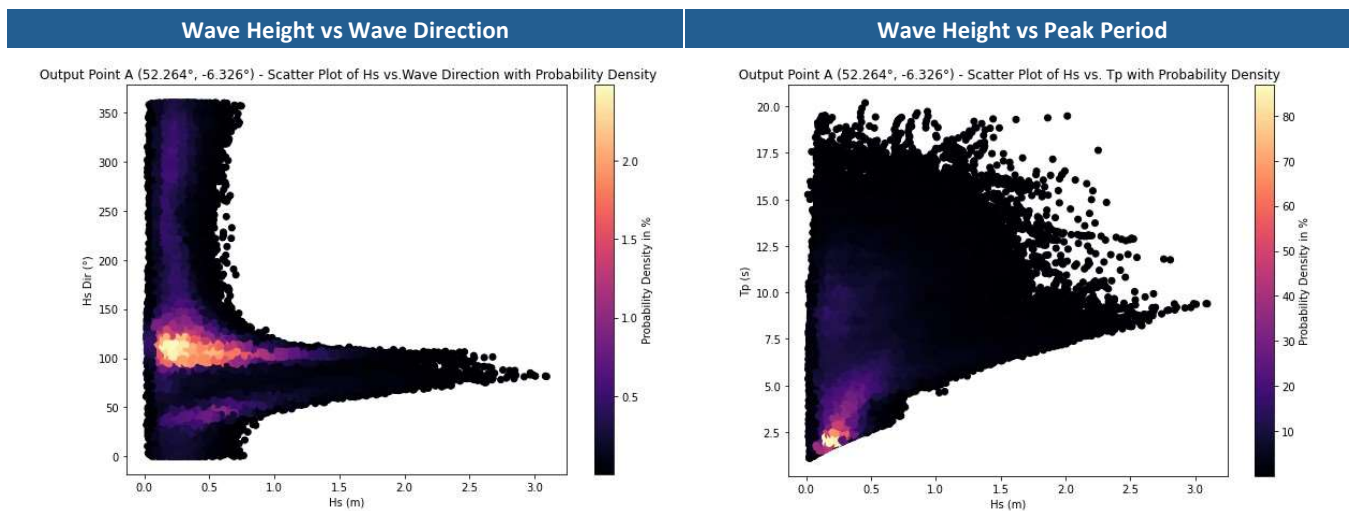


Figure 8-22: Point A – NE Rosslare Port – Scatter Plots (H_s vs Dir, left) (H_s vs T_p , right) (2002-2022)

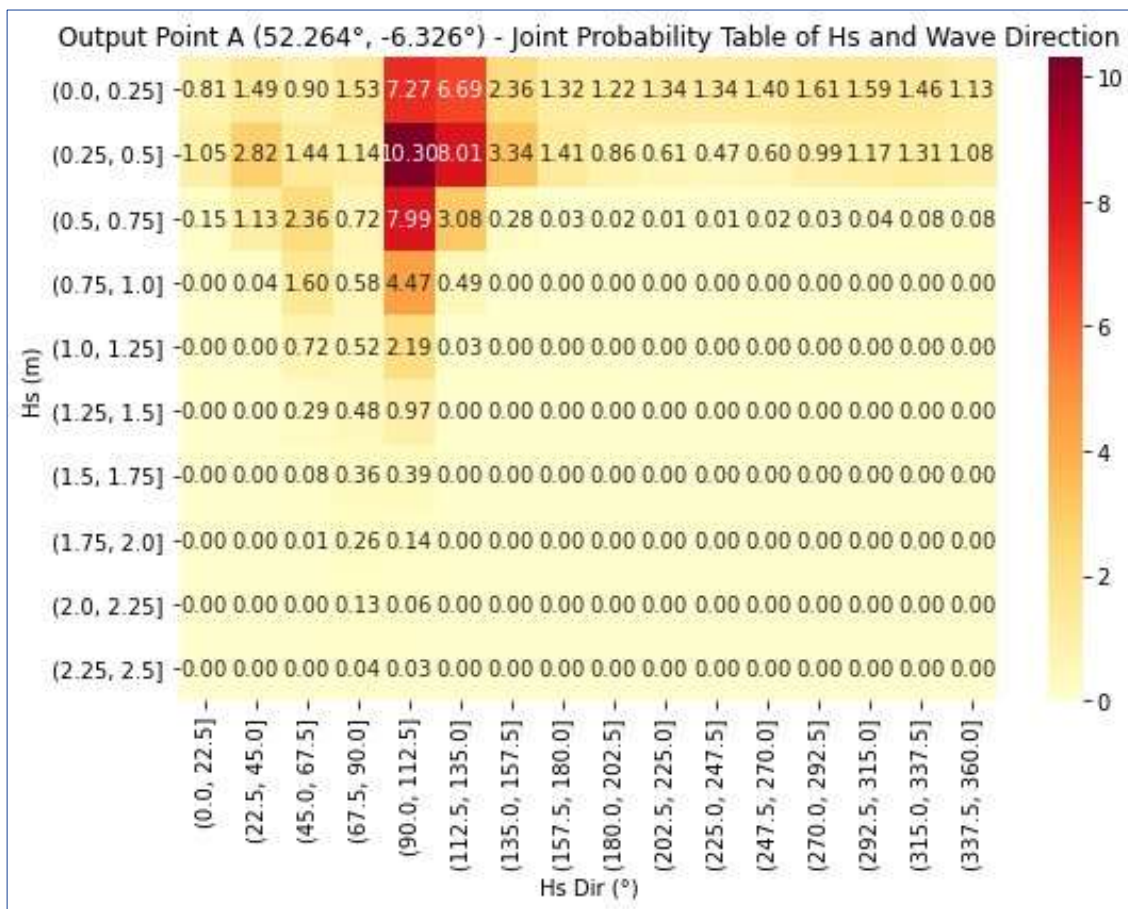


Figure 8-23: Point A – NE Rosslare Port – Joint probability table (Hs vs Dir) (2002-2022)

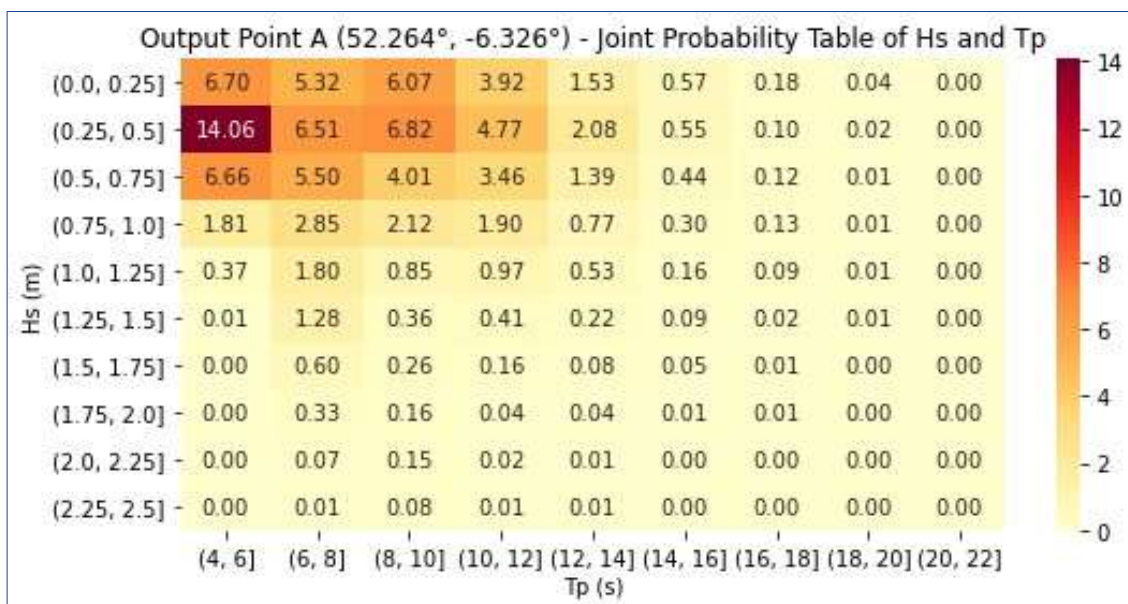


Figure 8-24: Point A – NE Rosslare Port – Joint probability table (Hs vs Tp) (2002-2022)

AVERAGE REGIME AT POINT B – NORTH OF THE PROPOSED DEVELOPMENT

The wave rose and the peak period rose presented in Figure 8-25 reveals a prevalence of easterly waves with a reduced occurrence of waves from other directions, particularly within the first and second sectors. In comparison with Point A, there is a clear reduction in the southeasterly (SE) wave component due to the shielding effect provided by Rosslare Port along with wave diffraction and refraction resulting from bathymetric changes.

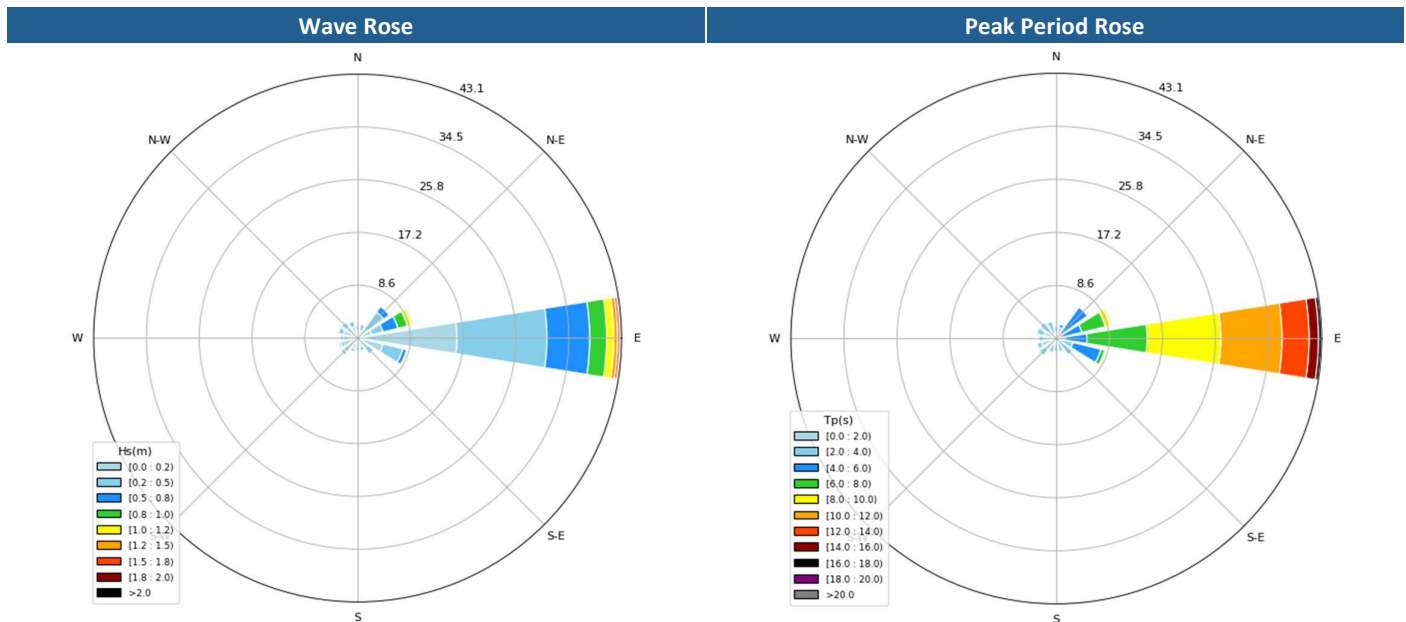


Figure 8-25: Point B – N Rosslare Port - Wave Rose and Peak Period Rose (2002-2022)

In terms of the combination of wave height and peak period, prevailing conditions remain the same as estimated in Point A ($H_s < 1$ m and $T_p < 12$ s) (Figure 8-26, Figure 8-27 and Figure 8-28). When analysed individually, wave heights below 1 m are associated with a probability of occurrence of 96.5% whereas peak periods up to 12 s have a probability of incidence of circa 90%.

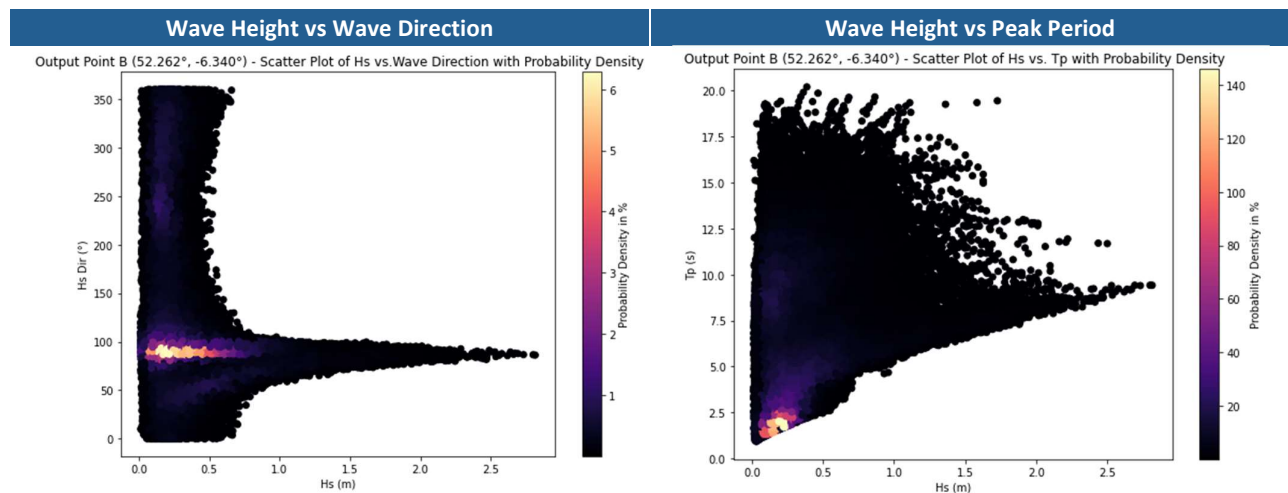


Figure 8-26: Point B – N Rosslare Port – Scatter Plots (Hs vs Dir, left) (Hs vs Tp, right) (2002-2022)

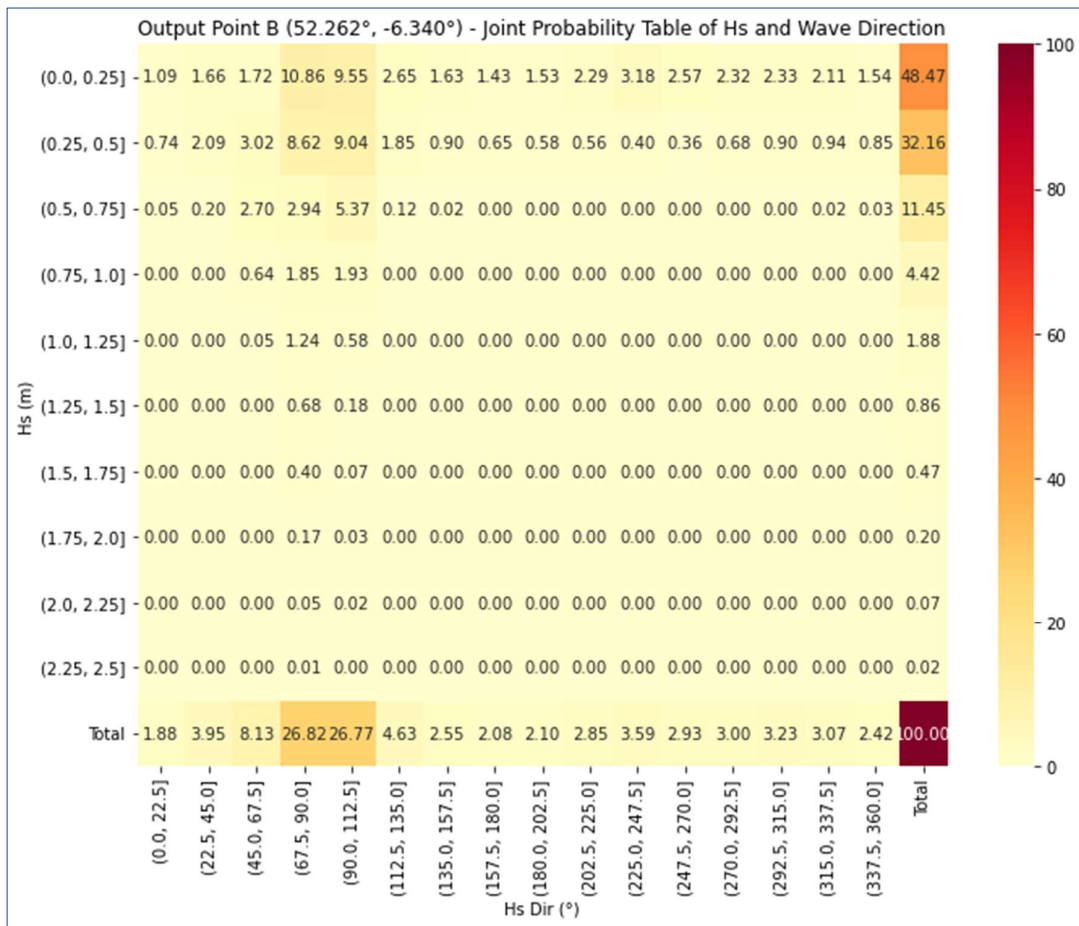


Figure 8-27: Point B – N Rosslare Port – Joint probability table (Hs vs Dir) (2002-2022)

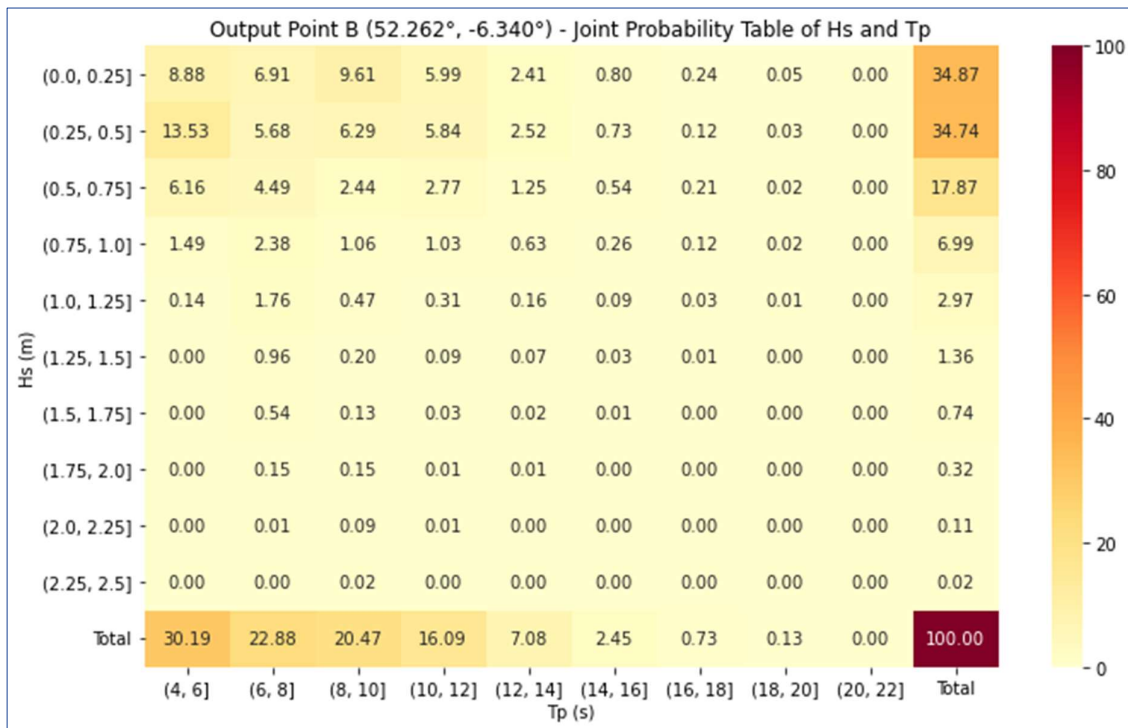


Figure 8-28: Point B – N Rosslare Port – Joint probability table (H_s vs T_p) (2002-2022)

EXTREME ANALYSIS

The Generalised Extreme Value (GEV) method combined with the block maxima data selection, is used to estimate extreme wave events. It should be highlighted that while the extreme analysis performed considering all wave directions results in a good distribution fit, as shown in the results, the directional assessment does not provide satisfactory results for some wave directions due to the limited number of values included within those direction ranges. Wave directions have been categorized as follows for the directional extreme values assessment:

- North (N) [337.5°, 22.5°)
- North-East (NE) [22.5°, 67.5°)
- East (E) [67.5°, 112.5°)
- South-East (SE) [112.5°, 157.5°)
- South (S) [157.5°, 202.5°)
- South-West (SW) [202.5°, 247.5°)
- West (W) [247.5°, 292.5°)
- North-West (NW) [292.5°, 337.5°)

The extreme peak period is estimated considering a wave steepness of 1/5.

The GEV distribution, quantile-quantile (QQ) plot and the density diagram obtained for the nearshore locations are provided in Appendix D.

The extreme values for both point A and B are shown in Table 8-6, Table 8-7, Table 8-8, and Table 8-9.

Table 8-6: Extreme significant wave heights in metres for Point A – NE Rosslare ORE Port

Return Period (RP)	Extreme Significant Wave Height per Wave Direction (in meters)								
	All	N	NE	E	SE	S	SW	W	NW
2-Year	2.3	0.7	1.8	2.3	1.1	0.6	0.6	0.6	0.6
10-Year	2.8	0.8	1.9	2.8	1.2	0.7	0.7	0.6	0.7
20-Year	3.0	0.8	2.0	3.0	1.3	0.7	0.7	0.6	0.7
50-Year	3.1	0.8	2.0	3.1	1.3	0.7	0.8	0.7	0.7
100-Year	3.3	0.8	2.0	3.3	1.4	0.7	0.9	0.7	0.7

Table 8-7: Extreme peak wave period in seconds for Point A – NE Rosslare ORE Port

Return Period (RP)	Extreme Peak Wave Period Wave Direction (in seconds)								
	All	N	NE	E	SE	S	SW	W	NW
2-Year	8.0	3.4	6.5	8.0	4.5	3.1	3.1	3.1	3.1
10-Year	9.5	3.7	6.8	9.5	4.8	3.4	3.4	3.1	3.4
20-Year	10.2	3.7	7.1	10.2	5.0	3.4	3.4	3.1	3.4
50-Year	10.5	3.7	7.1	10.5	5.0	3.4	3.7	3.4	3.4
100-Year	11.1	3.7	7.1	11.1	5.3	3.4	3.9	3.4	3.4

Table 8-8: Extreme Wave Heights in metres in Point B – N Rosslare ORE Port

Return Period (RP)	Extreme Significant Wave Height per Wave Direction (in meters)								
	All	N	NE	E	SE	S	SW	W	NW
2-Year	2.0	0.6	1.1	2.0	0.6	0.5	0.5	0.5	0.5
10-Year	2.5	0.7	1.2	2.5	0.7	0.5	0.5	0.6	0.6
20-Year	2.6	0.7	1.3	2.7	0.7	0.5	0.5	0.6	0.6
50-Year	2.8	0.7	1.4	3.1	0.7	0.6	0.5	0.6	0.6
100-Year	2.9	0.7	1.6	3.4	0.8	0.6	0.5	0.6	0.6

Table 8-9: Extreme peak wave period in seconds for Point B – N Rosslare ORE Port

Return Period (RP)	Extreme Peak Wave Period Wave Direction (in seconds)								
	All	N	NE	E	SE	S	SW	W	NW
2-Year	7.1	3.1	4.5	7.1	3.1	2.8	2.8	2.8	2.8
10-Year	8.6	3.4	4.8	8.6	3.4	2.8	2.8	3.1	3.1
20-Year	8.9	3.4	5.0	9.2	3.4	2.8	2.8	3.1	3.1
50-Year	9.5	3.4	5.3	10.5	3.4	3.1	2.8	3.1	3.1
100-Year	9.9	3.4	5.9	11.4	3.7	3.1	2.8	3.1	3.1

8.3 HYDRODYNAMIC ASSESSMENT

This section presents the analysis performed to evaluate the hydrodynamic phenomena (current and tidal water levels) in the Proposed Development for both the present port configuration and the future port development.

The Hydrodynamic Model (HD Model) has been calibrated based on the following sources:

- Rosslare tidal gauge, used for the calibration of the model against water levels
- Current parameters obtained in the metocean survey, used for the calibration of the model against current speed and direction

8.3.1 METHODOLOGY

8.3.1.1 GENERAL

This section summarises the methodology and the key assumptions considered in the hydrodynamic numerical model performed to evaluate current and tidal conditions in Rosslare Europort.

8.3.1.2 NUMERICAL MODEL

The flow and water level modelling were performed with MIKE21 HD Flow Model, which is a modelling system for 2D free-surface flows.

MIKE21 Flow Model is applicable to the simulation of hydraulic and environmental phenomena in lakes, estuaries, bays, coastal areas and seas. It may be applied wherever stratification can be neglected.

The hydrodynamic (HD) module is the basic module in the MIKE 21 Flow Model. It provides the hydrodynamic basis for the computations performed in the Environmental Hydraulics modules. The hydrodynamic module simulates water level variations and flows in response to a variety of forcing functions in lakes, estuaries and coastal regions. The effects and facilities include:

- bottom shear stress (considered in the present analysis)
- wind shear stress (considered in the present analysis)
- barometric pressure gradients (considered in the present analysis)
- Coriolis force (excluded from the analysis, as its effects are negligible for a relatively small spatial area)
- momentum dispersion (considered in the present analysis)
- sources and sinks (considered in the present analysis – River Slaney)
- evaporation (excluded from the analysis, as it has negligible effects on the Study Area)
- flooding and drying (considered in the present analysis)
- wave radiation stresses (excluded from the analysis)

8.3.1.3 INPUT DATA

The input data used for the hydrodynamic assessment was the same as for the wave propagation described in section 8.1.1.3, with the exception of waves, since wave forcing is not included in the flow model.

8.3.1.4 MODEL SET UP

MESH

In this study, a triangular mesh is employed covering an approximate area of 2,400 km², following the methodology described in section 8.1.1.4 Mesh.

KEY PARAMETERS

The key model parameters are outlined in the table below. These parameters were determined following a validation of the model using data obtained during the survey campaign. The selection of these parameters is guided by achieving a balance between computational efficiency and the accuracy of the results (Table 8-10).

Table 8-10 Key Flow Model Parameters

Model Parameter	Description
Time Step	30s
Simulation Period	at least one spring tide and one neap tide
Time Formulation	Instationary formulation Geographical space discretization: High order
Critical CFL (Courant–Friedrichs–Lewy) Number	0.8
Manning Number	50

BOUNDARY CONDITIONS

Tidal levels obtained from MIKE21 Global Tide Tool are considered in the model boundaries as varying in time and along the boundary.

8.3.2 MODEL CALIBRATION

8.3.2.1 FLOW SPEED AND DIRECTION

The metocean survey undertaken as part of Rosslare ORE project was used to obtain current and wave data to calibrate the hydrodynamic studies performed in this project stage. Two measurement devices were installed at the North-east of Rosslare port as indicated in Figure 8-29.

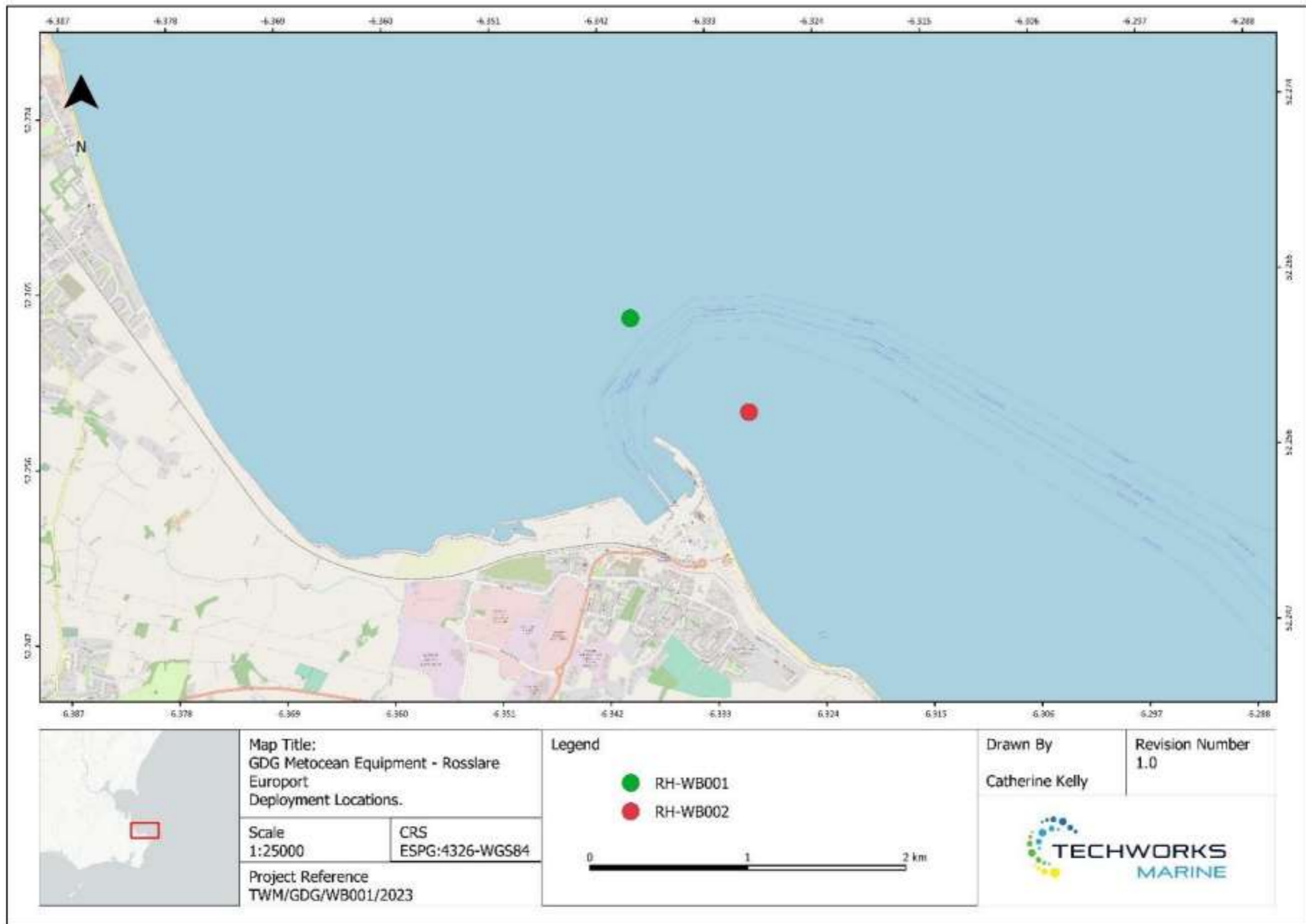


Figure 8-29: Measurement Buoys Location

Figure 8-30 to Figure 8-33 illustrate the comparison between flow speed and direction obtained from the model and the values registered in the survey buoys between 9/1/2024 to 23/1/2024. The comparison reveals that the flow model values generally align with the trends observed in the buoy data, showing good agreement with both the average and peak values.

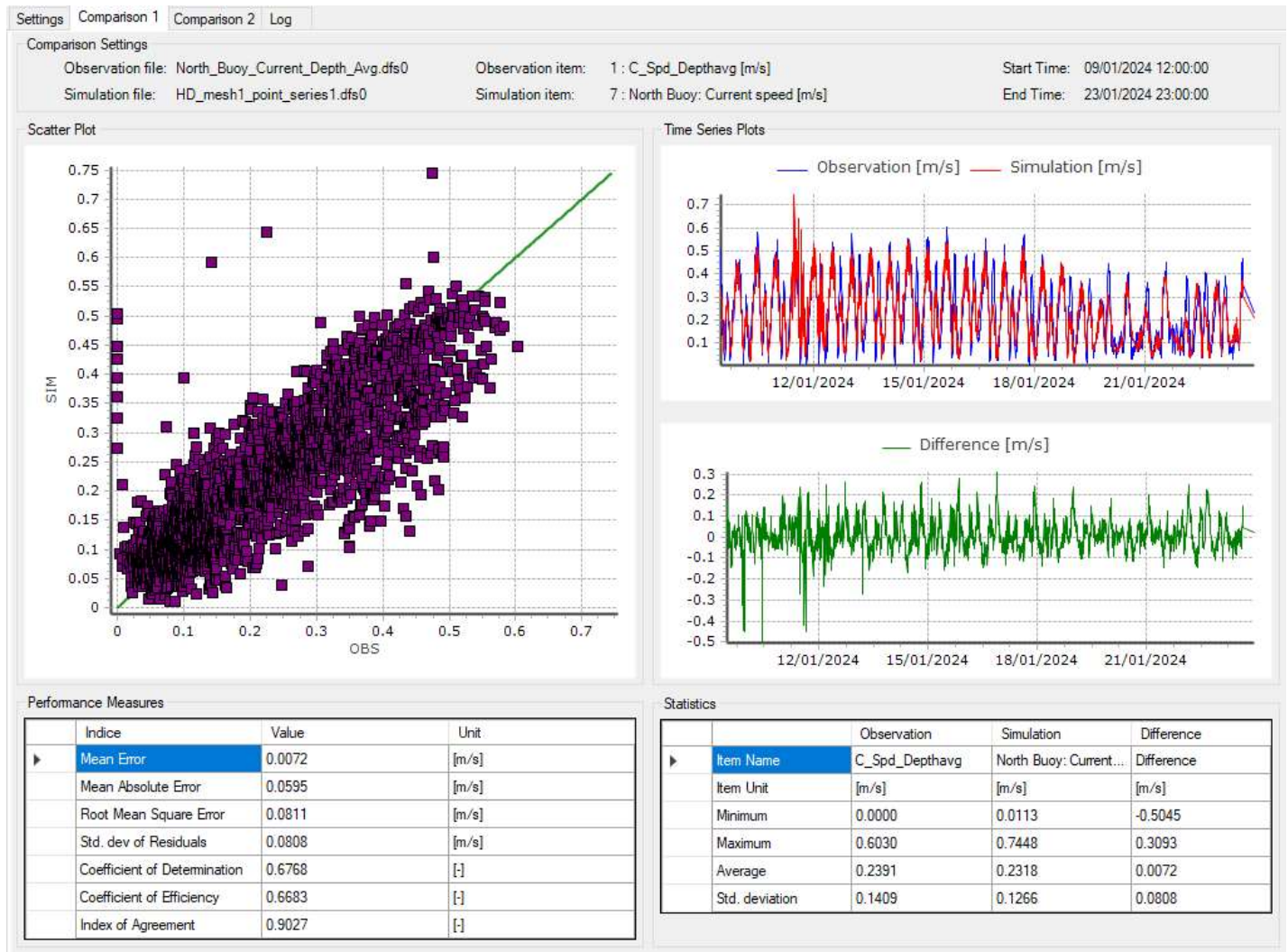


Figure 8-30: Comparison of Measured Depth-Average Current Speed (WB001) and Simulated Depth-Average Current Speed (Source: MIKE21 Time Series Comparator)

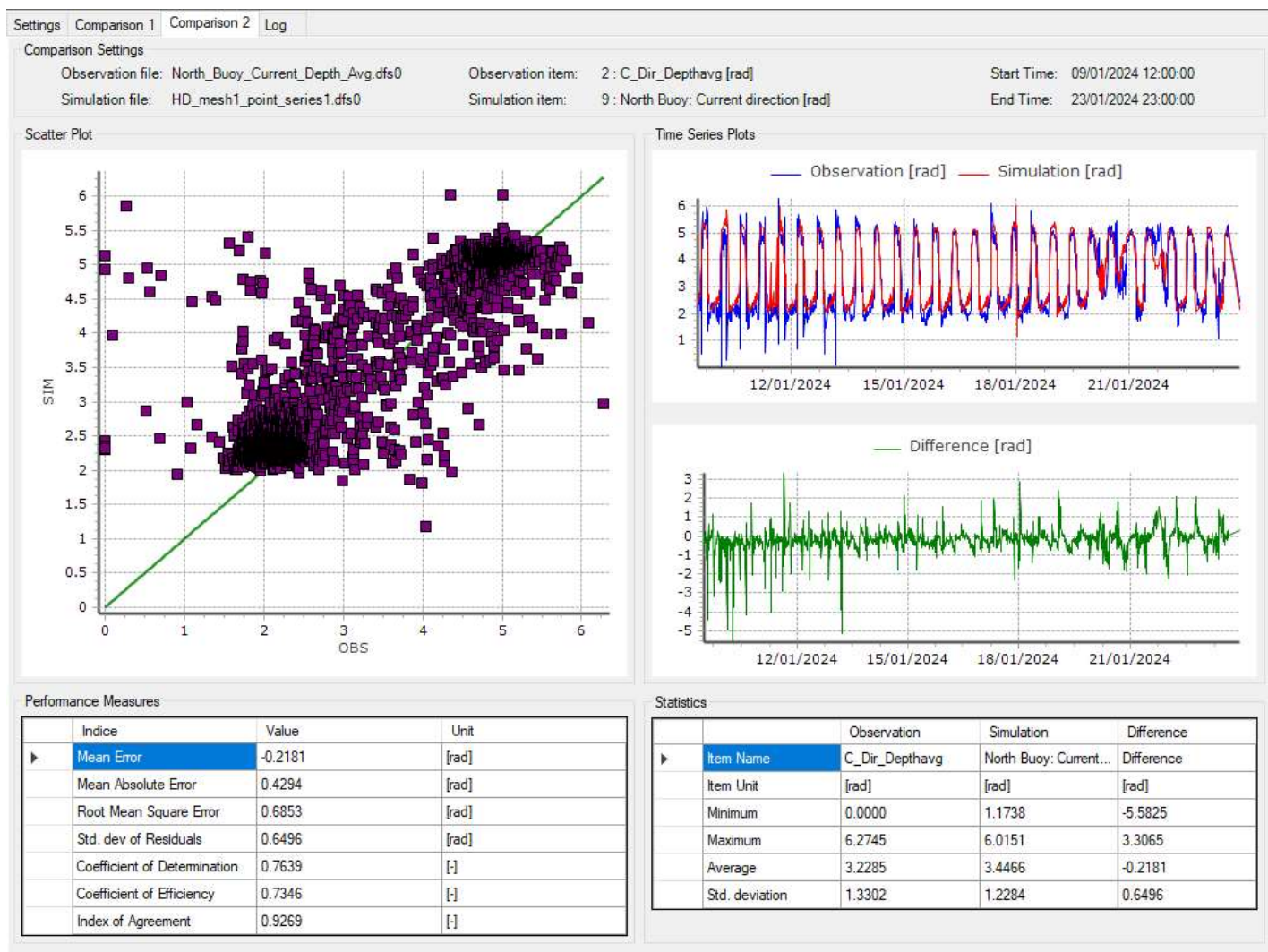


Figure 8-31: Comparison of Measured Depth-Average Current Direction (WB001) and Simulated Depth-Average Current Direction (Source: MIKE21 Time Series Comparator)

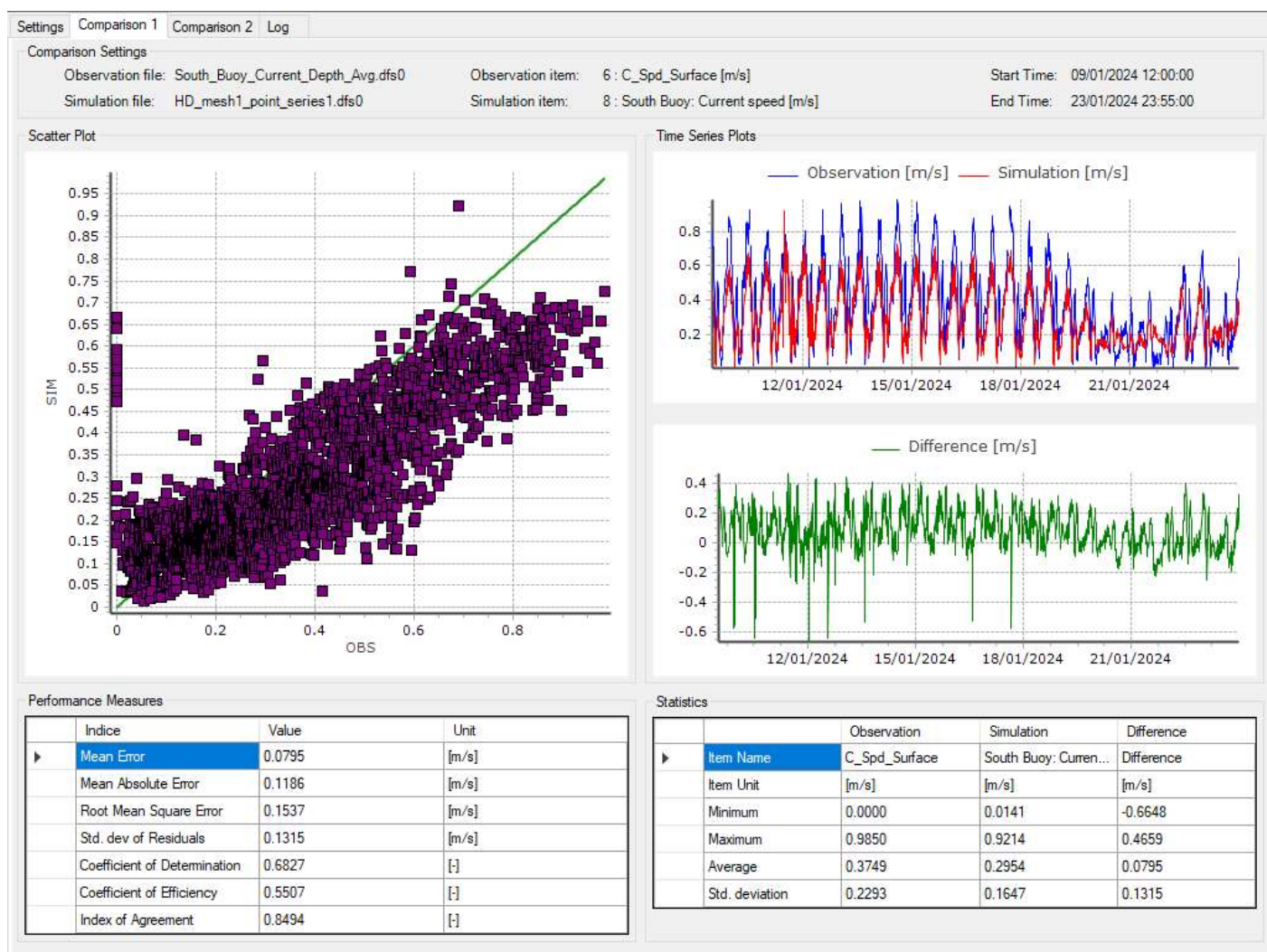


Figure 8-32: Comparison of Measured Depth-Average Current Speed (WB002) and Simulated Depth-Average Current Speed (Source: MIKE21 Time Series Comparator)



Figure 8-33: Comparison of Measured Depth-Average Current Direction (WB002) and Simulated Depth-Average Current Direction (Source: MIKE21 Time Series Comparator)

8.3.2.2 WATER LEVELS

The water levels obtained from the model have been calibrated against the water levels registered in the tidal gauge currently installed in Rosslare Harbour (SmartBay, 2023).

Figure 8-34 reveals that the model tends to overestimate water levels, but it represents properly the general variation of the measured tidal levels (neaps and springs). The difference in the results could be due to the wave effect and meteorological effects not included in the hydrodynamic model. A minor deviation in the tidal phase is observed, which is likely transient in nature and potentially influenced by meteorological factors.

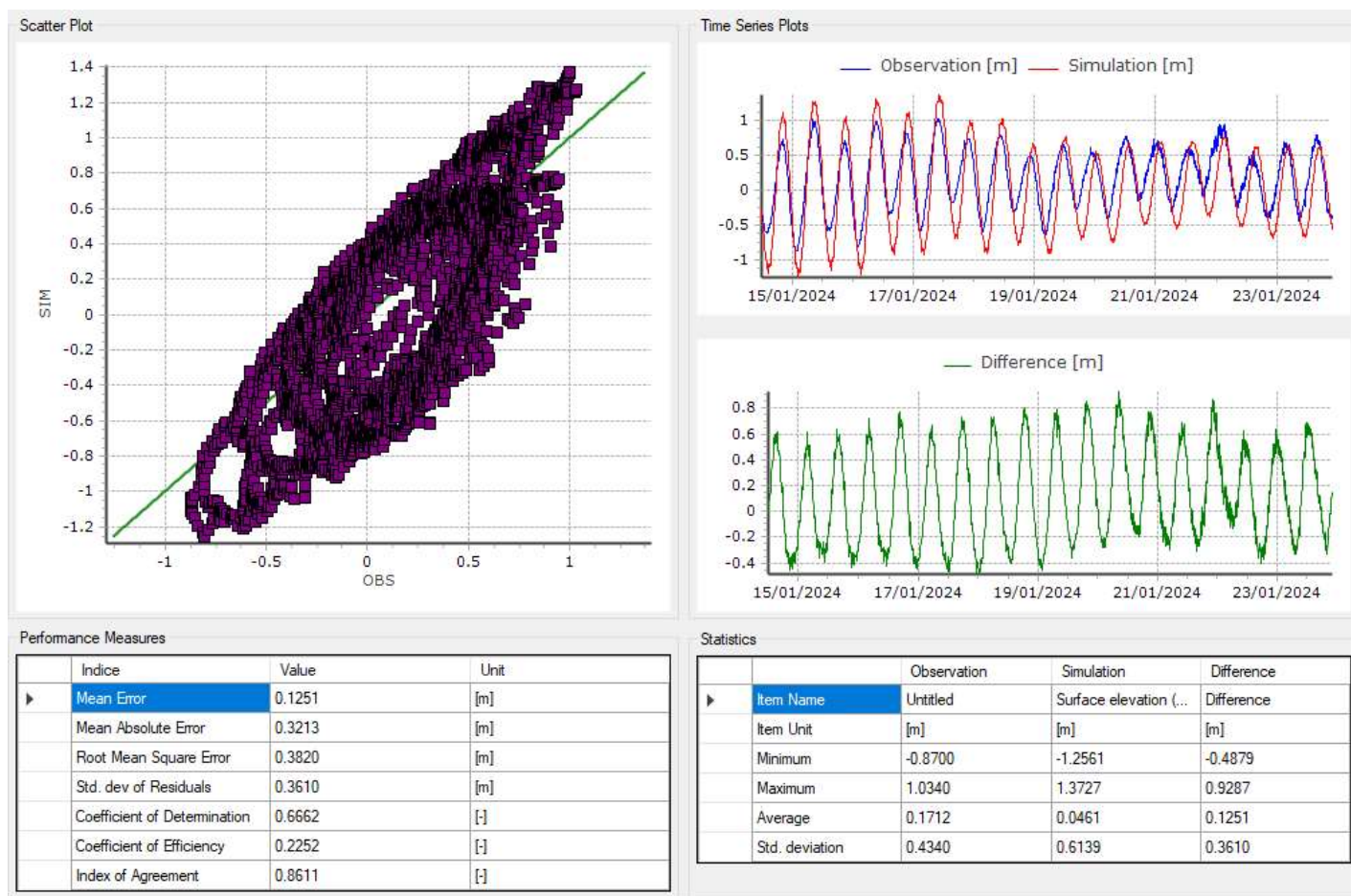


Figure 8-34: Comparison of Measured Water Level (ODM) and Simulated Surface Elevation
(Source: MIKE21 Time Series Comparator)

8.4 DREDGING DISPERSAL ASSESSMENT

This section presents the assessment of the sediment dispersal due to the proposed dredging and disposal works within the dredging and reclamation areas.

Capital dredging will be undertaken to deepen the navigation channel and Berth 2 to a navigable depth of -10m CD, and to achieve a navigable depth of -12m CD at Berth 1. The total area for dredging is 48.4ha. Reclamation of land from the marine area to the west of the marine dredge area, including infilling of the existing small boat harbour using the marine dredged material and imported rockfill to create 27.7ha of additional land for the Proposed Development. Reclamation will be undertaken in sections created by perimeter bunds and surrounded on the seaward facing sides by rock armour. Figure 8-35 shows the designated dredging and reclamation areas.



Rosslare ORE Hub
 Environmental Impact Assessment Report

General Site View

Legend
Rosslare ORE Hub
 Proposed Development Boundary
 Dredge Area
 Reclamation Area
Indicative Reclamation Sequencing
 Phase 1 - Outer Area
 Phase 2 - Central Area
 Phase 3 - Small Boat Harbour Area

Coordinate Reference System: EPSG:2157
 Project Number: 23172
 Date: 18/03/2025
 Author, Organisation: NC, GDG
 Revision: 00

Figure 8-35: Preliminary Indicative Construction Sequence considering dredging and reclamation area

8.4.1 DREDGING OPERATIONS

As described in detail in Chapter 6: Project description, dredging and reclamation works are planned to be conducted over three stages. Once the perimeter bunds are constructed using imported rockfill (Stage 1), dredging is expected to proceed efficiently from soft overlying sediments to stiffer underlying sediments using a Trailer Suction Hopper Dredger (TSHD) and backhoe dredger or to combine these elements using a Cutter Suction Dredger (CSD) (Stage 2 and 3). Technical Appendix 7: Geotechnical Interpretative Report of this EIAR provides information on marine seabed material from 28 No. marine boreholes collected within the proposed dredging area, as shown in Figure 8-36.

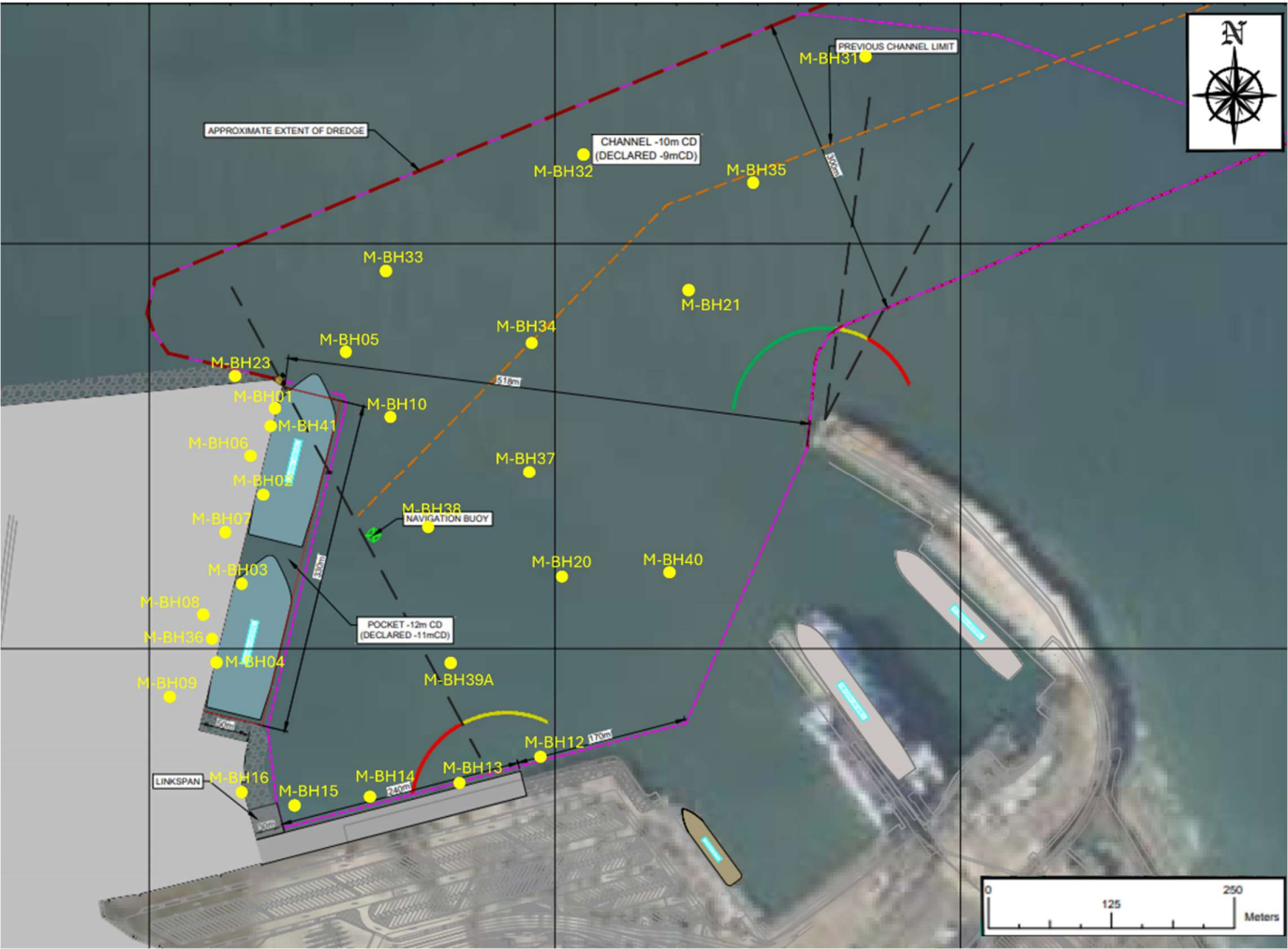


Figure 8-36: Marine Borehole locations within the dredging area

The total estimated sediment volumes including over-dredge allowances for the entire dredging area are estimated in Table 8-11.

Table 8-11: Total estimated dredged fractions for considering all the dredging area

Material Type	Volume (m ³)
Marine Deposits	550,000
Glacial Till	450,000
Weathered Rock and Bed Rock	400,000
Total	1,400,000

Considering the construction of the reclamation area, as well as the dredging and disposal of dredged material, three stages have been modelled as described below:

Stage 1: Perimeter Bunds

Stage 1 involves constructing over 1,000 m of perimeter bunds using approximately 400,000 m³ of imported rockfill, forming the boundary of the reclamation area and supporting future rock armour for wave protection. While the construction phase programme in Chapter 6: Project Description allows a total duration of 6 to 8 months for this stage, the modelling assumes that the reclamation area will be constructed within 3 months to ensure the worst case scenario from a sediment dispersion perspective is considered. A conservative assumption of 1% loss of displaced sediment into the water column has been modelled and it has been assumed that all release of sediment at Stage 1 will be at a single location near the outer end of the reclamation site, to facilitate worst case scenario modelling of the sediment plume. The sediment dispersed by the rockfill is anticipated to consist of coarse silt and fine sand, as specified in Table 8-12:

Table 8-12: Sediment material considered for Stage 1

Sediment type	Volume (m ³)	Fraction (%)	D50 (mm)
Coarse Silt	2,000	50	0.04675
Fine Sand	2,000	50	0.1875

Stage 2 Dredging: Suction Dredging

In this phase, the modelling assumes the Trailing Suction Hopper Dredging (TSHD) or Cutter Suction Dredging (CSD) technique will be used to remove 550,000 m³ of soft marine deposits. While the construction phase programme in Chapter 6: Project Description allows a total duration of 12 weeks for this stage, a 2-month period has been modelled to ensure the worst case scenario from a sediment dispersion perspective is considered. The model assumes dredged material will be disposed of during operations, with half the time allocated to dredging and the other half to disposal within the reclamation area.

Dredging will begin in the outermost area, handling 100,000 m³, after which the dredger will proceed with the remaining 450,000 m³ in the innermost area. The material to be dredged and disposed of in Stage 2 consists of clay, silt, sand, and gravel, as detailed in Table 8-13:

Table 8-13: Sediment Material considered for Stage 2

Sediment type	Volume (m ³)	Fraction (%)	D50 (mm)
Clay	225,500	21	0.00135
Silt	115,500	41	0.02675

Sand	165,000	30	0.535
Gravel	44,000	8	13.5

Stage 3 Dredging: Backhoe or CSD

For Stage 3 dredging, the construction phase programme in Chapter 6: Project Description allows a total duration of 9 months of Backhoe dredging or a 3.5 months duration of CSD operations to remove 850,000 m³ of deeper till and bedrock. The modelling assumes a mechanical dredging technique using a backhoe excavator is used over 8 months to ensure the worst case scenario from a sediment dispersion perspective is considered..

The soft marine deposits are estimated at 50,000 m³ in the outermost area and 800,000 m³ in the inner area. The dredging will start with the outer zone (50,000 m³, approximately ½ month), followed by the inner zone (800,000 m³, approximately 7½ months). The material to be dredged and disposed of in Stage 3 is expected to consist of clay and fine silt, as specified in Table 8-14:

Table 8-14: Sediment Material considered for Stage 3

Sediment type	Volume (m ³)	Fraction (%)	D50 (mm)
Clay	340,000	40	0.0018
Fine Silt	510,000	60	0.0117

The dredging point for both Stages 2 and 3 is centrally located within the outermost and innermost areas. The disposal point for all stages, located at the outer boundary of the reclamation area, is the weir-box, as this represents a worst-case scenario for sediment dispersion.

8.4.2 MODELLING SOFTWARE

The tidal flow simulations which form the basis of the study were undertaken using MIKE 21 Flow Model Flexible Mesh (FM) modelling system developed by DHI. The MIKE system is a state of the art, industry standard, modelling system, based on a flexible mesh approach. Using these flexible mesh modelling systems, it is possible to simulate the mutual interaction between currents and sediment transport by dynamically coupling the relevant modules in both two and three dimensions. The Flow Model FM modules include the Hydrodynamic Module (HD) and the Mud Transport (MT) Module.

The MIKE 21 Flow Model FM Hydrodynamic (HD) Module is a 2-dimensional depth-averaged hydrodynamic programme that resolves the shallow water equations, or Navier Stokes Momentum, and continuity equations (Constantin and Foias, 1988; Roe, 1981). These are resolved using a finite volume scheme. The Riemann solver (Roe, 1981) is used to determine the fluxes within the domain mesh, with various approximation schemes applied to resolve second order variance. The flow velocity is derived from the depth integrated resolution of the shallow water equations. Tide-induced bottom stresses are determined by a quadratic friction law which utilises drag coefficient and flow velocity. The simulated drag coefficient is calculated by resolving the Manning number (M) for bed friction (Manning et al., 1980).

The main features and effects included in the Hydrodynamic Module are:

- Flooding and drying
- Momentum dispersion
- Bottom shear stress
- Coriolis force
- Wind shear stress
- Barometric pressure gradients
- Ice coverage
- Tidal potential
- Precipitation/evaporation
- Wave radiation stresses
- Sources and sinks

The Mud Transport (MT) module (DHI Group, 2017) describes erosion, transport and deposition of mud or sand/mud mixtures under the action of currents and (if appropriate) waves. The module notably takes into account non-cohesive material which is ideal for simulating sediment dispersion from dredging activities (DHI Group, 2017a). The hydrodynamic basis for the MT Module is calculated using the Hydrodynamic Module of the MIKE 21 Flow Model FM modelling system and the MT is implemented as a coupled model with the two running concurrently. The following processes may be included in the simulation:

- Multiple sediment fractions
- Inclusion of non-cohesive sediments
- Multiple bed layers
- Flocculation
- Hindered settling
- Bed shear stress from combined currents and waves
- Forcing by waves
- Consolidation
- Tracking sediment spills
- Morphological update of the bed

In the MT-module, the settling velocity varies, according to the salinity, if included, and the concentration taking into account flocculation in the water column. Bed erosion can either be non-uniform, i.e. the erosion of soft and partly consolidated bed, or uniform, i.e. the erosion of a dense

and consolidated bed. The bed is described as layered and is characterised by the density and shear strength (DHI Group, 2017a).

The Hydrodynamic model results are presented below). The Hydrodynamic model was used within the dredging dispersal modelling, its calibration and validation is part of the hydrodynamical modelling section of this report.

8.4.3 METHODOLOGY

8.4.3.1 MODELLING SIMULATIONS

The modelling approach incorporates the use of the MIKE 21 FM Mud Transport Module, which is driven by the Hydrodynamic Module.

The modelling scenario developed to address the study objectives involved simulating the dredging and disposal cycles of the three considered stages for Rosslare Europort ORE Hub port expansion. The three stages were defined considering the worst-case situation where the highest volume to be dredged and disposed is continuously dispersed into the water column.

Further information regarding the modelling of the dredge cycle can be found in section 8.3.3.3 Modelling Setup.

MODELLING SETUP

The computational mesh used for both the Hydrodynamic and Mud Transport modules in the Mike 21 software is a triangular mesh covering approximately 2,400 km². The mesh resolution, as shown in is set at 2 km in offshore areas where the water depth exceeds 75m MSL, and ranges from 200 to 150 meters in the shallower areas near Rosslare Europort Figure 8-37.

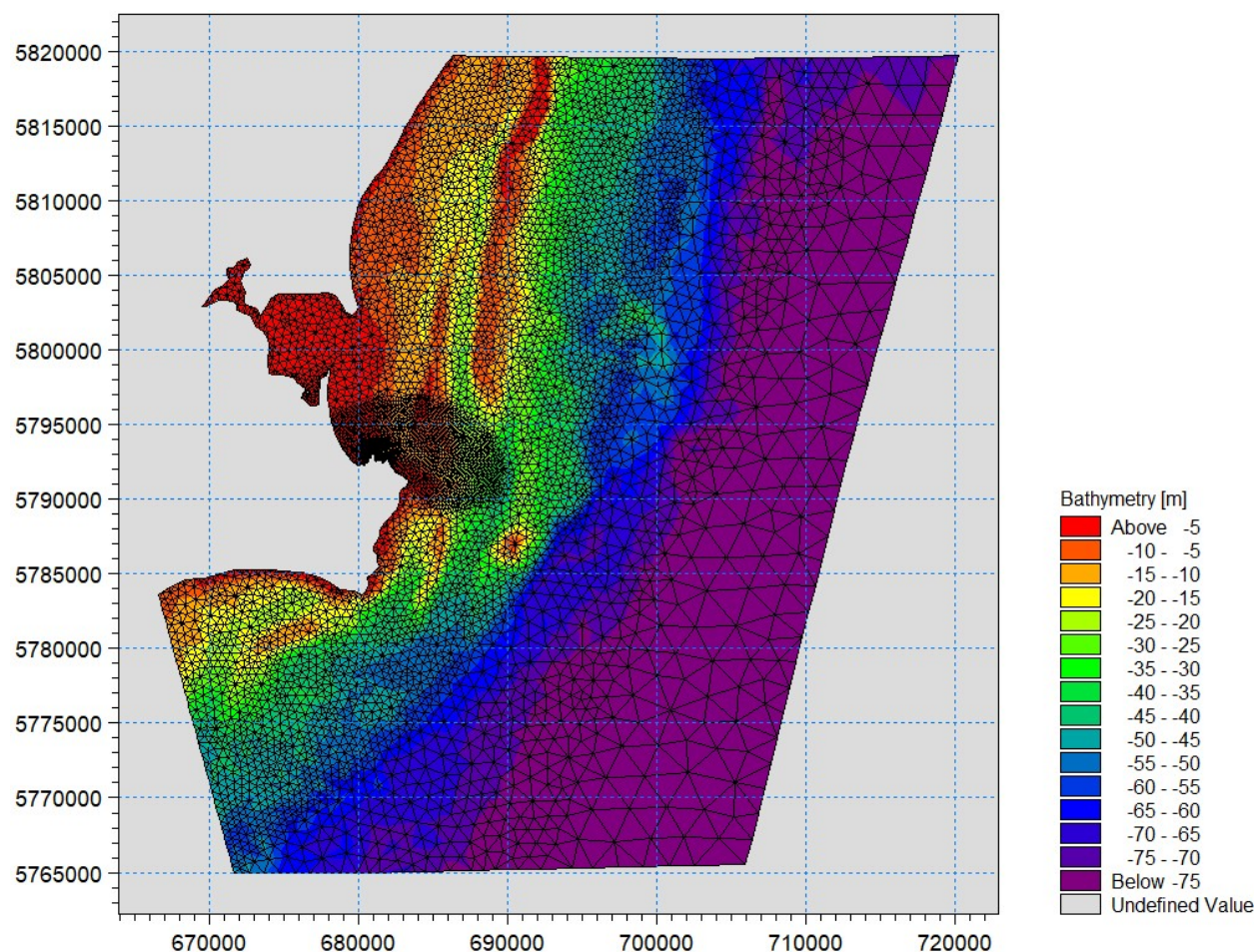


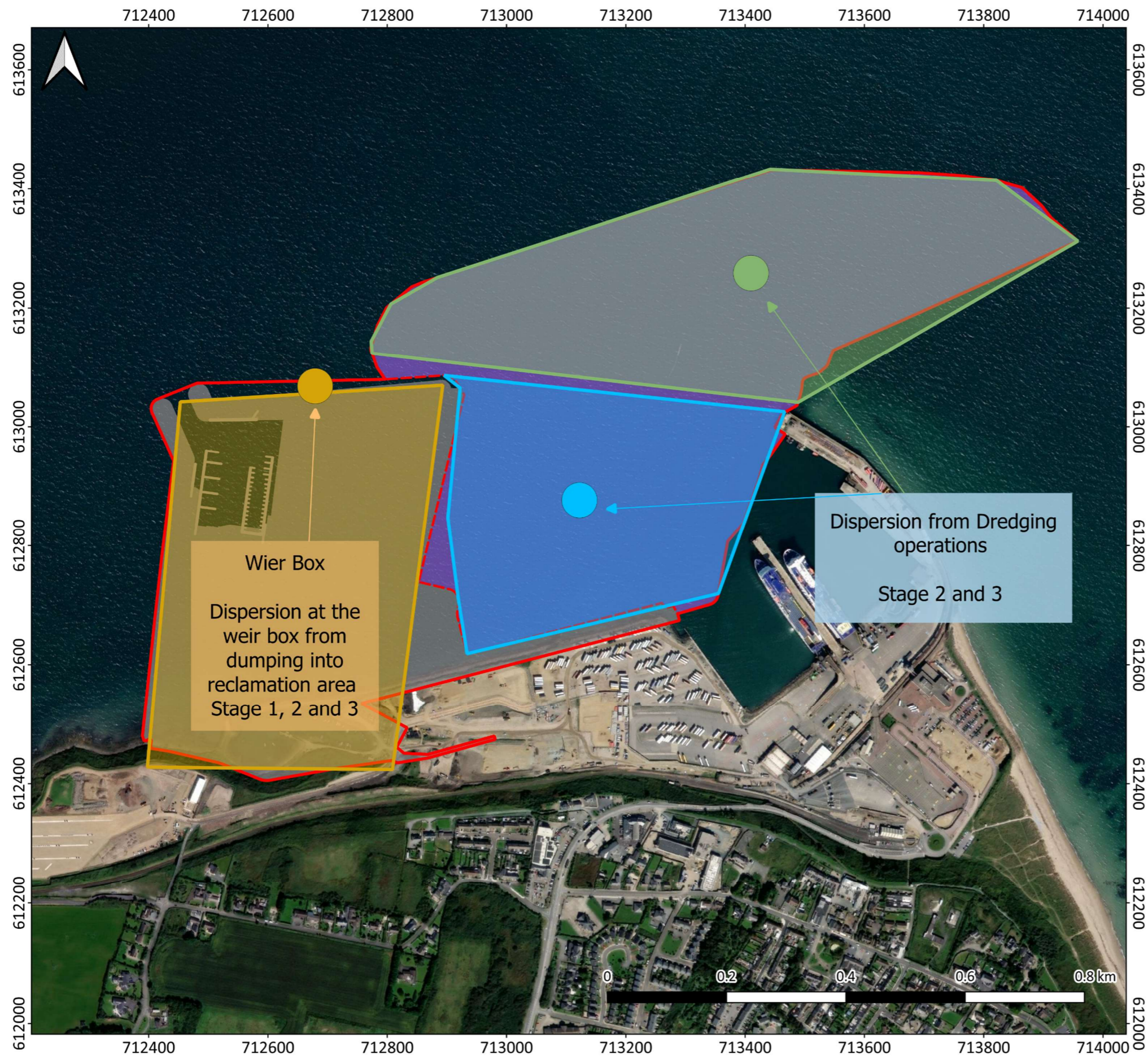
Figure 8-37: Model Mesh

The three stages represent three separate scenarios focusing on modelling the dispersion of material during both dredging and disposal operations. Each Stage represent different disposal and dredge cycles. Table 8-15 shows the duration of each cycle considering the three different stages.

Table 8-15: Duration of dredge cycle components

Stage 1			Stage 2			Stage 3		
Cycle	Duration (Months)	Hours per day	Cycle	Duration (Months)	Hours per day	Cycle	Duration (Months)	Hours per day
Disposal	3	12	Dredging	2	12	Dredging	8	20
-	-	-	Disposal	2	12	Disposal	8	20

Figure 8-38 shows the dredging and disposal locations considered within the 3 stages. The dredging point for both Stages 2 and 3 is centrally located within the outermost and innermost areas. The disposal point, located at the weir box at the outer boundary of the reclamation area, is in a more exposed location, as this represents a worst-case scenario for sediment dispersion.



Rosslare ORE Hub
 Environmental Impact Assessment Report

Dredging and Disposal Locations

Legend
Rosslare ORE Hub
 Proposed Development Boundary
 Dredge Area
 Reclamation Area
Indicative Dredging and Disposal Dispersion
 Dredging Operations - Outermost Area
 Dredging Operations - Innermost Area
 Reclamation Dumping Area

Coordinate Reference System: EPSG:2157
 Project Number: 23172
 Date: 08/04/2025
 Author, Organisation: NC, GDG
 Revision: 00

Figure 8-38: Dredging and disposal locations considered for the sediment dispersal

The representative material for the sediment dispersal considering disposal modelling scenario was chosen as the average of all provided sediment sample data, as outlined in Table 8-16. The selected representative sediment sample comprises three sediment classes and is detailed in Table 8-17. The critical shear stress for particle motion was determined using the following equation (Van Rijn, 1984).

$$\tau_c = \theta^*(s - 1)\rho_m g d_{50}$$

where τ_c is the critical bed shear stress, θ is the dimensionless Shields parameter for the given particle size, s is the specific gravity of the particles and is calculated as the ratio of specific weight of sediment to the specific weight of water, ρ_m is the density of water, g is the constant for acceleration due to gravity, and d_{50} is the median particle size.

The drag coefficient, K , for each sample was derived using the following formula;

$$K = d_{50} \left(\frac{g \rho_m (\rho_p - \rho_m)}{\mu^2} \right)^{1/3}$$

where g is the acceleration due to gravity, d_{50} is median grain size, ρ_p is the density of the particle, ρ_m is the density of water and μ is the dynamic viscosity of a liquid. The settling velocity (U_t) is then calculated according to the following equation;

$$U_t = \left(\frac{4 g d_{50}^{(1+n)} (\rho_p - \rho_m)}{3 b \mu^n \rho_m^{(1-n)}} \right)^{1/(2-n)}$$

whereby the b and n coefficients are tabulated to the value of K (Table 8-16) (McCabe et al., 2005) (Tilton et al., 2007).

Table 8-16: Determination settling velocity coefficients b and n determined based on drag coefficient K

Flow Regime	Drag coefficient (K)	b	n
Stokes	$K < 3.3$	24	1
Intermediate	$3.3 < K < 43.6$	18.5	0.6
Newton	$43.6 < K < 2360$	0.44	0

Table 8-17 Model input sediment properties for dredging and disposal operations

Stages	Representative Material Type	Settling Velocity (m/s)	Shield's parameter (dimensionless)	Critical Shear Stress for deposition (N/m ²)
Stage 1 Perimeter Bunds	Coarse Silt	0.000862	0.1467	0.0682
	Fine Sand	0.013874	0.0609	0.1137
Stage 2	Clay	0.00000064	0.29143	0.00351
	Silt	0.0002824	0.18742	0.04986
	Sand	0.0460450	0.03293	0.17526
	Gravel	0.6603337	0.05566	8.22557

Stages	Representative Material Type	Settling Velocity (m/s)	Shield's parameter (dimensionless)	Critical Shear Stress for deposition (N/m ²)
Stage 3	Clay	0.0000011	0.28868	0.004647
	Fine Silt	0.0000540	0.23744	0.027629

The spill rates associated with disposal in the reclamation area and dredging activities (Stages 2 and 3) represent the percentage of dredged material that disperses into the wider environment beyond the containment boundaries at the point of dredging (for dredging activities) and at the weir box (for disposal). Perimeter Bunds accounts for spills from the reclamation area rockfill, Stage 2 involves a 1% spill rate from TSHD or CSD, and Stage 3 includes a 3% loss during mechanical dredging. The spill rate for disposal at the reclamation area is estimated at 1%, which reflects the material that escapes beyond the weir box and disperses into the surrounding environment. Table 8-18 outlines the spill rates for both dredging and disposal activities for each stage. These spill rates are based on the dispersal of sediment into the wider environment and do not represent the rate of material loss from the barge itself.

Table 8-18: Spilling rates for both Dredging and disposal activities at each stage.

Stages	Disposal Spilling rate	Dredging Spilling rate
Stage 1 Perimeter Bunds	1 %	-
Stage 2	1 %	1 %
Stage 3	1 %	3 %

8.4.4 MODEL RESULTS

The results were gathered from several locations, including three sites within 200 meters of Rosslare Europort (Points 1, 2, and 3) and three sites 2.0 km offshore (Points 4, 5, and 6). Additional data was gathered from six nearby Special Areas of Protection and Conservation (SPAs and SACs), representing the closest point of each area to Rosslare Europort. These include Seas Off Wexford cSPA (Point 2) (it overlaps with Proposed Development Boundary), Carnsore Point SAC (Point 7), Wexford Harbour and Slobbs SPA (Point 8), The Raven SPA (Point 9), Blackwater Bank SAC (Point 10), and Long Bank SAC (Point 11).

Table 8-19 provides a list of the results from the extracted points, while the location of these points can be seen in Figure 8-39

Table 8-19 Point locations for the extracted numerical results.

Point Number	Name	Longitude (m)	Latitude (m)
Point 1	Nearshore West	679481	5793210
Point 2	Nearshore Centre (Seas Off Wexford cSPA)	680981	5793210
Point 3	Nearshore East	682481	5793210
Point 4	Offshore West	679481	5795010

Point Number	Name	Longitude (m)	Latitude (m)
Point 5	Offshore Centre	680981	5795010
Point 6	Offshore East	682481	5795010
Point 7	Carnsore Point SAC	683241	5791984
Point 8	Wexford Harbour and Slobbs SPA	678383	5799453
Point 9	The Raven SPA	680168	5802163
Point 10	Blackwater Bank SAC	687009	5792050
Point 11	Long Bank SAC	683043	5794430

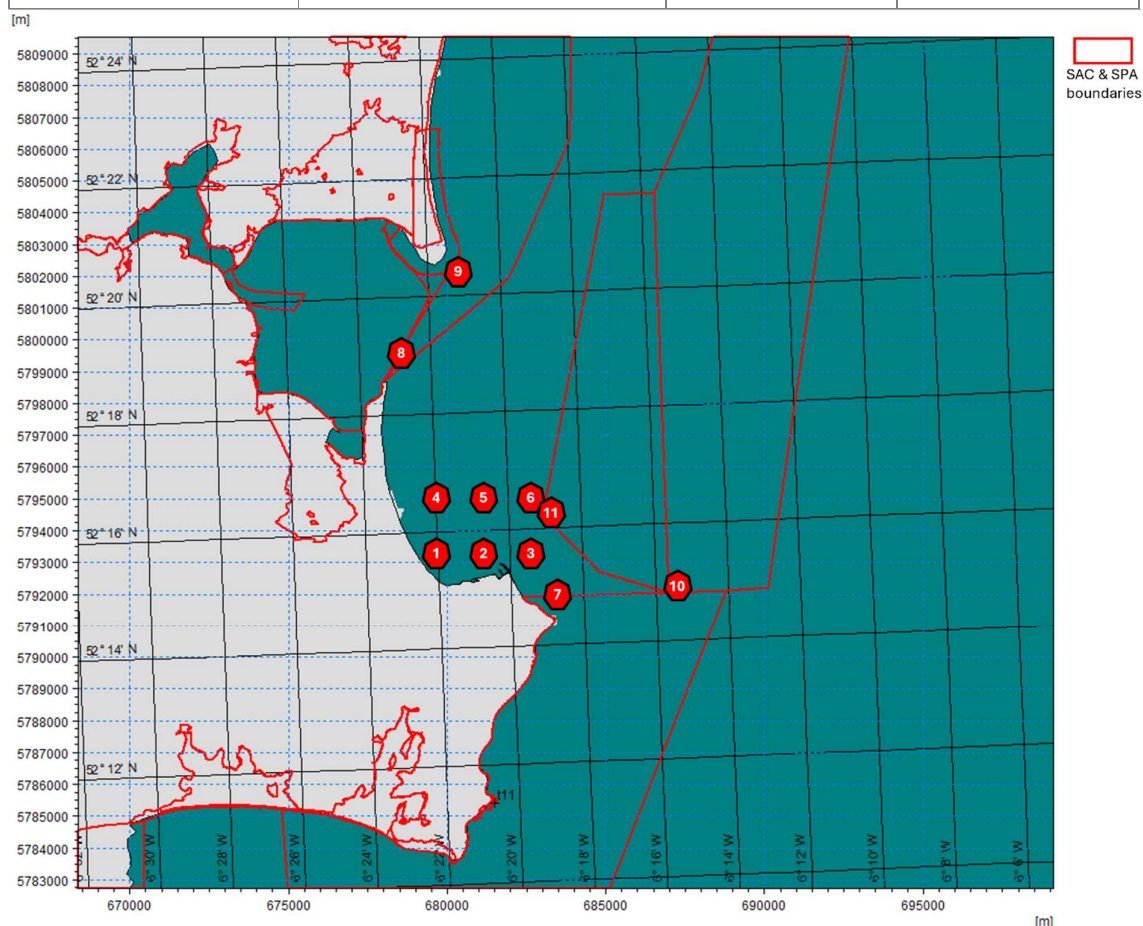


Figure 8-39: Location of the extracted results points.

8.4.4.1 SUSPENDED SEDIMENT CONCENTRATION (SSC)

STAGE 1: PERIMETER BUNDS

- The maximum total Suspended Sediment Concentration (SSC) observed at the points located in front of the project development during the 3-month disposal period is approximately 0.00023 Kg/m³ (0.23 mg/L) at the nearshore eastern point of Rosslare harbour
- Figure 8-40, Figure 8-41 and Figure 8-42 illustrate the distribution of sediment plumes resulting from the disposal of material beyond the reclamation area. The highest SSC is observed at the

disposal point on the outer boundary of the reclamation area at the weirbox, which overlaps with the Seas off Wexford SPA, reaching 0.007 Kg/m^3 (7 mg/L). Both the maximum and average SSC values are concentrated near the area between the west and east of Rosslare Harbour, indicating that the sediment remains confined within the port's area of influence. The SSC values are negligible south of Greenore Point and similarly low in areas to the west, beyond Rosehill Bay Beach.

- The Maximum Total SSC values calculated at each of the 11 points is shown in Table 8-20. It highlights that, apart from the higher values near the port, the points representing the other SAC and SPA areas have maximum SSC results below 0.00145 Kg/m^3 (1.45 mg/L).

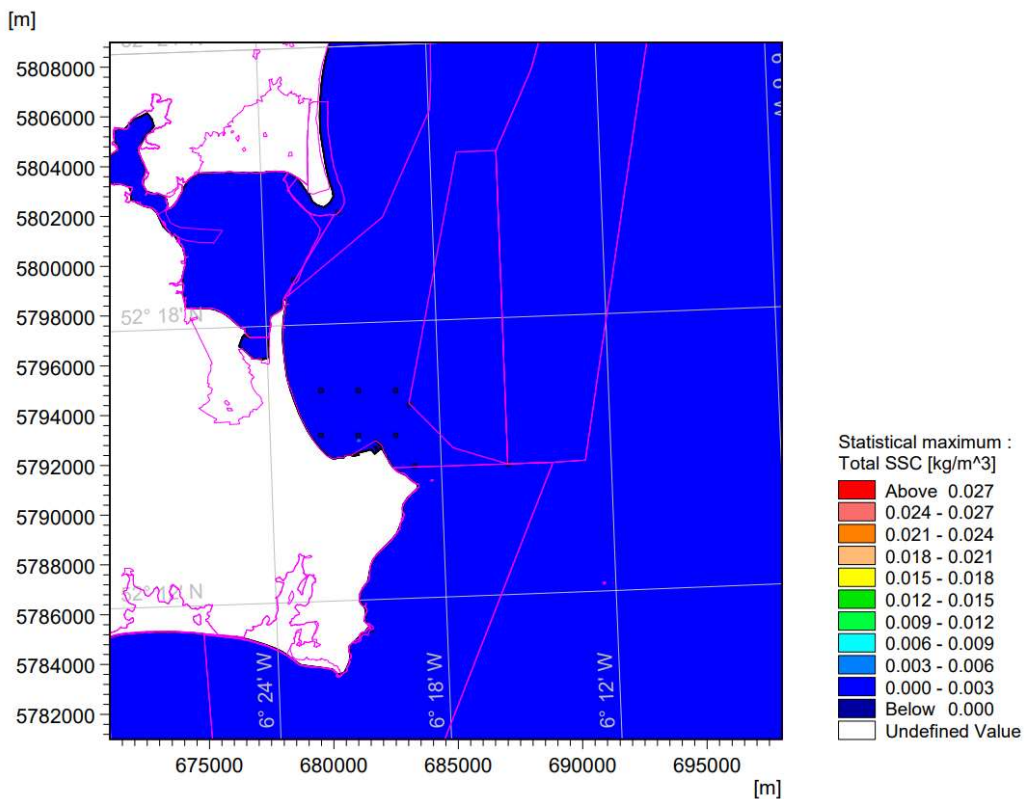


Figure 8-40: Maximum total Suspended Sediment Concentration (SSC) from the 3-month disposal simulation (Perimeter Bunds Stage)

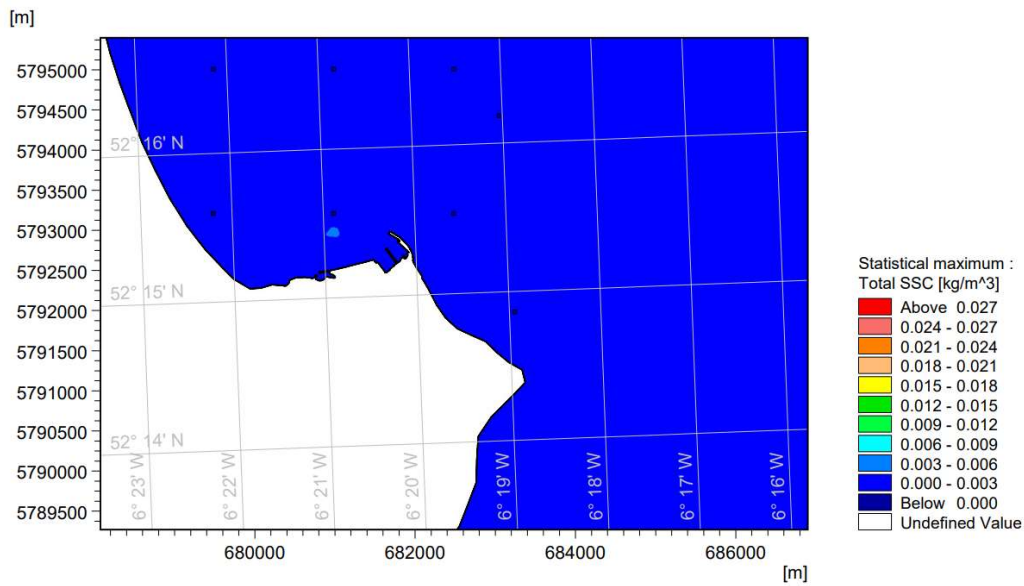


Figure 8-41: Close-up view of the port area showing the results of the maximum total Suspended Sediment Concentration (SSC) from the 3-month disposal simulation (Perimeter Bunds Stage)

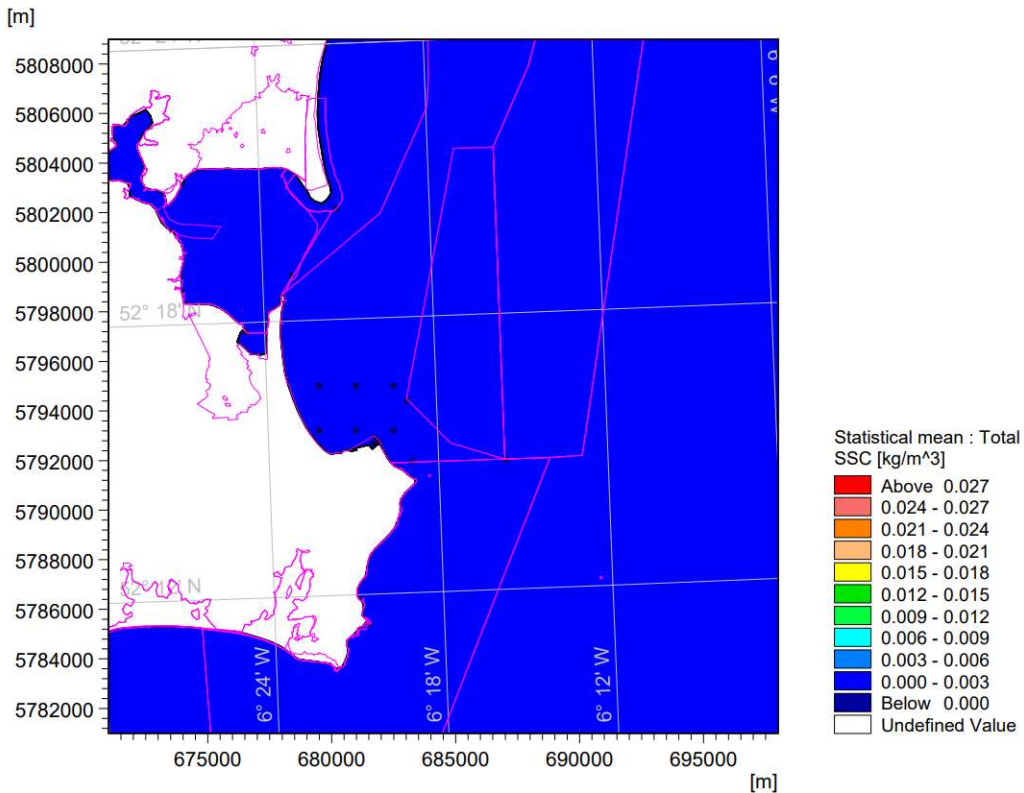
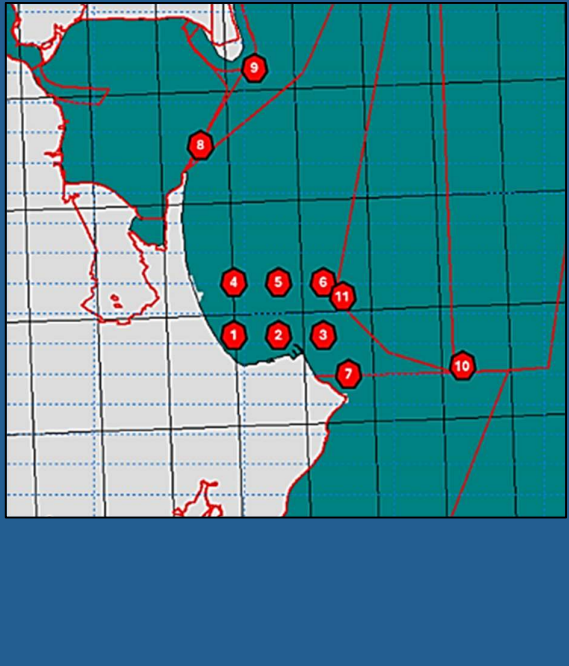


Figure 8-42: Average total Suspended Sediment Concentration (SSC) from the 3-month disposal simulation (Perimeter Bunds Stage)

Table 8-20: Maximum total Suspended Sediment Concentration SSC for the extracted numerical results (Perimeter Bunds Stage)

Point Number	Name	Max total SSC (kg/m ³)	
1	Nearshore West	0.000027888	
2	Nearshore Centre (Seas Off Wexford cSPA)	0.000038337	
3	Nearshore East	0.000231187	
4	Offshore West	0.000000178	
5	Offshore Centre	0.000034072	
6	Offshore East	0.000017577	
7	Carnsore Point SAC	0.001457500	
8	Wexford Harbour and Slobs SPA	0.000000013	
9	The Raven SPA	0.000000025	
10	Blackwater Bank SAC	0.000012435	
11	Long Bank SAC	0.000020682	

STAGE 2: TRAILING SUCTION HOPPER DREDGER

- The maximum total Suspended Sediment Concentration (SSC) observed during the two-month dredging and disposal period at the locations in front of the Proposed Development is around 0.00242535 Kg/m³ (2.43 mg/L) at the nearshore central point of Rosslare Harbour (P2), which overlaps with the Seas off Wexford cSPA.
- From Figure 8-43 to Figure 8-45 we observe the distribution of the maximum and average sediment plumes caused by material disposal beyond the reclamation area. The peak SSC is found at the weirbox, located on the outer boundary of the reclamation zone, with concentrations reaching 0.015 Kg/m³ (15 mg/L).
- The highest SSC values are concentrated near Rosslare Harbour, extending 1.5 km west to Rosehill Bay Beach and 2.5 km southeast to Greenore Point. South of Greenore Point, SSC values become negligible, and similarly low concentrations are found to the west, beyond Rosehill Bay Beach.
- The maximum SSC values calculated at all 11 locations is presented in Table 8-21. Aside from the elevated concentrations near the port, which overlaps with the Seas off Wexford SPA, the SSC levels at the SAC and SPA sites remain below 0.00516202 Kg/m³ (5.16 mg/L), as observed at the Carnsore Point SAC.

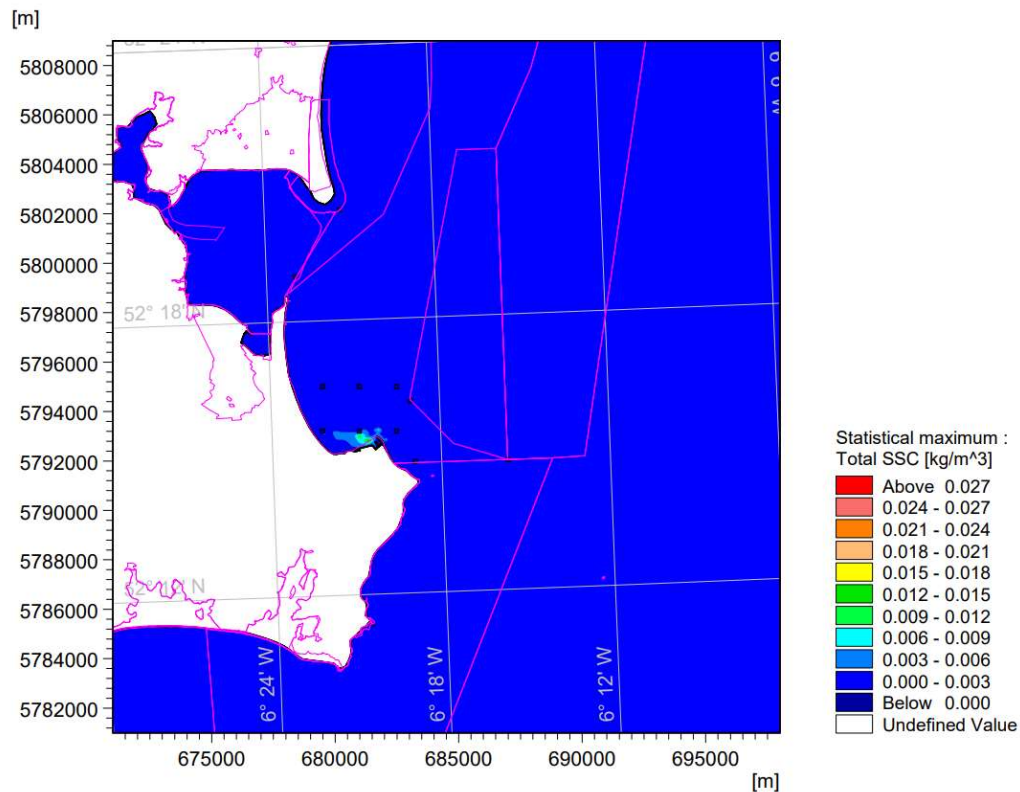


Figure 8-43: Maximum total Suspended Sediment Concentration (SSC) from the 2-month dredging and disposal simulation (Stage 2)

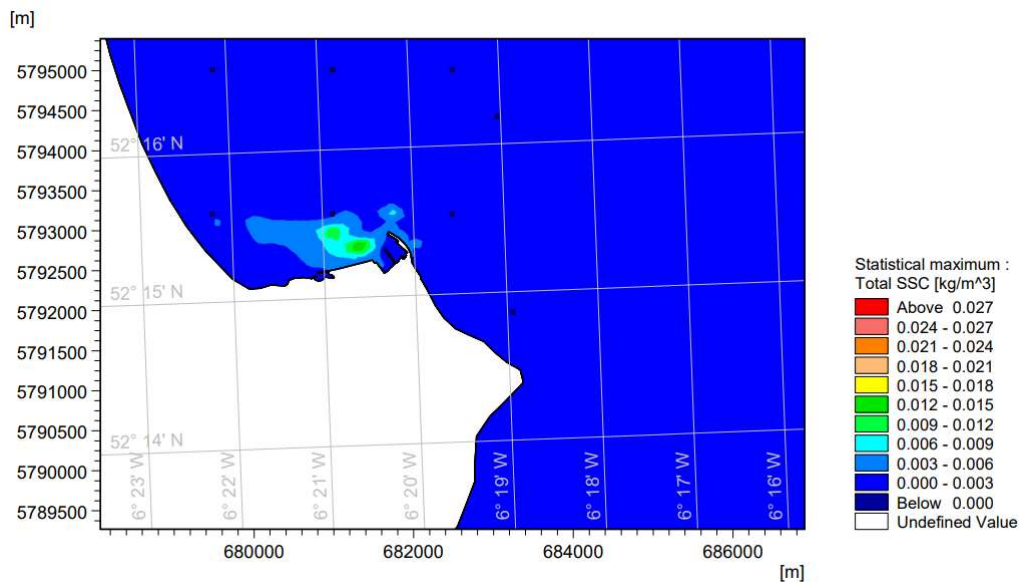


Figure 8-44: Close-up view of the port area showing the results of the maximum total Suspended Sediment Concentration (SSC) from the 2-month dredging and disposal simulation (Stage 2)

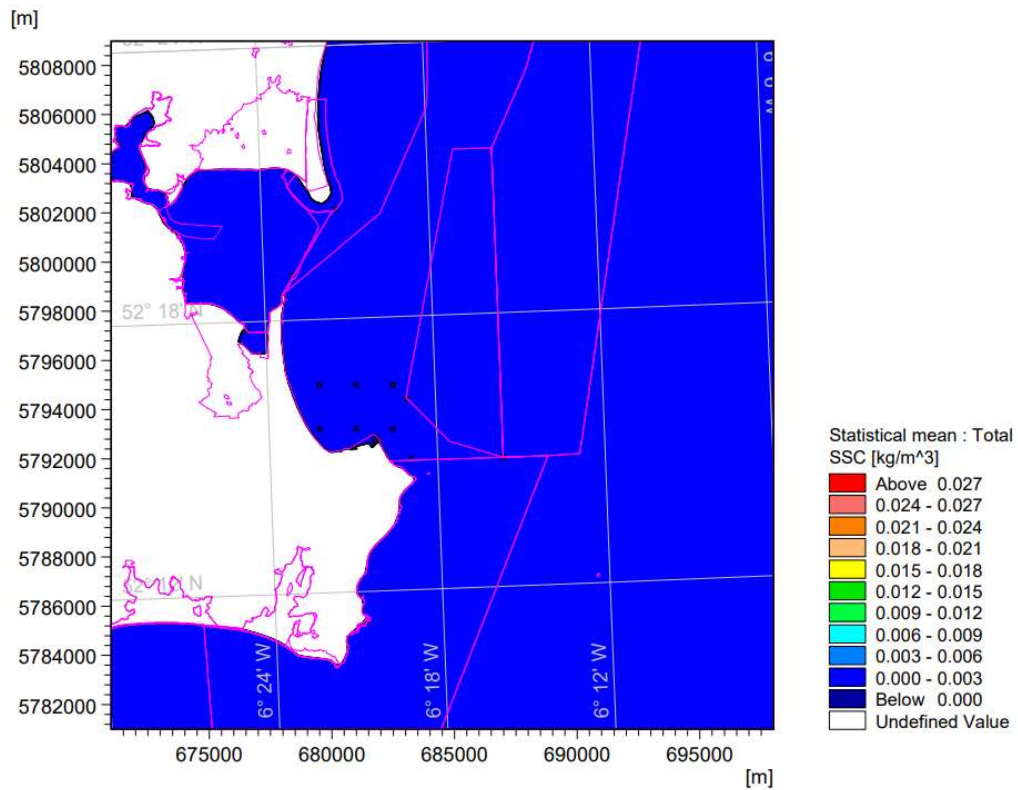
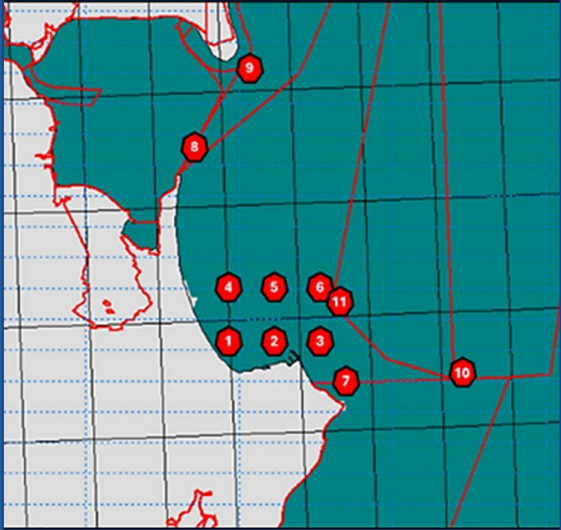


Figure 8-45: Average total Suspended Sediment Concentration (SSC) from the 2-month dredging and disposal simulation (Stage 2)

Table 8-21: Maximum total Suspended Sediment Concentration SSC for the extracted numerical results (Stage 2)

Point Number	Name	Max total SSC (kg/m ³)	
1	Nearshore West	0.00118989	
2	Nearshore Centre (Seas Off Wexford cSPA)	0.00242535	
3	Nearshore East	0.00094153	
4	Offshore West	0.00081174	
5	Offshore Centre	0.00031321	
6	Offshore East	0.00010552	
7	Carnsore Point SAC	0.00516202	
8	Wexford Harbour and Slobbs SPA	0.00014776	
9	The Raven SPA	0.00024671	
10	Blackwater Bank SAC	0.00011443	
11	Long Bank SAC	0.00010336	

STAGE 3: BACKHOE DREDGER

- The maximum total Suspended Sediment Concentration (SSC) observed at the points located in front of the project development during the 8-month dredging and disposal period is approximately 0.0017290Kg/m³ (1.73mg/L) at the nearshore centre point of Rosslare harbour, which overlaps with the Seas off Wexford SPA.
- From Figure 8-46 to Figure 8-48 one can observe the distribution of the maximum and the average sediment plumes resulting from the disposal of material beyond the reclamation area. The highest SSC is observed at weirbox location, in outer boundary of the reclamation area, which overlaps with the Seas off Wexford SPA, reaching 0.02 Kg/m³ (20 mg/L). As for Stage 1 and Stage 2, the maximum and average SSC values are concentrated near Rosslare Harbour, at 1.5km to the west (Rosehill Bay Beach) and 2.5km to the south-east (Greenore Point). The SSC values are negligible south of Greenore Point and similarly low in areas to the west, beyond Rosehill Bay Beach.
- The Maximum Total SSC values calculated at each of the 11 points is presented in Table 8-22. It highlights that, apart from the higher values near the port, the points representing the other SAC and SPA areas have maximum SSC results below 0.0099627Kg/m³ (9.96 mg/L) which is observed at Carnsore Point SAC.

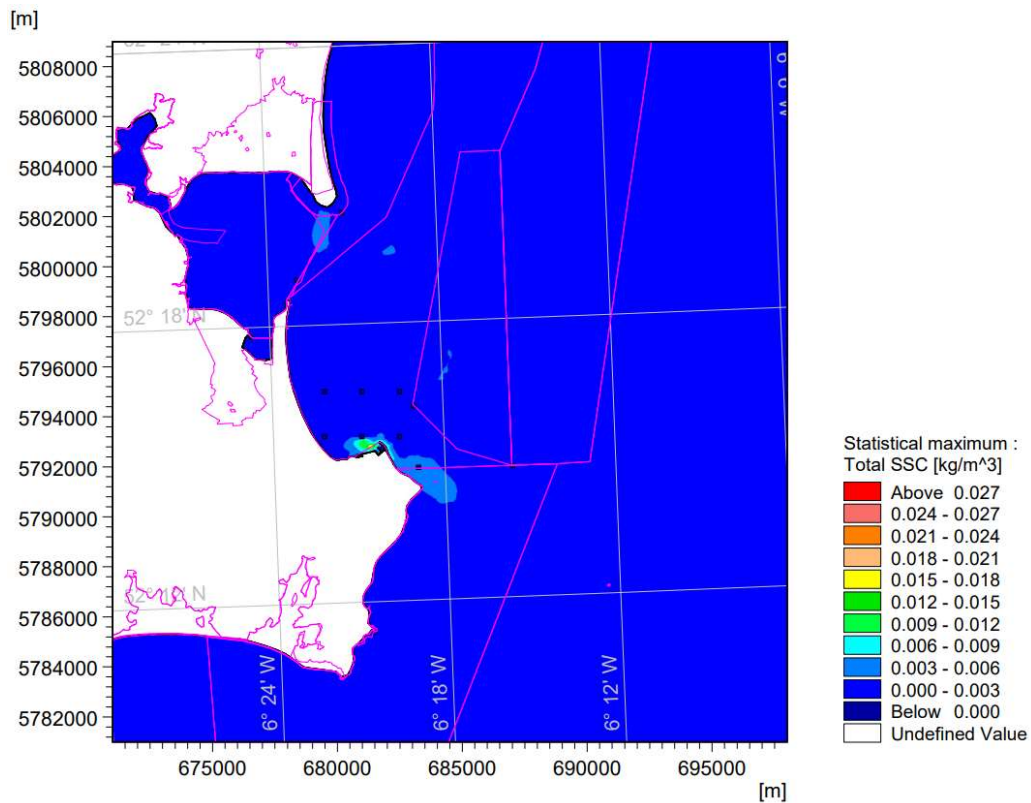


Figure 8-46: Maximum total Suspended Sediment Concentration (SSC) from the 8-month dredging and disposal simulation (Stage 3)

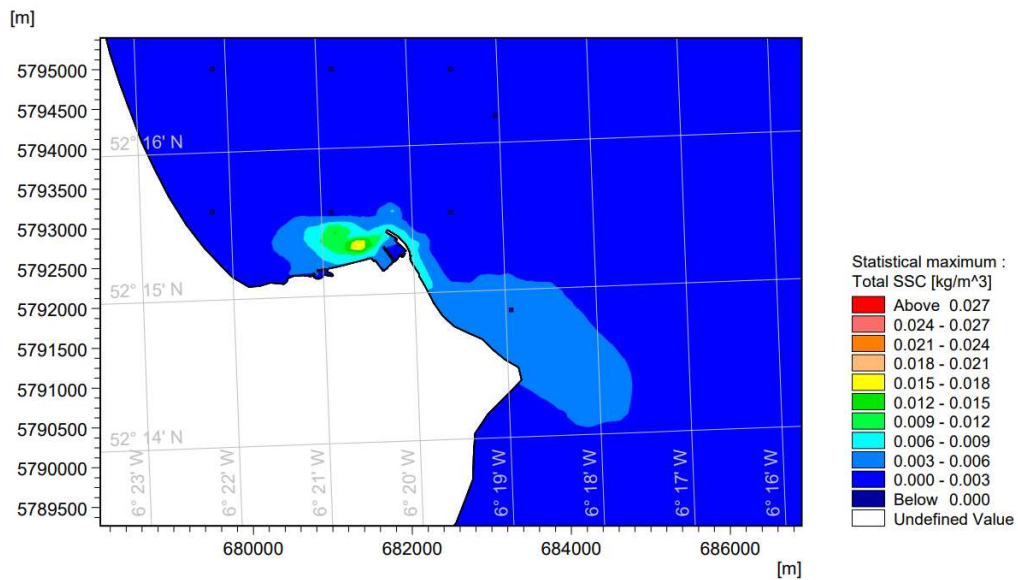


Figure 8-47: Close-up view of the port area showing the results of the maximum total Suspended Sediment Concentration (SSC) from the 8-month dredging and disposal simulation (Stage 3)

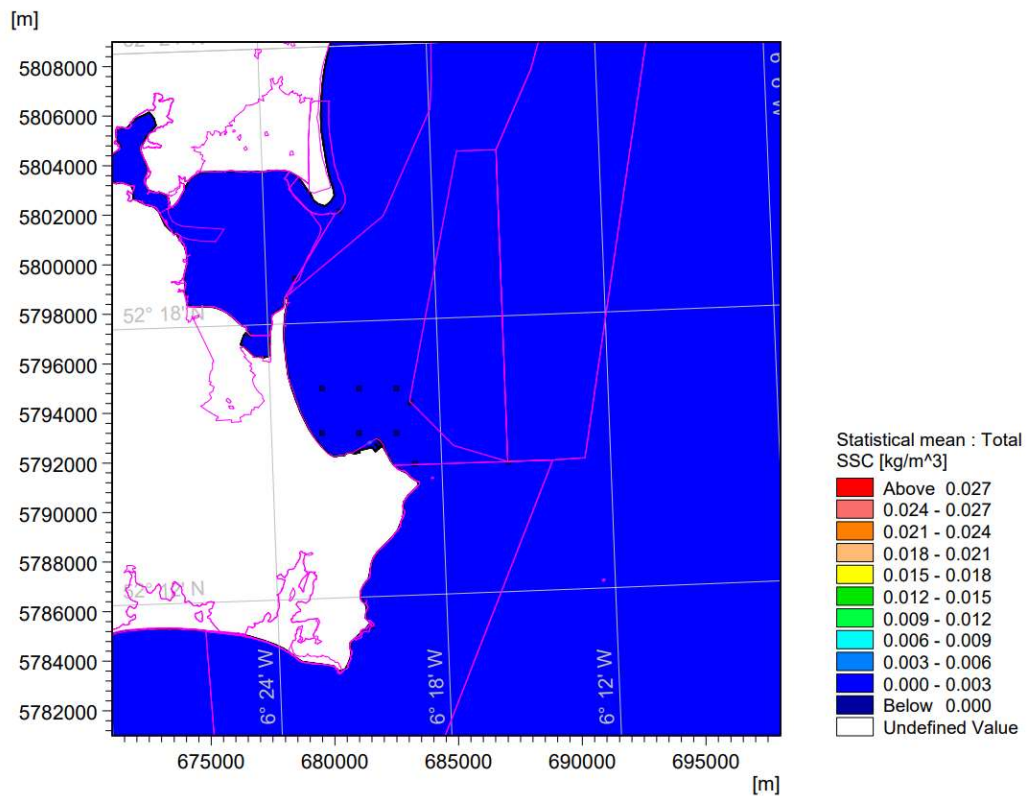
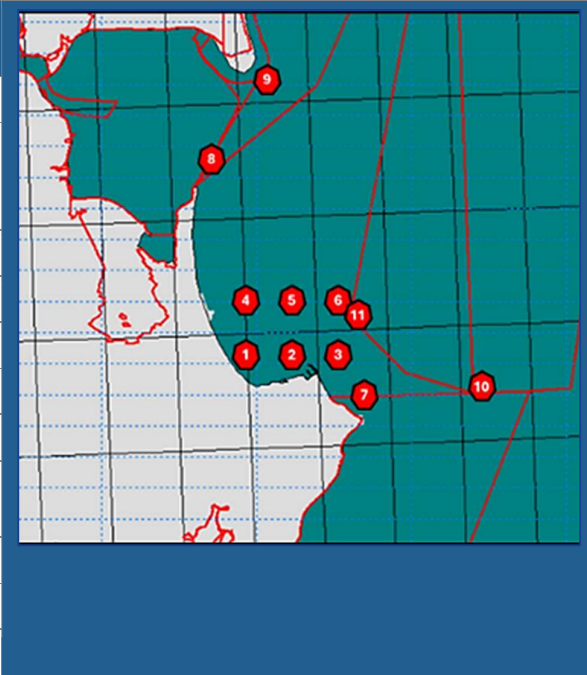


Figure 8-48: Average total Suspended Sediment Concentration (SSC) from the 8-month dredging and disposal simulation (Stage 3)

Table 8-22: Maximum total Suspended Sediment Concentration SSC for the extracted numerical results (Stage 3)

Point Number	Name	Max total SSC (kg/m ³)	
1	Nearshore West	0.0006343	
2	Nearshore Centre (Seas Off Wexford cSPA)	0.0017290	
3	Nearshore East	0.0006237	
4	Offshore West	0.0001254	
5	Offshore Centre	0.0002479	
6	Offshore East	0.0005284	
7	Carnsore Point SAC	0.0099627	
8	Wexford Harbour and Slobs SPA	0.0014411	
9	The Raven SPA	0.0002859	
10	Blackwater Bank SAC	0.0003939	
11	Long Bank SAC	0.0020431	

8.4.4.2 BED THICKNESS CHANGE

STAGE 1: PERIMETER BUNDS STAGE

- The same analysis is presented here for the evolution of bed thickness. The maximum total bed thickness over the 3-month disposal simulation period is depicted from Figure 8-49 to Figure 8-51
- The maximum total bed thickness change observed during the simulation at any of the 11 selected points is approximately 0.0026 cm, as shown in Table 8-23. This maximum value occurs in the nearshore area close to Rosslare Harbour, which overlaps with the Seas off Wexford SPA. For the other SAC and SPA areas, the highest bed thickness change is at Carnsore Point SAC, with a value of 0.0082 cm, which is considered negligible.
- Across the entire area, the largest bed thickness change is observed near the disposal site at the outer boundary of the reclamation area, which overlaps with the Seas off Wexford SPA, with a maximum of 8 cm during the 3-month disposal period. Figure 8-49 to Figure 8-51 show that the sediment deposited on the seabed remains confined to the area around the outer boundary of the reclamation site. Bed thickness changes beyond a 1 km radius from Rosslare Harbour are considered negligible (less than 2 cm), including all other SAC and SPA areas.

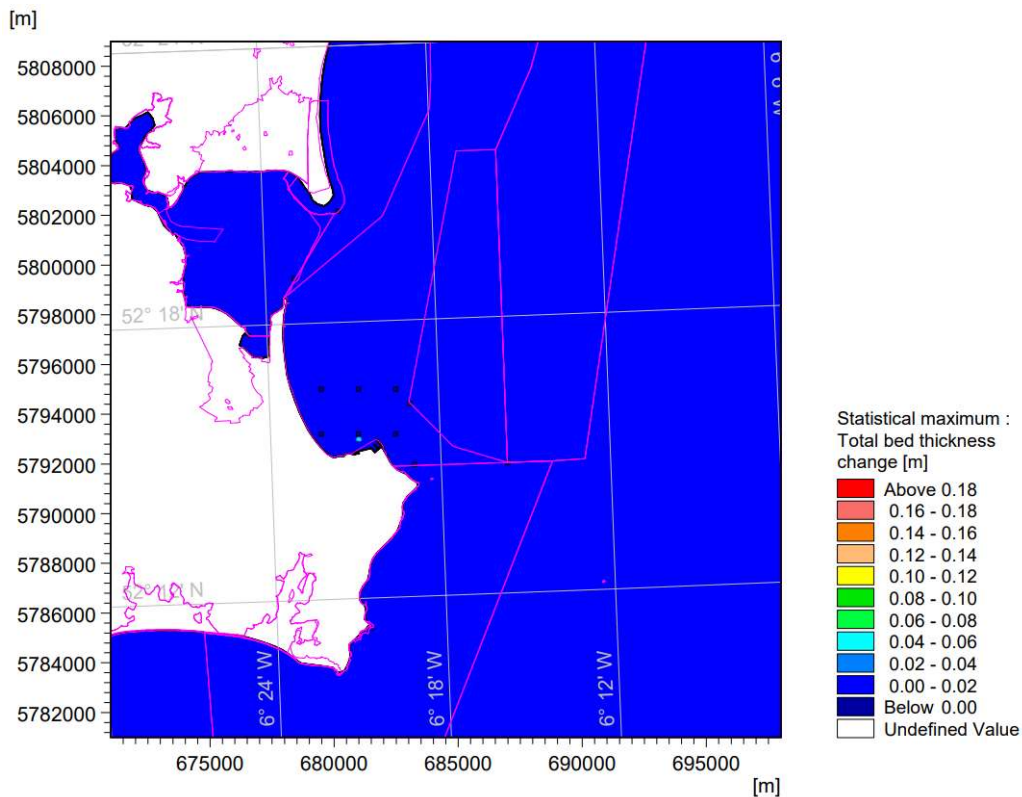


Figure 8-49: Maximum Bed thickness change from the 3-month disposal simulation (Perimeter Bunds Stage)

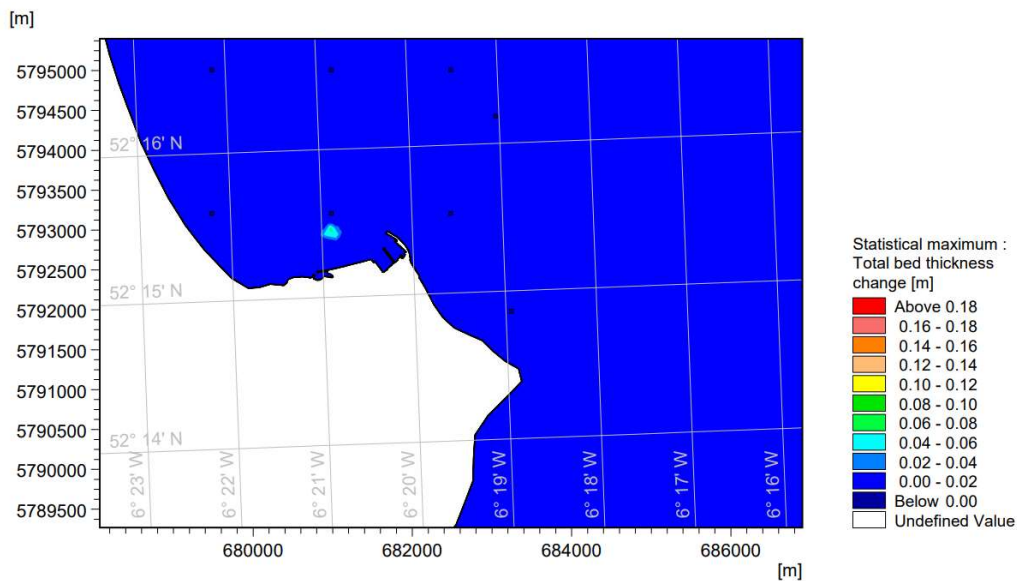


Figure 8-50: Close-up view of the port area showing the results of the maximum bed thickness change from the 3-month disposal simulation (Perimeter Bunds Stage)

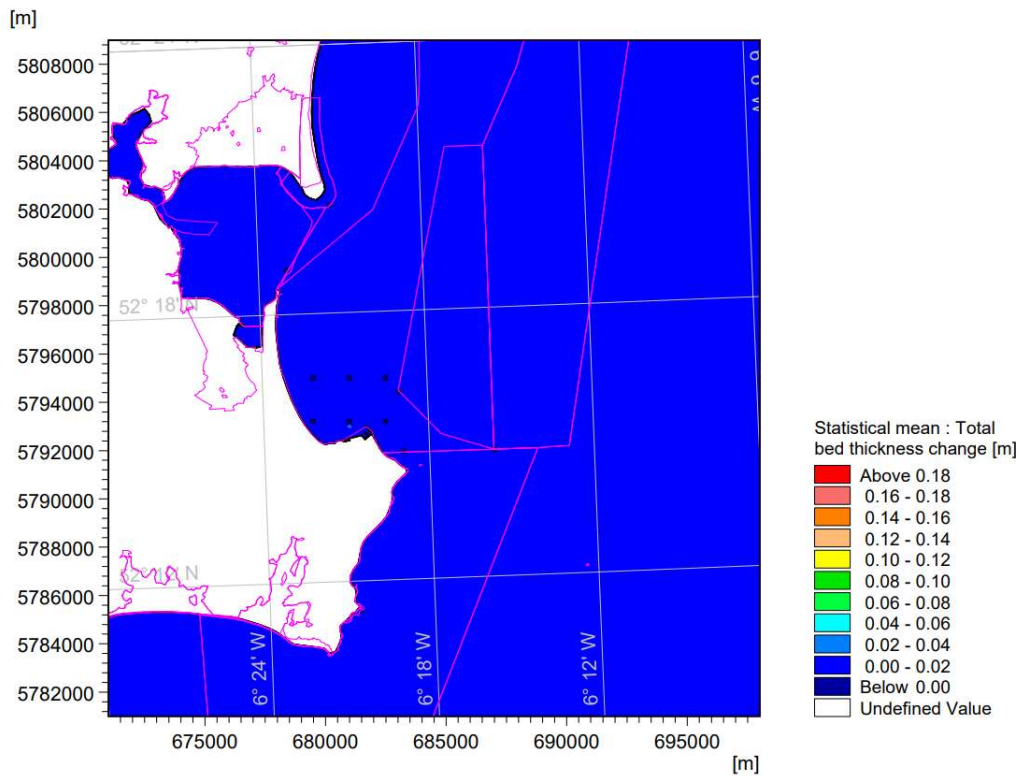


Figure 8-51: Average bed thickness change from the 3-month disposal simulation (Perimeter Bunds Stage)

Table 8-23: Total bed thickness change for the extracted numerical results (Perimeter Bunds Stage)

Point Number	Name	Max Total bed thickness change (m)	
1	Nearshore West	0.000017698	
2	Nearshore Centre (Seas Off Wexford cSPA)	0.000026413	
3	Nearshore East	0.000019322	
4	Offshore West	0.000000223	
5	Offshore Centre	0.000001482	
6	Offshore East	0.000001726	
7	Carnsore Point SAC	0.000082105	
8	Wexford Harbour and Slobbs SPA	0.000000145	
9	The Raven SPA	0.000000166	
10	Blackwater Bank SAC	0.000002337	
11	Long Bank SAC	0.000002476	

STAGE 2: TRAILING SUCTION HOPPER DREDGER

Figure 8-52 to Figure 8-54 illustrate the maximum bed thickness change during the 2-month dredging and disposal simulation period.

- The largest bed thickness increase, reaching 6 cm, is found near the disposal site at the weirbox location, which overlaps with the Seas off Wexford SPA, during the two-month period. Sediment deposition remains confined around the outer boundary of the reclamation area. For the other SAC and SPA locations, the highest bed thickness change is at Carnsore Point SAC and is 0.030 cm. According to Table 8-24, changes in bed thickness are up to 0.025 cm within the harbour area and less than 0.001 cm within a 1 km radius of the Proposed Development.

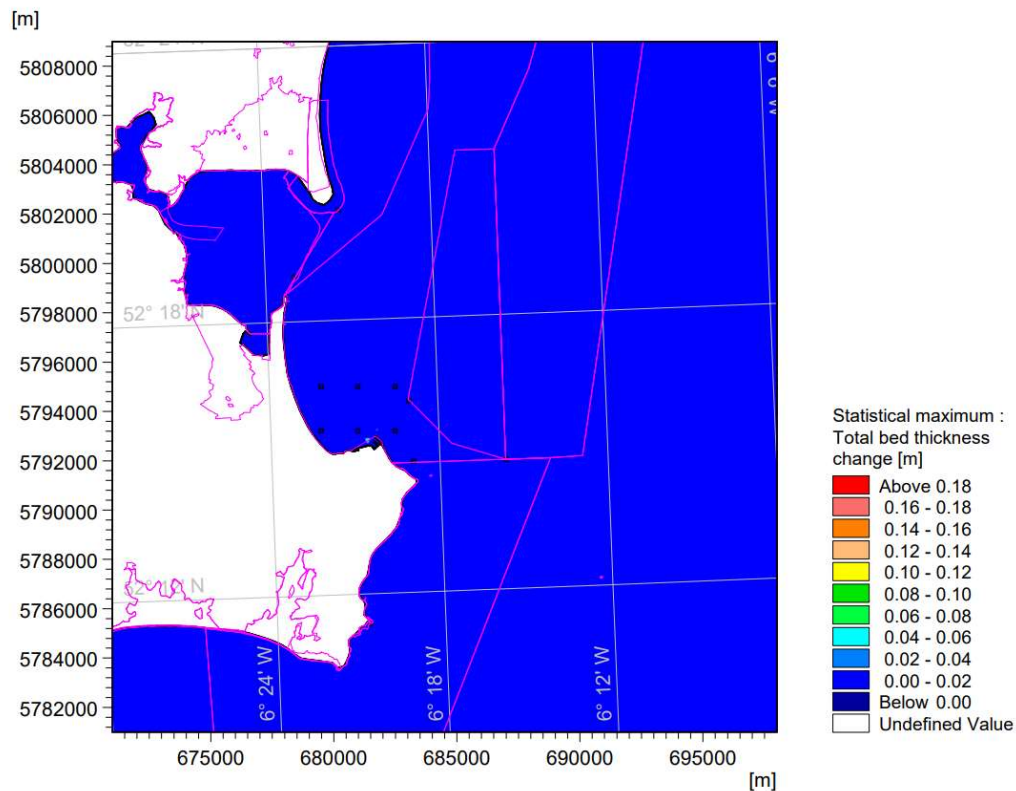


Figure 8-52: Maximum Bed thickness change from the 2-month dredging and disposal simulation (Stage 2)

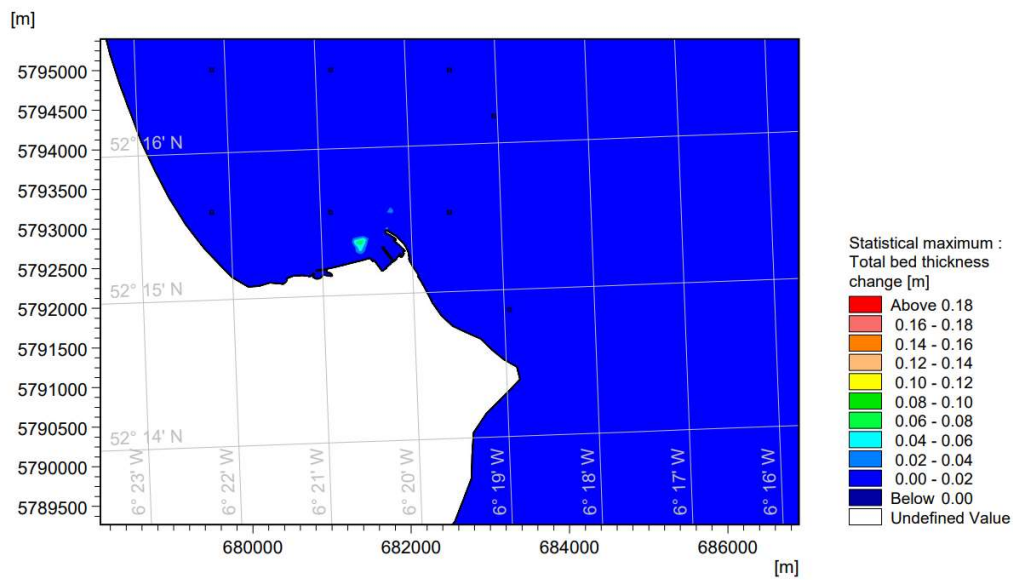


Figure 8-53: Close-up view of the port area showing the results of the maximum bed thickness change from the 2-month dredging and disposal simulation (Stage 2)

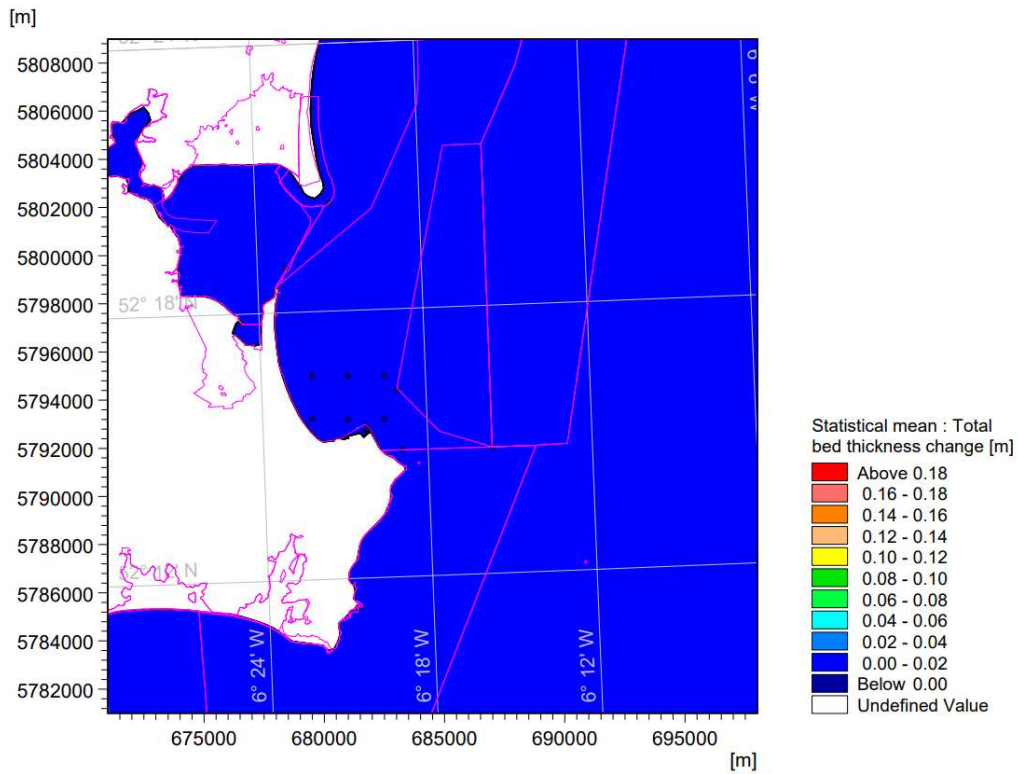
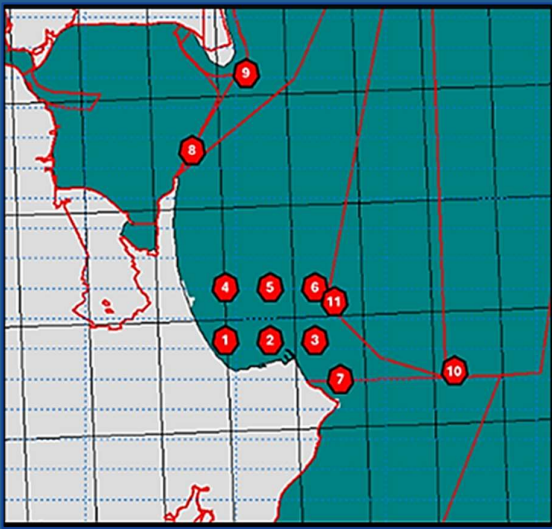


Figure 8-54: Average bed thickness change from the 2-month dredging and disposal simulation (Stage 2)

Table 8-24: Total bed thickness change for the extracted numerical results (Stage 2)

Point Number	Name	Max Total bed thickness change (m)	
1	Nearshore West	0.00016318	
2	Nearshore Centre (Seas Off Wexford cSPA)	0.00027738	
3	Nearshore East	0.00023141	
4	Offshore West	0.00001150	
5	Offshore Centre	0.00000777	
6	Offshore East	0.00000878	
7	Carnsore Point SAC	0.00030370	
8	Wexford Harbour and Slob SPA	0.00000105	
9	The Raven SPA	0.00000223	
10	Blackwater Bank SAC	0.00002555	
11	Long Bank SAC	0.00000743	

STAGE 3

- The same analysis is presented here for the evolution of bed thickness for Stage 3. The maximum total bed thickness over the 8-month dredging and disposal simulation period is depicted from Figure 8-55 to Figure 8-57.
- The maximum total bed thickness change observed occurs in the nearshore area close to Rosslare Harbour, which overlaps with the Seas Off Wexford cSPA. For the other SAC and SPA areas, the highest bed thickness change is at Carnsore Point SAC, with a value of 0.037 cm, which is considered negligible.

The sediment deposited on the seabed remains confined to the area around the outer boundary of the reclamation site. As shown in Table 8-25, bed thickness changes are up to 0.02 cm in the harbour area and less than 0.001 cm in the area located within 1 km radius of the Proposed Development.

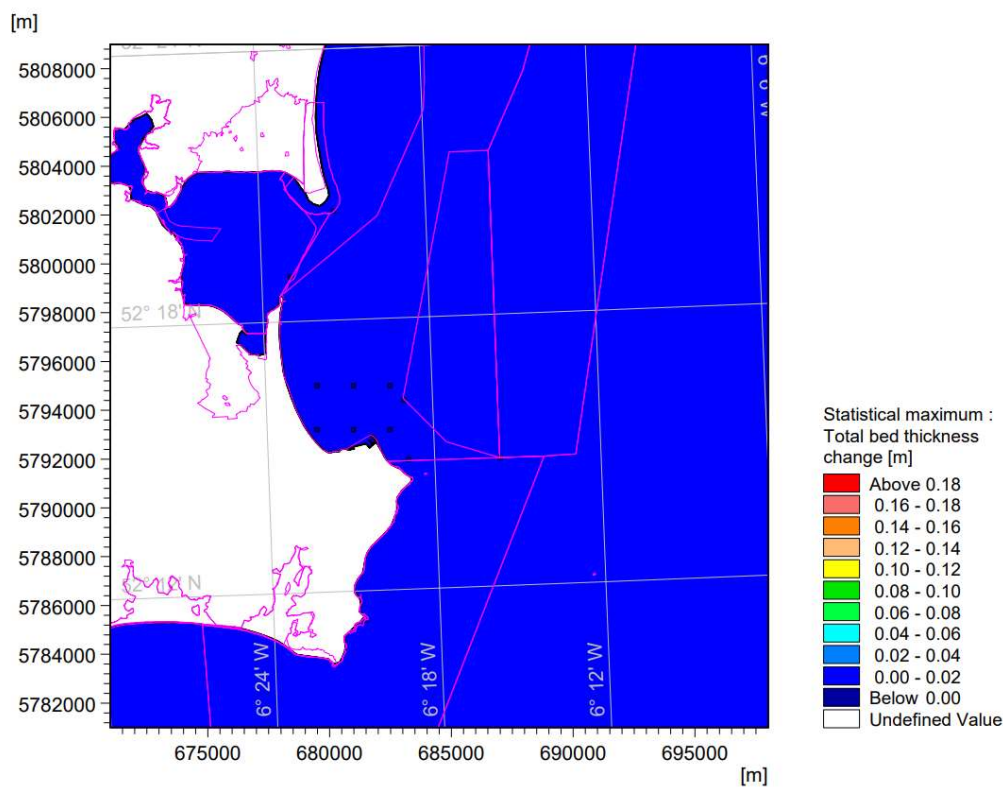


Figure 8-55: Maximum Bed thickness change from the 8-month dredging and disposal simulation (Stage 3)

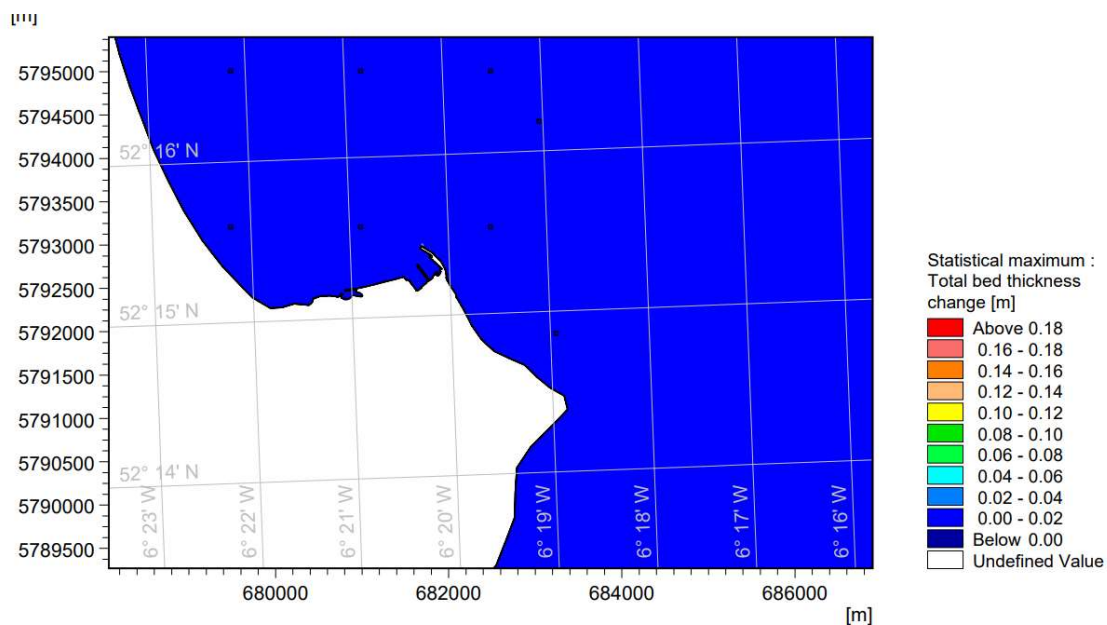


Figure 8-56: Close-up view of the port area showing the results of the maximum bed thickness change from the 8-month dredging and disposal simulation (Stage 3)

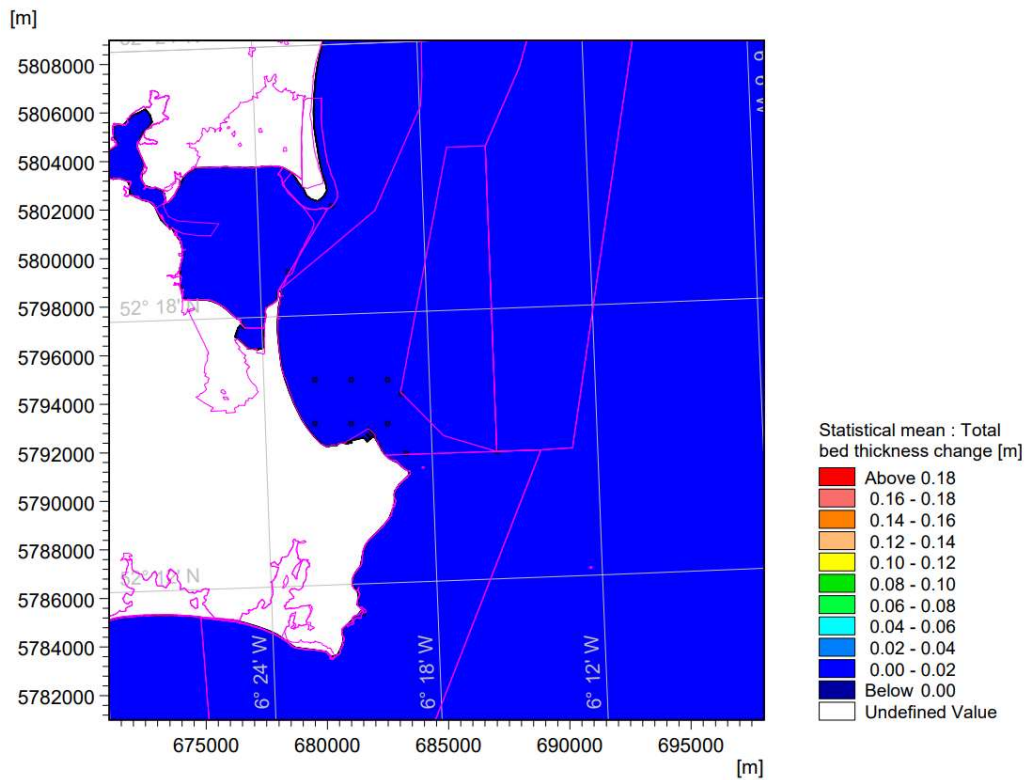


Figure 8-57: Average bed thickness change from the 8-month dredging and disposal simulation (Stage 3)

Table 8-25: Total bed thickness change for the extracted numerical results (Stage 3)

Point Number	Name	Max Total bed thickness change (m)	
1	Nearshore West	0.00006333	
2	Nearshore Centre (Seas Off Wexford cSPA)	0.00019784	
3	Nearshore East	0.00002240	
4	Offshore West	0.00001060	
5	Offshore Centre	0.00006961	
6	Offshore East	0.00014191	
7	Carnsore Point SAC	0.00037089	
8	Wexford Harbour and Slob SPA	0.00000891	
9	The Raven SPA	0.00000494	
10	Blackwater Bank SAC	0.00003655	
11	Long Bank SAC	0.00028329	

8.5 SEDIMENT TRANSPORT MODELLING

This section presents the numerical modelling analysis performed to evaluate the sediment transport phenomena in the Proposed Development for both the present port configuration and the Proposed Development.

Sediment transport modelling was conducted using the MIKE 21 Flow Model Flexible Mesh (FM) (DHI Group, 2017b), developed by DHI. The Sand Transport Module (DHI Group, 2024) was utilized, incorporating the effects of both the hydrodynamic modelling module (HD) (DHI Group, 2017c) and the spectral wave modelling module (SW) (DHI Group, 2023a). The validation and results of these modules have been presented in the preceding sections based on the following sources:

- Rosslare tidal gauge, used for the calibration of the model against water levels
- Current parameters obtained in the metocean survey, used for the calibration of the model against current speed and direction

Validation of the wave model was performed using data obtained for the nearby Splaugh Buoy (MetOcean Charts, 2023).

8.5.1 METHODOLOGY

8.5.1.1 GENERAL

This section summarises the methodology and the key assumptions considered in the sand transport model used to evaluate the sediment transport conditions with and without the Proposed Development at Rosslare Europort.

8.5.1.2 NUMERICAL MODEL

Both Wave and Hydrodynamic conditions (flow and water level) modelling were performed with MIKE21 SW (see section 8.1.1.2) and HD Flow Model (see section 8.2.1.2).

In addition to the above, the Sand Transport Module from the flexible mesh model (MIKE 21 Flow Model Flexible Mesh (FM)) was employed to simulate sediment transport processes. This module is specifically designed to model the transport of non-cohesive sediments (sand) under the combined influence of waves and currents. The Sand Transport Module integrates seamlessly with the hydrodynamic (HD) and spectral wave (SW) models to provide a comprehensive simulation of sediment dynamics. Key features of the Sand Transport Module include:

- Calculation of sediment transport rates due to combined wave and current action
- Simulation of bed level changes resulting from sediment erosion and deposition
- Consideration of sediment transport in both bedload and suspended load forms
- Inclusion of wave-induced sediment transport processes, such as wave asymmetry and streaming
- Dynamic coupling with hydrodynamic and wave models to account for time-varying flow and wave conditions

- Ability to simulate sediment transport in complex coastal and estuarine environments with unstructured meshes

The Sand Transport Module was utilized to evaluate sediment transport patterns and bed level changes in the study area under the combined influence of hydrodynamic and wave conditions. This allowed for a detailed understanding of sediment dynamics, which is critical for coastal management, erosion control, and infrastructure design.

8.5.1.3 INPUT DATA AND BOUNDARY CONDITIONS

The input data used for the sediment transport modelling is the same as for the wave propagation described in section 8.1.1.3.

8.5.1.4 MODEL SET UP

MESH

A triangular mesh is employed covering an approximate area of 2,400 km², following the methodology described in section 8.1.1.4 Mesh.

BOUNDARIES

Boundary conditions were established based on the available data near the edges of the mesh, as shown in Figure 8-58. Along the defined mesh boundaries, wave conditions remain spatially uniform but change over time. These conditions are defined by significant wave height (H_s), peak wave period (T_p), directional spreading, and wave directions for both swell and wind-generated waves, as well as water surface elevations influenced by tides.

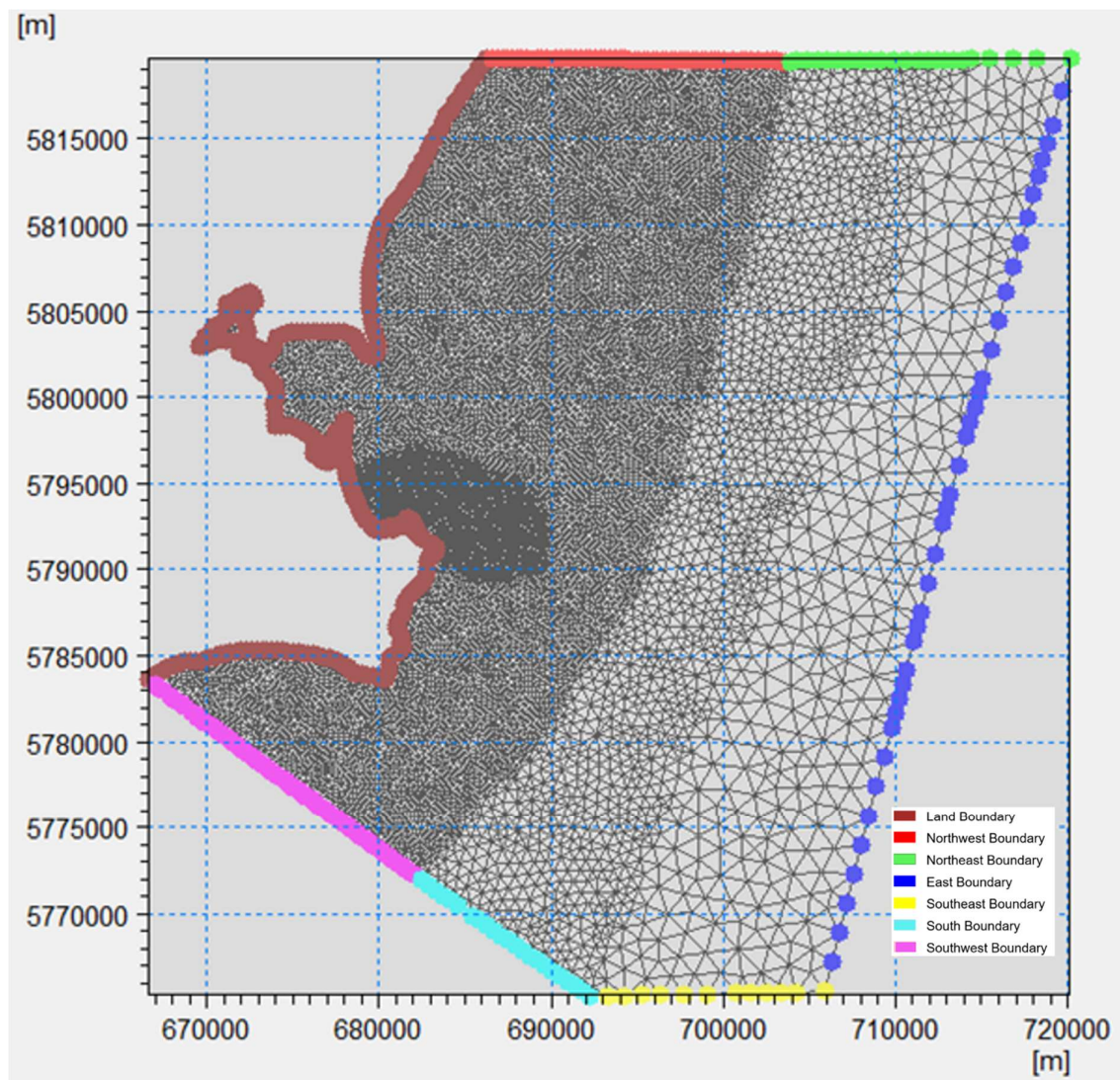


Figure 8-58: Model Boundaries

KEY PARAMETERS

The objective of this study was to evaluate sediment transport under unfavourable conditions, focusing on conditions most susceptible to sediment movement. A representative winter month was selected to simulate wave propagation, incorporating surface wind fields as well as hydrodynamic conditions influenced by currents and tidal flow. This representative winter month was constructed by analysis of a 21 year hindcast ERA5 timeseries. It contains waves from all expected directional sectors and includes the higher set of significant wave height values from the full dataset.

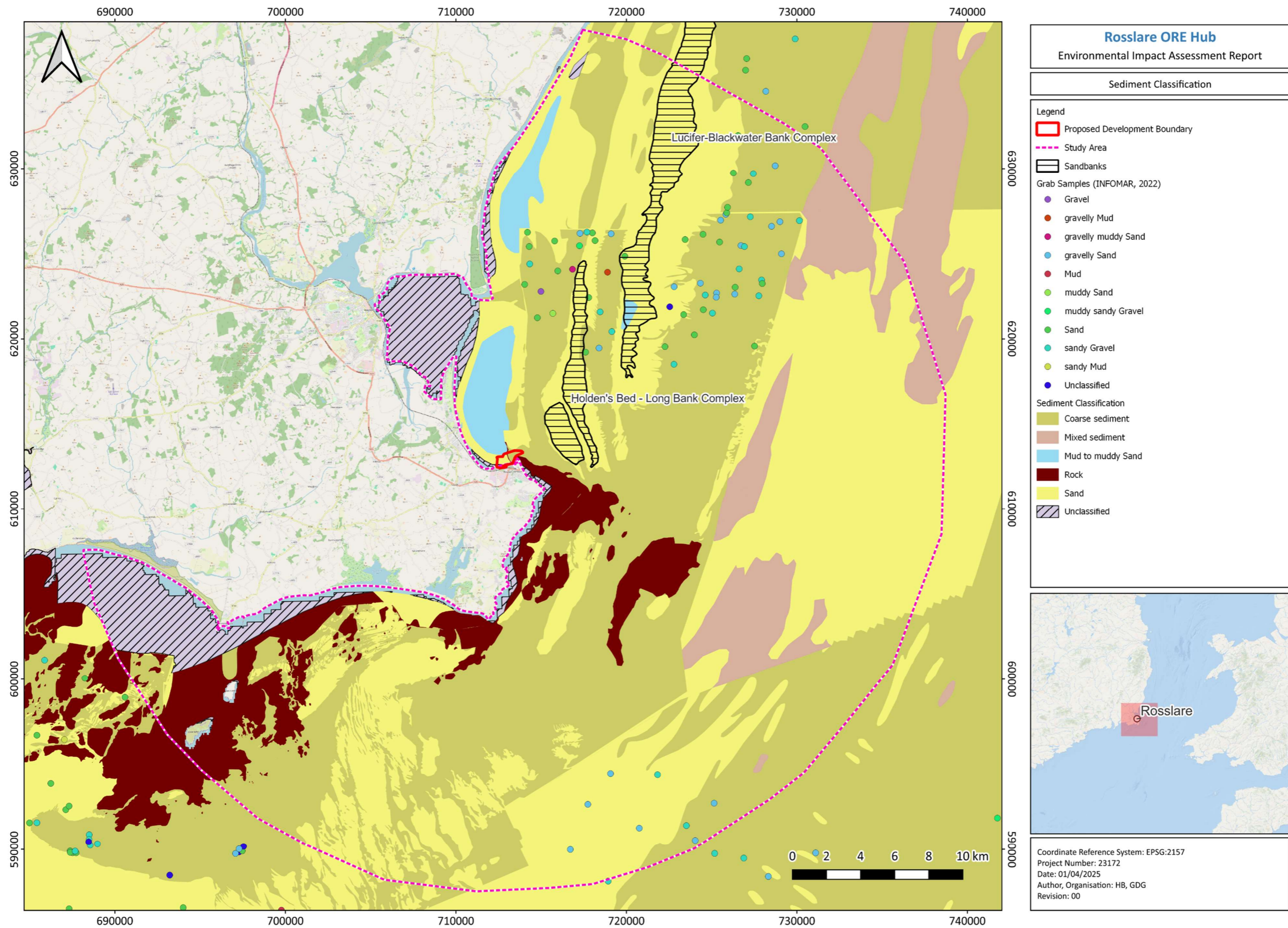
The computational mesh and bathymetry used are the same as those applied in the spectral wave propagation (SW) and hydrodynamic modelling (HD), as shown in Figure 8-4.

The key model parameters are presented in Table 8-26. These parameters were determined following the model calibration of both hydrodynamic modelling module (HD) and the spectral wave modelling module (SW).

Table 8-26: Key Model Parameters for Sediment transport modelling

Model Parameter	Description
Time Step	30 s
Simulation Period	From 1 st January 2022 to 1 st February 2022
Model Type	Wave and Current
Seabed Sediment properties	D50 Varying along the domain. Based on surveyed data (see Figure 8-59 and Figure 8-60) and data from EMODnet and INFOMAR.
Forcing	Wave Field from SW simulation
Boundary conditions	Zero sediment flux gradient

Figure 8-59 and Figure 8-60 show the sediment types and properties considered to define the D50 across the computational domain.



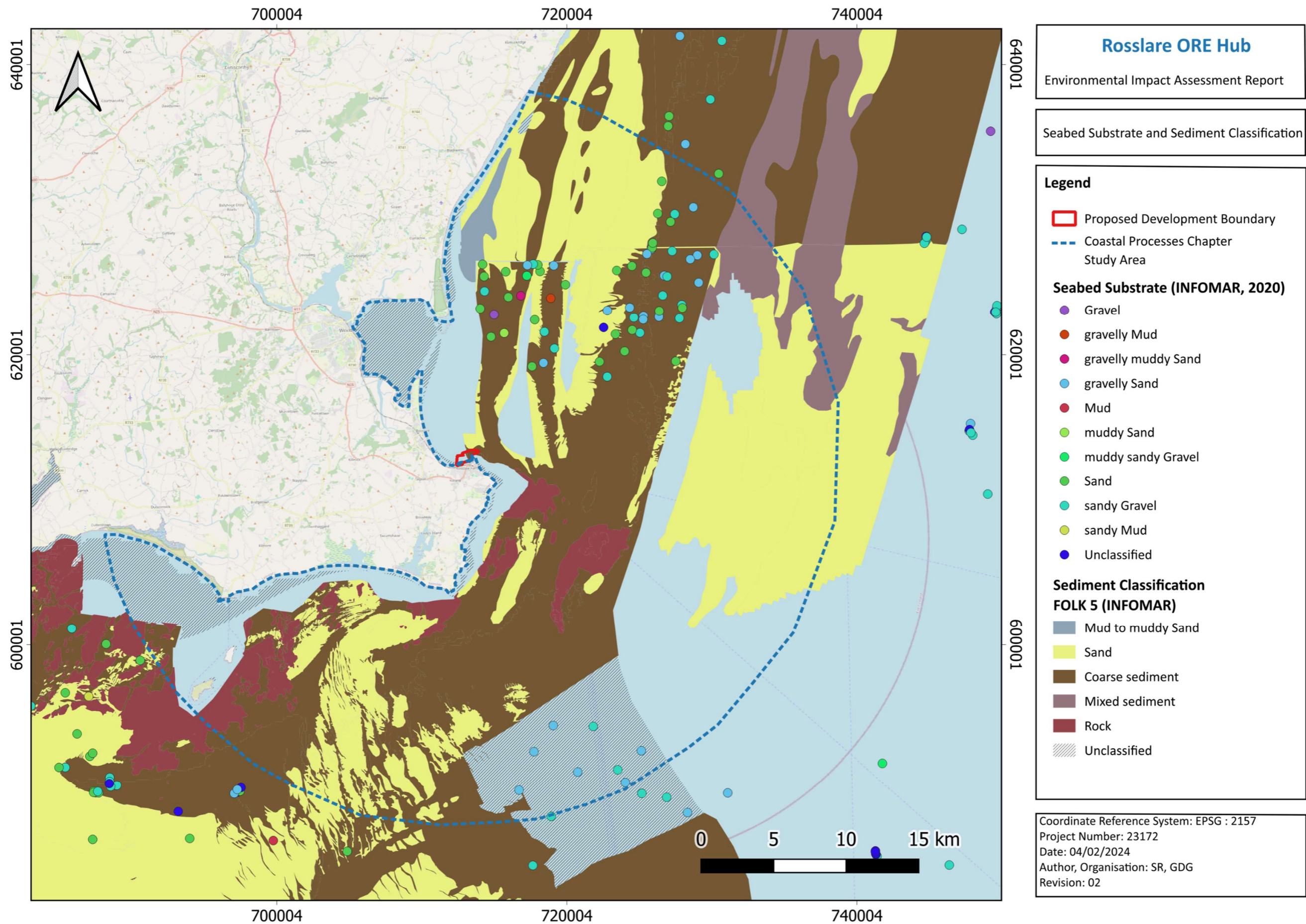


Figure 8-60: Coastal seabed substrate of the Rosslare Europort adjacent area, INFOMAR (2020, 2023)

8.5.2 RESULTS

The sediment transport modelling results include the statistical maximum and mean values for bed level change, total load transport, and suspended sediment concentration over an entire month based on conditions experienced in January 2022.

Figure 8-61 and Figure 8-62 compare the bed level changes associated with the baseline layout and the Proposed Development layout, showing respectively mean and maximum values for the modelled period (1 month).

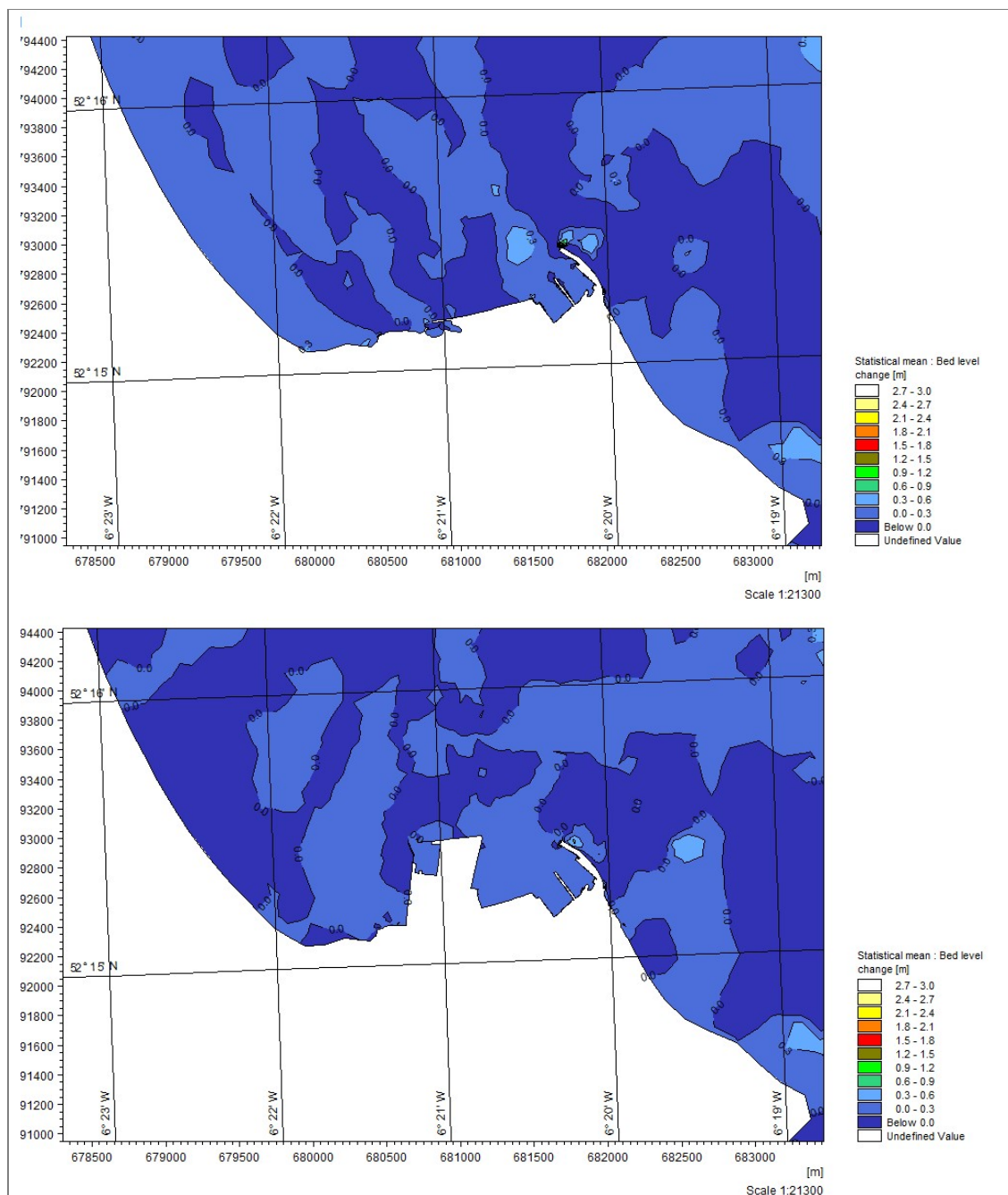


Figure 8-61: Statistical Mean of Bed Level Change for current layout (top) and Proposed Development layout (bottom)

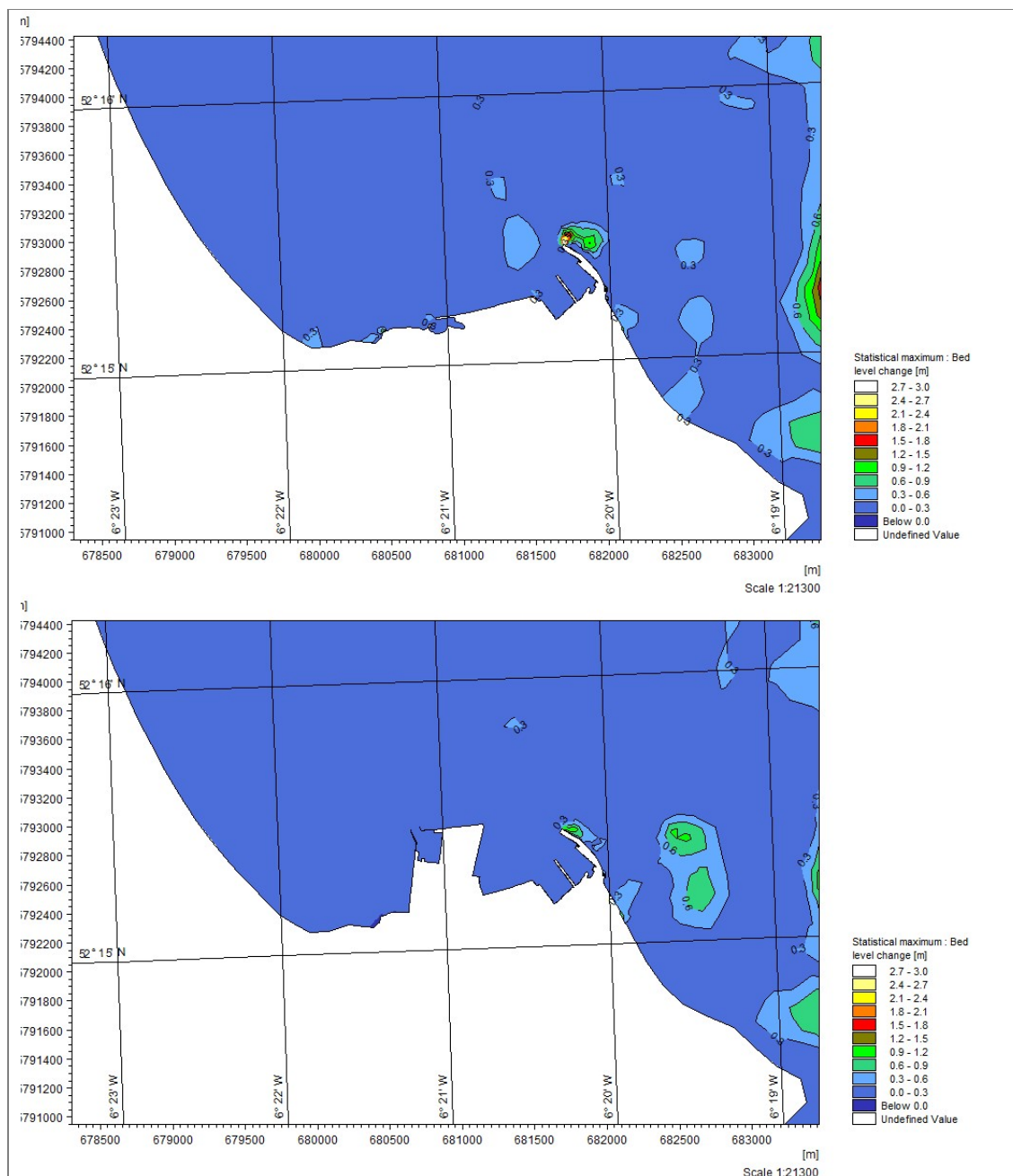
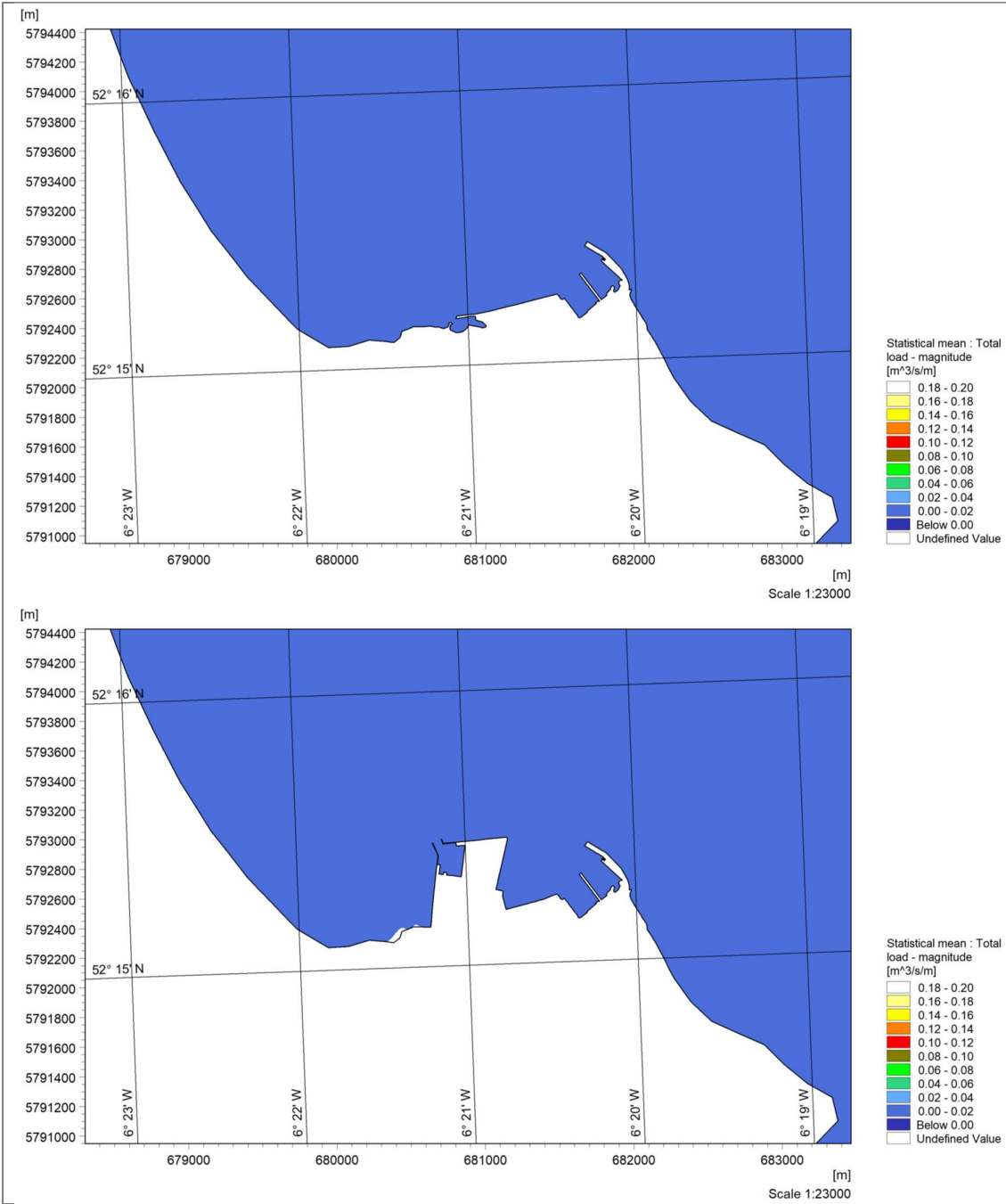


Figure 8-62: Statistical Maximum of Bed Level Change for current layout (top) and Proposed Development layout

Figure 8-61 and Figure 8-63 show that the current port layout results in greater sediment accumulation at the eastern extremity of the breakwater compared to with the Proposed Development in situ. The maximum bed level change for a typical winter month reveals a difference of circa 2.0 m in sediment accumulation, with the current port facilities only reaching about 3.0 m and with the Proposed Development included around 1.0 m at the eastern breakwater's tip. Additionally, the current port layout exhibits a maximum bed level change of about 0.5 m on the western side of the port, whereas with the Proposed Development included it shows a maximum

accumulation of approximately 0.5 m along the south-eastern stretch adjacent to the eastern breakwater.

Figure 8-63 and Figure 8-64 compare the Total Load for the current port only and the Proposed Development, showing respectively mean and maximum values for the modelled period (January 2022).



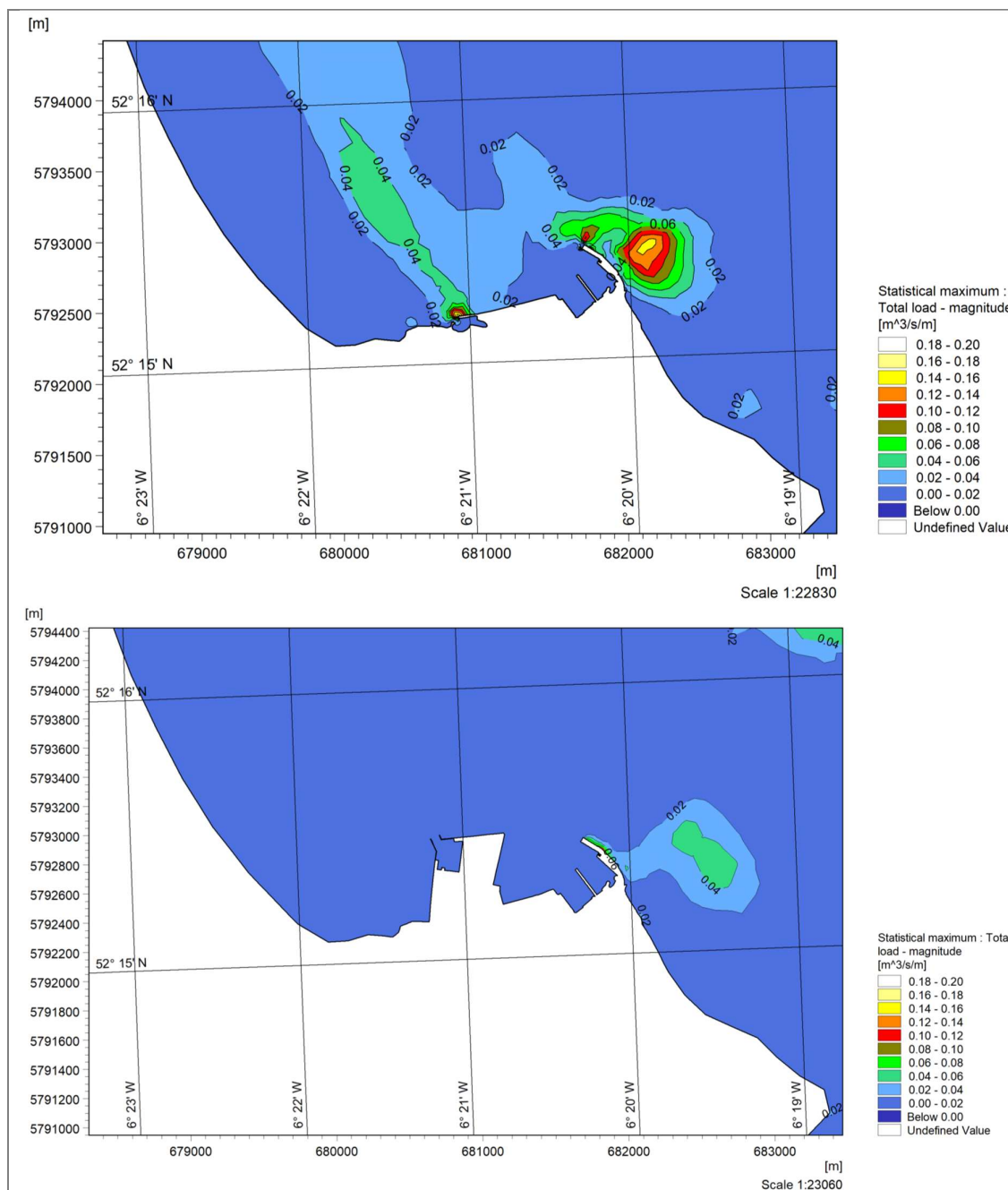
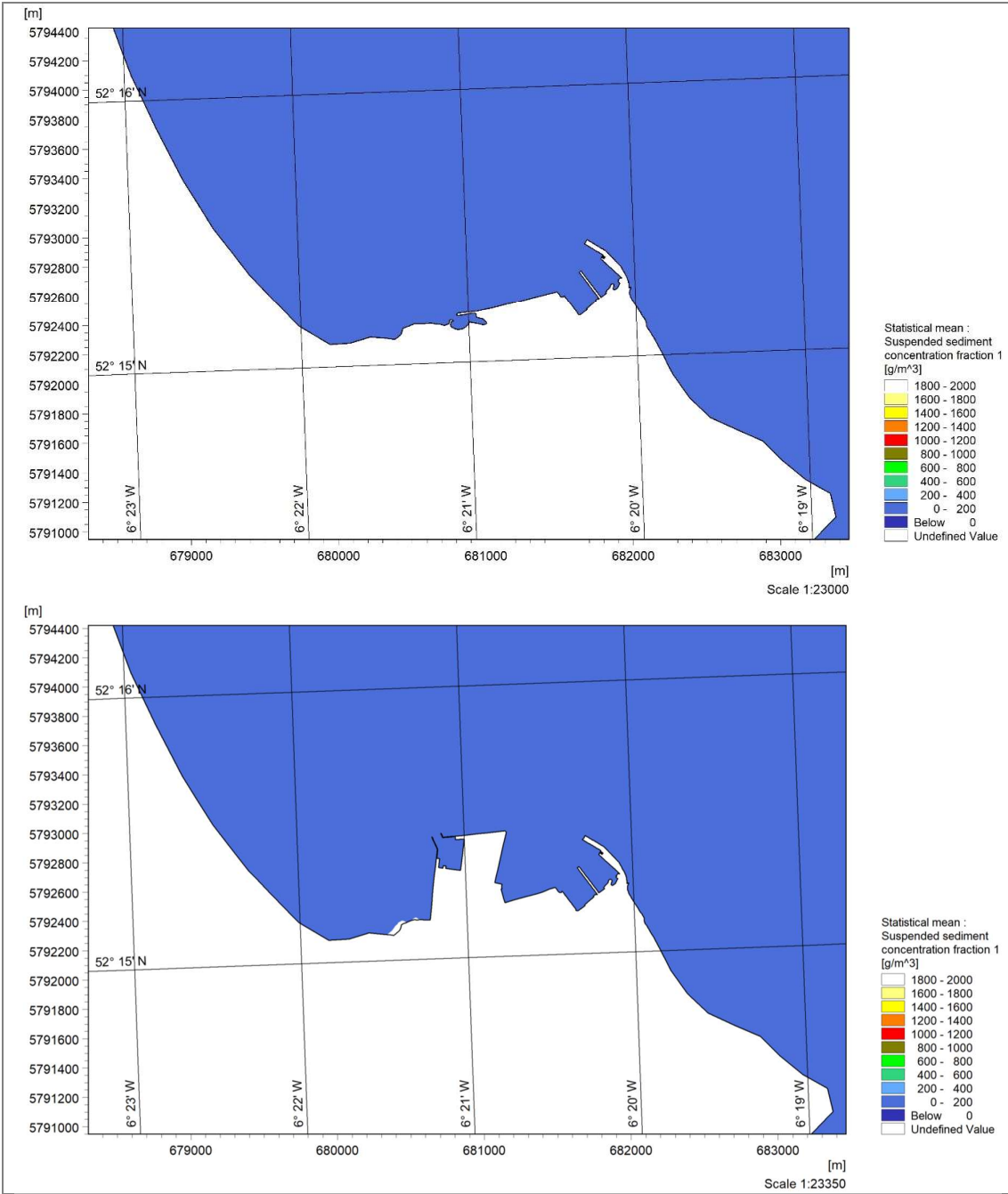


Figure 8-64: Statistical Maximum of Total Load for current port layout (top) and Proposed Development layout (bottom)

Figure 8-64 illustrates the total sediment load for both the current port only and with the Proposed Development included, confirming greater sediment accumulation on the eastern side of the eastern breakwater with the existing port only. It also shows sediment accumulation in the western part of the port, causing slight bed level changes in that area. Some sediment loading on the eastern side of the eastern breakwater is associated with the Proposed Development.

Figure 8-65 and Figure 8-66 compare the Suspended Sediment Concentration (SSC) for the existing port only and with the Proposed Development included, showing respectively mean and maximum values for the modelled period.



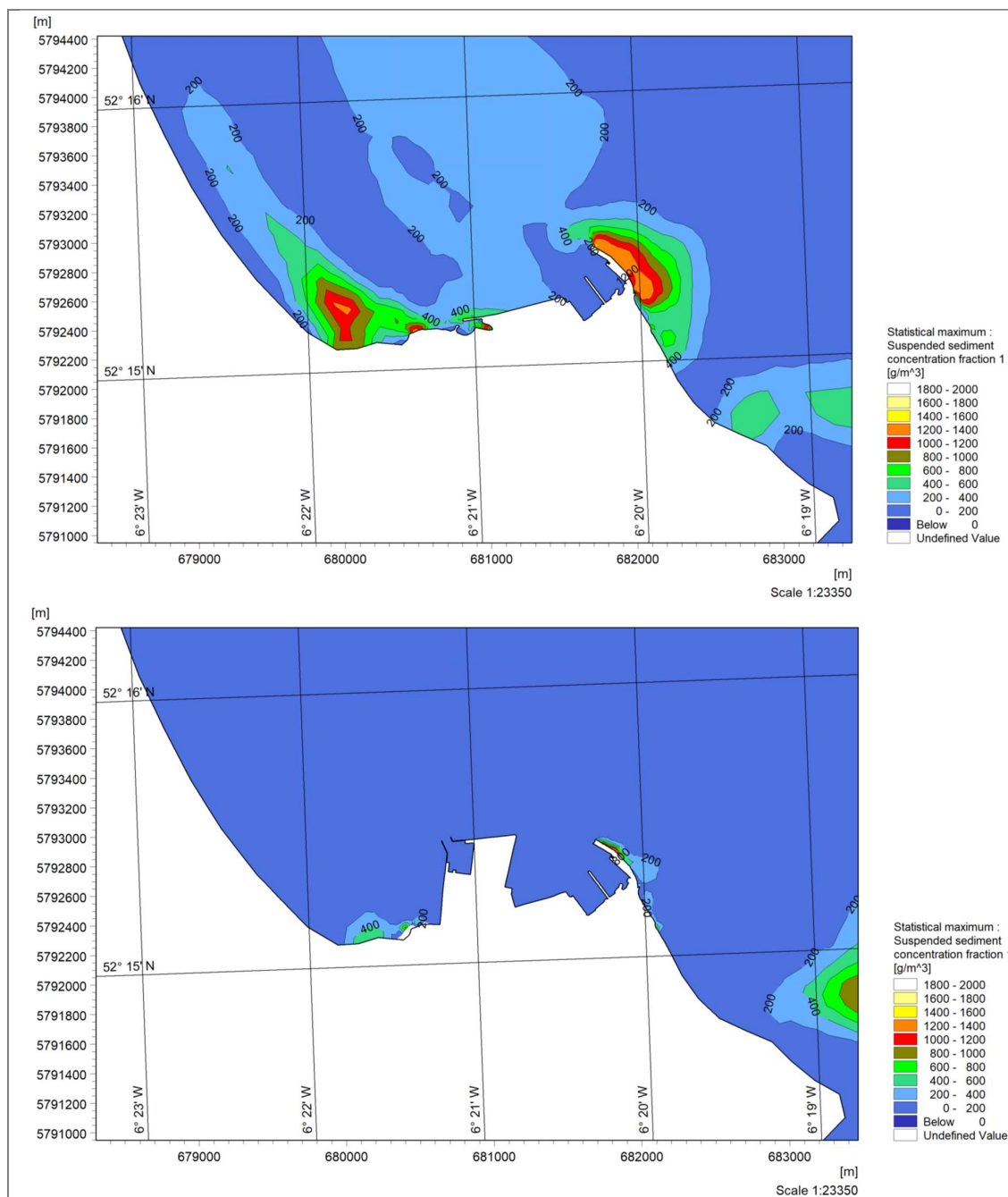


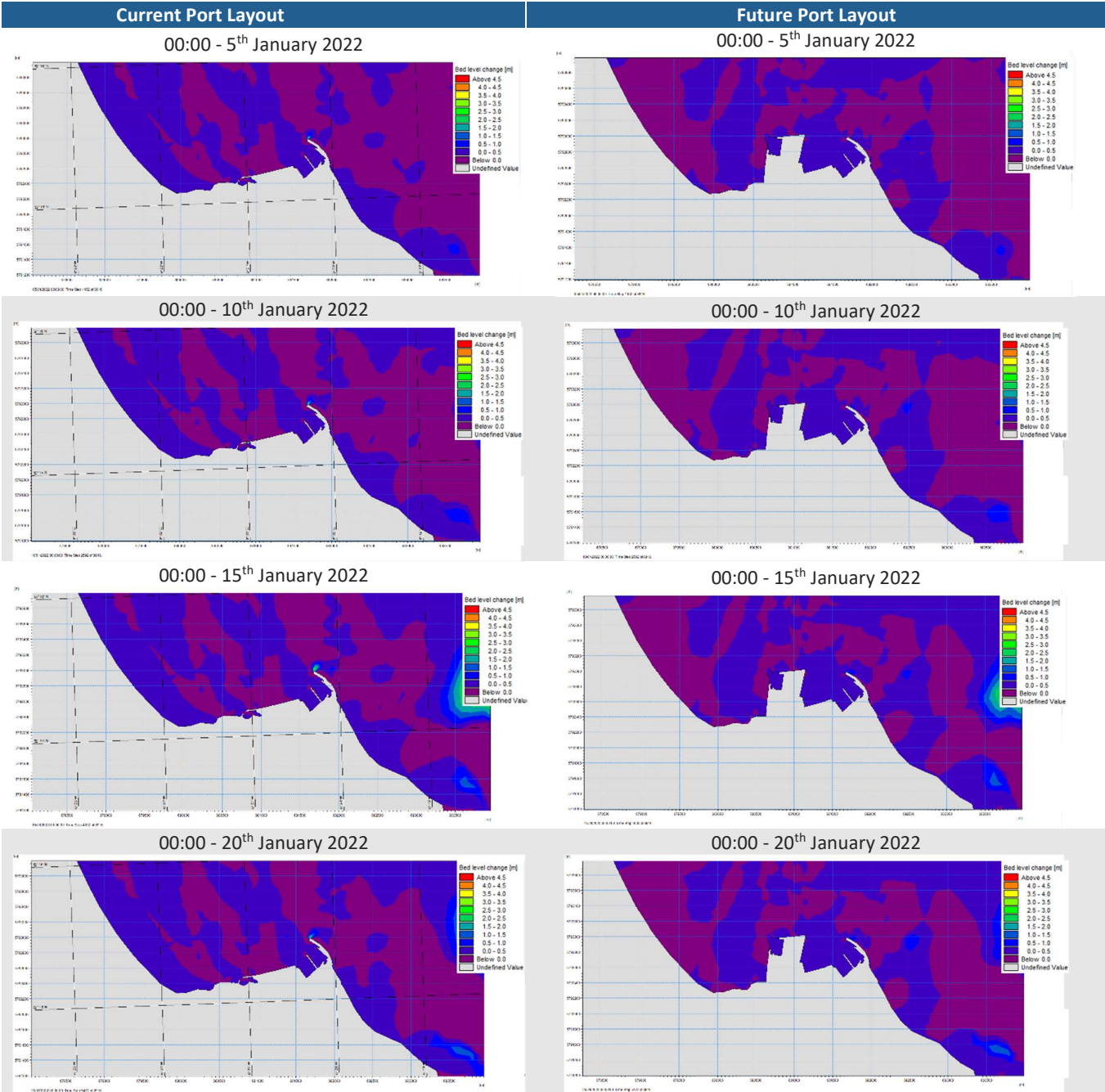
Figure 8-66: Statistical Maximum of Suspended Sediment Concentration (SSC) for current port layout (top) and Proposed Development layout (bottom)

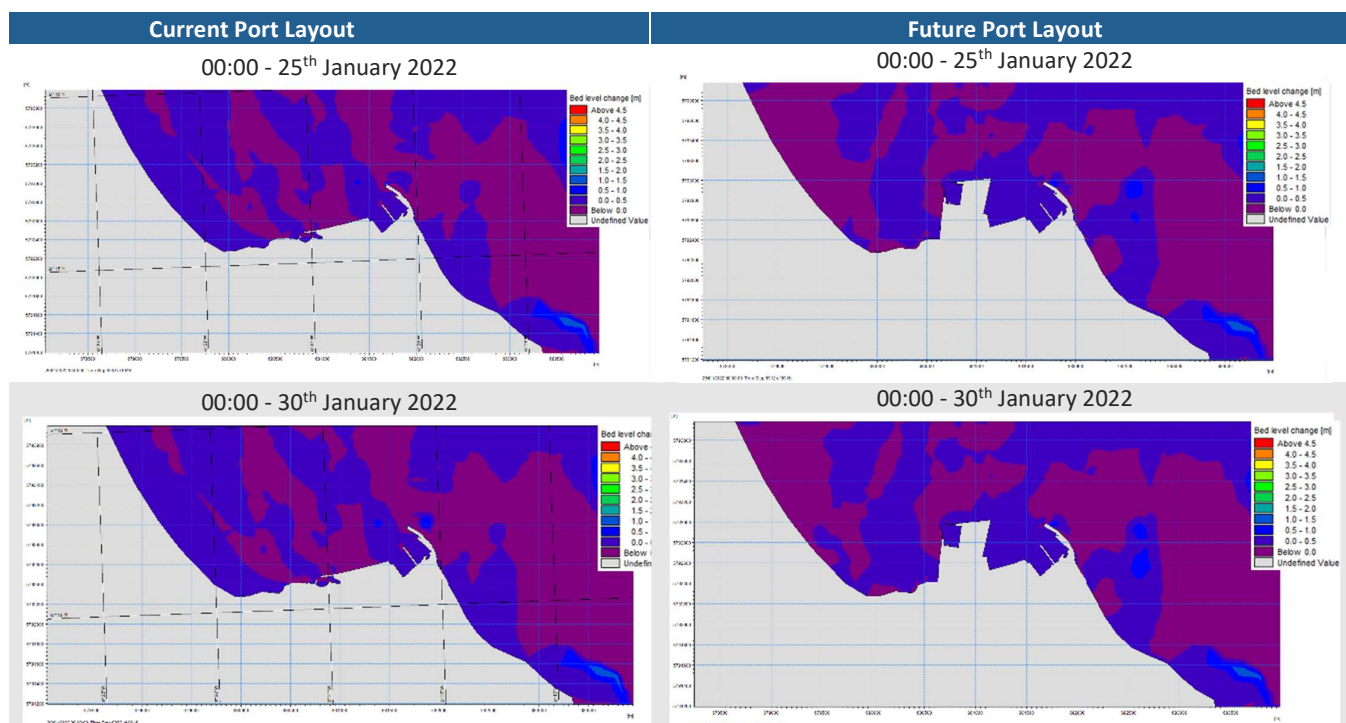
Figure 8-66 indicates that the current port only produces higher suspended sediment concentrations near the eastern side of the eastern breakwater and also increases suspended sediments on the western side of the port. In contrast, with the Proposed Development included lower suspended sediment concentrations on both the eastern and western sides of the port are generated.

Table 8-27 illustrates the bed level changes throughout the modelled period of January 2022. It displays simulation snapshots taken every 5 days, showing the bed level change values for both the current and Proposed Development layouts.

The Table 8-27 indicates that bed level changes are more pronounced in the current port layout, with greater changes observed near the eastern area of the eastern breakwater.

Table 8-27: Bed level Change throughout the modelled period of January 2022 for both Current and Proposed Development Layout





8.6 CONCLUSIONS AND RECOMMENDATIONS

8.6.1 WAVE PROPAGATION

The wave propagation modelling indicates the Rosslare Europort area is significantly protected from a relevant percentage of the swells entering the Irish Sea from the South.

The predominant wave directions near the port (at 1 km from existing facilities) are from east (E) to east-southeast (ESE), with a lower percentage of wave coming from the northeast (NE) and southeast (SE). The more extreme sea conditions are associated with westerly (W) waves. These conditions are result from offshore swells diffracting as they propagate within the Irish Sea and enter shallower waters.

Regarding the combination of significant wave height and peak period, the current conditions typically feature significant wave heights below 0.8 m combined with peak periods of up to 10 s. When analysed individually, wave heights below 1m and peak periods of up to 10 s are associated with an approximate occurrence probability of 90%.

Extreme wave conditions are estimated between 2.3 m and 3.3 m at the Northeast of the port (Point A) and between 2.0 m and 2.9 m at the North (Point B). These values are considerably lower for waves coming from the north and the west.

8.6.2 DREDGING DISPERSAL ASSESSMENT

The dredging dispersal model results reveal distinct trends in suspended sediment concentration (SSC) and bed thickness changes across the three stages of dredging and disposal at Rosslare

Europort. These variations are driven by differences in the duration and intensity of the operations at each stage.

The SSC values increased progressively with each stage, reflecting the longer dredging periods and disposal volumes. However, in all stages, the highest SSC concentrations were confined to the immediate vicinity of Rosslare Harbour, with minimal impact on SAC and SPA areas. Stage 3 had the highest overall SSC values due to its extended duration, but the dispersion patterns remained similar to those observed in earlier stages, with significant reductions in concentration beyond key geographical points like Greenore Point and Rosehill Bay Beach.

Bed thickness changes followed a similar pattern, with the largest changes consistently located near the disposal site, while negligible changes occurred beyond the port's influence. Stage 3 resulted in lower bed thickness changes due to its duration and the finer material being dispersed.

The model results suggest that sediment dispersal is effectively contained within the Rosslare Harbour area, with no significant adverse effects on protected environments.

8.6.3 SEDIMENT TRANSPORT MODELLING

The sediment transport modelling conducted for the study highlights differences between the existing port only and with the Proposed Development included, more particularly for:

Bed Level Changes:

Compared to baseline, inclusion of the Proposed Development has a reduction in sediment accumulation on the eastern extremity of the eastern breakwater.

Maximum bed level changes for the existing port only reach approximately 3.0 m, compared to around 1.0 m with the Proposed Development included at the same location.

Sediment Accumulation:

Modelling of the existing port only results in sediment accumulation along the western side of the port, leading to slight bed level changes in this area.

Modelling including the Proposed Development results in reduced sediment accumulation in both the eastern and western sections of the port, indicating improved sediment transport conditions.

Suspended Sediment Concentration (SSC):

Modelling including the Proposed Development shows a reduction in suspended sediment concentrations across both eastern and western areas of the port compared to the existing port only.

The sediment transport modelling conducted for this study indicates no evidence of changes in sediment accumulation or erosion at Rosslare Strand when comparing the existing port only to the scenario including the Proposed Development.

REFERENCES

- CDS, 2023. Climate Data Store - ERA hourly data on single levels from 1940 to present. Available at: [ERA5 hourly data on single levels from 1940 to present](#). Date Accessed: [March, 2023]
- Constantin, P., and Foias, C., 1988. Navier-Stokes Equations. The University of Chicago, Chicago, London.
- Coughlan, M., Guerrini, M., Creane, S., O'Shea, M., Ward, L.S., Van Landeghem, J.J.K., Murphy, J., Doherty, P., (2021). *"A new seabed mobility index for the Irish Sea: Modelling seabed shear stress and classifying sediment mobilisation to help predict erosion, deposition, and sediment distribution "*, Continental Shelf Research, Volume 229, 104574 ,ISSN 0278-4343, <https://doi.org/10.1016/j.csr.2021.104574>
- DHI Group, 2023. MIKE 21 Documentation DHI Group. Danish Hydraulic Institute Hydraulic Institute, Hørsholm, Denmark. Available at: [MIKE 21 documentation](#). Date Accessed: [March, 2023]
- DHI Group, 2023a. MIKE 21 Spectral Waves FM. Danish Hydraulic Institute Hydraulic Institute, Hørsholm, Denmark. Available at: [MIKE 21 SW, Spectral Waves FM Module, User Guide](#). Date Accessed: [March, 2023]
- DHI Group, 2023b. MIKE 21 Tidal Analysis and Prediction Module. Scientific Documentation. Danish Hydraulic Institute Hydraulic Institute, Hørsholm, Denmark. Available at: [MIKE 21, Tidal Analysis and Prediction Module, Scientific Documentation](#). Date Accessed: [March, 2023]
- DHI Group, 2017. MIKE 21 & MIKE 3 Flow Model FM Mud Transport Module - Scientific Documentation. Danish Hydraulic Institute Hydraulic Institute, Hørsholm, Denmark.
- DHI Group, 2017a. MIKE 21 Flow Model - Mud Transport Module - User Guide. Danish Hydraulic Institute Hydraulic Institute, Hørsholm, Denmark.
- DHI Group, 2017b. MIKE 21 Flow Model FM - Scientific Documentation. Danish Hydraulic Institute, Hørsholm, Denmark.
- DHI Group, 2017c. MIKE 21 Flow Model - Hydrodynamic Module. Danish Hydraulic Institute, Hørsholm, Denmark
- HI Group, 2024. MIKE 21 Flow Model FM: Sand Transport Module User Guide. DHI Water & Environment. Danish Hydraulic Institute, Hørsholm, Denmark
- EMODnet, 2020. European Marine Observation and Data Network. Available at: <https://emodnet.ec.europa.eu/>
- EMODnet, 2023. European Marine Observation and Data Network. Available at: <https://emodnet.ec.europa.eu/en/bathymetry>. Date Accessed: [March, 2023]
- GDG Irish Sea Model (2024) – Bathymetry file HSL- Rosslare-20feb23 5x5_CD.
- GDG Irish Sea Model (2024a) – Bathymetry files: "Bathymetry file "PH22005A"

GDG, 2024. Rosslare Europort ORE Hub Dredging Information Package Technical Note. Gavin and Doherty Geosolutions.

INFOMAR, 2020. Available at: <https://www.infomar.ie/> Date Accessed: [March 2023]

INFOMAR, 2023. Available at: <https://www.infomar.ie/surveys/hydrography/bathymetry>. Date Accessed: [March 2023]

Manning, R., Griffith, J., Pigot, T., and Vernon-Harcourt, L., 1980. On the flow of water in open channels and pipes.

McCabe, W., Smith, J., and Herriot, P., 2005. Unit Operations of Chemical Engineering. 7th Edition.

MetOcean Charts, 2023. Splaugh Buoy Data. Available at: <https://cilpublic.cil.ie/metocean/>. Date Accessed: [December, 2023]

Roe, P., 1981. Approximate Riemann solvers, parameter vectors, and difference schemes. Journal of Computational Physics, vol. 43, pp. 357-372

SmartBay, 2023. Ireland's Digital Ocean, SmartBay Tidal Database. Available at: <https://digitalocean.ie/Data/DownloadTideData?smartbay=True>

Techworks Marine, 2024. Gavin and Doherty Geosolutions - Rosslare Metocean Equipment Final Report.

Tilton, J., and Green, D., 2007. Perry's Chemical Engineer's Handbook - Section 6: Fluid and Particle Dynamics. 8th Edn

Van Rijn, 1984. Sediment transport, Part I: bed load transport. Journal of Hydraulic Engineering, vol. 110, no. 10.

APPENDIX A – OFFSHORE METOCEAN CONDITIONS: JOINT PROBABILITY TABLES

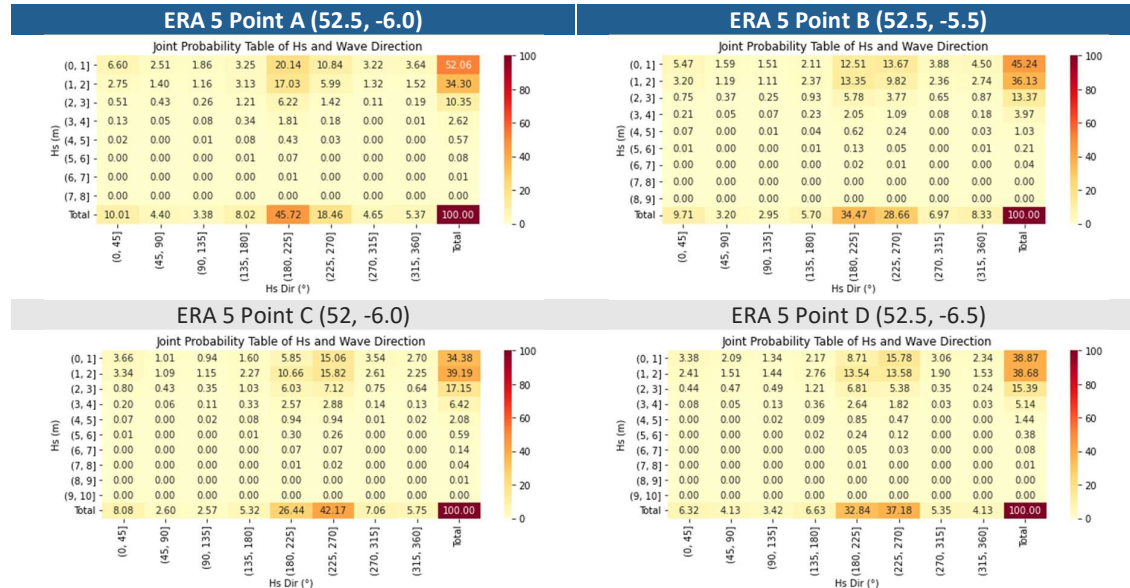


Figure A-1: Joint probability table H_s vs wave direction - offshore data points (1979-2022)

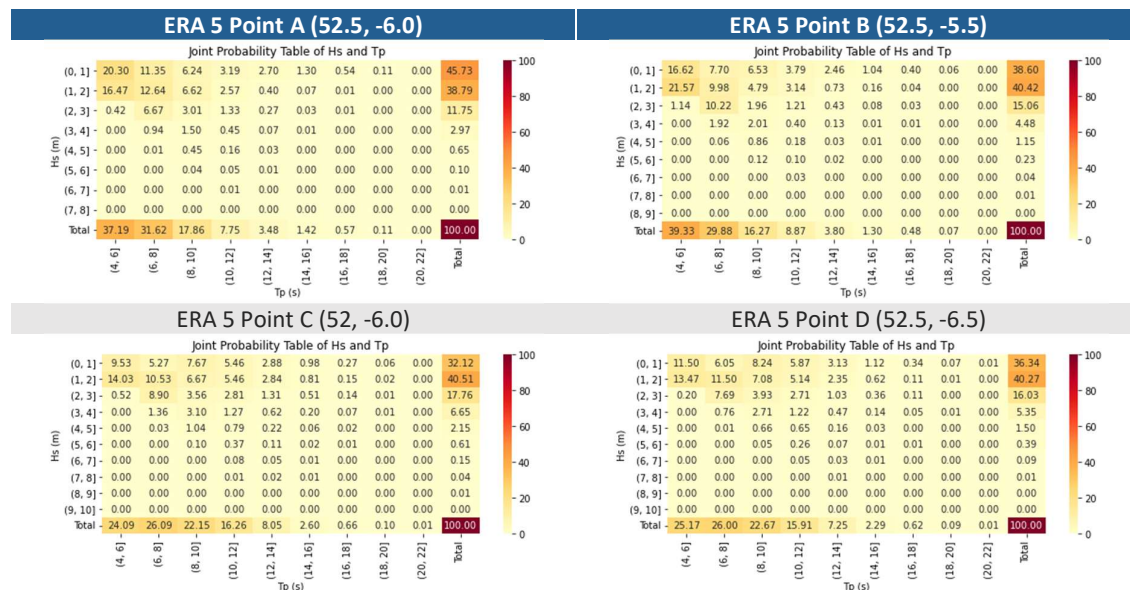


Figure A-2: Joint probability table H_s vs T_p - offshore data points (1979-2022)

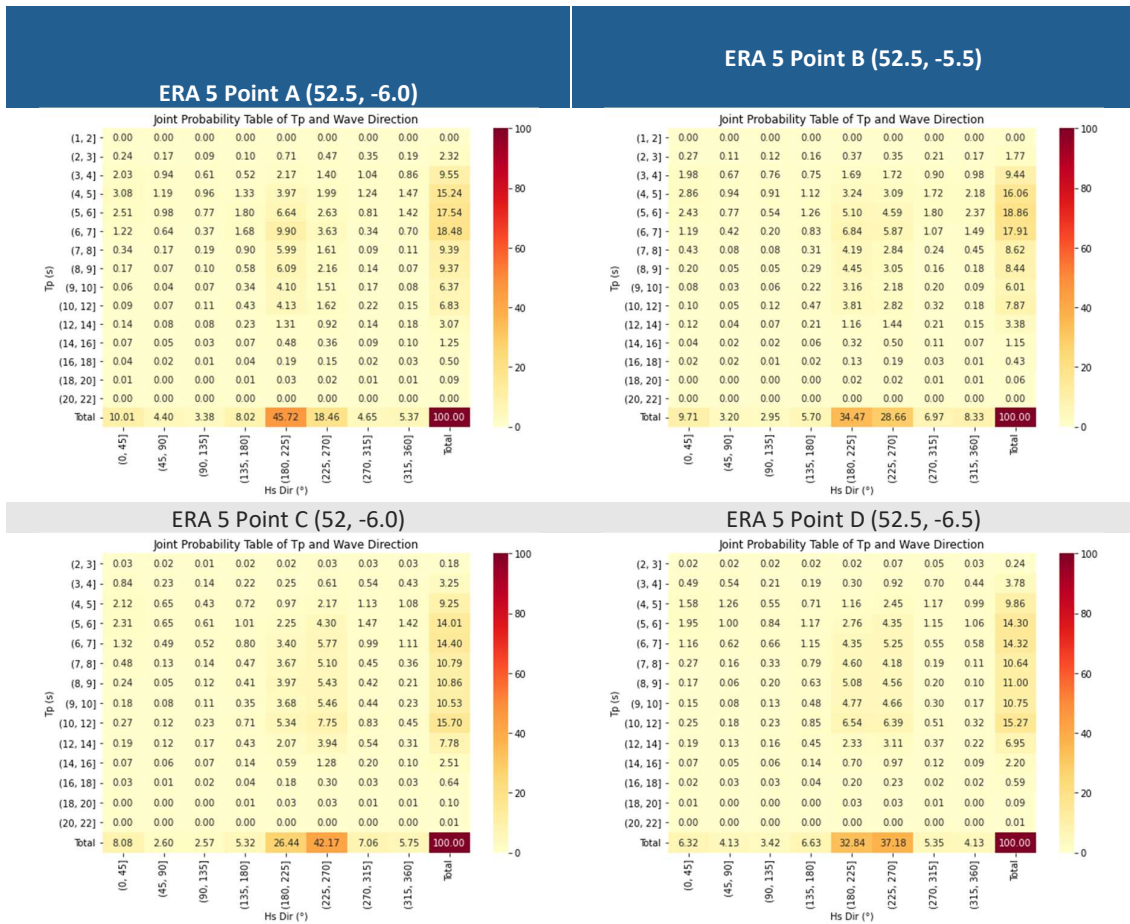


Figure A-3: Joint probability table T_p vs wave direction - offshore data points (1979-2022)

APPENDIX B – OFFSHORE METOCEAN CONDITIONS: EXTREME ANALYSIS RESULTS

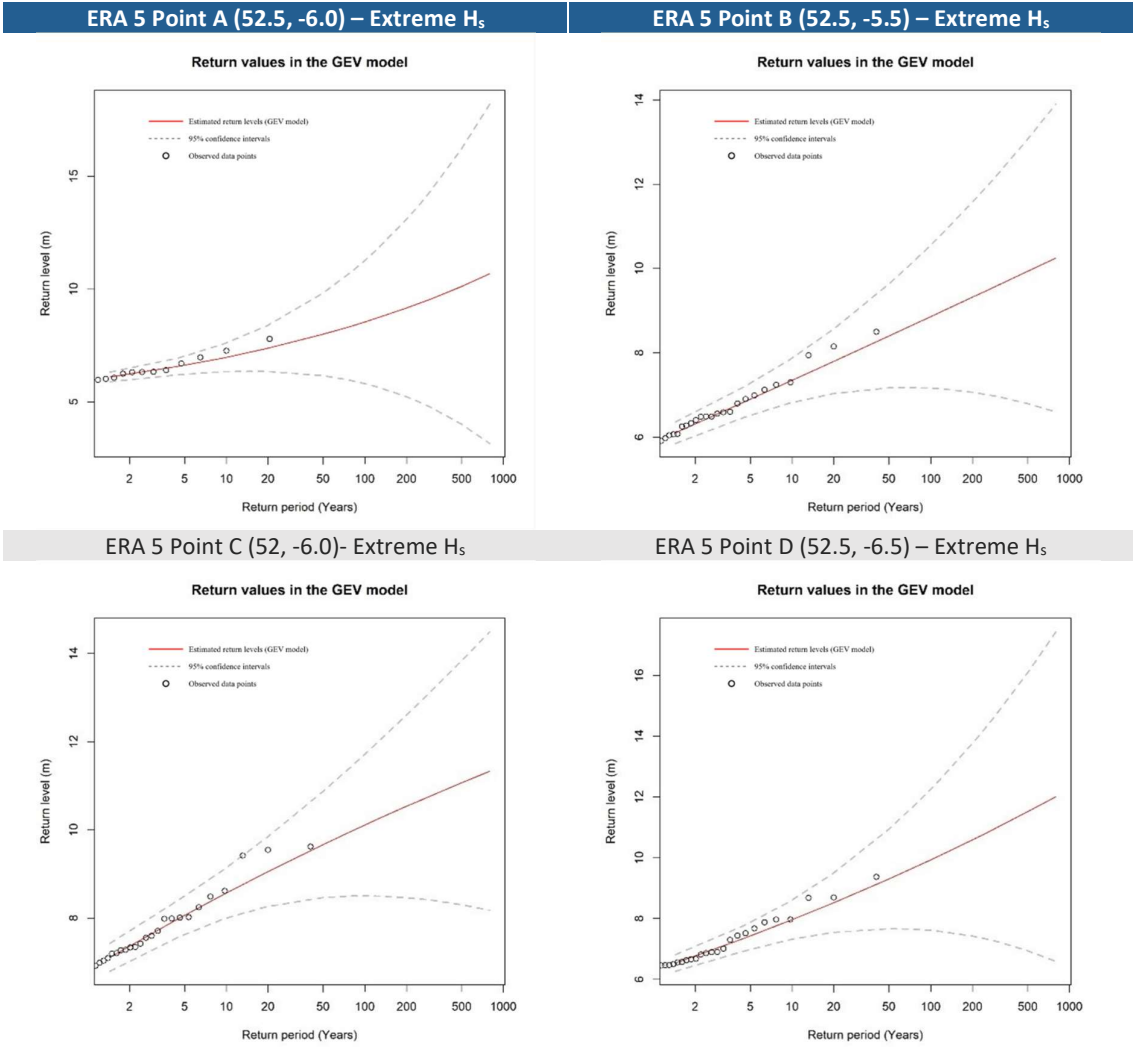
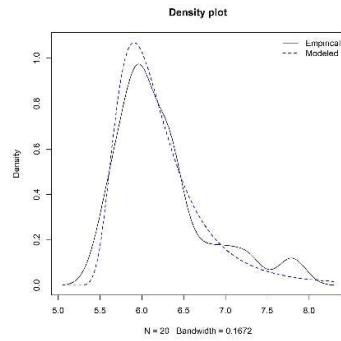
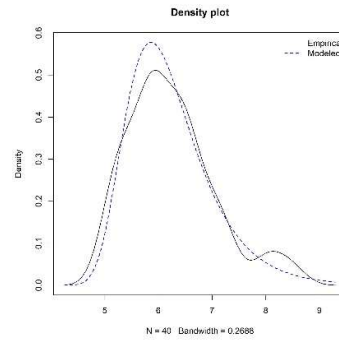


Figure B-1: Return Period Analysis for each point

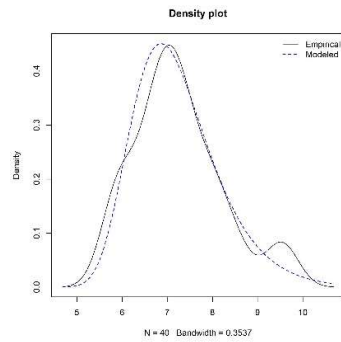
ERA 5 Point A (52.5, -6.0) - Density Diagram



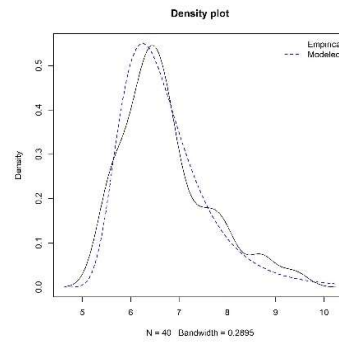
ERA 5 Point B (52.5, -5.5) - Density Diagram



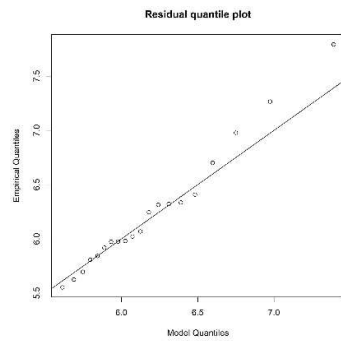
ERA 5 Point C (52, -6.0) - Density Diagram



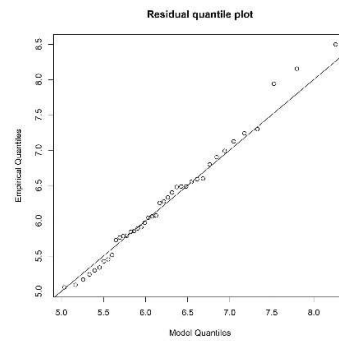
ERA 5 Point D (52.5, -6.5) - Density Diagram



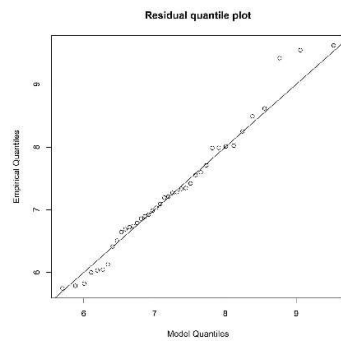
ERA 5 Point A (52.5, -6.0) – QQ Plot



ERA 5 Point B (52.5, -5.5) – QQ Plot



ERA 5 Point C (52, -6.0) – QQ Plot



ERA 5 Point D (52.5, -6.5) – QQ Plot

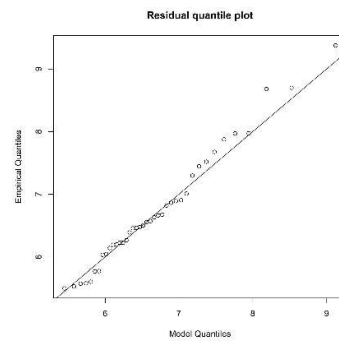


Figure B-2: Density Diagrams and Residual Quantile Plots for each point

APPENDIX C – NEARSHORE METOCEAN CONDITIONS: DENSITY DIAGRAM AND NON- EXCEEDANCE CURVES

C.1 POINT A – NE ROSSLARE PORT

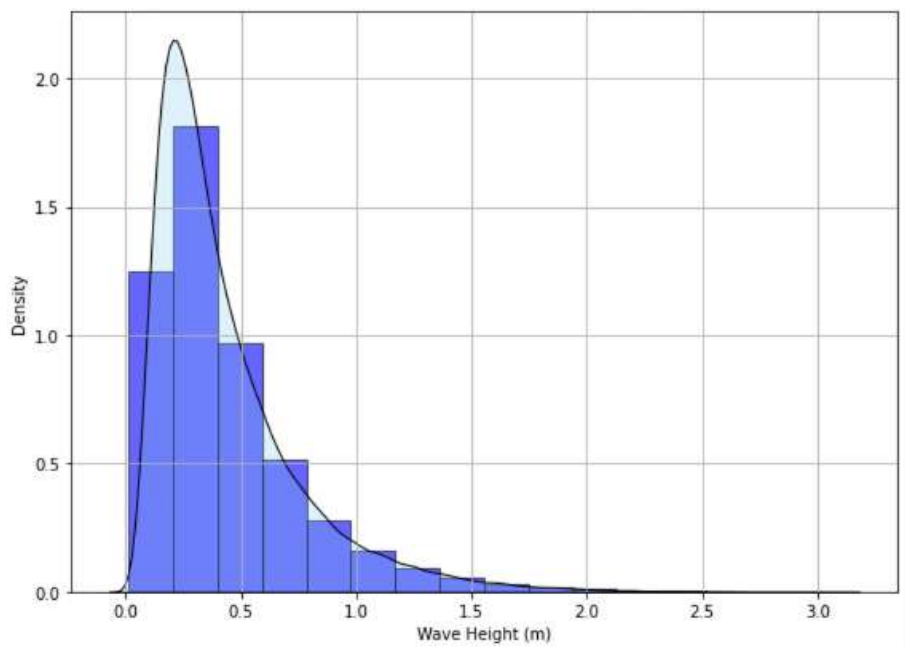


Figure C-1: Density Diagram Point A

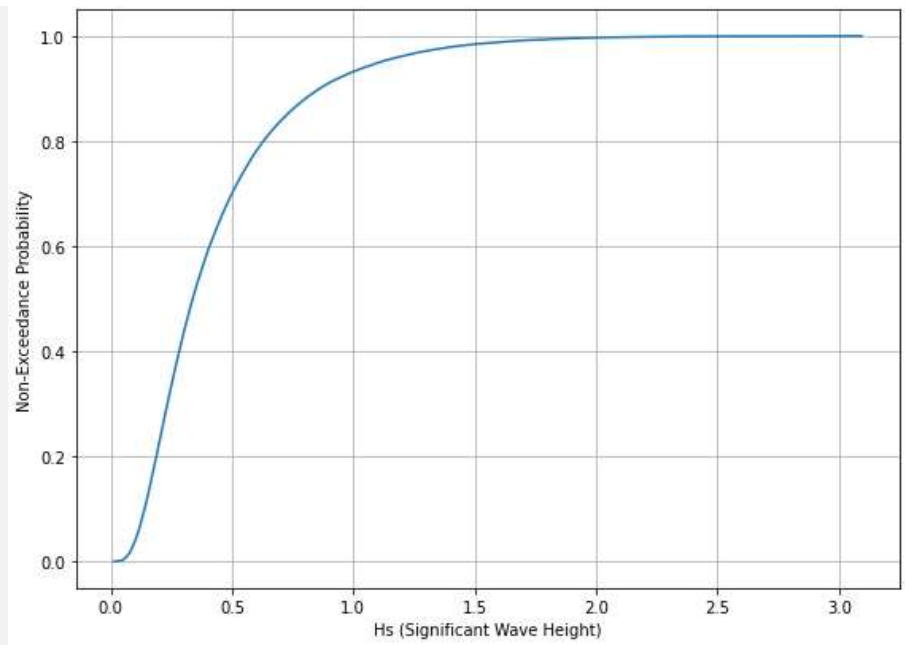


Figure C-2: Non-exceedance probability Point A

C.2 POINT B – N ROSSLARE PORT

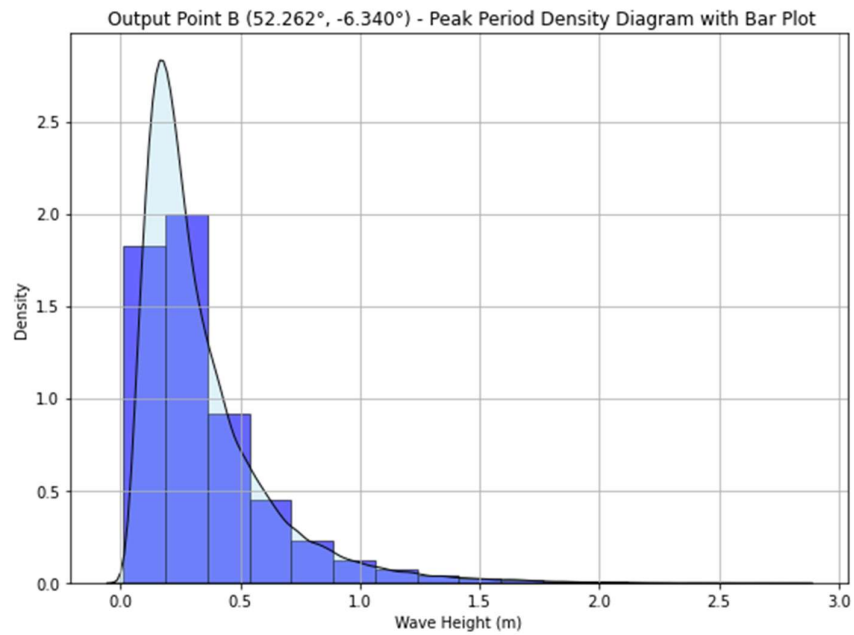


Figure C-3: Density Diagram Point B

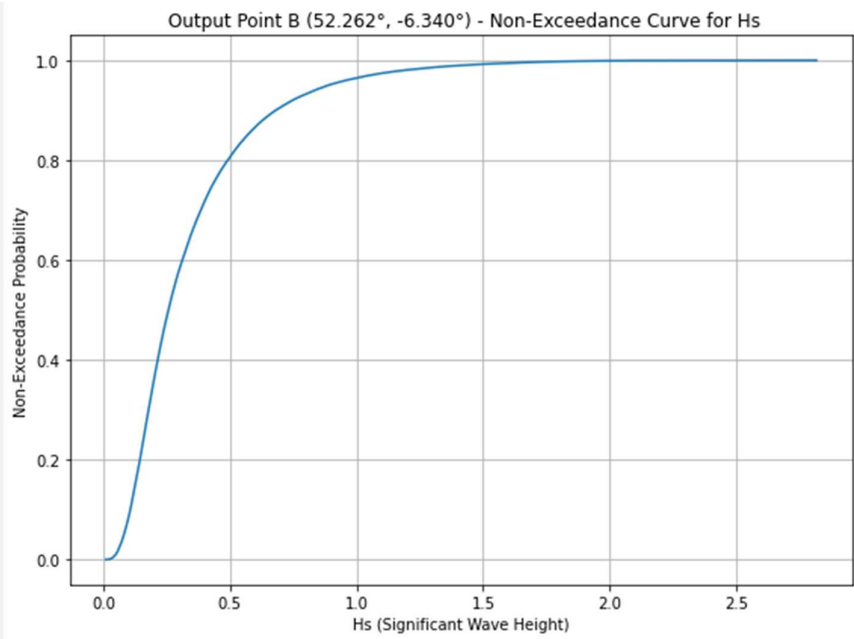


Figure C-4: Non-Exceedance Probability Point B

APPENDIX D – NEARSHORE METOCEAN CONDITIONS: EXTREME CONDITIONS DIAGRAMS

D.1 POINT A – NE ROSSLARE PORT

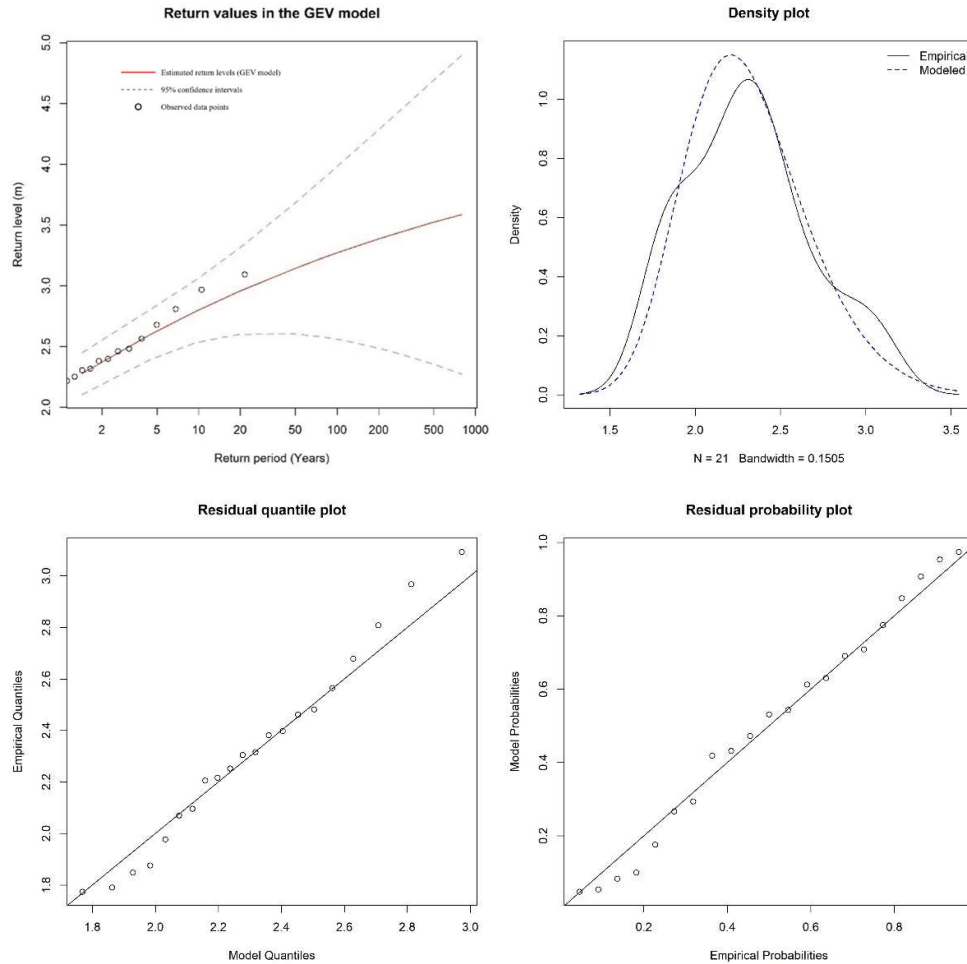


Figure D-1: Return Period analysis, Density plot and Residual quantile and probability for point A

D.2 POINT B – N ROSSLARE PORT

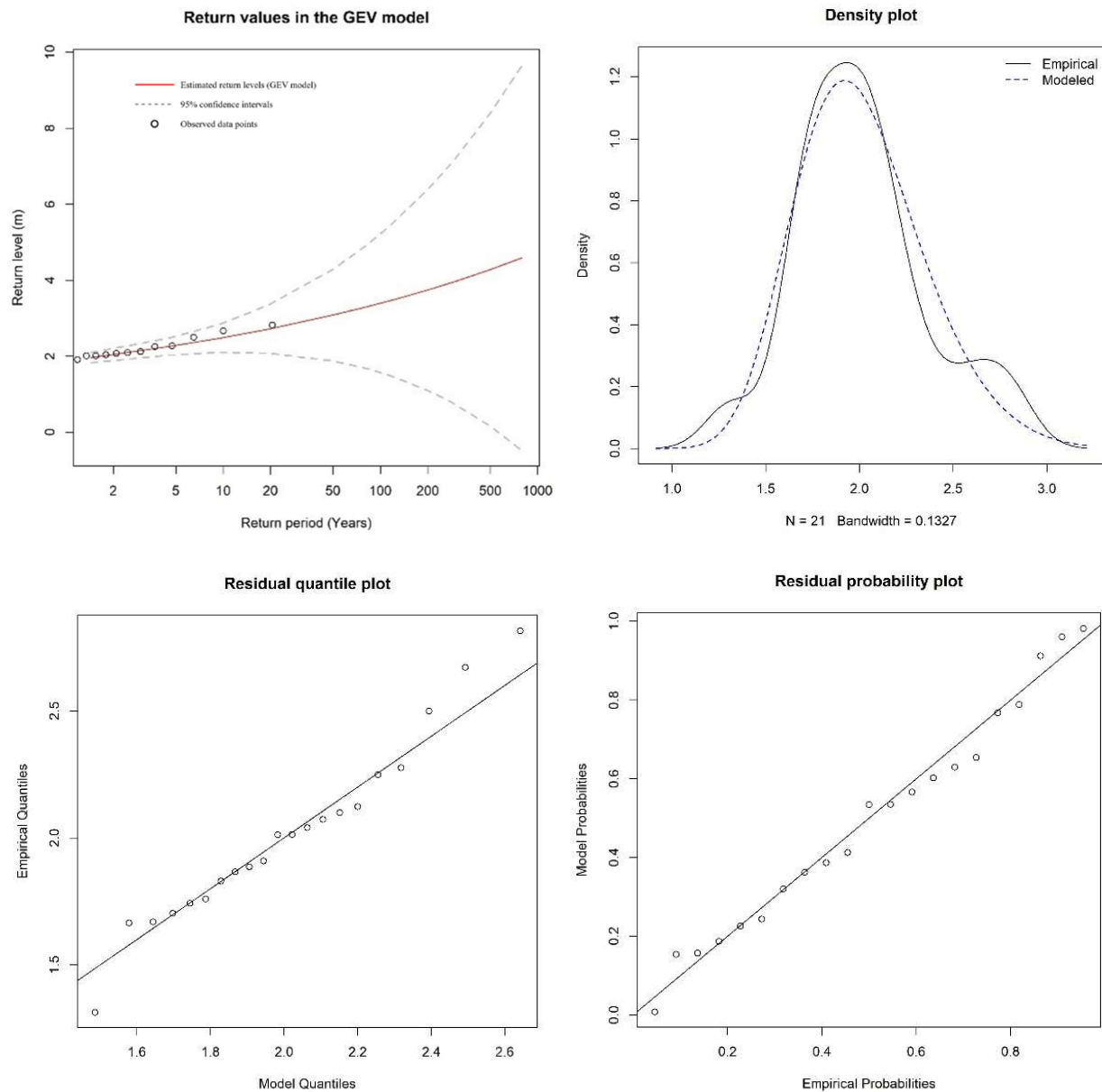


Figure D-2: Return Period analysis, Density plot and Residual quantile and probability for point B

APPENDIX E – METOCEAN SURVEY REPORT

See attached at end of document.

APPENDIX F – WALKOVER SURVEY REPORT

F.1 INTRODUCTION

Rosslare Harbour was visited for a site walkover survey on 29 November 2023 by GDG.

The walkover was undertaken by Joey O'Connor, Paul Stafford, Niamh Connolly and Charlotte Manwaring. The walkover was undertaken in two teams in the morning to facilitate access requirements and time constraints, with all four surveyors working in one team for the afternoon walkover.

Access to the Terminal 7 OPW construction site was controlled by John Paul Construction with access to the Harbour controlled by Rosslare Europort. Site induction from John Paul Construction was required to access the John Paul Construction site, which included the western area of the harbour, at Ballygeary, which was being developed to upgrade port border infrastructure. Controlled access ensured safety of surveyors, though limited the areas the site walkover could access.

Weather on the day was overcast with a slight wind.

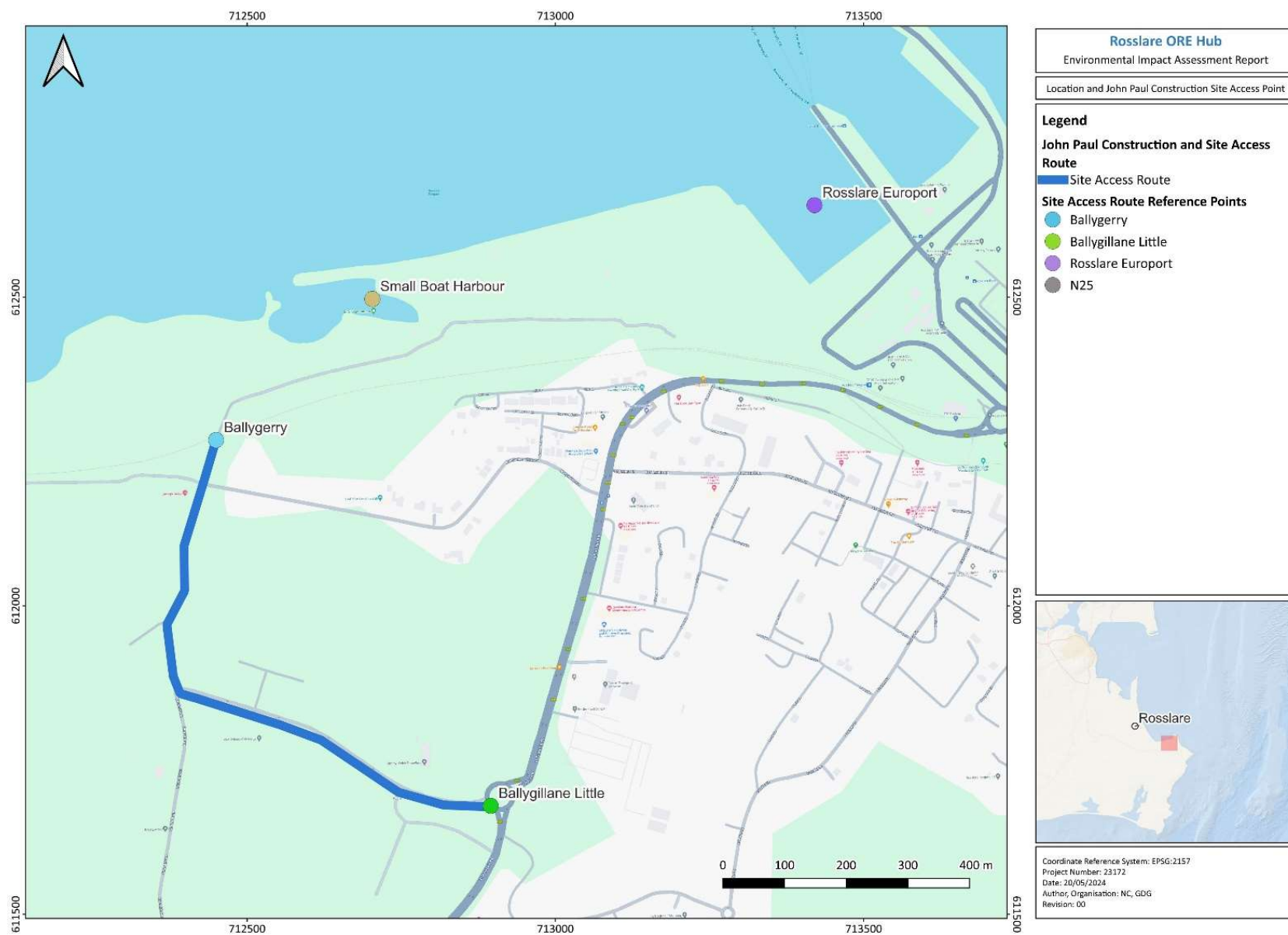


Figure E-1 Location and John Paul Construction site access point

F.1.1 APPLICABLE STANDARDS AND REFERENCES

BS 5930:2015+A1:2020 Code of practice for site investigations

BS 10175:2011 (+A2:2017) Investigation of potentially contaminated sites - code of practice

Land contamination risk management (LCRM), Environment Agency, 2021

F.2 METHODOLOGY

The walk over survey area is divided into the John Paul Construction Site and small boat harbour (i.e. the western area) and Rosslare Harbour port and beach (i.e. the eastern area).

The walk over survey was conducted to describe the characteristics and uses of the site at the time of survey, including general condition of the site and the surrounding area.

The following characteristics were considered at each location surveyed:

- Current use and status of the site
- General condition of site and surrounding land use
- Presence of surface staining and odours
- Records of any bedrock or superficial geology, including made ground composition
- Topography and surface condition – open ground, hardstanding and other geotechnical or surface features
- Local surface water features
- Ecological feature
 - Presence and type of vegetation
 - Signs of any vegetation dieback
 - Presence and extent of any non-native invasive plants such as Himalayan balsam, Japanese Knotweed or Giant hogweed
- Buildings and below or above ground structures such as fuel tanks
- Above and likely below ground services
- Access to and security of the site
- Potential presence of any asbestos cement material within buildings or throughout the site
- Communications or discussions with site personnel

Specific sites within the survey area were identified for targeted survey:

- Old harbour and storage area near containers for signs of contamination (Figure E-2)
 - Characterise potential waste
 - Visual check for any fuel spillages/slick by boats, noting any odours
- Water features/contamination
 - Assess the Milltown Rosslare waterbody at closest accessible point (Figure E-3)
 - Assess any freshwater inputs, such as rivers, streams and field drains, into the coastal area that are not accounted for on EPA maps
 - Assess condition of bedrock at coastline
 - Transition zone/soil bedrock interface

- Visible groundwater seepages
- Pipeline or sewage outfalls
 - Note any discoloured water and odours
- Milltown Roslare_010 waterbody at closest accessible point
 - Measurement of stream channel width and water column depth
 - Provide flow estimation
 - Record any evidence of point-source contamination nearby
- Rosslare Harbour Wastewater Treatment Plant (WWTP) (Figure E-3):
 - Photograph and general description
 - Note any nearby field drains, pipework or obvious outflow points



Figure E-2 Potential waste/dump sites for inspection (yellow boxes)



Figure E-3 Hydrological features including target watercourse and WWTP

F.3 RESULTS

F.3.1 OVERVIEW

Table E-1 provides an overview of the site at the time of the site visit. Figure E-4 shows the location of the areas visited within the western area, which includes the John Paul Construction site. Figure E-5 shows the locations visited in the eastern area, which includes the port.

Table E-1 Overview of walkover survey site

Area	Description	Surrounding area
Western Area, including small boat harbour at Ballygeary (1) and John Paul construction compound (2) and border control construction site (3)	<p>Access to this area is via Churchtown Road. There is a vehicle security gate for the site south of the railway line. Vehicle access was therefore over the railway bridge. A site carpark was located to the left (west) part of the site adjacent and across from the site compound.</p> <p>The site compound had further turnstile gate access control and comprises of a series of portacabins over two levels.</p> <p>A material storage area was located to the west of the carpark and site compound. This area was also used for sub-contractor offices.</p> <p>The small boat harbour is located in the middle of this area and comprised built stone causeways, a number of small fishing boats and small boat sheds.</p> <p>Access to the eastern area of the construction site was down a newly built road and at the time of the site visit foundations were being constructed as part of the redevelopment in this area.</p>	<p>North – rocky shoreline and sea beyond.</p> <p>South – Railway line with a combination of open land and residential properties.</p> <p>East – Rosslare harbour</p> <p>West – open fields and farmland.</p>

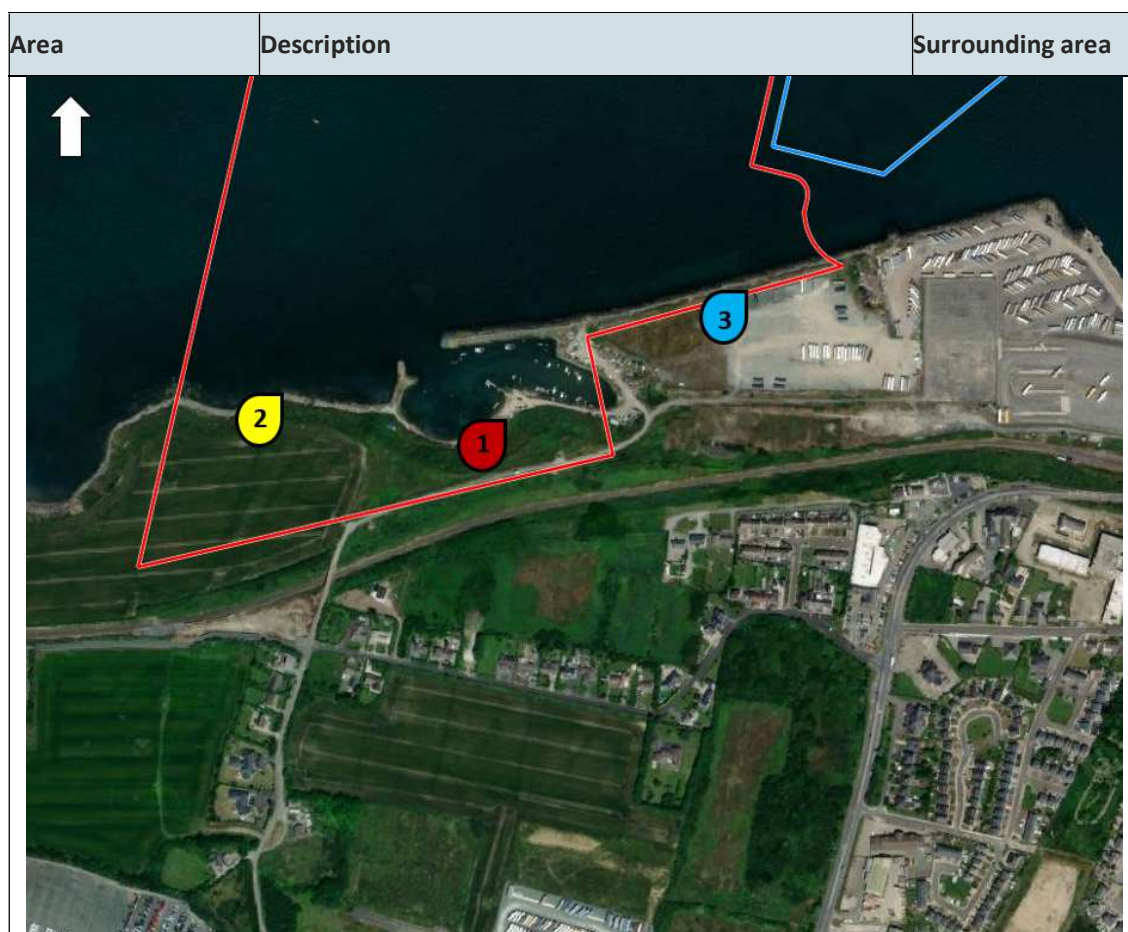


Figure E-4: Areas visited in Western area

Eastern Area, including beach (1) Rosslare Port (2) and northern breakwater (3)	Access to the eastern area and port was via the public access road from the town down an incline to a roundabout. Access to the terminal, goods area for lorries and the eastern beach is from this roundabout.	North – harbour walls and sea beyond.
	The terminal building and car park area are to the east of the port. Construction work was being undertaken within this area at the time of the walkover survey, including the removal of former railway line.	South – Railway line and access road. Land slopes steeply to the south up to the town with a combination of commercial and residential properties.
	The harbour is divided into two berth areas with a northern breakwater extending out to sea. There were a number of disused tanks / containers towards the seaward end of the breakwater seawall.	East – harbour walls and sea beyond.
	A light house is located on the end of the harbour wall.	West – Port area currently under redevelopment.
	Much of the area is under concrete / tarmac hardstanding.	

Area	Description	Surrounding area
	<p>The southern area of the port is currently used for goods customs.</p> <p>The eastern beach was surveyed at low tide, allowing to the seaward sections of the northern breakwater and associated coastal defences adjacent to the terminal building.</p>	

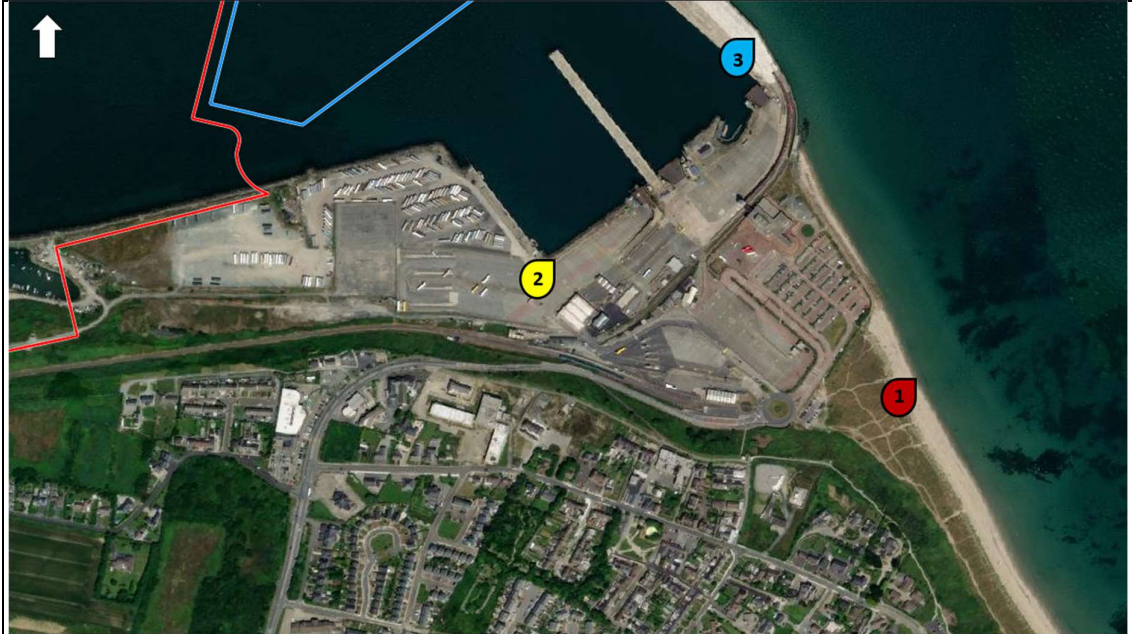


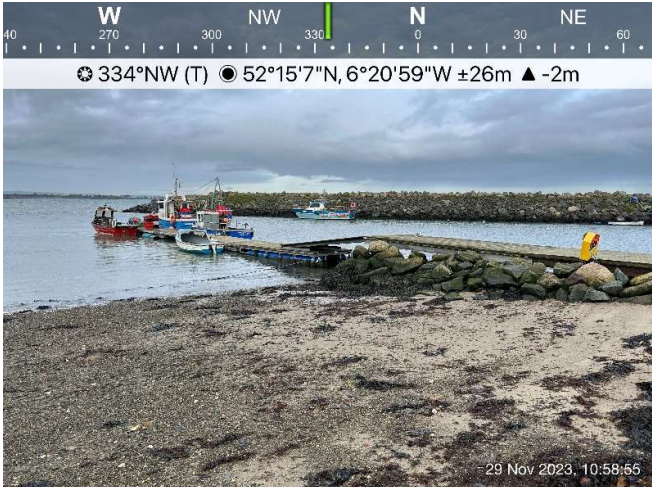

Figure E-5: Areas visited in Eastern area

F.3.2 EASTERN AREA LOCATION 1 SUMMARY – SMALL BOAT HARBOUR

Date of Inspection: 29/11/2023

Weather conditions: overcast some rain

Site Usage and Access

Current Site Usage	<p>Small boat harbour with stone harbour walls that extend eastward and two smaller walls that extend NE& NW. With pontoons and a number of fishing boats.</p>  <p>334°NW (T) 52°15'7"N, 6°20'59"W ±26m ▲ -2m</p> <p>29 Nov 2023, 10:58:55</p>
Site Accessibility	<p>Access is restricted through John Paul construction site. Photo below shows exit from the small boat harbour.</p>  <p>132°SE (T) 52°15'8"N, 6°20'52"W ±4m ▲ 1m</p> <p>29 Nov 2023, 10:49:21</p>

Site Description

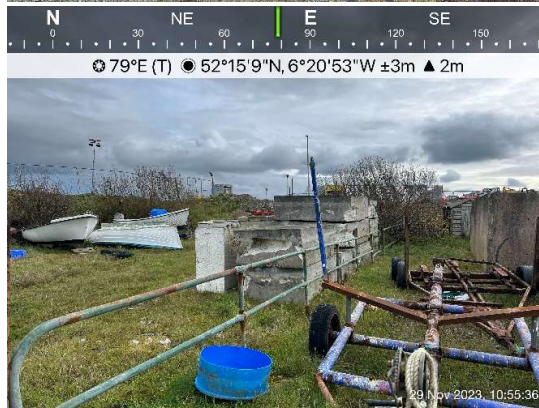
Profile

The boat harbour is largely at sea level.

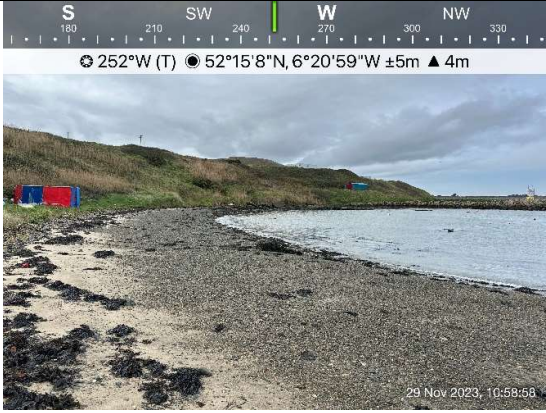

Eastern and Southern area there are a number of small shed structures



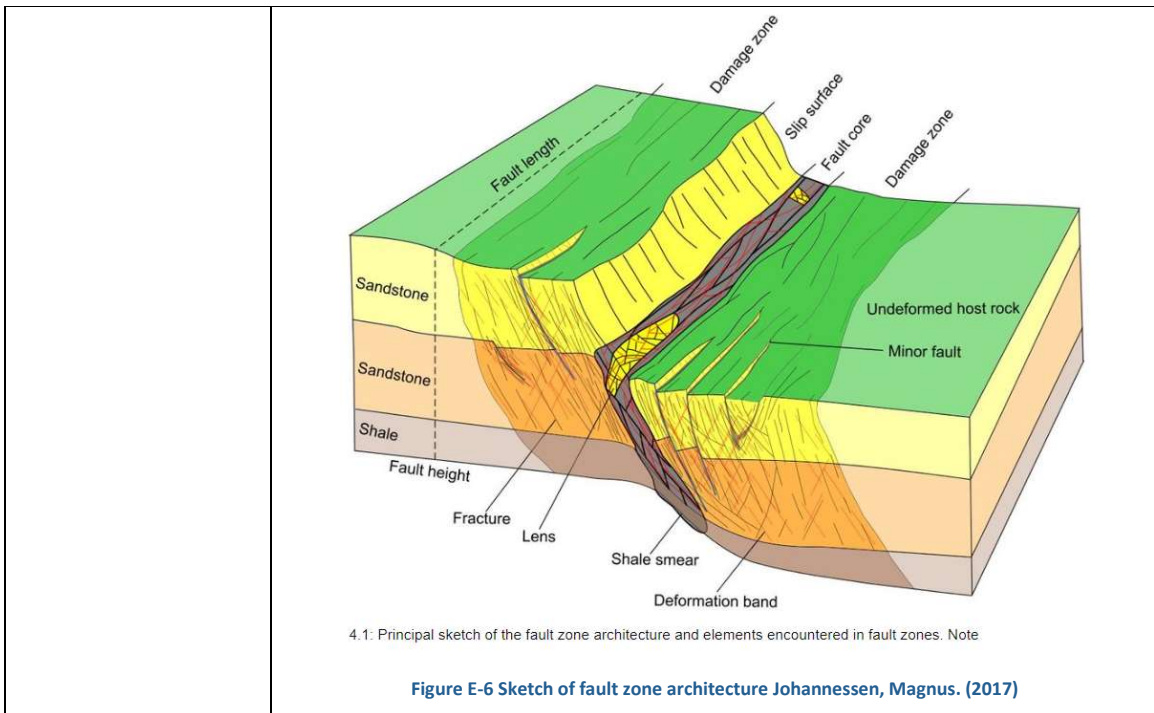
Largely tidy but some areas of rubbish build up and many lobster and whelk pots.



Land rises steeply to the south and to land currently used as the John Paul Site compound.

		
Surface covering	Beach areas / rough vegetation / hardcore surfaces	
Structures	Harbour walls etc	
Geology		 <p>Metamorphic rocks – Greenore Point Group Amphibolite</p> <p>The onsite geology is mainly comprised of Precambrian amphibolites with small sections of Ordovician conglomerates and sandstones which sit unconformably (out of sequence) on top of the older amphibolites due to local faulting or extensive erosion (nonconformity).</p> <p>The metamorphic amphibolites found onsite are referred to as the Greenore Point Group and have been described by the Geological Survey of Ireland as a “thick sequence of amphibolites probably igneous in origin with both plutonic and volcanic components”. Extensive foliation is evident throughout the outcrop found onsite indicating a moderate to high degree of metamorphism has occurred. Foliation is caused by an alignment of minerals when a rock experiences intense shearing forces or differential pressures as a result of burial.</p> <p>The mineral assemblage within the Greenore Point Group comprise of hornblende, plagioclase, garnet, quartz, epidote, and biotite.</p> <p>The engineering properties of amphibolite can vary depending on factors such as mineral composition, texture, and fabric. General properties of amphibolite can be considered to be:</p>

	<ul style="list-style-type: none"> • Strength: Amphibolite tends to have good compressive strength due to its dense mineral composition. However, the strength can vary depending on the degree of metamorphism and the presence of structural weaknesses such as foliation or fractures. • Durability: Amphibolite is typically durable and resistant to weathering and erosion, making it suitable for various engineering applications. • Elastic Modulus: It exhibits a relatively high elastic modulus, making it suitable for applications where stiffness and strength are important, such as in building foundations or as dimension stone. • Abrasion Resistance: Amphibolite is typically resistant to abrasion, which makes it suitable for use in applications where wear resistance is essential, such as in road construction or as railway ballast. • Thermal Conductivity: The thermal conductivity of amphibolite can vary depending on its mineral composition and fabric. Generally, it has moderate thermal conductivity, which can influence its suitability for use in thermal applications such as heat exchangers or as a construction material in environments with temperature variations. <p>There are minor deposits of sedimentary rocks in the form of Ordovician sandstones, mudstones, and conglomerates. Due to port development, there are no visible outcrops across the site. The formations are described as dark grey mudstones with play grey laminated/thin-bedded siltstone to coarse-grained sandstones and conglomerates. There is evidence of soft sediment deformation throughout the formation. As these formations are heterogeneous in lithology the associated engineering properties will be variable depending upon the geology encountered.</p> <p>It should be noted that the area has undergone extensive brittle structural deformation with faults and fractures identified across the site. Due care is required before undertaking development. The extent of the fault zone associated with the strike-slip faults found onsite is not known. The properties of the fault zone, including its composition, fault gouge, and fault rocks, can influence ground behaviour during construction and may present challenges during development.</p>
--	---



Properties in Proximity

Land use	North: stone harbour walls and sea beyond South: slope rising up to the area currently used by John Paul construction compound. East: John Paul construction site West: continuation of shoreline
Watercourses	None

Obvious Contamination

Noxious smells	None noted
Waste	Areas highlighted with yellow boxes on Figure E-2 are not “dump” sites however rubbish is found in certain areas within the Small Boat Harbour.
Discoloured water	None noted
Surface staining	None noted
Suspected Asbestos	None noted
Vegetation dieback	None noted

Ecology

Any notable receptors	 <p>No notable receptors.</p>
Invasive species (e.g. Japanese Knotweed, Giant Hogweed)	None noted


Tanks and Drums

Above ground tanks	None
Subsurface tanks	None
Chemical drums	IBCs and plastic drums

Public Utilities

Overhead cables	Small wooden mounted cables
Manholes	None noted
Transformers	Not seen

Slope Stability

Any obvious instability	 <p>Exposed area in the left of the above photo. Blue building is a Sea Scout hut with flag poles</p>
Retaining walls, etc.	none

Miscellaneous

Condition of structures	Well used sheds. Some derelict.
Buried foundations	None noted
Underground voids, cellars	None
Evidence of mining activity	None


F.3.3 EASTERN AREA LOCATION 2 – FURTHER ALONG COAST FROM BOAT HARBOUR

Date of Inspection: 29/11/2023	Weather conditions: overcast, some rain
--------------------------------	---

Site Usage and Access

Current Site Usage	Beach area with steep slope up to John Paul compound.
Site Accessibility	Access along the shoreline beyond the boat harbour at low tide

Site Description

Profile	
Surface covering	Stoney shoreline and vegetated slope
Structures	None
Geology	Metamorphic – Greenore Point Group Amphibolite

Properties in proximity

Land use	North: open sea South: steep grass slope riding up to John Paul compound East: Small boat harbour West: continuation of the shoreline
Watercourses	none

Obvious Contamination

Noxious smells	n/a seaweed
Waste	None
Discoloured water	None
Surface staining	None
Suspected Asbestos	None
Vegetation dieback	None

Ecology

Any notable receptors	None
Invasive species (e.g. Japanese Knotweed, Giant Hogweed)	None

Tanks and Drums

Above ground tanks	None
Subsurface tanks	None
Chemical drums	None

Public Utilities

Overhead cables	None
Manholes	None
Transformers	None

Slope Stability

Any obvious instability	Steep slope
Retaining walls, etc.	none

Miscellaneous

Condition of structures	None
Buried foundations	None
Underground voids, cellars	None
Evidence of mining activity	None

F.3.4 EASTERN AREA LOCATION 3

Date of Inspection: 29/11/2023	Weather conditions: overcast, some rain
--------------------------------	---

Site Usage and Access

Current Site Usage	Area to the south of this location point is currently under construction.
Site Accessibility	Access is restricted through John Paul construction site.

Site Description

Profile	<p>Largely flat with harbour wall to the north and construction site to the south</p> 
Surface covering	Mixture of stone / vegetation
Structures	
Geology	None seen as all made ground

Properties in proximity

Land use	<p>North: Sea</p> <p>South: John Paul construction site</p> <p>East: Rosslare Harbour</p> <p>West: coastline and small boat harbour</p>
Watercourses	none

Obvious Contamination

Noxious smells	None
----------------	------

Waste	Area of suspected waste “Dump” highlighted on Figure E-2 is now part of the John Paul construction site and there is no evidence of this at the time of the site visit
Discoloured water	none
Surface staining	none
Suspected Asbestos	none
Vegetation dieback	none

Ecology

Any notable receptors	None noted
Invasive species (e.g. Japanese Knotweed, Giant Hogweed)	None noted



Tanks and Drums

Above ground tanks	None noted
Subsurface tanks	None noted
Chemical drums	None noted

Public Utilities

Overhead cables	None noted
Manholes	None noted
Transformers	None noted

Slope Stability

Any obvious instability	none
Retaining walls, etc.	Harbour coastal defences present

Miscellaneous

Condition of structures	None noted
Buried foundations	None noted
Underground voids, cellars	None noted
Evidence of mining activity	None noted


F.3.5 EASTERN AREA LOCATION 1- BEACH

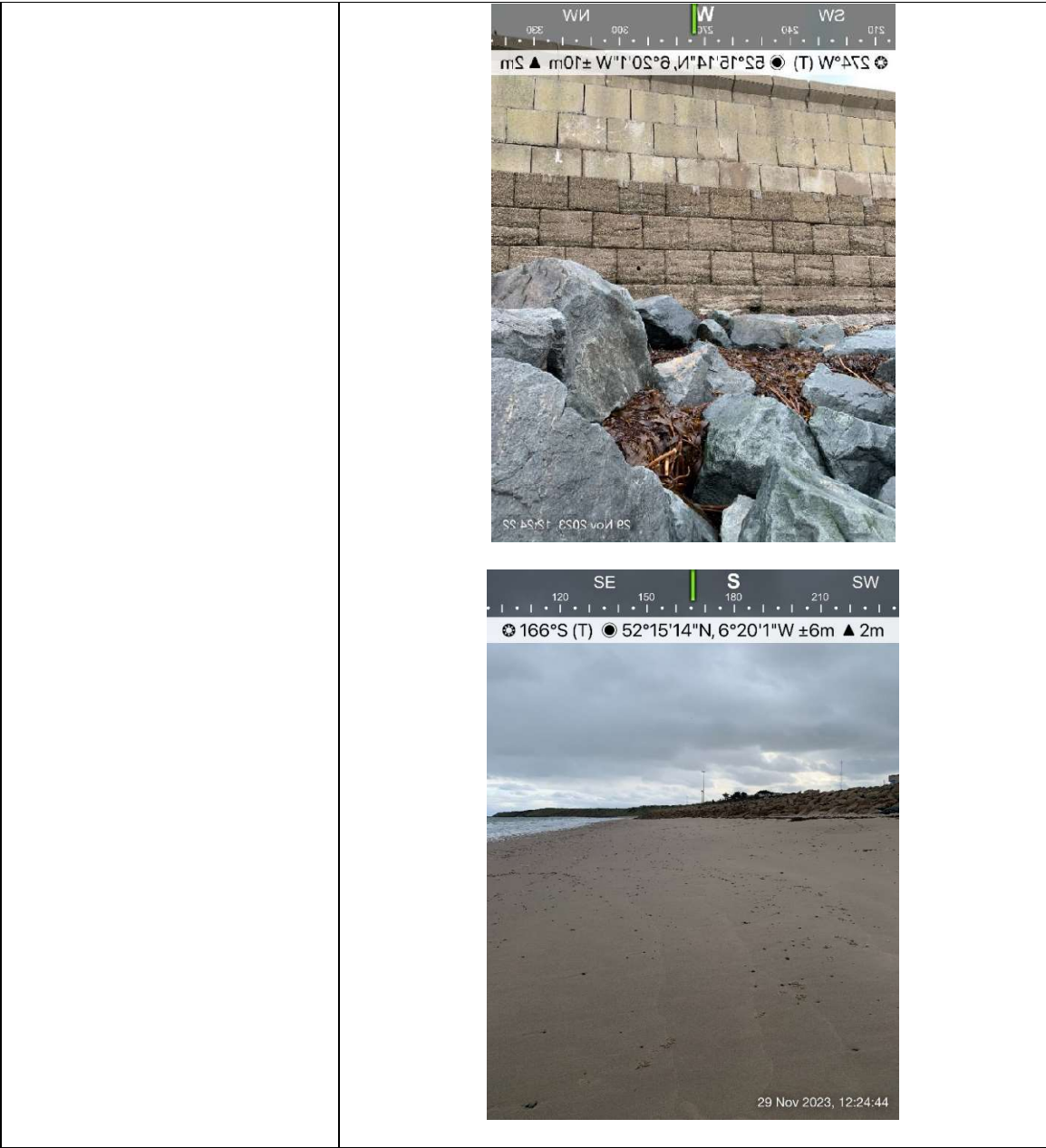
Date of Inspection: 29/11/2023	Weather conditions: overcast. windy
--------------------------------	-------------------------------------


Site Usage and Access

Current Site Usage	Beach
Site Accessibility	Access from harbour road and car park

Site Description

Profile	<p>Level beach leading to vegetated slope that rises steeply to the southwest</p>  <p>The three photographs illustrate the beach profile. The top photo shows a wide, sandy beach with tall grass on the right and a cloudy sky. The middle photo shows a rocky shoreline with waves crashing against the rocks. The bottom photo shows a view of the beach from a distance, with waves breaking on the shore and a cloudy sky.</p>
---------	--



	 <p>The top photograph shows a close-up of a sandy beach with several dark, irregularly shaped rocks scattered across the surface. The middle photograph shows a rocky coastline with waves breaking against the shore. The bottom photograph shows a wide, sandy beach with a vegetated slope in the background.</p>
Surface covering	Sand with some areas of rock exposed at low tide. Harbour walls and coastal defences
Structures	
Geology	Metamorphic rocks

Properties in proximity

Land use	North: Sea and Harbour walls South: beach with vegetated slope leading up to the town East: Sea West: Rosslare port
Watercourses	none

Obvious Contamination

Noxious smells	None
Waste	None
Discoloured water	none
Surface staining	none
Suspected Asbestos	none
Vegetation dieback	none

Ecology

Any notable receptors	None noted
Invasive species (e.g. Japanese Knotweed, Giant Hogweed)	None noted

Tanks and Drums

Above ground tanks	None noted
Subsurface tanks	None noted
Chemical drums	None noted

Public Utilities

Overhead cables	None noted
Manholes	None noted
Transformers	None noted

Slope Stability

Any obvious instability	
-------------------------	---



Some local slips on the vegetated slopes

Retaining walls, etc.	Harbour coastal defences present
-----------------------	----------------------------------

Miscellaneous

Condition of structures	Harbour walls are old and repair work can be seen.
Buried foundations	None noted
Underground voids, cellars	None noted
Evidence of mining activity	None noted

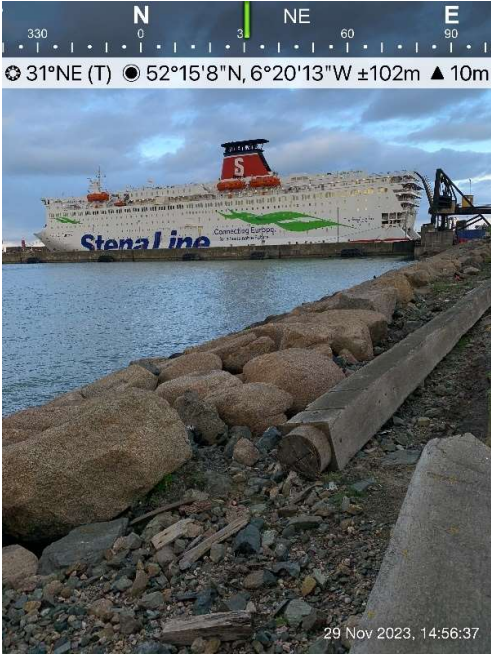
F.3.6 EASTERN AREA LOCATION 2 – ROSSLARE EUROPORT ENVIRONS

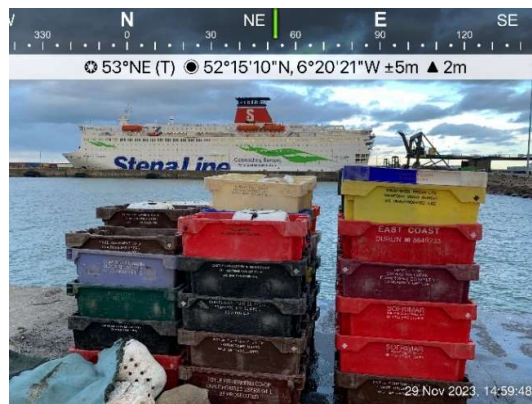
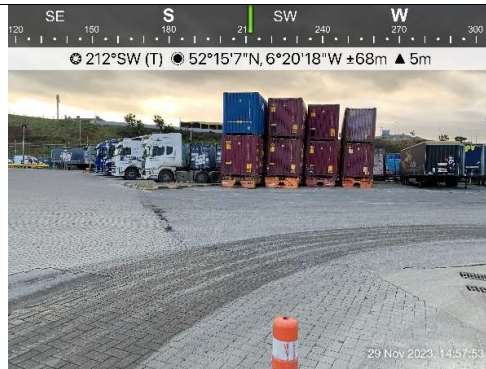
Date of Inspection: 29/11/2023	Weather conditions: overcast windy
--------------------------------	------------------------------------

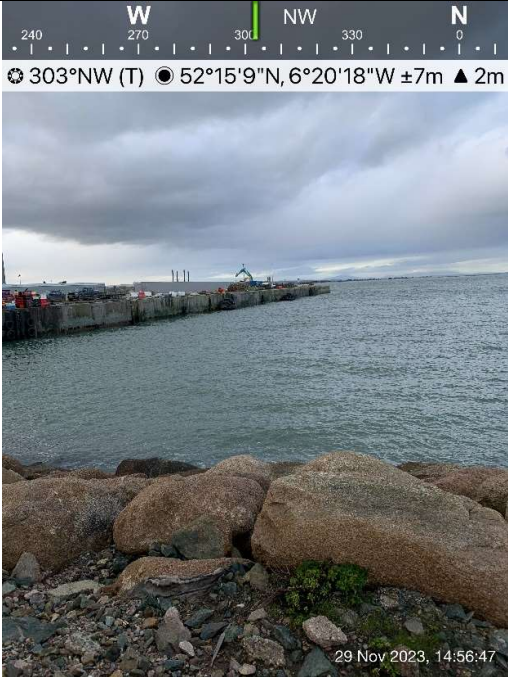


Site Usage and Access


Current Site Usage	Rosslare port.
Site Accessibility	Limited access

Site Description

Profile	<p>Largely flat</p> 
---------	--



	 
Surface covering	<p>Mixture of concrete and areas of made ground hardstanding</p> 

	
Structures	
Geology	N/A

Properties in proximity

Land use	Rosslare port
Watercourses	none

Obvious contamination

Noxious smells	Fish smells
Waste	Small areas of waste amongst fishing gear
Discoloured water	None but puddles present
Surface staining	none
Suspected Asbestos	none
Vegetation dieback	None but limited vegetation in areas of stone hardstanding

Ecology

Any notable receptors	None
Invasive species (e.g. Japanese Knotweed, Giant Hogweed)	None

Tanks and Drums

Above ground tanks	None seen in this area but likely to be present near buildings
Subsurface tanks	
Chemical drums	

Public Utilities

Overhead cables	
Manholes	
Transformers	

Slope Stability

Any obvious instability	Largely flat
Retaining walls, etc.	n/a

Miscellaneous

Condition of structures	
Buried foundations	Likely to be present



Rosslare ORE Hub Environmental Impact Assessment Report
Technical Appendix 8: Coastal Processes

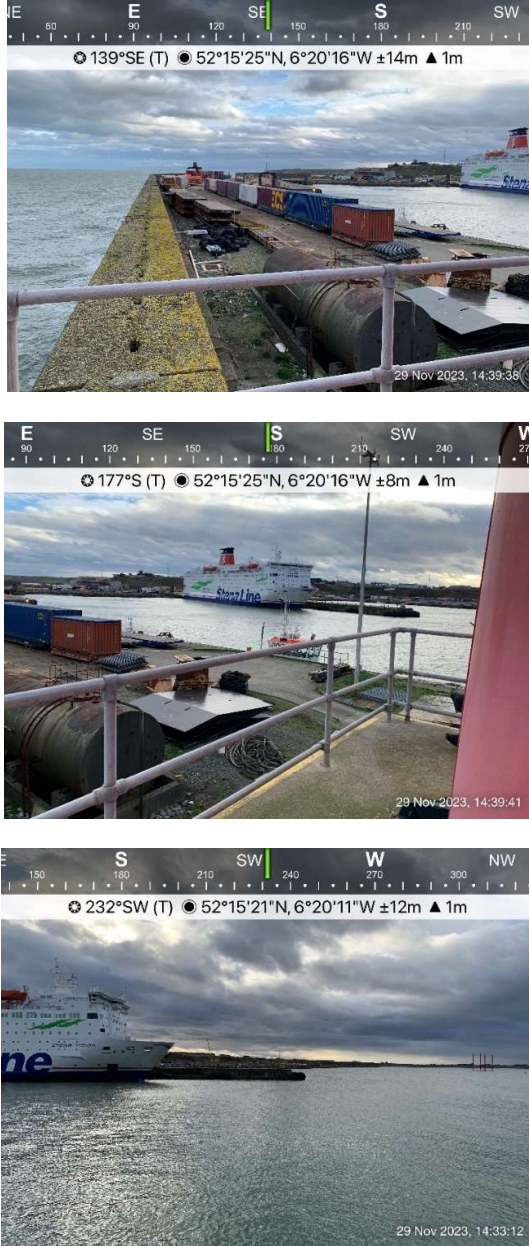
F.3.7 WESTERN AREA LOCATION 3 – HARBOUR WALL & LIGHTHOUSE

Date of Inspection: 29/11/2023	Weather conditions: overcast windy
--------------------------------	------------------------------------

Site Usage and Access

Current Site Usage	Rosslare port.
Site Accessibility	Limited access

Site Description

Profile	<p>Largely flat with steep/vertical harbour walls</p>  <p>The first photograph shows a view from a concrete pier looking out towards the sea. A large ship is visible in the distance. The second photograph shows a view from a higher vantage point, looking down at the pier and out towards the sea. The third photograph shows a view from a pier looking out towards the sea, with a large ship visible in the distance.</p>
---------	---



SE S SW W
120 150 180 210 240 270
192°S (T) 52°15'33"N, 6°21'17"W ±1032m ▲ 14m

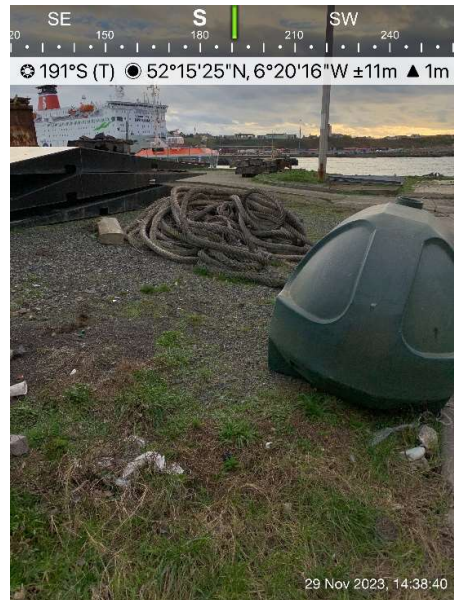
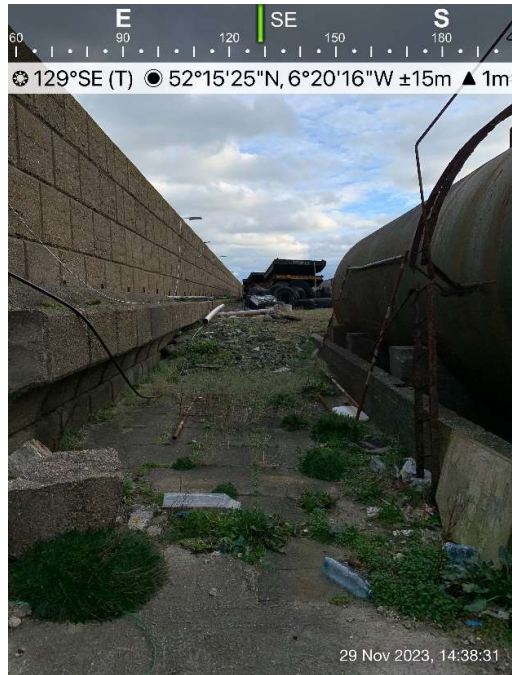


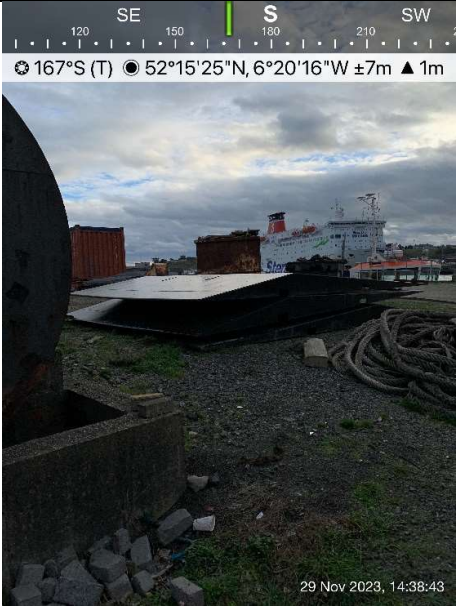

SW W NW N
240 270 300 330 0 30
312°NW (T) 52°15'21"N, 6°20'11"W ±7m ▲ 1m



E SE S SW
90 120 150 180 210 240
170°S (T) 52°15'25"N, 6°20'15"W ±44m ▲ 2m





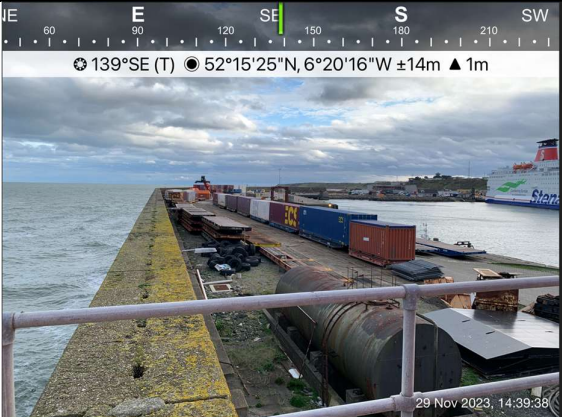
		
Surface covering	Concrete and made ground hardstanding	
Structures		
Geology	N/A	

Properties in proximity

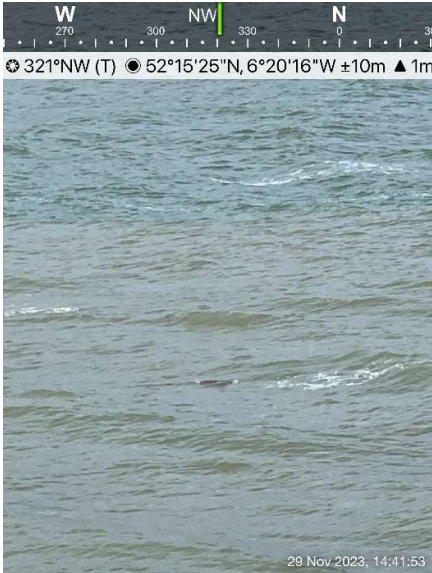
Land use	Harbour wall limited access and used mostly for redundant storage
Watercourses	none

Obvious Contamination

Noxious smells	None
Waste	Areas of waste


		
Discoloured water	none	
Surface staining	none	
Suspected Asbestos	none	
Vegetation dieback	none	

Ecology

Any notable receptors	Grey seal noted in water off northern end of breakwater.	
Invasive species (e.g. Japanese Knotweed, Giant Hogweed)	None noted	

Tanks and Drums

Above ground tanks	Yes
--------------------	-----

		
Subsurface tanks	None noted	
Chemical drums	None noted	

Public Utilities

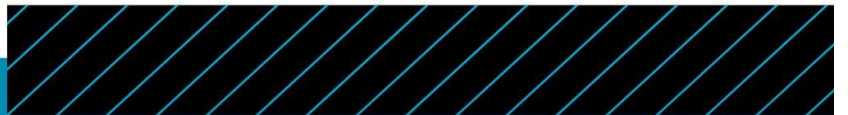
Overhead cables	some
Manholes	Yes
Transformers	None noted

Slope Stability

Any obvious instability	None noted
Retaining walls, etc.	Harbour walls

Miscellaneous

Condition of structures	Harbour walls are old and repairs can be seen.
Buried foundations	Likely to be present see info about former railway line
Underground voids, cellars	None noted although see comment above
Evidence of mining activity	None noted



Rosslare ORE Hub

EIAR Technical Appendices

Technical Appendix 8:

Coastal Processes

Appendix E: Metocean Survey Report



TECHWORKS
MARINE



GDG – Rosslare

Metocean Equipment Final Report

Submitted to Gavin & Doherty Geosolutions by
TechWorks Marine

Project Ref: TWM/GDG/WB001/2023



Document History

Project Reference: TWM/GDG/WB001/2023

Report name: GDG Rosslare Metocean Equipment Final Report

Date and Revision number:

Reporting Date – 05/07/24

Revision – 3.0

This document has been prepared by:

Document					
Revision No.	Description	Prepared By	Checked By	Approved By	Issue Date
1	Issued for client approval	CK, IL	SMcG	SMcG	22/05/24
2	Client comments received	JMcC	SMcG	SMcG	14/06/24
3	Client comments applied	CK	SMcG	SMcG	05/07/24

Signatory Legend:

COK: Charlotte O’Kelly

Managing Director

PT: Philip Trickett

Technical Director

SMcG: Sinead McGlynn

Chief Operations Officer

CK: Catherine Kelly

Marine Scientist

JMcC: Jack McCarthy

Marine Scientist

IL: Ingvar Lukas

Oceanographic Data Scientist

Contents

Figures	3
Tables.....	4
1. Executive Summary	5
2. Introduction.....	6
2.1. Deployment locations	6
2.2. Maintenance visits.....	7
3. Data Overview	8
3.1. Data Quality Control Methodology	8
3.2. Parameter Description.....	8
3.3. Collected Data Statistics.....	9
4. Data Presentation.....	10
4.1. RH-WB001 (North Buoy) Parameter Statistics	10
4.2. RH-WB002 (South Buoy) Parameter Statistics	10
4.3. Time Series Plots.....	11
4.4. Scatter plots	14
4.5. Roses.....	20
5. Joint Probability Tables	25
5.1. WB001	25
5.2. WB002.....	27
6. General State of the Irish Climate- December 2023 to March 2024	29
6.1. Storms	29
7. Conclusion.....	30
8. Appendices.....	31
WB001 Current Speed per bin:.....	32
WB002 Current Speed per bin:.....	36

Figures

Figure 1: Map of deployment locations.....	7
Figure 2: Time series plot of WB001 significant wave height – H_s (m)	11
Figure 3: Time series plot of WB001 mean zero crossing period - T_z (m/s)	12
Figure 4: Time series plot of WB001 peak period - T_p (s).....	12
Figure 5: Time series plot of WB002 significant wave height - H_s (m)	13
Figure 6: Time series plot of WB002 mean zero crossing period - T_z (s).....	13
Figure 7: Time series plot of WB002 peak period - T_p (s).....	14
Figure 8: WB001 peak period as a function of significant wave height.	15
Figure 9: WB001 mean zero crossing period as a function of significant wave height.	15
Figure 10: WB002 peak period as a function of significant wave height.....	16
Figure 11: WB002 Scatterplot Comparison of Significant Wave Height vs Peak Period	17
Figure 12: WB002 mean zero crossing period as a function of significant wave height.	16
Figure 13: WB001 and WB002 comparison of Significant Wave Height vs Average Zero Crossing period	17
Figure 14: WB001 and WB002 comparison of Significant Wave Height vs Peak Period	18
Figure 15: WB001 Depth Averaged current speed.....	18
Figure 16: WB001 current direction.	19
Figure 17: WB002 Depth Averaged current speed.....	19
Figure 18: WB002 current direction.	19
Figure 19: WB001 wave rose showing direction the waves are coming from.....	21
Figure 20: WB002 wave rose showing direction the waves are coming from.....	22
Figure 21: WB001 current rose showing direction current is going to.	23
Figure 22: WB002 current rose showing direction current is going to.	24

Tables

Table 1: Deployment coordinates	6
Table 2: List of parameters collected during campaign.....	8
Table 3. Data return statistics for each of the met ocean buoys from December 2023 to March 21 st 2024.	9
Table 4: RH-WB001 parameter statistics for wave and currents	10
Table 5: RH-WB002 parameter statistics for wave and currents	10
Table 6. WB001 Significant wave height (Hs) - Mean direction joint probability percentage table	25
Table 7: WB001 current speed - current direction (depth averaged) joint probability percentage table	25
Table 8: WB001 peak period (Tp) - Significant wave height (Hs) joint probability percentage table ..	26
Table 9: WB001 zero mean crossing period (Tz) - Significant wave height (Hs) joint probability percentage table	26
Table 10: WB002 Significant wave height (Hs) - Mean direction joint probability percentage table ..	27
Table 11: WB002 Current speed - current direction (depth averaged) joint probability percentage table	27
Table 12: WB002 peak period (Tp) - Significant wave height (Hs) joint probability percentage table	28
Table 13: WB002 zero mean crossing period (Tz) - Significant wave height (Hs) joint probability percentage table	28

1. Executive Summary

TechWorks Marine (TWM) were contracted by Gavin O'Doherty Geosolutions (GDG) to deploy metocean equipment consisting of two wave buoys labelled RH-WB001 and RH-WB002. These systems were deployed onsite for a minimum of 3 months as part of surveys underway by GDG for the redevelopment of Rosslare Europort.

The main purpose of the metocean survey was to collect accurate oceanographic information from the project site that will be used to:

- Feed into the port infrastructure design
- Estimate workability ranges at the port to define the construction strategy; and
- Inform the Coastal Processes chapter of the EIAR.

The scope of the services included the installation, maintenance, repair and decommissioning of the following devices:

- Two (2) measurement devices (WB001 and WB002) along the export route to record currents and waves.

The wave buoys were deployed on 14/12/2023. The monitoring campaign ended on 21/03/2024 and the buoys were recovered on 20/04/2024.

This report details the final dataset that was delivered to GDG after the recovery of all systems. All systems functioned well for the duration of the measurement campaign. The average data return for all systems was 93%.

2. Introduction

TechWorks Marine were contracted by Gavin and Doherty Geosolutions (GDG) to deploy, maintain and recover two wave buoys as part of the MetOcean surveys for the ongoing development of Rosslare Europort. The buoys, which are named RH-WB001 and RH-WB002, were deployed on the 14/12/2023 and were recovered on 20/04/2024. The relevant authorities were made aware of the presence of these systems at the locations stated.

Two acoustic listening devices (FPODs) were also deployed on the 2T sinkers attached to each buoy, owned and operated by the Irish Whale and Dolphin Group. They do not form part of the scope of this work.

2.1. Deployment locations

The following section outline the deployment locations and depths for RH-WB001 and RH-WB002. The map below shows the positions of each system deployed. It should be noted that the identifiers of the buoys were switched on the AIS license issued, but for the purposes of this report and the data delivery, the buoys labels are appended with North/South for clarity.

Table 1: Deployment coordinates

	Depth	Deployment Locations Decimal Degrees		Deployment Locations Degrees & Decimal Minutes	
Item	(m)	Latitude	Longitude	Latitude	Longitude
RH-WB001 (North Buoy)	6-7	52.26323° N	6.34034° W	52° 15.7922' N	06° 20.418' W
RH-WB002 (South Buoy)	5-6.5	52.25798° N	6.32991° W	52° 15.4788' N	06° 19.7946' W

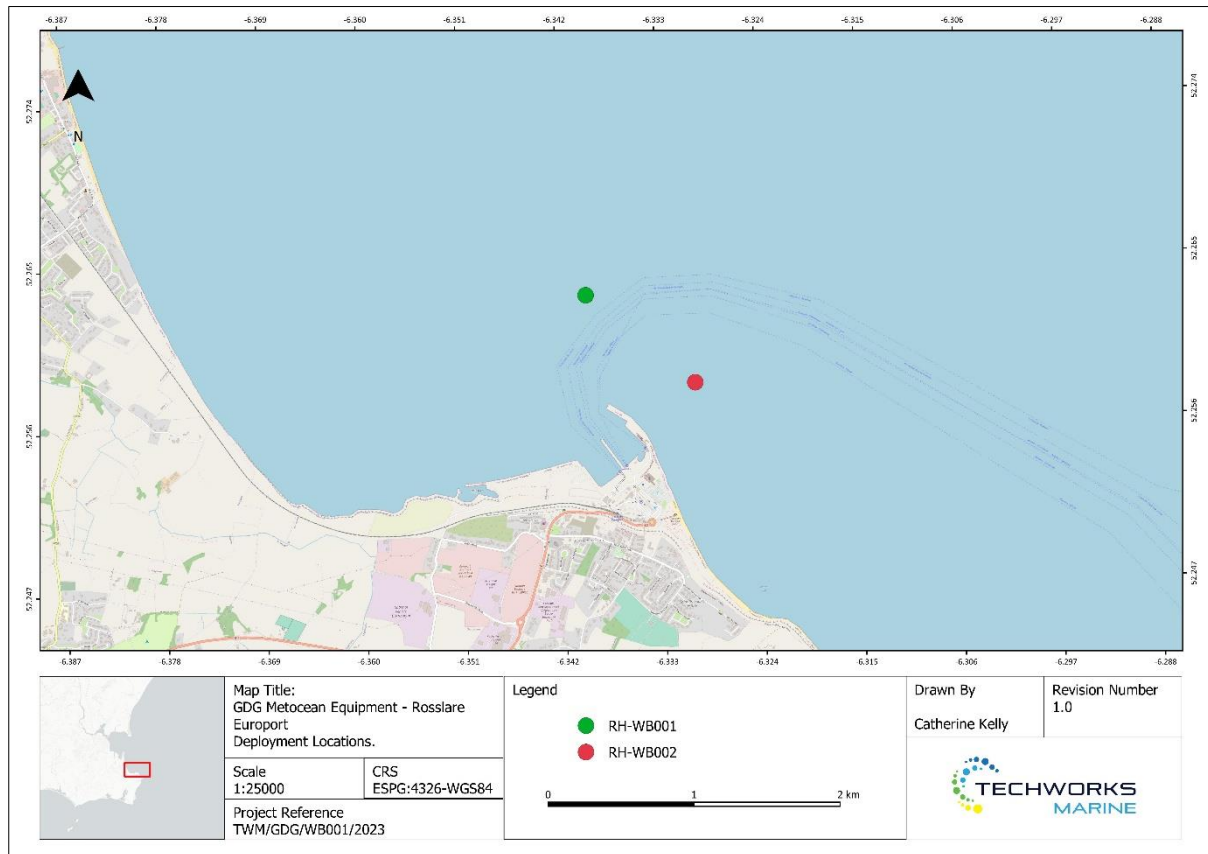


Figure 1: Map of deployment locations

2.2. Maintenance visits

Two unscheduled maintenance visits occurred during the project. The first visit occurred on the 13th January 2024 after the AIS unit on RH-WB001 stopped transmitting. The decision was made to switch out the AIS units on both buoys. The TechWorks Marine field team completed these works from the side of a small vessel, without removing the buoys from the water.

The second unscheduled maintenance visit occurred on the 7th February 2024 due to battery failure on RH-WB001. The battery failure occurred after a period of low solar charge and resulted in a data gap between 23rd January and 7th February (15 days). Due to the nature of the work a larger vessel was needed to remove the buoy from the water. The work was completed without incident and the batteries maintained good voltage levels for the remainder of the project.

The client and relevant authorities onsite were made aware of these visits at the time and notified when the maintenance was completed. Due to the gap in data collection, the measurement campaign was extended by a further week from the initial completion date of 14th March 2024.

3. Data Overview

3.1. Data Quality Control Methodology

Data processing to convert the raw data received from the buoy to the correct units is carried out after receipt of the data from the TMBB. The post-processed data consists of sensor output for each sensor (wave and ADCP), which has been visually inspected and from which null (zero) values, physically unrealistic peaks (e.g. significant wave height increasing unrealistically over a period of 10 minutes and dropping off again during the next timestep), duplicate timesteps, periods of sensor failures or erroneous data, and unrealistic differences between consecutive timestamps have been removed.

ADCP data have been processed in Nortek's post-processing software "*Ocean Contour*", which provides data visualisation, interactive QA/QC and data averaging capabilities. ADCP data have been filtered by removing side-lobes, correcting for instrument tilt, and only keeping data with >50% signal correlation.

Data from the wave sensor was collected every 17.5 minutes and data from the ADCP was collected every 10 minutes.

3.2. Parameter Description

Table 2: List of parameters collected during campaign.

Instrument	Parameter Measured	Unit
Wave Buoy 001 and 002		
SeaView SVS-603 HR	Significant Wave Height (Hs)	m
	Maximum Wave Height (Hmax)	m
	Peak Period (Tp)	s
	Mean Zero crossing period (Tz)	s
	Maximum Period (Pmax)	s
	Mean Wave Period (T01)	s
	Mean Wave Direction (Mean_Wave_Dir)	°
	Peak Wave Direction (Peak_Wave_Dir)	°
Nortek Signature 500 AD2CP	Current Speed per bin	m/s
	Current Direction per bin	°
	Heading	°
	Pitch and Roll	°

3.3. Collected Data Statistics

The following table displays the data return statistics for WB001 and WB002. The overall data returns are excellent with the exception of WB001 for January and February due to a battery failure.

Table 3. Data return statistics for each of the met ocean buoys from December 2023 to March 21st 2024.

Statistics	Dec-23	Jan-24	Feb-24	Mar-24	Total
WB001 Current	99.0%	72.6%	77.2%	99.6%	84.4%
WB001 Wave	100%	80.3%	84.1%	100%	89.1%
WB002 Current	100%	99.6%	99.3%	100%	99.4%
WB002 Wave	100%	100%	99.8%	100%	100%

4. Data Presentation

The data collected from both buoys during the period December 2023 to April 2024 is outlined below. The descriptive statistics for each recorded parameter on WB001 and WB002 are presented in Tables 4 and 5 below.

4.1. RH-WB001 (North Buoy) Parameter Statistics

Table 4: RH-WB001 parameter statistics for wave and currents

	Mean	Stn. Dev.	Min	50%	75%	90%	95%	99%	Max
Hs (m)	0.52	0.35	0.1	0.41	0.61	0.97	1.37	1.8	2.21
Hmax (m)	0.85	0.56	0.16	0.66	0.99	1.55	2.18	2.86	3.47
Tp (s)	5.73	2.28	1.34	5.75	6.87	8.83	10.24	11.51	14.84
Tz (s)	3.19	0.81	1.67	3.05	3.75	4.35	4.72	5.2	6.6
Tm-1,0 (s)	4.55	1.17	2.22	4.47	5.31	6.04	6.59	7.88	10.22
Pmax (s)	7.96	1.73	4	7.5	9	10.5	11.5	13	17.5
Peak_Dir (deg)	114.54	-	-	-	-	-	-	-	-
Mean_Dir (deg)	110.67	-	-	-	-	-	-	-	-
C_Spd_Depthavg	0.24	0.13	0	0.22	0.33	0.42	0.46	0.54	0.65
C_Dir_Depthavg	182.55	-	-	-	-	-	-	-	-

4.2. RH-WB002 (South Buoy) Parameter Statistics

Table 5: RH-WB002 parameter statistics for wave and currents

	Mean	Std. Dev.	Min	50%	75%	90%	95%	99%	Max
Hs (m)	0.56	0.36	0.11	0.44	0.67	1.03	1.42	1.81	2.03
Hmax (m)	0.9	0.57	0.18	0.71	1.06	1.66	2.27	2.87	3.23
Tp (s)	6.3	1.83	1.52	6.13	7.01	8.9	10.14	11.51	14.84
Tz (s)	3.48	0.7	1.84	3.44	3.96	4.41	4.71	5.15	5.67
Tm-1,0 (s)	4.91	0.98	2.48	4.86	5.53	6.16	6.63	7.44	8.55
Pmax (s)	8.33	1.59	4	8	9	10.5	11.5	12.5	16.5

Peak_Dir (deg)	89.19	-	-	-	-	-	-	-	-
Mean_Dir (deg)	93.54	-	-	-	-	-	-	-	-
C_Spd_Depthavg	0.34	0.2	0	0.31	0.46	0.63	0.72	0.87	1.04
C_Dir_Depthavg	175.98	-	-	-	-	-	-	-	-

4.3. Time Series Plots

Figures 2 to 4 shows the time series of significant wave height, mean zero crossing period and peak period for WB001.

Figures 5 to 7 shows the time series of significant wave height, mean zero crossing period and peak period for WB001.

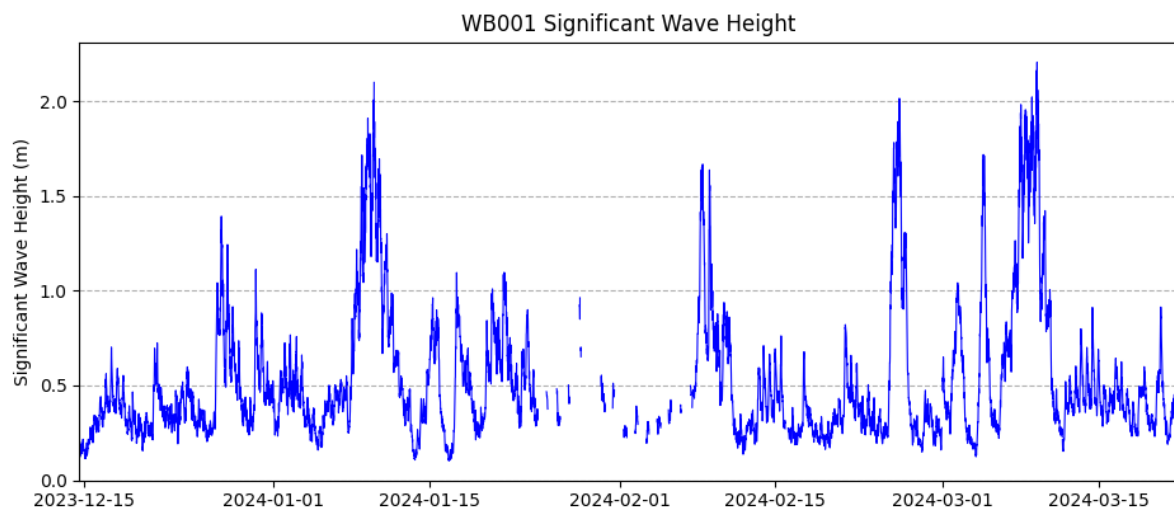


Figure 2: Time series plot of WB001 significant wave height – H_s (m)

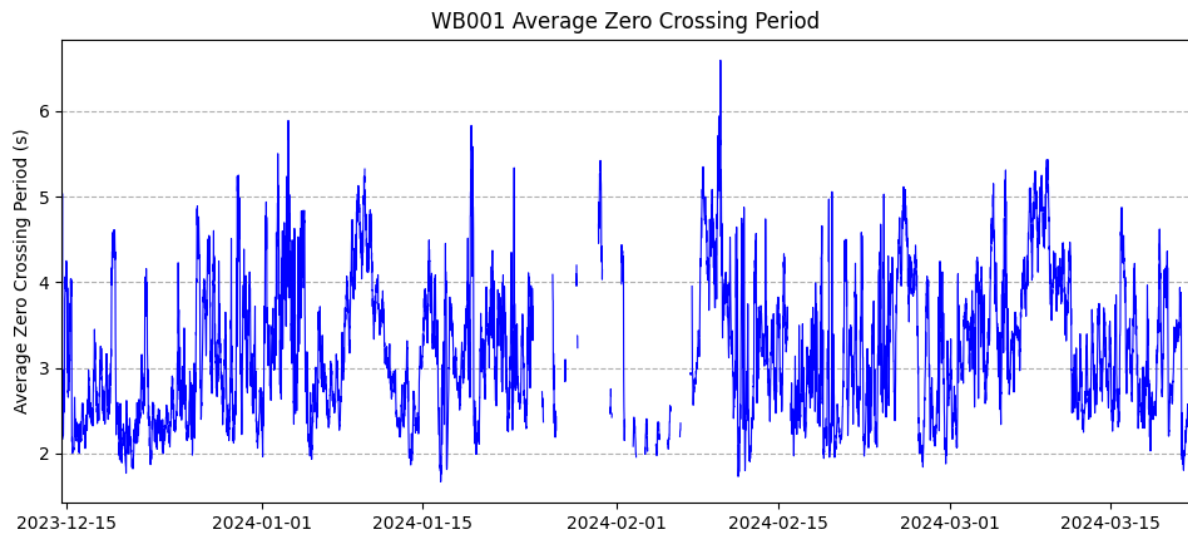


Figure 3: Time series plot of WB001 mean zero crossing period - T_z (m/s)

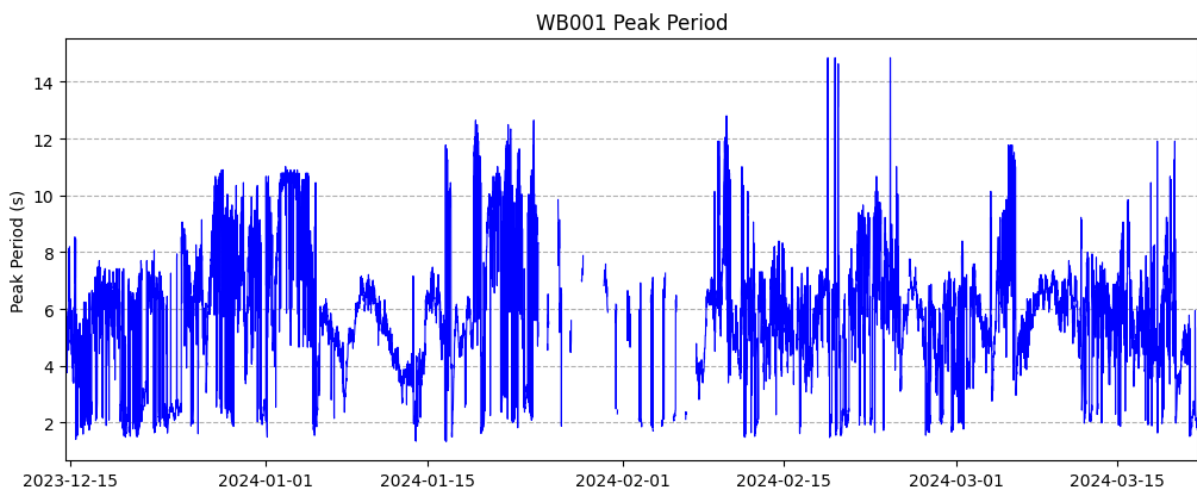


Figure 4: Time series plot of WB001 peak period - T_p (s)

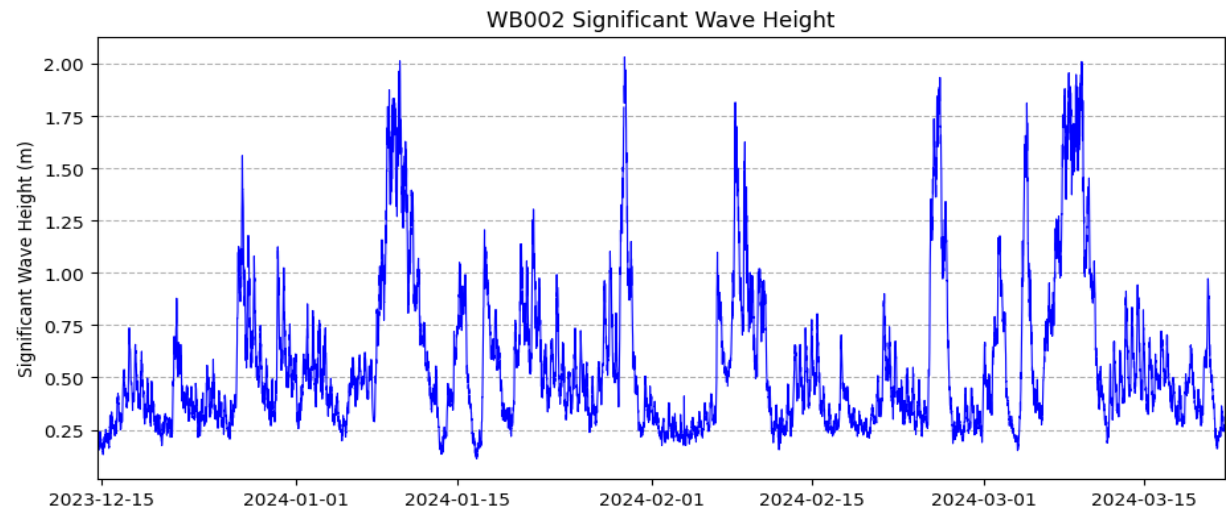


Figure 5: Time series plot of WB002 significant wave height - H_s (m)

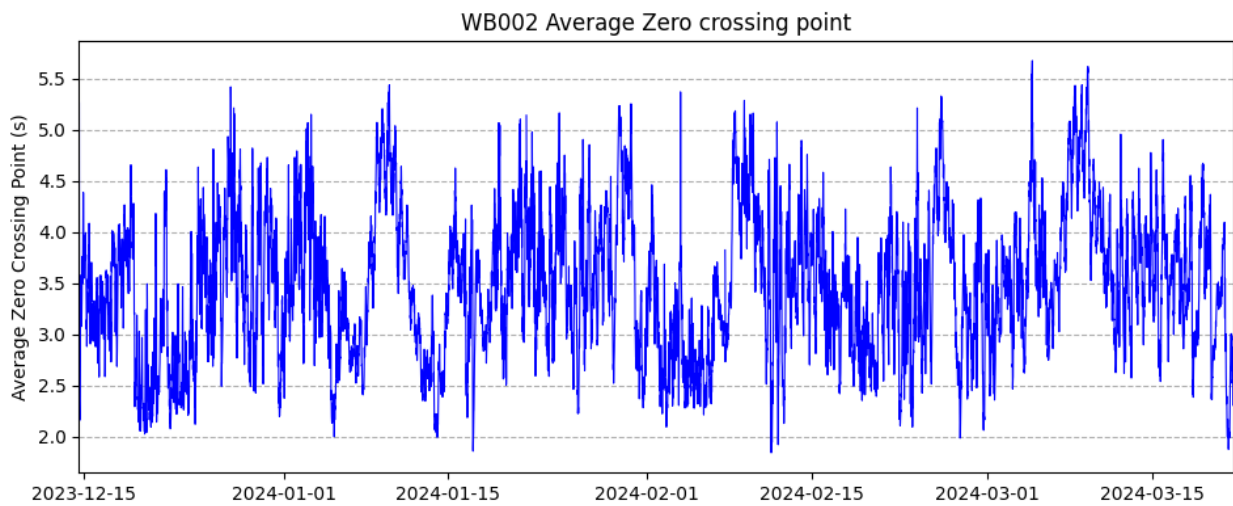


Figure 6: Time series plot of WB002 mean zero crossing period - T_z (s)

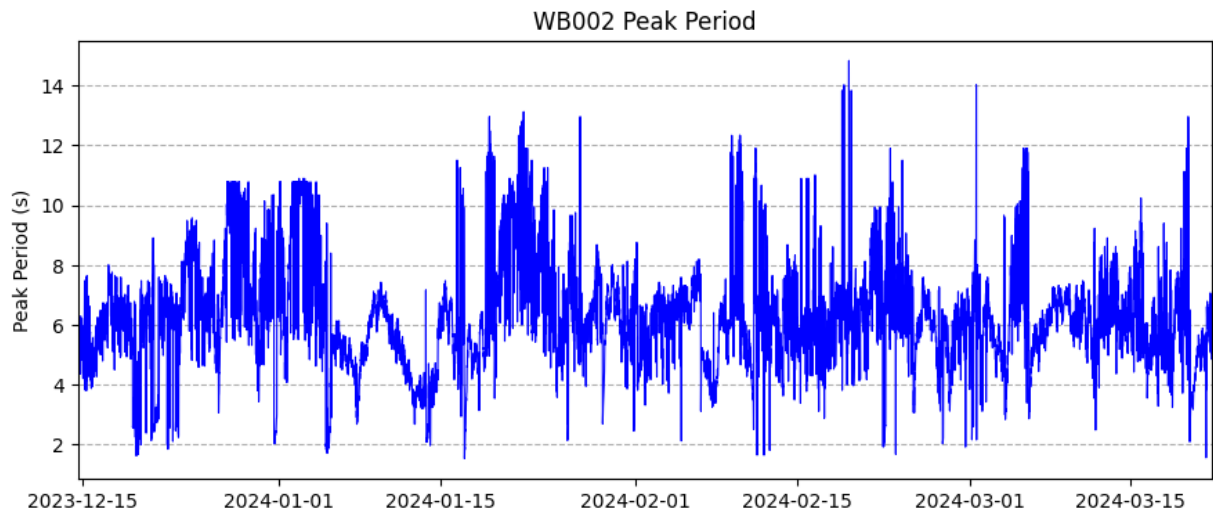


Figure 7: Time series plot of WB002 peak period - T_p (s)

4.4. Scatter plots

Figures 8 and 9 present scatter plots of significant wave height versus periods for WB001 and Figures 10 and 11 present similar for WB002. The data suggests that higher significant wave heights are generally associated with longer average zero crossing periods. This pattern could be due to the increased energy and dynamics of wave systems during this period of time.

As seen in Figures 12 and 13, WB001 and WB002 follow similar patterns in these wave parameter relationships.

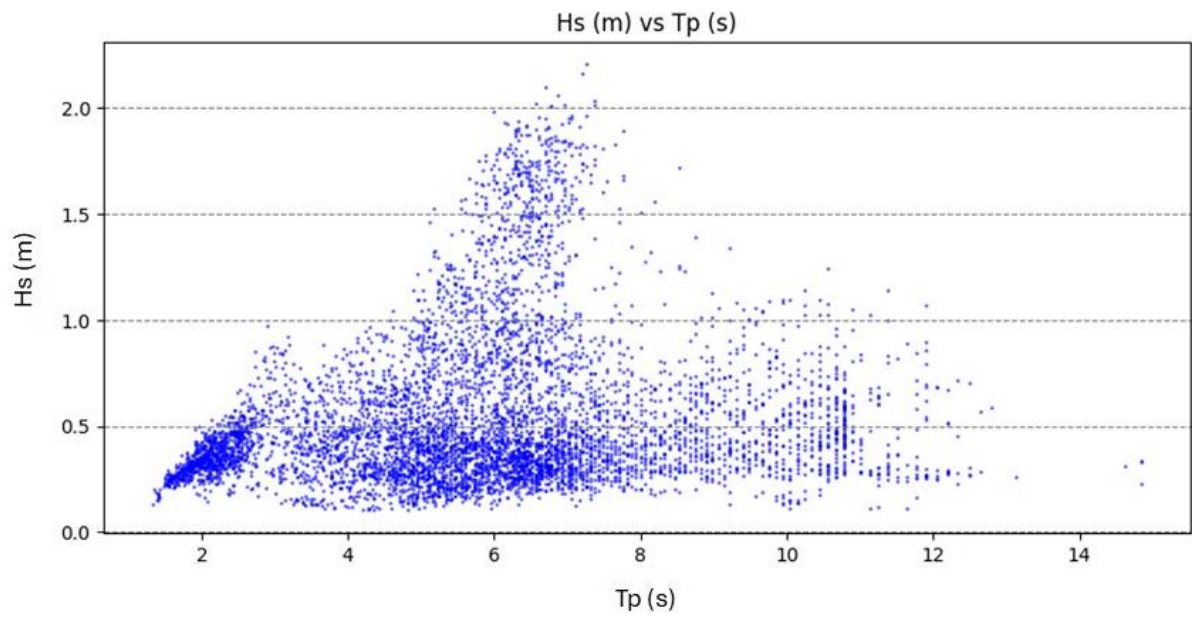


Figure 8: WB001 peak period as a function of significant wave height.

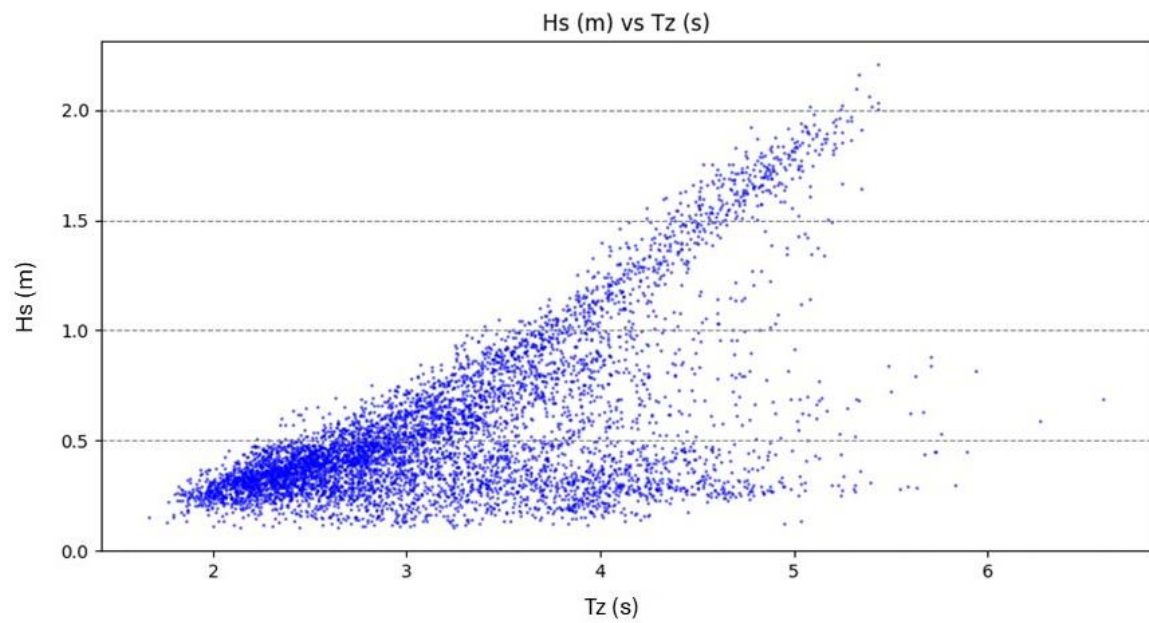


Figure 9: WB001 mean zero crossing period as a function of significant wave height.

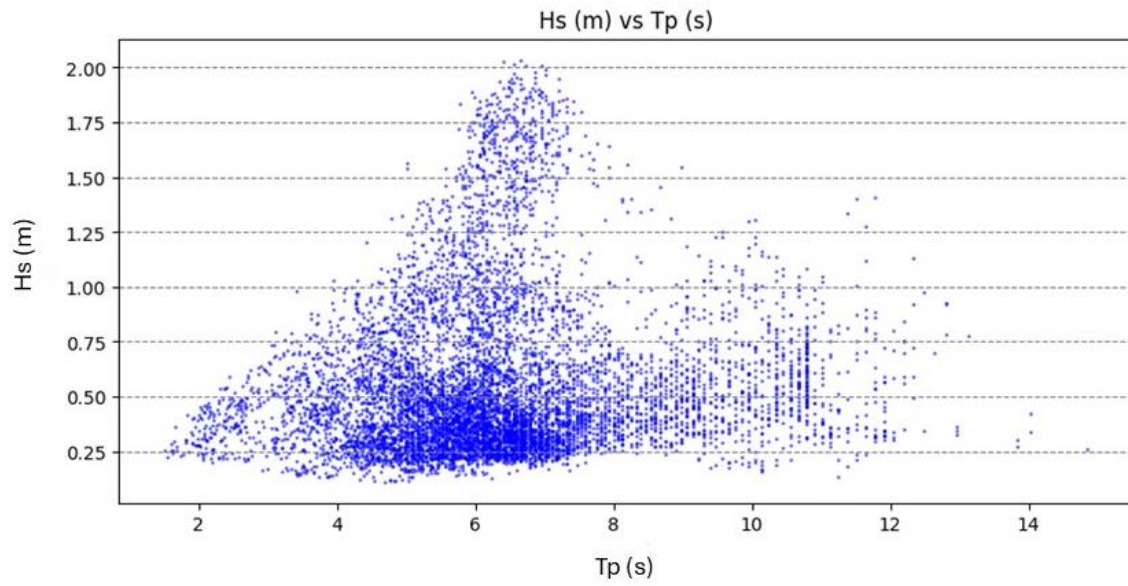


Figure 10: WB002 peak period as a function of significant wave height.

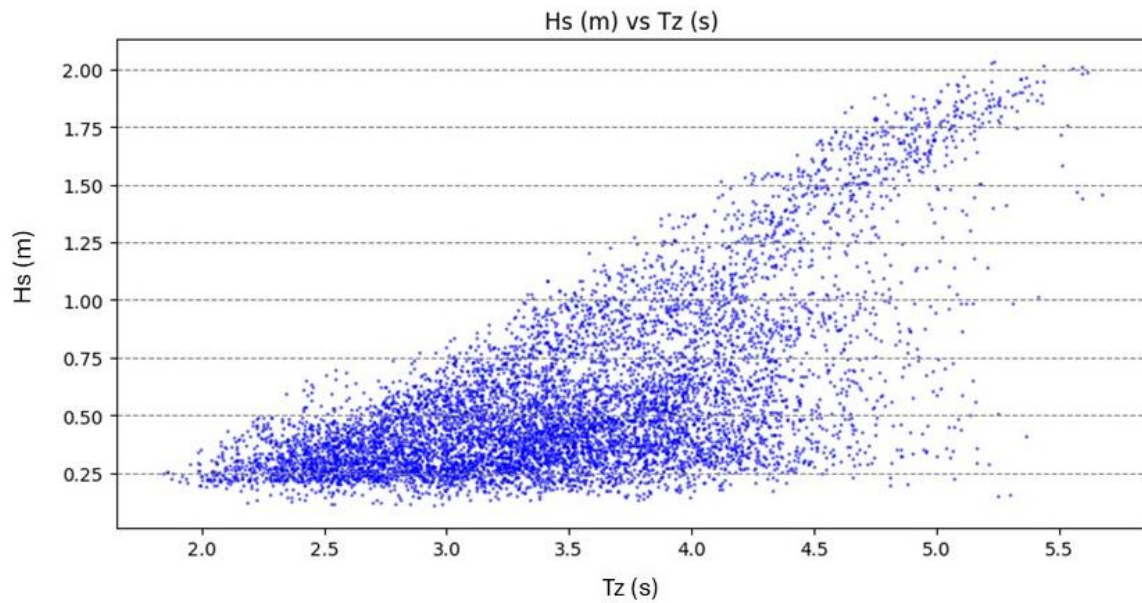


Figure 11: WB002 mean zero crossing period as a function of significant wave height.

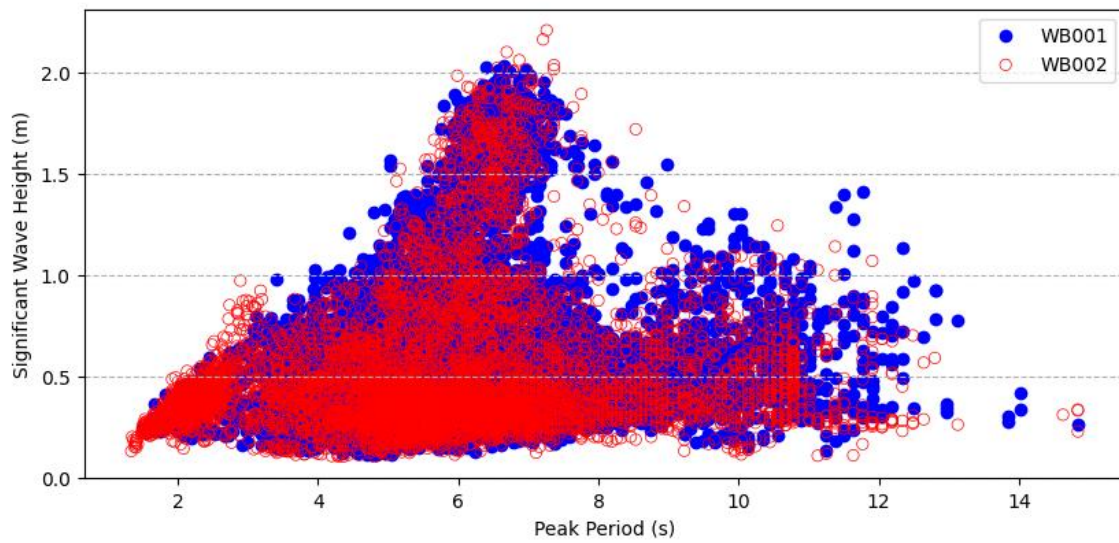


Figure 12: WB002 Scatterplot Comparison of Significant Wave Height vs Peak Period

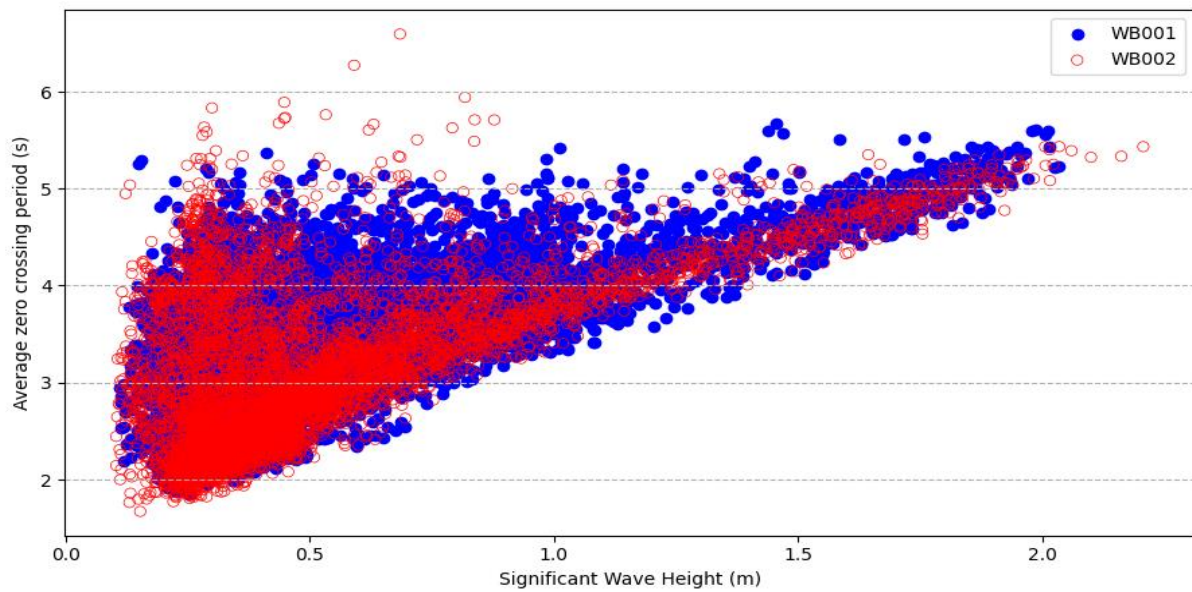


Figure 13: WB001 and WB002 comparison of Significant Wave Height vs Average Zero Crossing period

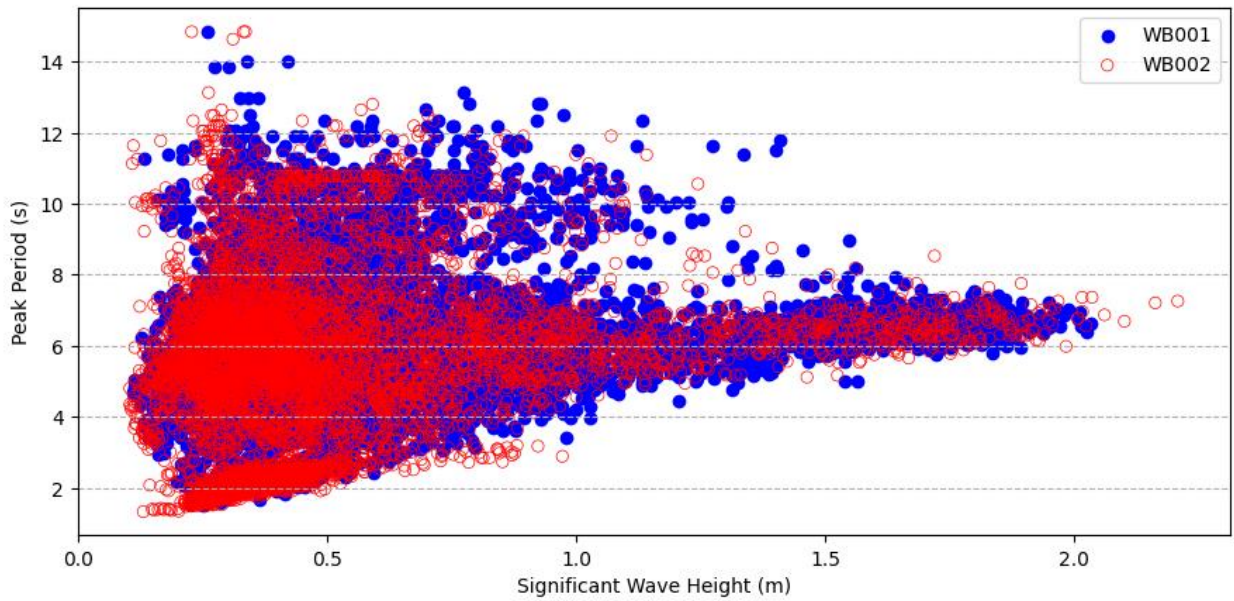


Figure 14: WB001 and WB002 comparison of Significant Wave Height vs Peak Period

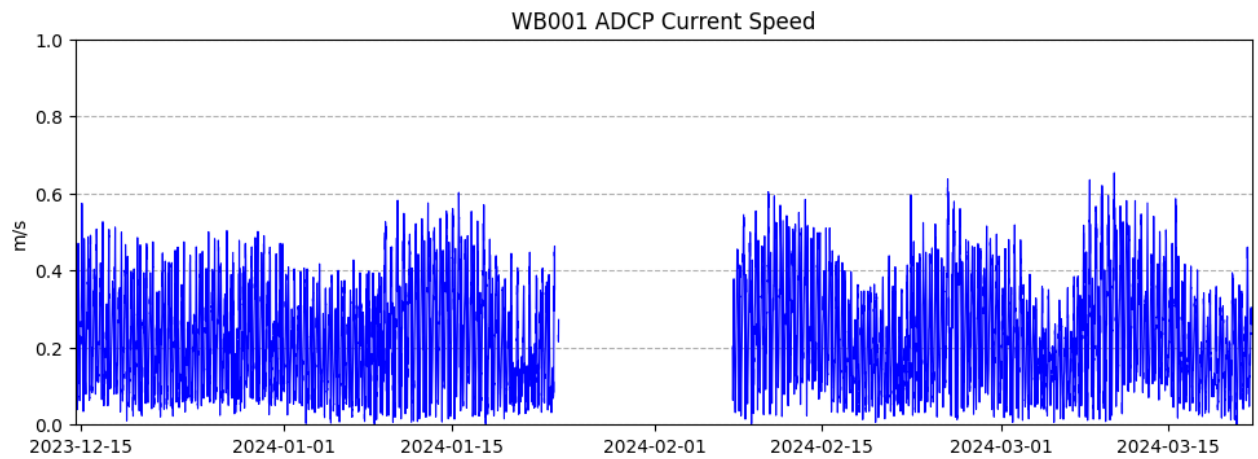


Figure 15: WB001 Depth Averaged current speed.

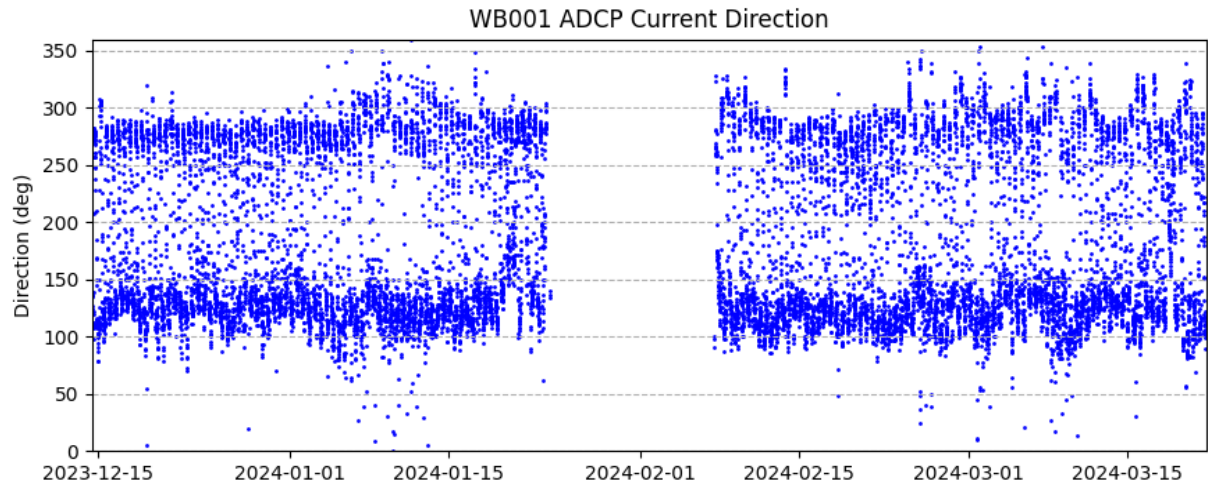


Figure 16: WB001 current direction.

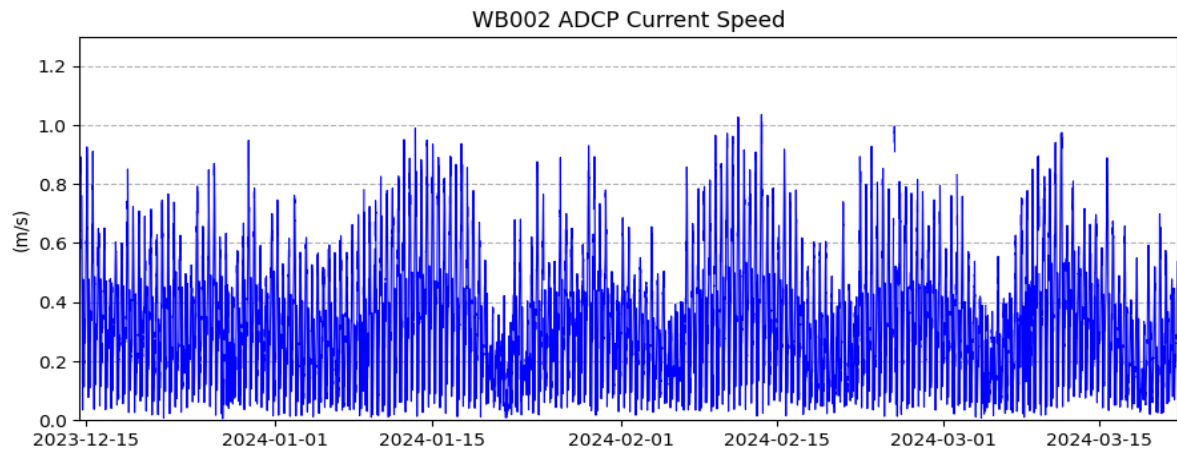


Figure 17: WB002 Depth Averaged current speed.

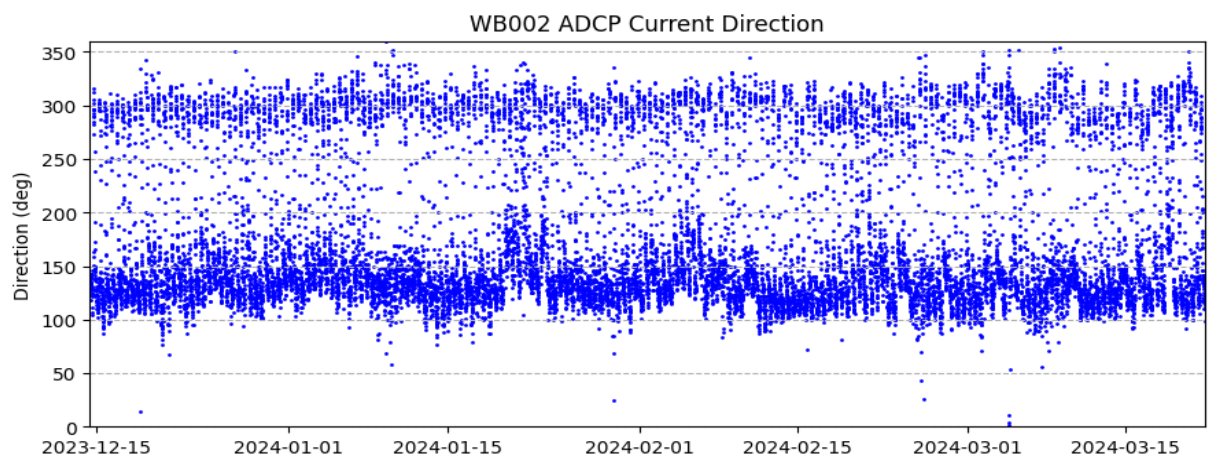


Figure 18: WB002 current direction.

4.5. Roses

Figure 18 shows the WB001 (North Buoy) significant wave height in relation to wave direction. Generally, the directionality of the waves are coming from the East (57%) with highest wave heights between 1.60 and 2(m). Figure 19 shows the WB002 (South Buoy) significant wave height in relation to wave direction, which has a larger spread of waves coming from the North/Easterly direction. The majority of these waves are between 0.40 and 0.80 (m).

Figure 20 displays a current speed rose for WB001, indicating that the majority of currents are coming from the South East with a small westerly component. The highest speed of currents are coming from the South East and East with speeds of >0.50 (m/s). WB002 follows a similar pattern in Figure 21. However, WB002 exhibits more extremes in speed, with highest speeds more predominantly from the South East.

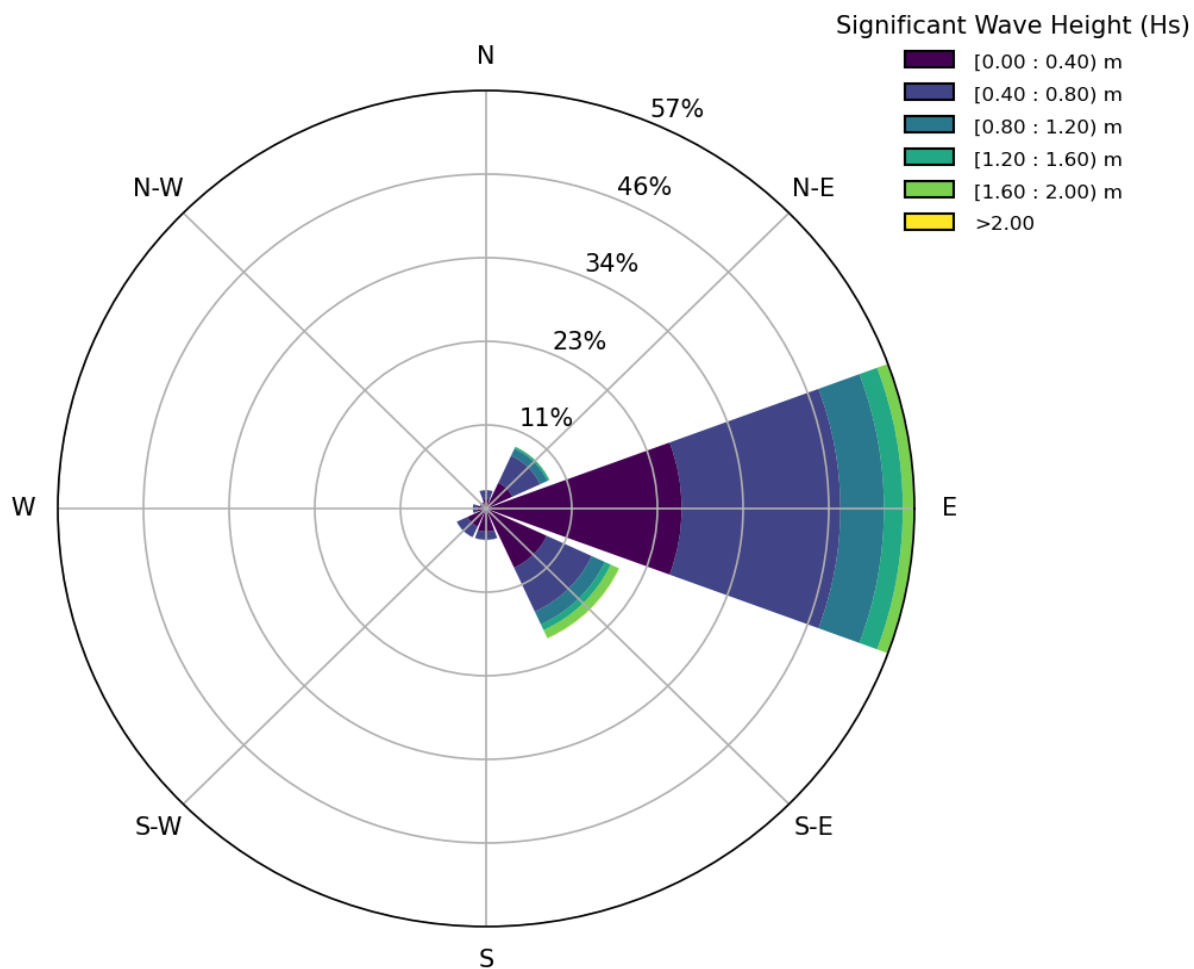


Figure 19: WB001 wave rose showing direction the waves are coming from.

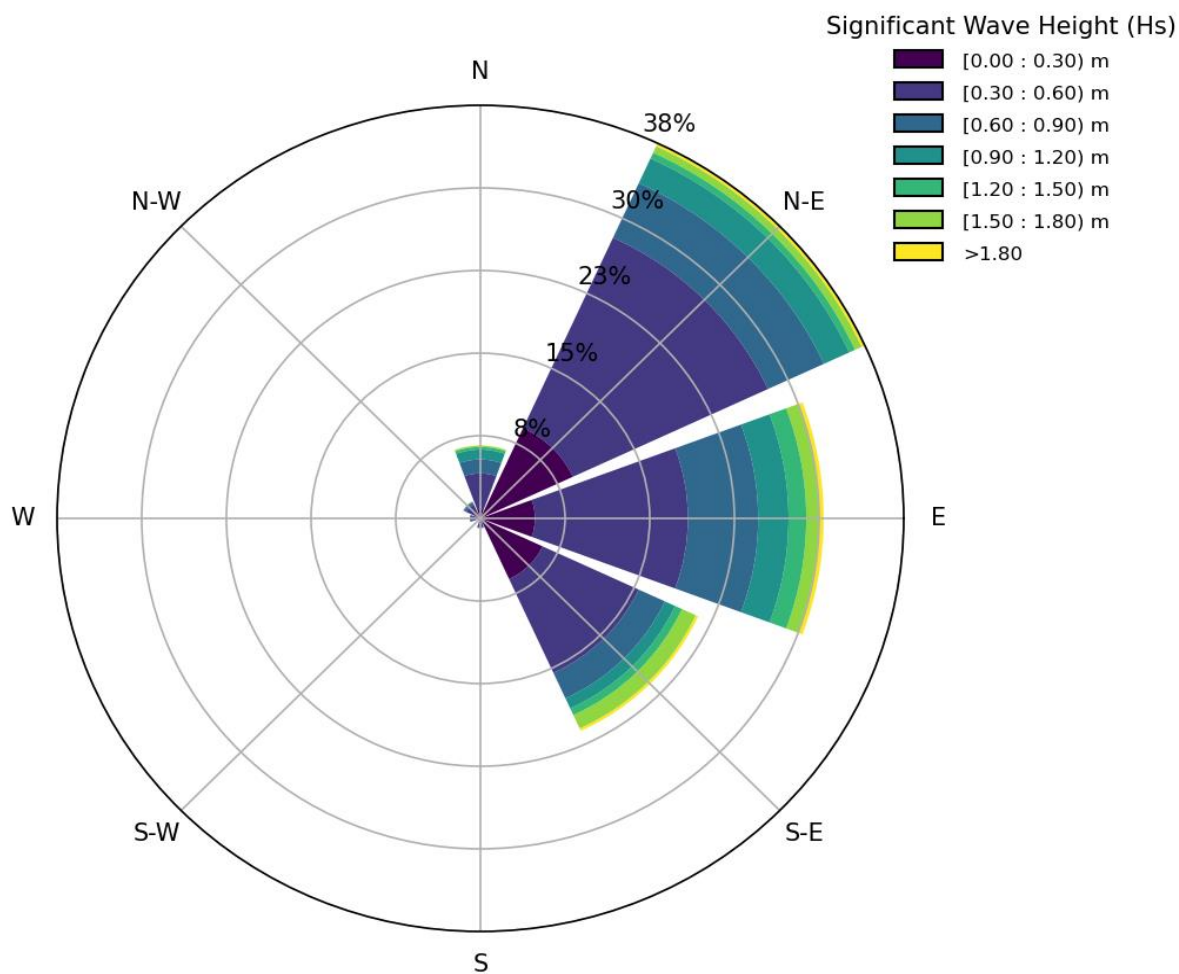


Figure 20: WB002 wave rose showing direction the waves are coming from.

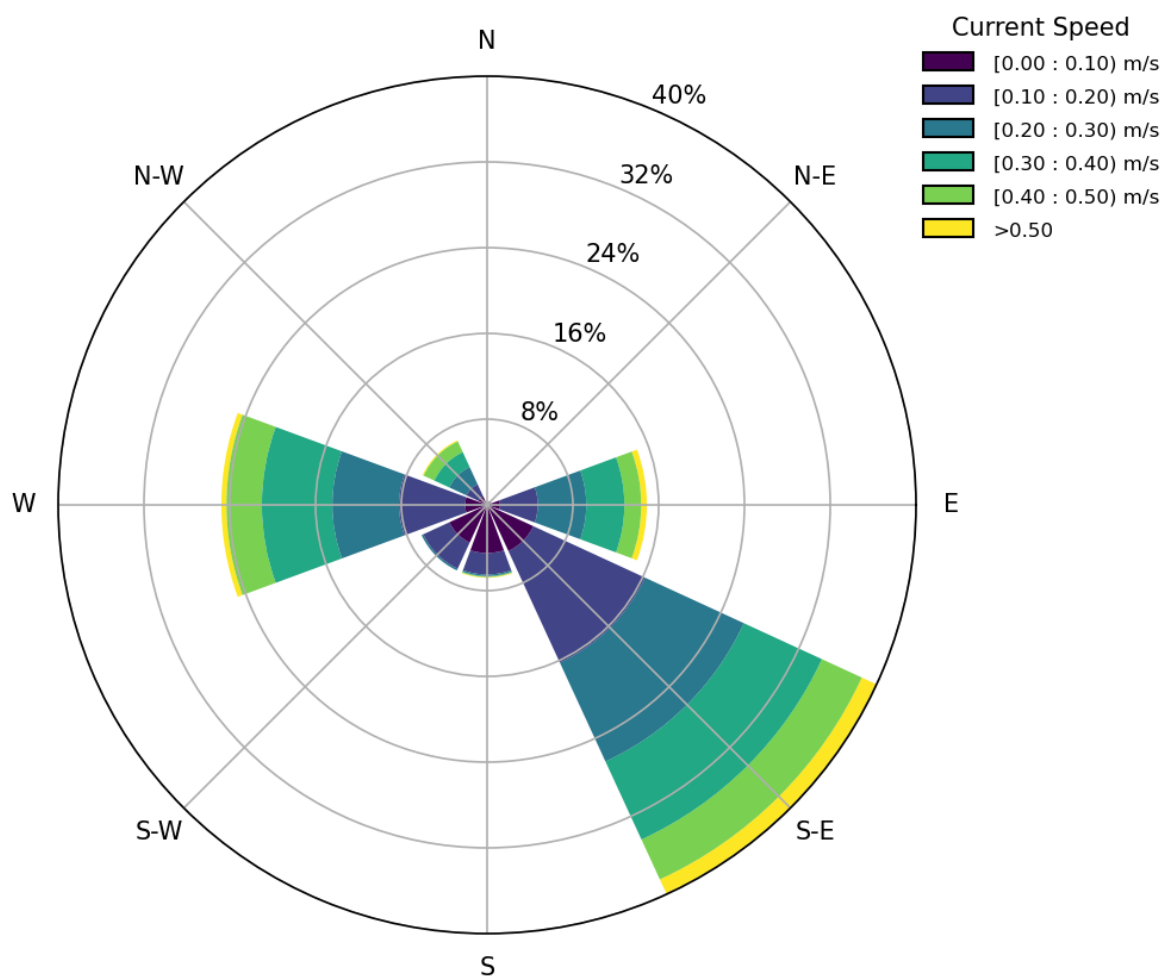


Figure 21: WB001 current rose showing direction current is going to.

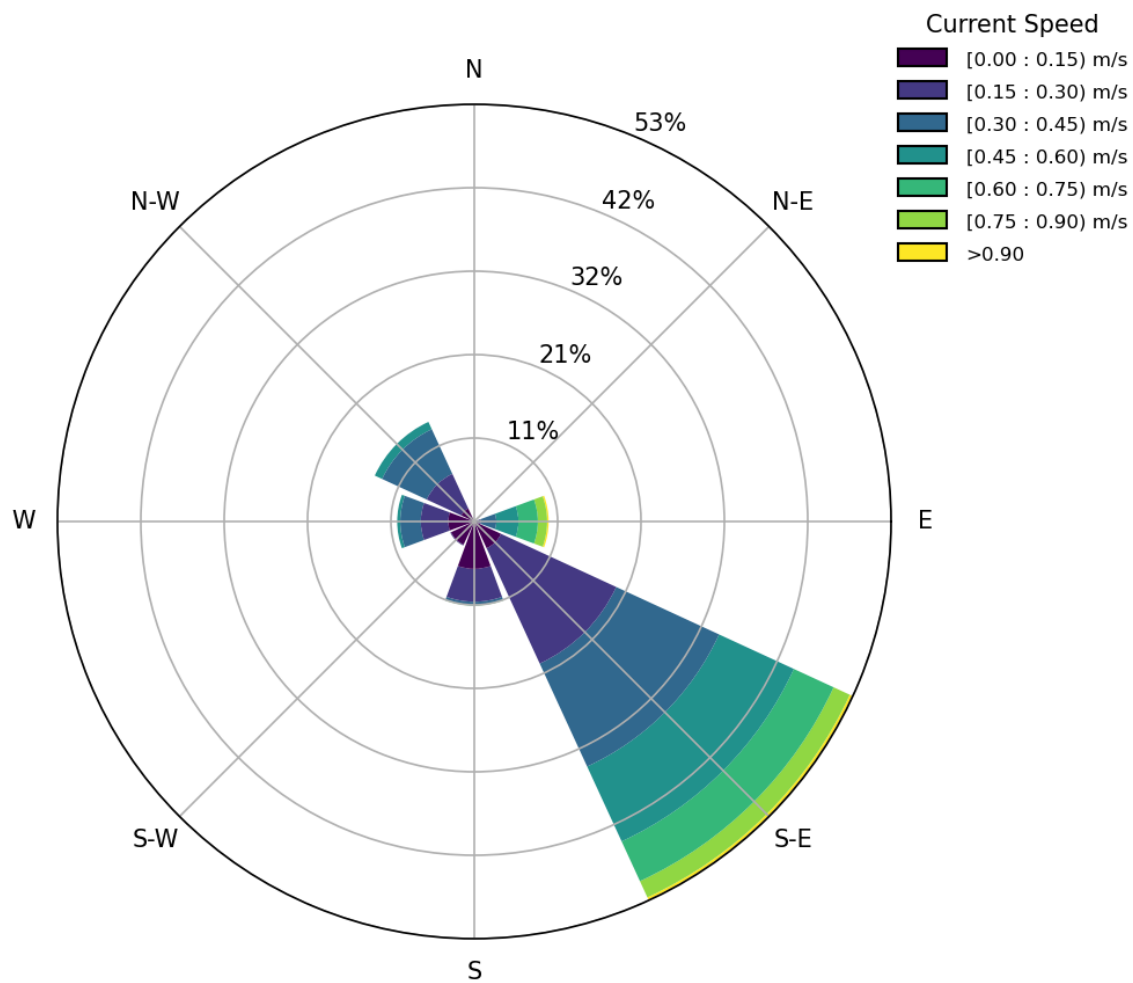


Figure 22: WB002 current rose showing direction current is going to.

5. Joint Probability Tables

5.1. WB001

Table 6. WB001 Significant wave height (Hs) - Mean direction joint probability percentage table

Mean Direction (deg)													
Hs (m)		(345, 15]	(15, 45]	(45, 75]	(75, 105]	(105, 135]	(135, 165]	(165, 195]	(195, 225]	(225, 255]	(255, 285]	(285, 315]	(315, 345]
	(2.5, 3.0]	0.	0.	0.	0.	0.	0.	0.	0.	0.	0.	0.	0.
	(2.0, 2.5]	0.	0.	0.	0.04	0.1	0.	0.	0.	0.	0.	0.	0.
	(1.5, 2.0]	0.	0.01	0.17	1.26	2.28	0.	0.	0.	0.	0.	0.	0.
	(1.0, 1.5]	0.	0.07	0.56	2.47	2.3	0.	0.	0.	0.	0.	0.	0.
	(0.5, 1.0]	0.32	1.28	2.43	12.53	7.23	0.51	0.36	0.4	0.11	0.01	0.32	0.03
	(0.0, 0.5]	1.25	2.84	5.76	27.74	13.31	4.94	2.58	2.26	2.5	1.03	0.49	0.53

Table 7: WB001 current speed - current direction (depth averaged) joint probability percentage table

Current Direction - Depth Averaged (deg)									
Current Speed - Depth Averaged (m/s)		(337.5, 22.5]	(22.5, 67.5]	(67.5, 112.5]	(112.5, 157.5]	(157.5, 202.5]	(202.5, 247.5]	(247.5, 292.5]	(292.5, 337.5]
	(0.65, 0.70]	0.	0.	0.	0.01	0.	0.	0.	0.
	(0.60, 0.65]	0.	0.	0.02	0.05	0.02	0.	0.	0.
	(0.55, 0.60]	0.	0.	0.2	0.4	0.03	0.	0.03	0.02
	(0.50, 0.55]	0.	0.	0.31	1.01	0.03	0.	0.43	0.09
	(0.45, 0.50]	0.	0.	0.6	1.73	0.03	0.	1.15	0.32
	(0.40, 0.45]	0.	0.	0.95	2.33	0.03	0.	2.08	0.78
	(0.35, 0.40]	0.	0.	1.66	3.54	0.03	0.	2.81	0.7
	(0.30, 0.35]	0.	0.	1.88	4.5	0.03	0.01	3.81	0.83
	(0.25, 0.30]	0.	0.	2.37	4.97	0.03	0.03	3.12	0.99
	(0.20, 0.25]	0.02	0.	2.04	5.03	0.1	0.13	3.02	0.77
	(0.15, 0.20]	0.02	0.01	2.06	5.34	0.27	0.68	3.18	0.64
	(0.10, 0.15]	0.03	0.04	1.52	6.06	1.65	1.94	2.92	0.55
	(0.05, 0.10]	0.08	0.11	0.94	4.07	3.5	2.93	1.71	0.63
	(0.0, 0.05]	0.13	0.23	0.28	0.75	1.04	0.97	0.4	0.28

Table 8: WB001 peak period (T_p) - Significant wave height (H_s) joint probability percentage table

		T_p (s)														
H_s (m)		(1.0, 2.0]	(2.0, 3.0]	(3.0, 4.0]	(4.0, 5.0]	(5.0, 6.0]	(6.0, 7.0]	(7.0, 8.0]	(8.0, 9.0]	(9.0, 10.0]	(10.0, 11.0]	(11.0, 12.0]	(12.0, 13.0]	(13.0, 14.0]	(14.0, 15.0]	(15.0, 16.0]
	(2.5, 3.0]	0.	0.	0.	0.	0.	0.	0.	0.	0.	0.	0.	0.	0.	0.	0.
	(2.0, 2.5]	0.	0.	0.	0.	0.	0.08	0.06	0.	0.	0.	0.	0.	0.	0.	0.
	(1.5, 2.0]	0.	0.	0.	0.	0.39	2.72	0.58	0.03	0.	0.	0.	0.	0.	0.	0.
	(1.0, 1.5]	0.	0.	0.	0.1	1.82	2.66	0.31	0.15	0.17	0.14	0.06	0.	0.	0.	0.
	(0.5, 1.0]	0.	1.44	1.79	4.33	5.3	5.08	2.61	1.42	1.26	1.71	0.44	0.15	0.	0.	0.
	(0.0, 0.5]	4.73	8.41	4.8	9.12	12.81	11.75	5.72	2.64	1.89	2.19	0.85	0.21	0.03	0.08	0.

Table 9: WB001 zero mean crossing period (T_z) - Significant wave height (H_s) joint probability percentage table

		T_z (s)						
H_s (m)		(1.0, 2.0]	(2.0, 3.0]	(3.0, 4.0]	(4.0, 5.0]	(5.0, 6.0]	(6.0, 7.0]	(7.0, 8.0]
	(2.5, 3.0]	0.	0.	0.	0.	0.	0.	0.
	(2.0, 2.5]	0.	0.	0.	0.	0.14	0.	0.
	(1.5, 2.0]	0.	0.	0.	2.89	0.83	0.	0.
	(1.0, 1.5]	0.	0.	1.67	3.58	0.15	0.	0.
	(0.5, 1.0]	0.	5.05	17.3	2.72	0.42	0.04	0.
	(0.0, 0.5]	2.3	40.53	15.4	6.44	0.54	0.	0.

5.2. WB002

Table 10: WB002 Significant wave height (Hs) - Mean direction joint probability percentage table

Mean Direction (deg)													
Hs (m)		(345, 15]	(15, 45]	(45, 75]	(75, 105]	(105, 135]	(135, 165]	(165, 195]	(195, 225]	(225, 255]	(255, 285]	(285, 315]	(315, 345]
	(2.5, 3.0]	0.	0.	0.	0.	0.	0.	0.	0.	0.	0.	0.	0.
	(2.0, 2.5]	0.01	0.	0.01	0.	0.04	0.	0.	0.	0.	0.	0.	0.
	(1.5, 2.0]	0.12	0.54	0.51	1.01	1.89	0.1	0.	0.	0.	0.	0.	0.04
	(1.0, 1.5]	0.42	0.63	2.12	1.58	1.76	0.06	0.	0.	0.	0.	0.	0.06
	(0.5, 1.0]	1.36	2.55	11.98	6.32	4.95	2.15	0.	0.	0.07	0.2	0.1	0.78
	(0.0, 0.5]	2.42	6.61	23.48	7.87	7.98	7.78	0.33	0.04	0.25	0.46	0.49	0.94

Table 11: WB002 Current speed - current direction (depth averaged) joint probability percentage table

Current Direction – Depth Averaged (deg)									
Current Speed - Depth Averaged (m/s)		(337.5, 22.5]	(22.5, 67.5]	(67.5, 112.5]	(112.5, 157.5]	(157.5, 202.5]	(202.5, 247.5]	(247.5, 292.5]	(292.5, 337.5]
	(1.0, 1.05]	0.	0.	0.01	0.05	0.	0.	0.	0.
	(0.95, 1.0]	0.	0.	0.04	0.1	0.	0.	0.	0.
	(0.90, 0.95]	0.	0.	0.15	0.26	0.	0.	0.	0.
	(0.85, 0.90]	0.	0.	0.22	0.47	0.	0.	0.	0.
	(0.80, 0.85]	0.	0.	0.3	0.77	0.01	0.	0.	0.
	(0.75, 0.80]	0.	0.01	0.65	0.99	0.01	0.	0.	0.
	(0.70, 0.75]	0.	0.	0.7	1.31	0.	0.	0.	0.
	(0.65, 0.70]	0.	0.	0.83	1.74	0.03	0.	0.	0.
	(0.60, 0.65]	0.	0.	0.93	2.44	0.01	0.	0.	0.
	(0.55, 0.60]	0.	0.	1.04	3.	0.01	0.	0.	0.01
	(0.50, 0.55]	0.	0.	0.84	3.47	0.03	0.	0.06	0.14
	(0.45, 0.50]	0.01	0.	0.9	3.96	0.04	0.	0.32	0.86
	(0.40, 0.45]	0.01	0.	0.88	4.31	0.05	0.	0.75	1.76
	(0.35, 0.40]	0.01	0.	0.51	4.46	0.11	0.01	0.89	2.1
	(0.30, 0.35]	0.02	0.	0.59	5.52	0.19	0.	0.96	2.32
	(0.25, 0.30]	0.02	0.	0.31	6.11	0.45	0.	0.99	1.93

	(0.20, 0.25]	0.01	0.01	0.2	5.54	1.24	0.01	1.04	1.61
	(0.15, 0.20]	0.01	0.	0.15	4.41	2.37	0.09	1.42	1.27
	(0.10, 0.15]	0.06	0.	0.06	2.41	3.3	0.91	1.73	0.9
	(0.05, 0.10]	0.05	0.	0.04	1.1	2.3	1.85	1.26	0.7
	(0.0, 0.05]	0.09	0.03	0.07	0.29	0.46	0.47	0.33	0.23

Table 12: WB002 peak period (T_p) - Significant wave height (H_s) joint probability percentage table

		T_p (s)														
H_s (m)		(1.0, 2.0]	(2.0, 3.0]	(3.0, 4.0]	(4.0, 5.0]	(5.0, 6.0]	(6.0, 7.0]	(7.0, 8.0]	(8.0, 9.0]	(9.0, 10.0]	(10.0, 11.0]	(11.0, 12.0]	(12.0, 13.0]	(13.0, 14.0]	(14.0, 15.0]	(15.0, 16.0]
	(2.5, 3.0]	0.	0.	0.	0.	0.	0.	0.	0.	0.	0.	0.	0.	0.	0.	0.
	(2.0, 2.5]	0.	0.	0.	0.	0.	0.06	0.	0.	0.	0.	0.	0.	0.	0.	0.
	(1.5, 2.0]	0.	0.	0.	0.	0.33	3.03	0.81	0.02	0.	0.	0.	0.	0.	0.	0.
	(1.0, 1.5]	0.	0.	0.01	0.28	2.41	2.71	0.49	0.15	0.27	0.2	0.1	0.01	0.	0.	0.
	(0.5, 1.0]	0.	0.3	1.92	5.02	6.67	6.65	3.33	1.78	1.75	2.32	0.48	0.21	0.01	0.	0.
	(0.0, 0.5]	0.37	1.96	3.23	7.71	15.58	16.06	6.91	2.69	1.81	1.34	0.8	0.11	0.02	0.04	0.

Table 13: WB002 zero mean crossing period (T_z) - Significant wave height (H_s) joint probability percentage table

		T_z (s)					
H_s (m)		(1.0, 2.0]	(2.0, 3.0]	(3.0, 4.0]	(4.0, 5.0]	(5.0, 6.0]	(6.0, 7.0]
	(2.5, 3.0]	0.	0.	0.	0.	0.	0.
	(2.0, 2.5]	0.	0.	0.	0.	0.06	0.
	(1.5, 2.0]	0.	0.	0.	2.86	1.34	0.
	(1.0, 1.5]	0.	0.	1.76	4.63	0.25	0.
	(0.5, 1.0]	0.	3.16	19.12	7.98	0.19	0.
	(0.0, 0.5]	0.25	23.72	28.77	5.72	0.19	0.

6. General State of the Irish Climate- December 2023 to March 2024

December was mainly dominated by Atlantic low pressure systems. However, storm Erin and storm Fergus crossed the country on Saturday 9th and Sunday 10th December. Storm Gerrit and storm Geraldine brought further wet and windy weather towards the end of the year. Rainfall was above average in most of the country.

2024 began with Atlantic low pressure in control bringing rain or showers. The last week of January brought the wettest and windiest period of the month, with storms Isha and Jocelyn in the north of the country, however this brought widespread wet and windy weather and some of the gusts were damaging, especially during storm Isha.

February was another mild Atlantic dominated month. The first week was a more low pressure dominated phase to the north and high to the south, bringing dry and relatively mild westerly airflow across the country. However, low pressure dominated the rest of the month bringing heavy showers crossing the country in a westerly airflow.

March saw Atlantic low pressure systems continuing to dominate with a southerly displaced Jetstream. Low pressure to the south pushed weather fronts northwards and brought some spells of rain to the south. The third week presented Atlantic low pressure, whilst the fourth week brought a showery north-westerly airflow.

6.1. Storms

In total, there were four major storms that occurred during the deployment period, mainly dominated on the North and West coasts and within the months of December and January.

7. Conclusion

Two metocean buoys (WB001 and WB002) were deployed on 14/12/2023 and retrieved on 20/04/24.

The wave climate in the Irish sea near Rosslare Europort during this time was relatively mild. There were no reported trends of extreme values, and there was no direct impact from storms reported.

The overall data return for the following instruments was 84.38% for the ADCP on WB001 and 89.13% for the wave sensor on WB001. This was due to the power issue identified for WB001, and as a result the measurement campaign was extended by 1 week. The data return for WB002 was 99% for the ADCP and 100% for the wave sensor. The total data return was 93% for the entire campaign.

8. Appendices

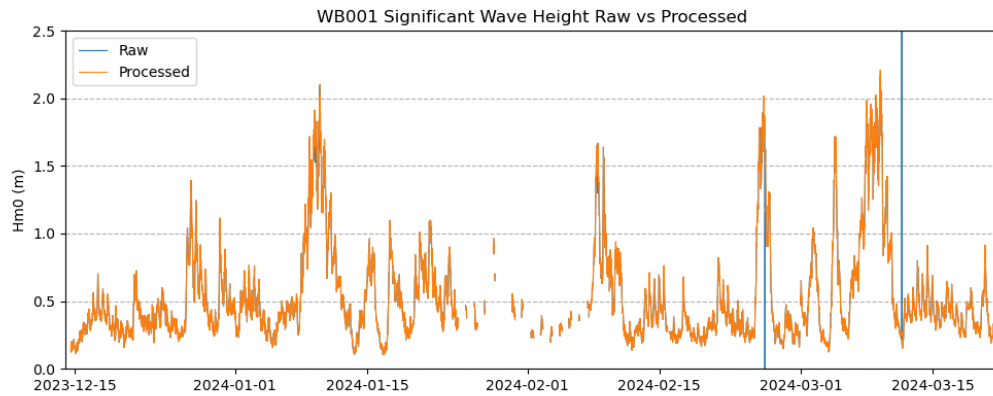


Figure 23: Raw vs processed wave height data for WB001.

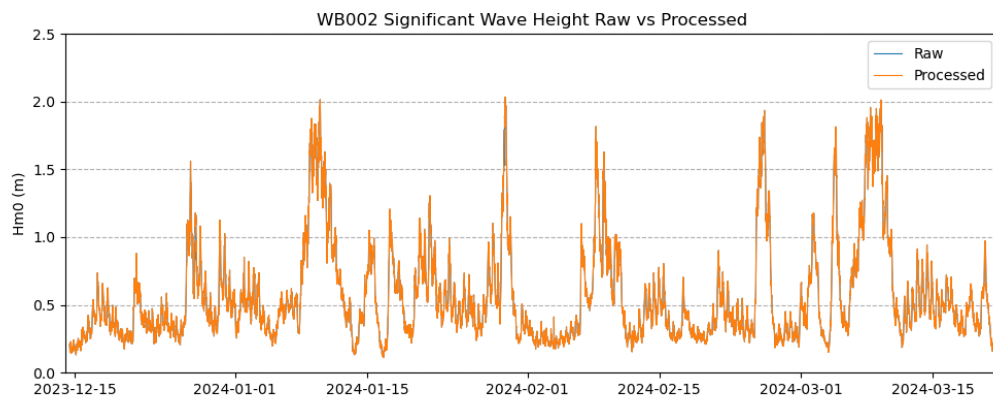
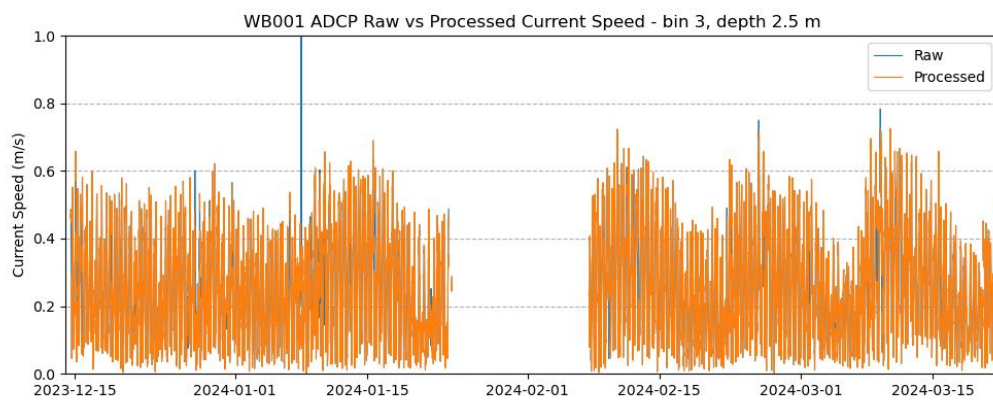
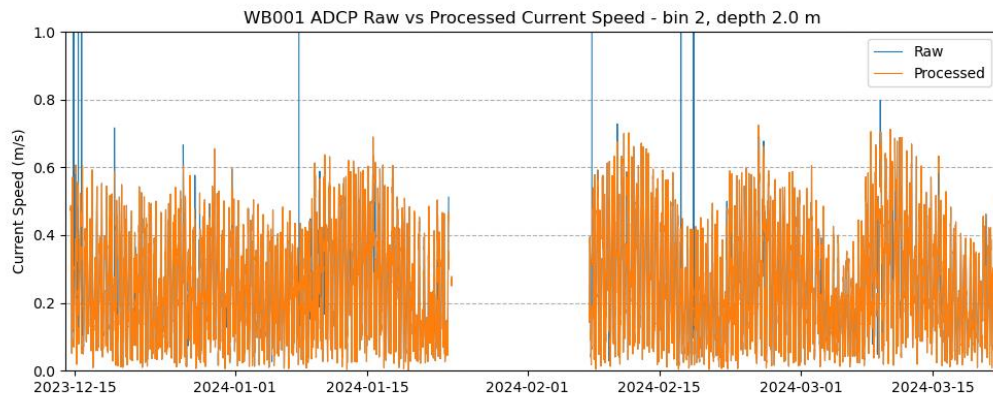
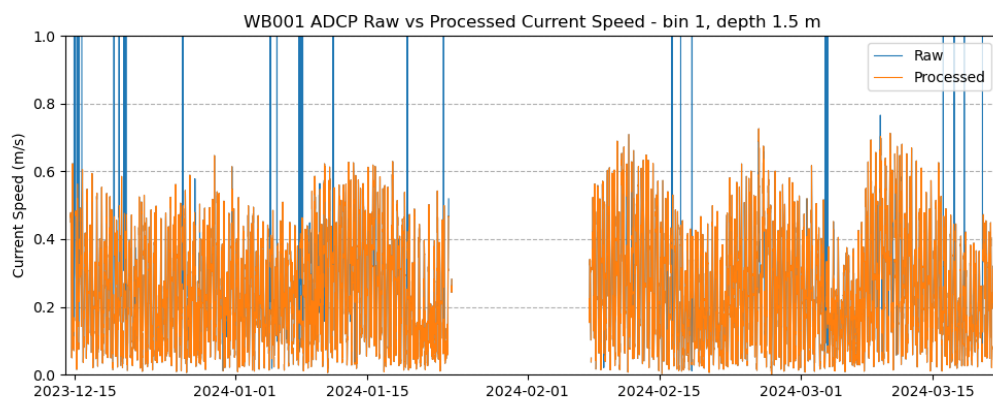
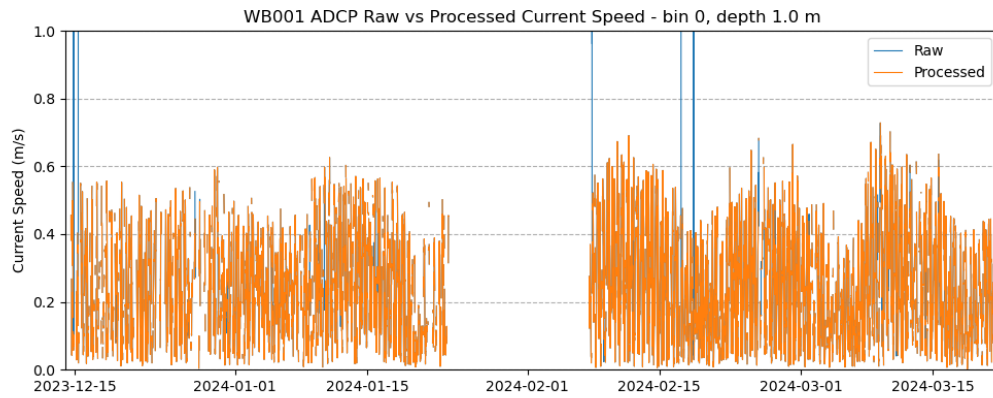
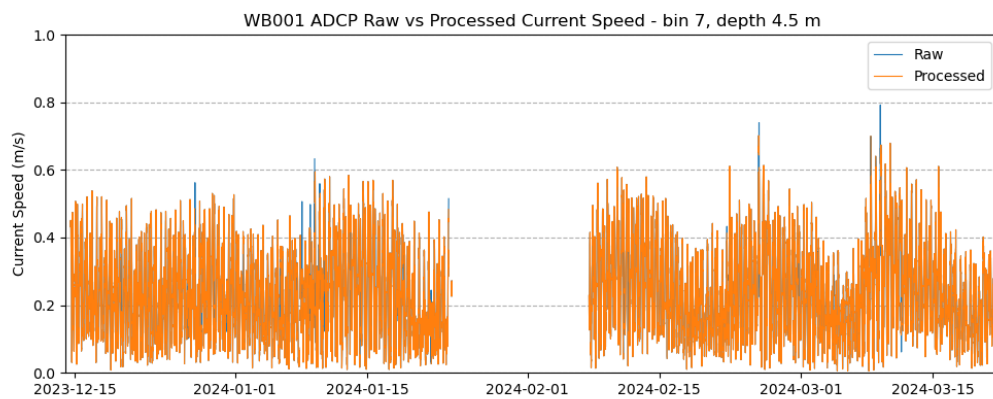
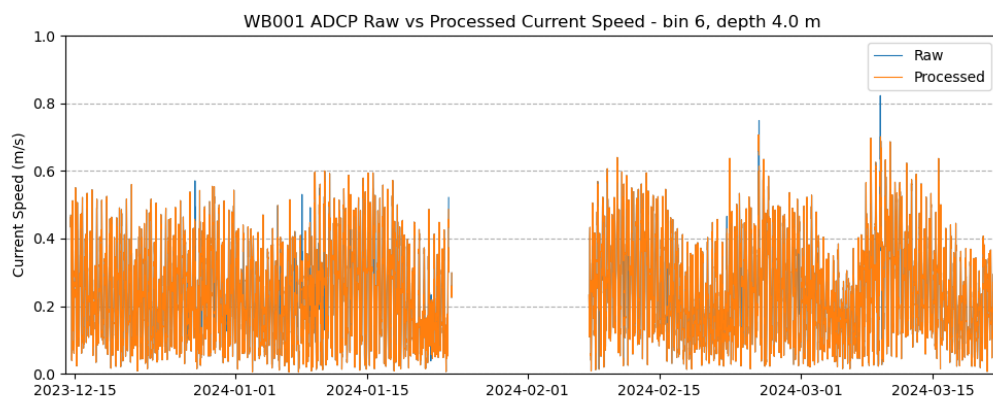
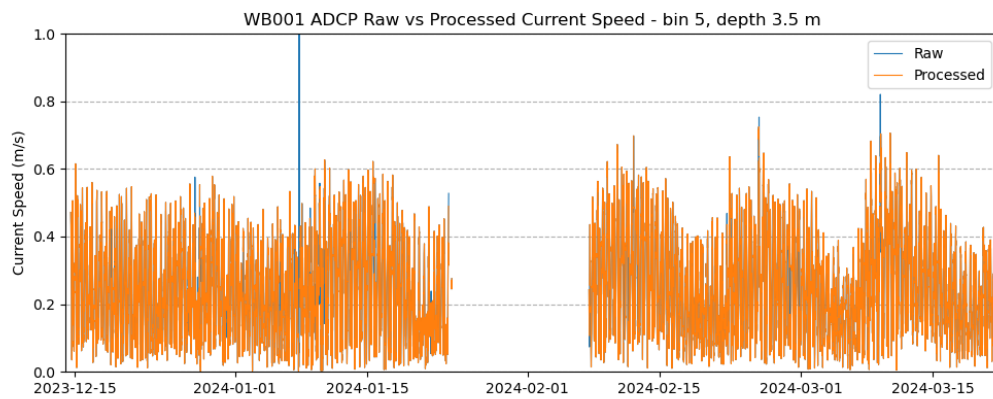
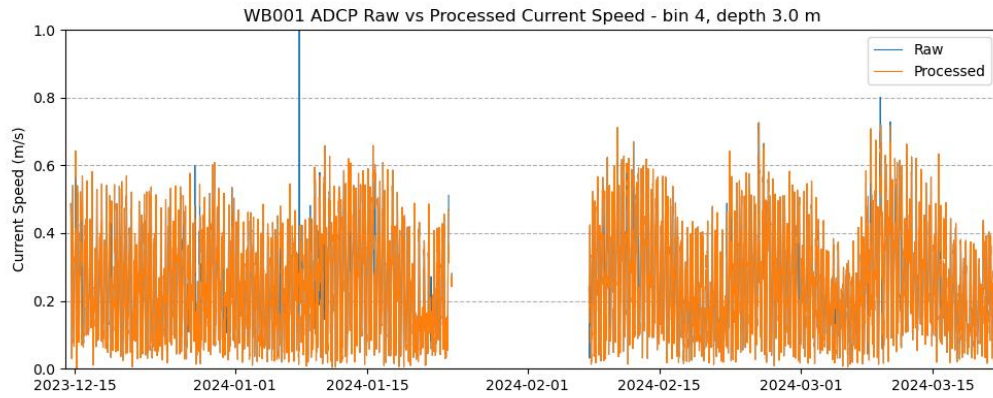
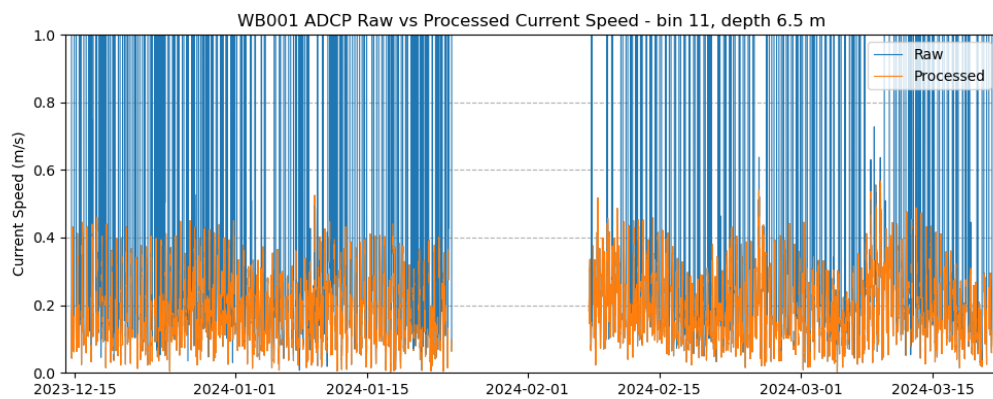
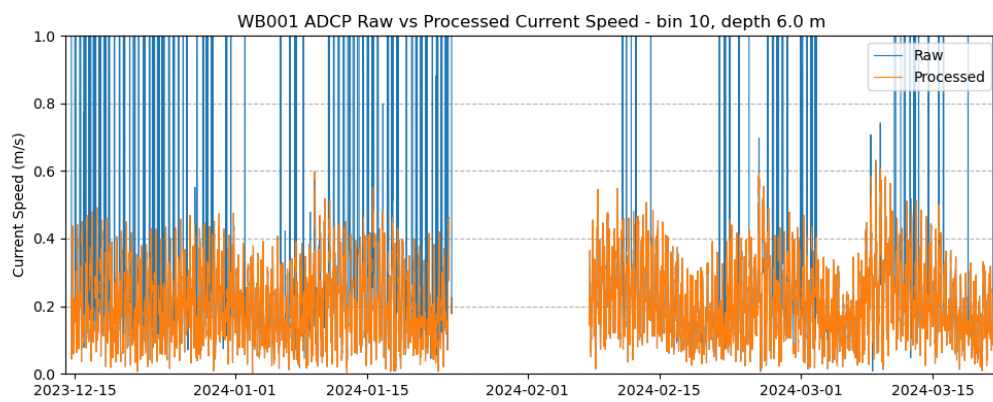
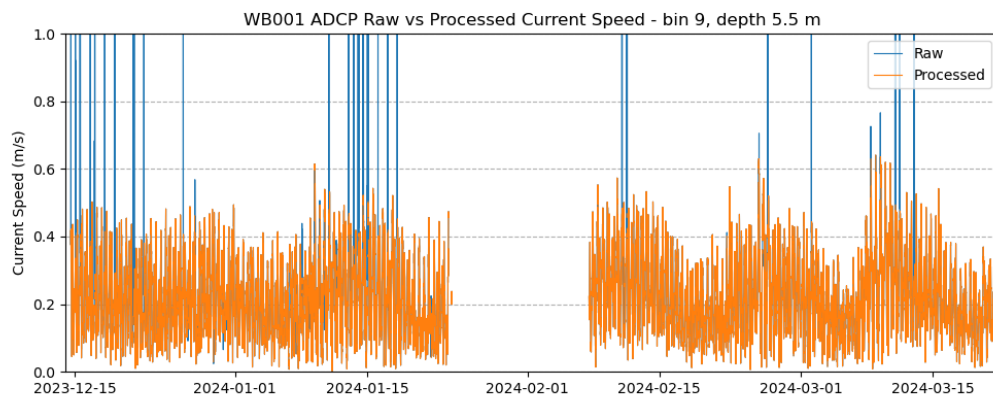
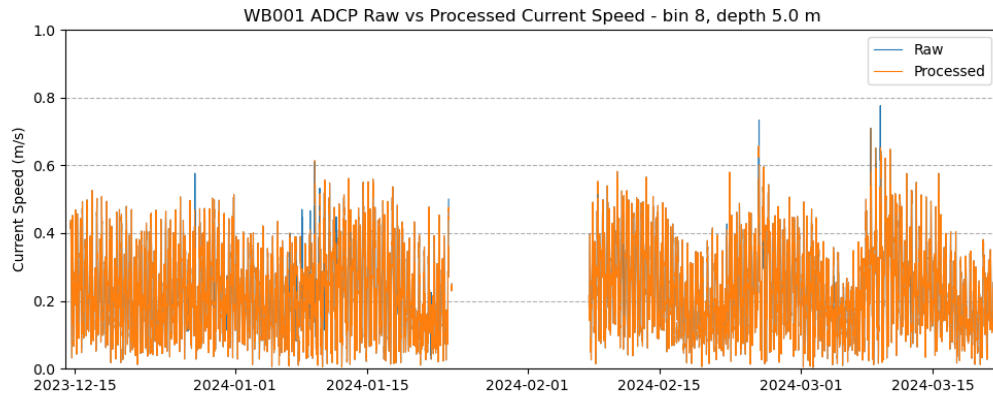


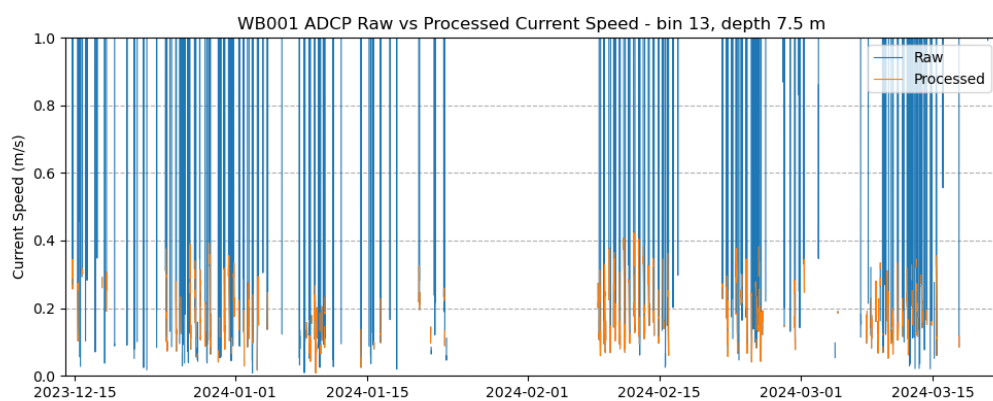
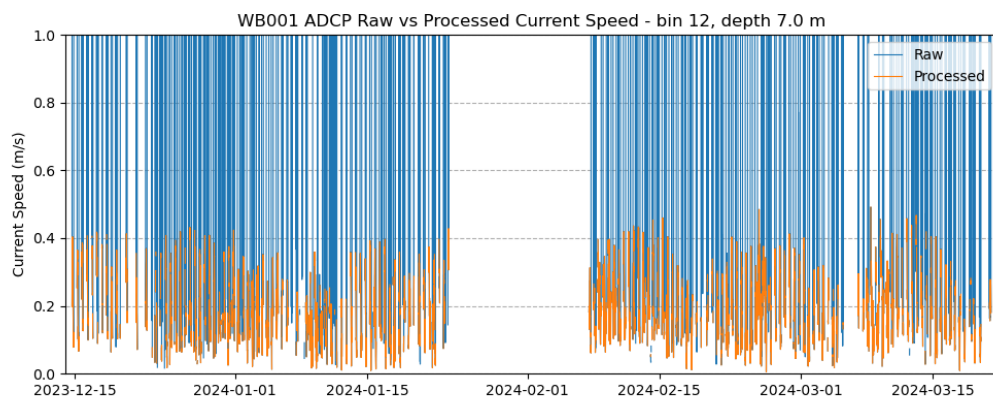
Figure 24: Raw vs processed wave height data for WB002.

WB001 Current Speed per bin:









WB002 Current Speed per bin:

